Functional analysis of a plant virus replication 'factory' using live cell imaging

Volha Linnik

A thesis submitted to fulfil the requirements for the degree
of
Doctor of Philosophy

The University of Edinburgh
2010

Declaration

I hereby declare that the work presented in this thesis is the result of my own investigation and composition, and it has not been submitted in any previous application for a degree or qualification at any institution. The work was done in the Molecular Plant Sciences Department, the University of Edinburgh, under the supervision of Prof. Karl Oparka. Any contributions of other parties are clearly acknowledged in the text.

Acknowledgements

First, I would like to thank my supervisor, Professor Karl Oparka, for giving me an opportunity to start a new project in his lab, for his kind guidance, support and high enthusiasm about my project throughout my PhD studies. He has been always open for discussions and full of helpful advice on my ideas and results. I would also like to thank the whole Oparka lab (all current and recent members) for the scientific atmosphere in the lab, their experimental expertise and help. Many thanks to Nynne, Christine and Jens for showing me the magic tricks for microscopy when I started my PhD in the lab. Big thanks go to Jess for correcting my Introduction chapter, to Jens for correcting my viral RNA imaging chapters and the Material and Methods chapter. Many thanks also go to Jens for taking me on the Pumilio project and for his sharing of my enthusiasm for the PVX project. Kate, Kirsti and Kathryn have been wonderful additions to my life in the lab.

I would also like to thank the Darwin Trust of Edinburgh for giving me an opportunity to come and study here at the Edinburgh University and make it possible for me to do my PhD. Many thanks go to the chartable educational trusts and funds that helped me to survive after the termination of the Darwin Trust funding. I would also like to thank Alex Fraser and Ellen Glendinning for their help on the official side and for all the letters they managed to provide for me so quickly.

A special thank you goes to my family, especially to my Mom, Dad, my brother and my Grandma. Without their love, support and care I would not be able to complete my PhD in two years time. A very special thanks to Nikolaj for his patience, valuable help, care and encouragement to keep on going no matter what difficulties had raised and who has had to live through all of this. I would also like to thank him for dedicating his time to correct all my thesis chapters.

List of abbreviations

a.a.	amino acids
Amp	Ampicillin
Amp^R	Ampicillin resistance
AMV	Alfalfa mosaic virus
AO	acridine orange
ASPV	Apple stem pitting virus
BiFC	bimolecular fluorescence complementation
BMV	Brome mosaic virus
BNYVV	Beet necrotic yellow vein virus
bp	base pairs
BP	recombination with B and P restriction sites in the gateway system
BSA	bovine serum albumin
BSMV	Barley stripe mosaic virus
BYV	Beet yellows virus
CaMV	Cauliflower mosaic virus
CFP	cyan fluorescent protein
CIP	calf intestinal alkaline phosphatase enzyme
CIRV	Carnation Italian ringspot virus
ClYMV	Clover yellow mosaic virus
Cm	Chloramphenicol
Cm^R	Chloramphenicol resistance
CMV	Cucumber mosaic virus
CP	coat protein
CPMV	Cowpea mosaic virus
CR	central rod
CS	cytoplasmic sleeve
CW	cell wall
CymRSV	Cymbidium ringspot virus
D	desmotubule
DAPI	4'-6-diamidino-2-phenylindole
DB	dense bundle
ddNTP	didesoxyribonucleotide triphosphate
DMSO	dimethyl sulfoxide
DNA	deoxyribonucleic acid
dNTP	deoxyribonucleotide triphosphate
DP	desmotubule-embedded proteins
d.p.a.	days post-agroinfiltration
d.p.b.	days post-bombardment
d.p.i.	days post-inoculation of local leaf tissue with the virus
dsDNA	double stranded deoxyribonucleic acid
EDTA	ethylenediaminetetraacetic acid

EM	electron microscopy
ER	endoplasmic reticulum
FABD2	fimbrin actin binding domain 2
FM	fibrous mass
FMDV	Foot-and-mouth-disease virus
FMV	Foxtail mosaic potexvirus
FP	fluorescent protein
FRAP	fluorescence recovery after photobleaching
GFLV	Grapevine fanleaf virus
GFP	green fluorescent protein
gRNA	genomic RNA
HDEL	ER retention signal sequence
HEL	helicase
HiFi PCR	High Fidelity Polymerase Chain Reaction
h.p.b.	hours post-bombardment
Kan	Kanamycin
Kan^R	Kanamycin resistance
kb	kilo basis
LB	Luria-Bertani media
LR	recombination with L and R restriction sites in the gateway system
LSCM	laser scanning confocal microscope
mCitrine	monomeric yellow fluorescent protein
MES	2-(N-Morpholine)-ethane sulfonic acid
mGFP	monomeric green fluorescent protein
MO	membranous organelle
MP	movement protein
mRFP	monomeric red fluorescent protein
mRNA	messenger RNA
MT	methyltransferase
MTOC	microtubule organising centre
mtRNA	mitochondrial RNAs
NE	nuclear envelope
NEB	New England Biolabs
NLS	nuclear localisation signal
nt	nucleotide
OD	optical density
ORF	open reading frame
PCR	Polymerase Chain Reaction
PD	plasmodesmata
PEMV	Pea enation mosaic virus
PM	plasma membrane
PMP	plasma membrane-embedded proteins
PMTV	Potato mop-top virus
POL	polymerase

PRO	protease
PSLV	Poa semilatent virus
PUF	Pumilio family
PUMHD	Pumilio Homology Domain
PVC	Peanut clump virus
PVM	Potato virus M
PVX	Potato virus X
RCNMV	Red clover necrotic mosaic virus
RdRp	RNA-dependent RNA polymerase
RNA	ribonucleic acid
RNP	ribonucleoprotein
SB	spherical body
SEL	size exclusion limit
SFV	Semliki forest virus
sgp	subgenomic promoter
sgRNA	subgenomic RNA
ShVX	Shallot virus X
SP	spoke-like extensions
Spec	Spectinomycin
$Spec^R$	Spectinomycin resistance
ssDNA	singe stranded deoxyribonucleic acid
ssRNA	single stranded ribonucleic acid
(-)ssRNA	negative single-stranded ribonucleic acid
(+)ssRNA	positive single-stranded ribonucleic acid
ST	sialyl-transferase
STP	single tailed particle
TAV	Tomato aspermy virus
TBE	Tris/Borate/EDTA
TE	Tris EDTA
TEV	Tobacco etch virus
TGB	triple gene block
TIP	TGB interacting proteins
TMV	Tobacco mosaic virus
TRV	Tobacco rattle virus
TYMV	Turnip yellow mosaic virus
UTR	untranslated region
UV	ultraviolet light
VRC	viral replication complex
vRNA	viral ribonucleic acid
YEP	yeast extract peptone
YFP	yellow fluorescent protein

Abstract

Plant viruses have developed a number of strategies that enable them to become obligate intracellular parasites of many agricultural crops. Potato virus X (PVX) belongs to a group of positive-sense, single-stranded plant RNA viruses that replicate on host membranes and form elaborate structures known as viral replication complexes (VRCs) that contain viral RNA (vRNA), proteins and host cellular components. VRCs are the principal sites of viral genome replication, virion assembly and packaging of vRNA for export into neighbouring cells. For many animal viruses, host membrane association is crucial for RNA export. For plant viruses, it is not yet known how vRNA is transported to and through plant plasmodesmata. PVX encodes genetic information required for its movement between cells; three viral triple gene block (TGB) movement proteins and a viral coat protein are essential for viral trafficking.

This research project studies the relationship between PVX and its host plants, *Nicotiana benthamina* and *Nicotiana tabacum*. A particular focus of this project is exploration of the structural and functional significance of the PVX VRC and how the virus recruits cell host components for its replication and movement between cells. The role of specific viral proteins in establishing the VRC, and the ways in which these interact with host organelles, was investigated. A combination of different approaches was used, including RNA-binding dyes and a Pumilio-based bimolecular fluorescence complementation assay for detection of the vRNA, fluorescent reporters for virus-encoded proteins, fluorescent reporters for host organelles involved in viral replication, and also transgenic tobacco plants expressing reporters for specific plant components (endoplasmic reticulum, Golgi, actin, microtubules and plasmodesmata). In addition, mutagenesis was used to study the functions of individual viral proteins in replication and movement. All of these approaches were combined to achieve live-cell imaging of the PVX infection process.

The PVX VRC was shown to be a highly compartmentalised structure; (+)-stranded vRNA was concentrated around the viral TGB1 protein, which was localised in discrete circular compartments within the VRC while coat protein was localised to the external edges of the VRC. The vRNA was closely associated with host components (endoplasmic reticulum and actin) shown to be involved in the formation of the VRC. The TGB2/TGB3 viral proteins were shown to colocalise with the host endomembranes (ER) and to exit these compartments in the form of motile granules. vRNA, TGB1, TGB2 and CP localised to plasmodesmata of the infected cells. TGB1 was shown to move cell-to-cell and recruit ER, Golgi and actin in the absence of viral infection. In the presence of virus, TGB1 targeted the VRCs in several neighbouring cells. A model of PVX replication and movement is proposed in which TGB1 functions as a key component for recruitment of host components into the VRC to enable viral replication and spread.

Contents

Table of figures

List of tables

Table of contents

1. Introduction

2. Materials and Methods

4. Analysis of PVX VRC formation in relation to viral gene products

5. Analysis of PVX VRC formation in relation to viral RNA

1. Introduction

1.1 Plant virus infection

1.1.1 Plant viruses

Plant viruses can be described as small microscopic obligate intracellular parasites that require and completely depend on host cells to accomplish their infection cycle. These molecular pathogens obtain many of their requirements from their host plant and use plant energy, ribosomes and related enzymes, nucleotides and amino acids synthesised by the host cell for their own purposes, such as initiation of viral replication, infection of the host plant and spread (Matthews, 1992; Nettleship and Foster, 2000; reviewed in Stange, 2006).

Genomes of plant viruses are predominantly ribonucleic acid (RNA)-based, with almost 75 % in the form of positive-sense single-stranded RNA ((+)ssRNA). Very few viruses have negative-sense single-stranded RNA ((-)ssRNA), single-stranded deoxyribonucleic acid (ssDNA) or double-stranded DNA (dsDNA) genomes. Plant viruses with segmented genomes (genomes with more than one molecule of nucleic acid) also exist. These plant viruses, unlike mammalian viruses, package each nucleic acid molecule into a single virus particle (Hillman, 1998; reviewed in Stange, 2006).

In order to recruit host factors for their needs, viruses have their own highly efficient mechanisms and encode genetic information required for their replication and movement (Ring and Blair, 2001). As plants do not have the capacity to copy viral RNA (vRNA), RNA viruses have their own replicase (RdRp, RNA-dependent RNA polymerase) to produce multiple copies of their RNA genome. A coat protein (CP) is necessary to encapsidate newly synthesised vRNA into viral infectious particles to protect it from degradation and breakage. Movement proteins (MPs) are necessary for trafficking the virus for cell-to-cell movement (Nettleship and Foster, 2000).

1.1.2 Symptoms induced by plant viruses

Plants respond to viral infections by developing a range of symptoms. Local lesions are developed near the site of virus entry into the leaf, and are the first diagnostic indication of viral infection of the plant. Infected cells of the leaf commonly lose chlorophyll and other pigments, producing chlorotic lesions. Necrotic lesions (Fig. 1_1) are formed when the infected cells die (Hillman, 1998).

Figure 1_1: Necrosis of *Nicotiana benthamiana* leaves infected with tobacco rattle virus (Adapted from Carette *et al*., 2002)

Systemic symptoms develop when the virus moves from an infected leaf into the remainder of the plant. Depending on the virus, these symptoms may include a broad range of developmental abnormalities, such as uneven growth, curling, and decreased plant size resulting in reduction of total crop yield. During virus infection a mosaic pattern can develop, which consists of dark and light green areas with a number of

shades in colour giving a mosaic effect in the infected leaves (for instance, during tobacco mosaic virus (TMV) infection) (Matthews, 1992).

The plant defence response against virus infection incorporates silencing of viral gene expression and salicylic acid mediated resistance. However, once the virus enters the plant, it may usurp host-plant machinery to enable its replication and movement (reviewed in Takemoto and Hardham, 2004). Plant viruses have the following features that help them to evolve and mutate quickly in order to adapt to their hosts and to overcome the defence barriers of the plant: short replication cycle with the production of a large number of viral genomes per host cell, a high probability to recombine, and a broad range of host plants they can infect. In addition, the viral replicase lacks repairing activity, leading to an enhanced rate of mutations in each replication cycle (reviewed in Stange, 2006).

1.1.3 Plant virus life cycle

The replication cycle of plant viruses can be explained using the potato virus X (PVX) life cycle as an example. PVX is transmitted mechanically from diseased plants to uninfected ones. PVX virions get into plant cells by physical injury of the cell wall and through breaks in the plasma membrane (reviewed in Scholthof, 2005). The wound site in the host cell can be formed by physical contact between a virus-infected plant and a healthy plant, or by human force (Hillman, 1998; Ring and Blair, 2001), for example cutting tools and handling of infected plants that cause mechanical wounding of leaf epidermal cells that results in initiation of a viral infection in a single epidermal plant cell (reviewed in Scholthof, 2005). Common insect pests of potato plants do not transmit PVX (Smith, 1957). Once the virus is in the plant cell, its genomic material uncoats, transcription takes place, followed by translation and expression of viral proteins, assembly of the virus and genome packaging (encapsidation) into stable particles (virions) and the release of the virions from the infected cells (Hillman, 1998; Ring and Blair, 2001). Encapsidation of the virus into particles is thought to give a number of

benefits to the virus. It protects the virus both during movement within an infected plant (especially throughout viral long-distance movement) and during spread to other host plants. In addition, it serves as one of the viral defence systems by protecting the viral genome from the replication and translation machinery of the host, and preventing the excessive overproduction of the virus in the host plant cell (Hull, 2002; Palukaitis *et al*., 2008).

1.1.4 Movement of viruses

To promote the development of disease, plant viruses spread locally (Fig. 1_2 and Fig. 1_3) from initially infected cells to non-infected plant tissues. Viruses move from cell-to-cell through plasmodesmata (PD; reviewed in Lucas, 1995; Ding, 1998; Oparka, 2004; reviewed in Epel, 2009), which are plant-specific intercellular membranous channels, and systemically between organs within the plant through the vascular system (Gilbertson and Lucas, 1996; reviewed in Oparka and Santa Cruz, 2000; Lucas *et al*., 2001; Ring and Blair, 2001; Taliansky *et al*., 2008). Evidence of viral systemic spread through the plant vascular tissue (Fig. 1_3) comes from appearance of virus particles in the phloem as seen in electron micrographs (Price, 1966; Esau *et al*., 1967). Chemical or physical disturbance of the flow of metabolites in the phloem may lead to the delay or even prevention of virus movement through the phloem (Roberts, 1952; Leisner and Turgeon, 1993).

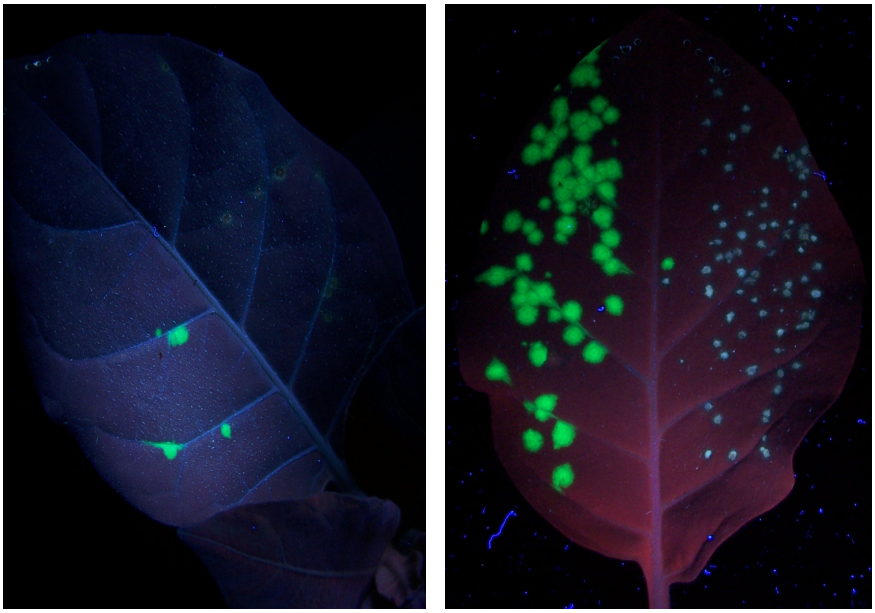

Figure 1_2: Local green viral lesions (green fluorescent protein (GFP)-expressing virus) on *Nicotiana tabacum* leaves are visualised with ultraviolet (UV) illumination

Figure 1_3: Virus spread within a plant (local, left and systemic, right)
Round fluorescent spots (green) show local lesions; a large area of fluorescence in the upper leaves corresponds to the part of the leaf where a systemic spread of the virus occurred.

1.1.4.1 Virus movement from cell-to-cell

Virus cell-to-cell movement takes place mainly in epidermal and mesophyl tissues (Trutnyeva *et al*., 2008). It involves transport of virus particles (virions) or ribonucleoproteins and occurs through PD (Hillman, 1998; Ring and Blair, 2001). Cell-to-cell movement usually happens early in the infection process, e.g. 5 h post-infection for TMV in *N. tabacum* plants (Fannin and Shaw, 1987). Similar pathways are used by the plant host to move endogenous macromolecules, suggesting that plant viruses take over the plant transport system for their own needs (Trutnyeva *et al*., 2008).

Components which are smaller than the size exclusion limit (SEL) of PD move through the channels by diffusion without modification of the PD SEL. Molecules larger than the PD SEL have to move by selective transport and require conformational changes to take place in the plasmodesmal pore. Variation in PD SEL depends on the plant cell type and cell age (reviewed in Roberts and Oparka, 2003). Transient expression of plasmids that encode GFP-MP fusions has shown that molecules with the molecular mass up to 50-kDa were able to move liberally via PD in sink plant leaves (Oparka *et al*., 1999). However, it has been proposed that viral MPs appear to associate with the secondary branched PD of source leaves and do not target simple plasmodesmata of young sink leaves (Tomenius *et al*., 1987; Itaya *et al*., 1998). Moreover, it is known that PD SEL decreases in leaves during the changes from simple to secondary PD (Oparka *et al*., 1999). The molecular mass of the viral proteins of Potato virus X is much larger that the SEL of PD. For instance, PVX replicase is a protein of 165-kDa (Doronin and Hemenway, 1996; Plante *et al*., 2000). The 'triple-gene block' movement proteins of Potato virus X are about 45-kDa and the viral coat protein is 25-kDa (Morozov *et al*., 1983). All 3 'triple-gene block' movement proteins and the coat protein of PVX are essential for virus cell-to-cell trafficking (Huisman *et al*., 1988; Skryabin *et al*., 1988; Chapman *et al*., 1992; Angell and Baulcombe, 1995; Angell *et al*., 1996; Kalinina *et al*., 1996; Santa Cruz *et al*., 1996; Santa Cruz *et al*., 1998; Morozov and Solovyev, 2003; Ju *et al*., 2007). This implies that PVX MPs are larger than the channels that interconnect

plant cells. However, plant viruses do not have the capacity to lyse the cell-wall barrier, consisting of cellulose and pectin. This indicates that the virus has to modify these channels before viral movement takes place in order to infect adjacent uninfected cells (Ring and Blair, 2001; Taliansky *et al*., 2008). These modifications are controlled by viral MPs (Trutnyeva *et al*., 2008). Some viral MPs have been reported to localise to PD resulting in an increase in PD SEL (Evert *et al*., 1977; Carrington *et al*., 1996). Some viruses (for instance, potato virus X, tobacco etch virus and beet yellows virus) may move via PD in the form of virions and cause alterations in the structure of plasmodesmal pore (Esau *et al*., 1967; Kitajima and Lauritis, 1969; Weintraub *et al*., 1976; Santa Cruz *et al*., 1998). The 30-kDa TMV MP also accumulates in plasmodesmata (Fig. 1_4) (Deom *et al*., 1987; Tomenius *et al*., 1987; Ding *et al*., 1992a) and increases the PD SEL (Wolf *et al*., 1989; Citovsky *et al*., 1993; Waigmann *et al*., 1994; Oparka *et al*., 1997a).

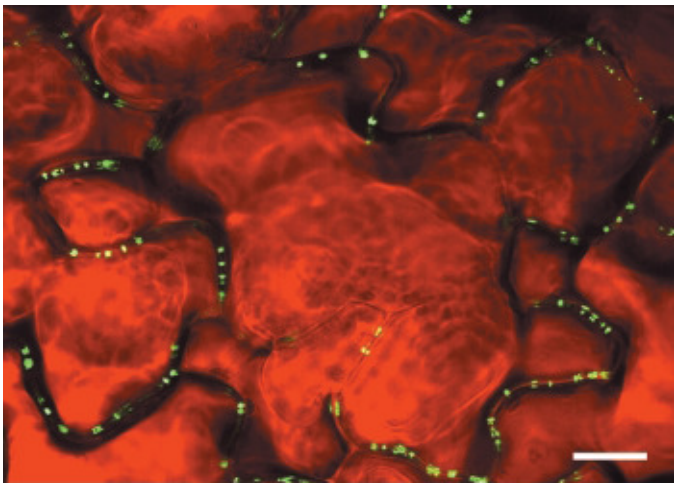

Figure 1_4: MP of TMV localises to PD (Adapted from Roberts and Oparka, 2003)
Confocal image of epidermal cells of the *N. tabacum* source leave of plants expressing the TMV MP-GFP fusion.
TMV MP-GFP fusion localises to the PD (green spots at the periphery of the epidermal cell walls). Bars, 10 mm.

One possible function of viral MPs is to mediate virus-induced accumulation of β-1,3-glucanase, a callose degrading enzyme. This event leads to the opening of PD for viral cell-to-cell trafficking (reviewed in Epel, 2009). Deposition of callose ((1→3)-β-glucan) at PD to regulate the plasmodesmal SEL is one of the control strategies of plants to direct the exchange of molecules through PD. This event has been reported to take place during wounding of plants (Hughes and Gunning, 1980). However, callose deposition could be also an early defense mechanism to prevent the spread of viruses. Support for this hypothesis comes from findings on callose depositions in pit fields of plants infected with PVX (Allison and Shalla, 1974). PVX TGB2 has been shown to increase PD SEL, allowing the passage of free GFP between PVX-infected cells (Tamai and Meshi, 2001). In addition, it was found that the second movement protein of PVX could associate with TGB2 interacting protein (TIP), a host factor that interacts with β-1,3-glucanase, which resulted in increased callose degradation (Fridborg *et al*., 2003). This could be a possible mechanism of regulation of the size exclusion limit of PD and PVX targeting of PD (reviewed in Boevink and Oparka, 2005). Moreover, callose was also found at PD of plants infected with many other viruses, such as TMV (Wu and Dimitman, 1970; Moore and Stone, 1972; Beffa *et al*., 1996), tomato bushy stunt virus (Pennazio *et al*., 1978), and maize dwarf mosaic virus (Choi, 1999), additionally supporting the hypothesis of a common defense mechanism to stop the spread of viruses in infected plant tissue.

1.2 Positive-sense RNA virus genome expression and replication

All (+)ssRNA viruses share similarities in their RNA replication processes. The differences only come from the variation in organisation of the viral genome, morphology of virus particles, and the host plant (reviewed in Sanfaçon, 2005). The replication process of these viruses is associated with host-derived intercellular membranes leading to the formation of functional viral replication complexes (VRCs) that incorporate vRNA, viral proteins, cell host organelles and cytoskeleton elements (Hills *et al*., 1987; Saito *et al*., 1987; Padgett *et al*., 1996; Heinlein *et al*., 1998; Mas and Beachy, 1999; Szecsi *et al*., 1999; Kawakami *et al*., 2004; Mackenzie, 2005; Novoa *et*

al., 2005; Miller and Krijnse-Locker, 2008). The precise role and involvement of plant host factors to accomplish successful viral replication and translation of their genome remains to be established (Whitham and Wang, 2004). PVX VRCs will be introduced in more detail in the following sub-chapter.

(+)ssRNA viruses encode a template-specific RdRp, the so-called viral replicase. RdRp is necessary for the synthesis of viral RNA and does not have a proofreading ability like DNA polymerases. Once a (+)ssRNA virus is in the host plant cell, uncoating of its genome takes place (reviewed in Thivierge *et al*., 2005). Next, the translation initiation factors and ribosomal subunits recognise the genomic RNA and translation initiation starts from the open reading frame at the 5' end of the RNA molecule (Le *et al*., 1997; Gallie, 1998; Browning, 2004). The components of the RdRp are then produced allowing synthesis of full-length complementary negative-sense RNA intermediate molecules from (+)RNA templates (without any DNA phase), followed by synthesis from a (-)RNA template of new genomic (+)RNA and shorter viral subgenomic RNAs (sgRNAs) that allow the translation of viral proteins (Noueiry and Ahlquist, 2003). The balance between viral RNA replication and translation is coordinated by the interaction of viral and host factors since the 5'>3' movement of ribosomes on the vRNA contradicts with the 3'>5' RdRp activity. This happens in both plants and animals (Gingras *et al*., 1999; Barry and Miller, 2002; Walter *et al*., 2002).

Viral (+)RNAs share characteristics with cellular messenger RNAs (mRNAs). The genomic viral (+)ssRNA can be translated directly by serving as an mRNA and used as a template for translation of viral proteins, allowing synthesis of a complementary negative strand RNA molecule (Ring and Blair, 2001). The genome organisation of some (+)RNA viruses (for instance, the PVX genome) is also similar to some eukaryotic cellular mRNAs. For instance, PVX RNA has a 5' untranslated region (UTR), a modified nucleotide sequence (so named cap structure or 5' cap), and a polyadenylated 3' end (3' poly(A) tail). However, there are a number of differences between viral RNAs and eukaryotic mRNAs. The viral 5' UTRs of some (+)RNA viruses vary significantly

in their length and structure at the 5' and 3' ends from those of cell host mRNAs (reviewed in Thivierge *et al*., 2005). In eukaryotic cells, translation is spatially and functionally separated from RNA synthesis. Unlike host cell mRNAs, vRNA synthesis follows rather than precedes translation. In addition, RNA virus replication and translation are coupled: many host and viral factors take part both in plant virus translation and viral replication (White *et al*., 1992; Novak and Kirkegaard, 1994).

(+)ssRNA plant viruses are infectious as 'naked' RNA. New (+)RNA is either packaged into virions covered with virus-specific CP (encapsidation of vRNA) or recruited for cell-to-cell transport to continue the infection process in neighbouring cells (vRNA trafficking). The host cytoskeleton is involved in trafficking of the viral genome. Viral nucleoproteins (protein-RNA complexes) assemble in the cytoplasm of the cell (for the majority of plant viruses) either as helices or as isometric particles (Harrison *et al.*, 1996). Generally, release of virions occurs by plant-cell death and membrane degradation (Ring and Blair, 2001).

The exact mechanism of PVX RNA transport to and through PD is still not fully clear, and the functional significance of the VRC structure for viral replication and spread remains to be discovered.

The positive-sense plant RNA virus genome expression and replication described above is schematically represented in Fig. 1_5 using potato virus X replication as an example of the replication processes of positive-sense single-stranded RNA viruses.

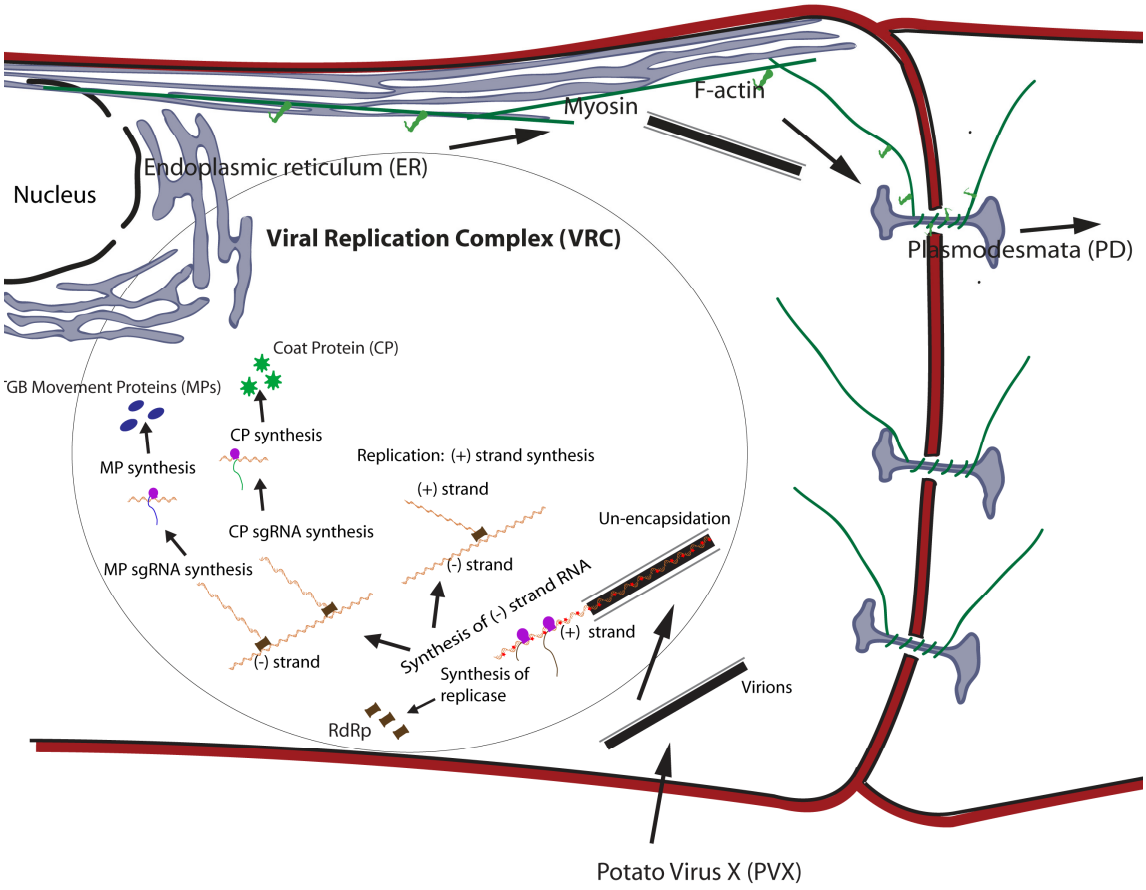

Figure 1_5: Schematic illustration of (+)ssRNA virus genome expression and replication

1.3 Potato Virus X

1.3.1 Plants infected with potato virus X

PVX belongs to the genus *Potexviruses*, family *Flexiviridae* (Adams *et al*., 2004). PVX is well-characterised genetically and is one of the most widespread of all the *Potexviruses*. There are different strains of this virus. PVX can infect crops from the *Solanaceae* plant family, including potato, tobacco (Fig. 1_6), tomato and pepper, causing systemic infections in these plants and resulting in crop yield losses (Chapman *et al*., 1992; Santa Cruz *et al*., 1996).

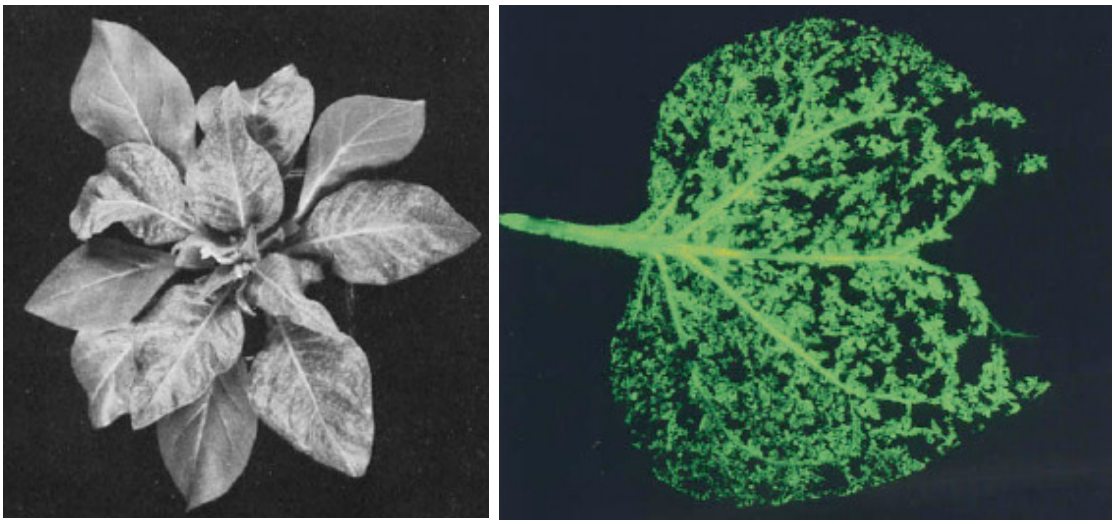

A B

Figure 1_6: PVX systemic infections in plants

A: Systemic PVX infections developed in a *N. clevelandii* plant at 13 days post-inoculation (Adapted from Chapman *et al*., 1992)

B: Systemic spread of PVX CP mutant construct in *N. benthamiana* showing distribution of virus across the leaf (Adapted from Santa Cruz *et al*., 1998).

Local PVX infections are developed when the virus infects members of the *Chenopodiaceae* and *Amaranthaceae* families. Infected plants develop different symptoms of infection, which depend on the PVX strain. Infected plants are often short in size, have small leaves, decreased leaf numbers and show chlorosis. A mild mottling can also be present. PVX infection can also cause plant leaf tip death (Smith, 1957).

1.3.2 PVX RNA

The PVX genome consists of a (+)ssRNA molecule (Ring and Blair, 2001). The genomic (~6.4 kb) RNA has an 84-nucleotide (84-nt) 5'-UTR and 72-nt 3'-UTR (AbouHaidar *et al*., 1998).

The PVX RNA encodes 5 open reading frames (ORFs; Fig. 1_7) (Huisman *et al*., 1988).

Figure 1_7: Schematic representation of PVX genomic RNA molecule
5 ORFs: replicase, 3 'triple-gene block' movement proteins and a viral coat protein.

The first ORF encodes a protein of 165-kDa, which is involved in viral replication (the viral replicase) and possesses methyltransferase, RNA helicase and RNA polymerase activities (Doronin and Hemenway, 1996; Plante *et al*., 2000). The central region of the genome encodes 3 overlapping ORFs ('triple-gene block' movement proteins (TGB MPs or TGBs)). The final ORF at the 3' end of the RNA molecule is the viral CP gene (Morozov *et al*., 1983). This protein is required for virion assembly and protects the virus during its spread in the plant tissue. Like TGB MPs, the CP of PVX is critical for virus cell-to-cell movement (Huisman *et al*., 1988; Skryabin *et al*., 1988; Chapman *et al*., 1992; Angell and Baulcombe, 1995; Angell *et al*., 1996; Kalinina *et al*., 1996; Santa Cruz *et al*., 1996; Santa Cruz *et al*., 1998; Morozov and Solovyev, 2003; Ju *et al*., 2007). PVX CP was found to accumulate in plasmodesmata of infected cells but does not gate plasmodesmata (i.e. does not modify the SEL of PD) (Oparka *et al*., 1996). However, it is transported with the infectious material from one cell to another (Santa Cruz *et al*., 1998). PVX CP mutants lacking the CP gene can move cell-to-cell but do not move systemically; however, the virus still assembles virus particles but they are not infectious (Chapman *et al*., 1992; Baucombe *et al*., 1995). In addition, CP phosphorylation was proposed to play an important role in initiating of translation during PVX infection (Lee and Lucas, 2001).

Both genomic (gRNA) and subgenomic (sgRNA) PVX RNAs are capped at the 5' end (Sonenberg *et al*., 1978) and polyadenylated at the 3' end (Morozov *et al*., 1981; Huisman *et al*., 1988). It was shown in radiographs that only genomic-size PVX RNA was present in PVX particles (Dolij *et al*., 1987). Six double-stranded forms of PVX sgRNAs with 3' poly(A) tails (3.6 kb, 3.0, 1.8 kb (Dolij *et al*., 1987) and 2.1, 1.4 and 0.9

kb (Dolij *et al*., 1987; Huisman *et al*., 1988) required for the expression of the TGB proteins and CP have been identified. PVX CP is translated from the 0.9 kb sgRNA (Grama and Mashkovsky, 1986). The data of *in vitro* translation studies show that TGB1 is expressed as a single translation product of the 2.1 kb sgRNA, suggesting that the ORF of the TGB1 gene is produced from a functionally monocistronic mRNA. TGB2 and TGB3 are both derived from the same 1.4 kb sgRNA. This mRNA is considered functionally bicistronic (Morozov *et al*., 1991; Zhou and Jackson, 1996; AbouHaidar *et al*., 1998; Verchot *et al*., 1998; Agranovsky and Morozov, 1999). Expression of the TGB2 and TGB3 proteins was proposed to involve a translation mechanism, in which PVX TGB3 ORF is translated by the leaky ribosome scanning mechanism through the TGB2 ORF from the same 1.4 kb sgRNA (sgRNAs of PVX are visualised in Fig. 5_2 E, Chapter 5) (Skryabin *et al*., 1988; Morozov *et al*., 1989; reviewed in Dreher and Miller, 2006). In the leaky ribosome scanning mechanism more than one translation initiation site can be used by ribosomes during the scanning at the 5' UTR sequence of the viral RNA (Verchot *et al*., 1998). Coupling of the expression of the TGB2 and TGB3 proteins is likely an evolutionary conserved mechanism to make sure that they are translated at levels that are most efficient for virus function. Support for this theory comes from the complementation experiments of TGB cell-to-cell movement defective mutants of beet necrotic yellow vein virus, where viral spread was dependent on the relative amounts of the 13K and 15K TGB proteins, respectively, and occurred only when these proteins were produced from the same bicistronic mRNA (Gilmer *et al*., 1992; Bleykasten-Grosshans *et al*., 1997).

Expression of TGB proteins is detected simultaneously early in viral infection (Niesbach-Klösgen *et al*., 1990; Donald e*t al*., 1993). The amounts of TGB2 and TGB3 are regulated in the cell relative to the TGB1 protein, CP and RNA-dependent RNA polymerase. The TGB2 and TGB3 are found at much lower amounts in infected cells compared to other viral proteins (Yang *et al*., 2000). However, the TGB3 protein is expressed in very low amounts probably due to a leaky ribosome scanning translation mechanism (Guilford and Forster, 1986; Dolja *et al*., 1987; Zhou and Jackson, 1996;

Morozov and Solovyev, 2003). For example, the transcript ratio of TGB1/TGB2/TGB3 for the potexvirus barley strip mosaic virus is 100/10/1, respectively (Lim *et al*., 2008). Moreover, PVX TGB3 protein is sometimes not even detected in infected cells (Gorshkova *et al*., 2003).

1.3.3 PVX viral replication complex (PVX VRC)

Once PVX is in the cell, the viral RNA replication is initiated and the MPs are produced (Santa Cruz *et al*., 1998). PVX forms complex perinuclear replication structures in the infected cells. The relationship of perinuclear inclusion bodies (also known as X-bodies (Iwanowski, 1903), amorphous bodies or amorphous inclusions, amoeboid bodies or vacuolate bodies) to the virus was studied in early work by Goldstein and Sheffield (Goldstein, 1926; Sheffield, 1939, 1949). Later, these bodies were named as viral replication complexes (Asurmendi *et al*., 2004). VRCs are often referred to as the principal centres of viral replication, translation and encapsidation in the host cell (Kikumoto and Matsui, 1961; Kozar and Sheludko, 1969; Allison and Shalla, 1973; Espinoza *et al*., 1991; Ju *et al*., 2005). PVX VRCs have also been proposed to be centres of active PVX protein synthesis during the viral replication process due to the fact that viral TGB proteins were found to localise to the PVX VRCs (Kozar and Sheludko, 1969; Shalla and Shepard, 1972; Samuels *et al*., 2007).

PVX VRCs are found in epidermal and hair cells of the infected leaves, in mesophyll cells and in the parenchymatous tissue of the veins (Smith, 1957). Electron micrographs show viral replication complexes that contain many of the structural host components of a plant cell, as well as PVX particles (virions) either in a regular stacked form of densely packed virus aggregates at the periphery of the VRC or sometimes distributed randomly throughout the VRC (Kozar and Sheludko, 1969; Shalla and Shepard, 1972; Tilsner *et al*., 2009). The association of PVX VRCs with cellular organelles (endoplasmic reticulum (ER), Golgi, vacuoles, mitochondria) has been identified (Kozar and Sheludko, 1969; Stols *et al*., 1970). Inclusions of virus particles were also identified in

chloroplasts of parenchyma cells of *Datura stramonium* infected with the PVX Xs strain, the most virulent PVX strain, but only at the earliest stages of infection. However, no viral particles were observed in the plastids of plants infected with the two less virulent PVX strains (Xk and Xr) (Kozar and Sheludko, 1969).

In living epidermal cells, the distinctive shape of the PVX VRC is approximately round or oval; however, elongated and more irregular shapes can also occur. There can be more than one VRC of different sizes in the cell. Small VRCs could be found in any position in the cytoplasm of cells infected with PVX and first appear at 4-5 days post-infection. At later stages of the viral infection VRCs mainly occur near the cell nucleus (Fig. 1_8) (Kozar and Sheludko, 1969; Santa Cruz *et al.*, 1996; Tilsner *et al.*, 2009). Mature VRCs are usually up to twice the size of the cell nucleus (Smith, 1957).

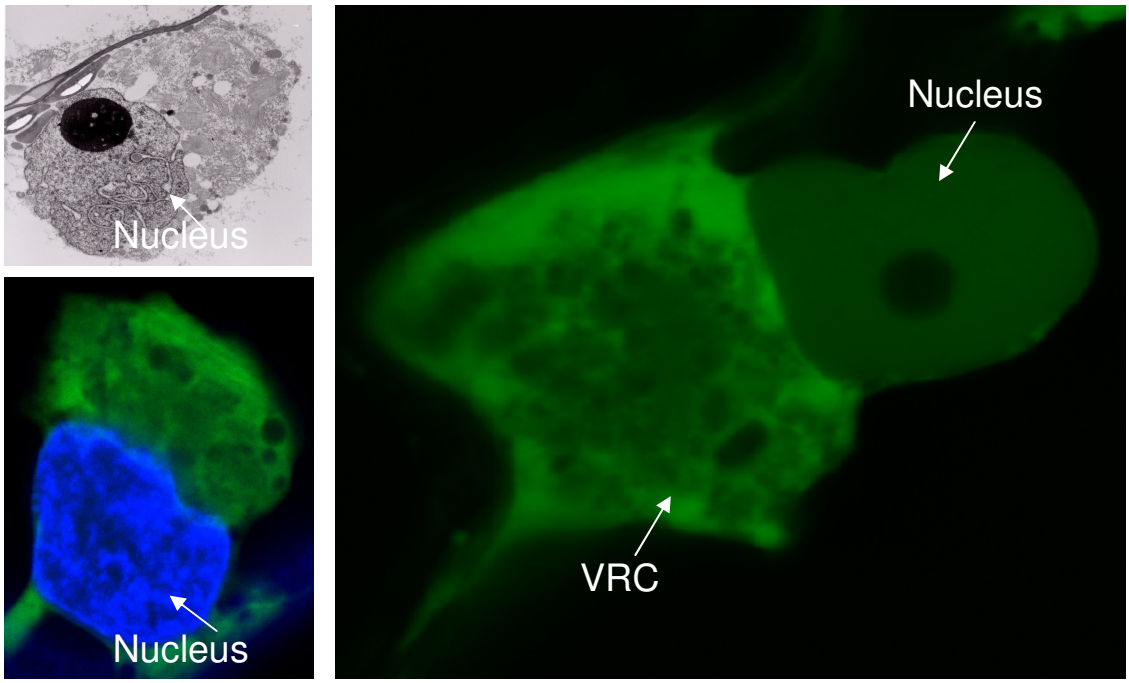

Figure 1_8: PVX VRCs next to the cell nucleus
Top left: Electron micrograph of a cell infected with PVX showing the VRC in close association with the nucleus

Lower left: Confocal image of a cell infected with PVX green construct expressing a GFP-CP fusion (pTXS.GFP-2A-CP) (Santa Cruz *et al*., 1996); VRC is shown in green and is positioned next to the cell nucleus which was stained with 4',6-diamidino-2-phenylindole (DAPI) (shown in blue).
(Left images are adapted from Tilsner *et al*., 2009)
Right image: Confocal image of a cell infected with pTXS.GFP showing a mature PVX VRC closely next to the nucleus in the magnified focus; the vacuoles within the VRC are seen (this thesis work).

1.3.4 PVX movement complex

Encapsidation of vRNA into virions takes place prior to viral transport into neighboring cells. Once the replication complex is ready for movement, vRNA is transported from the site of synthesis to and through PD (Christensen *et al*., 2009).

Several models of PVX RNA movement have been proposed. According to one model, the PVX genome can move either as a viral particle or in a the form of a virion-like ribonucleoprotein (RNP) complex consisting of PVX RNA, CP and TGB1, which is targeted to PD either by itself or via an interaction with TGB2 and TGB3 (Lough *et al*., 1998; Santa Cruz *et al*., 1998; Solovyev *et al*., 2000; Rodionova *et al*., 2003; Karpova *et al*., 2006; reviewed in Verchot-Lubicz *et al*., 2007). This PVX cell-to-cell movement model is based to some extent on the observation that *in vitro*-assembled vRNA-CP-TGB1 complexes move from cell-to-cell in microinjection studies *in vivo* (Lough *et al*., 1998).

In vitro experiments on PVX viral particle assembly discovered single-tailed particles (STPs) consisting of PVX RNA, CP and TGB1 (Lough *et al*., 1998, 2000; Atabekov *et al*., 2000, 2001, 2007; Rodionova *et al*., 2003; Karpova *et al*., 2006). PVX CP was localised at the 5' end of the vRNA. STPs can be formed from the CP and 5' end of the viral RNA in the complete absence of TGB1. However, binding of the TGB1 protein to

CP-vRNA complex and association with the CP subunits at the head of the STPs results in the unwinding of virion particles and in conversion of vRNA into a translatable form. Therefore, these PVX particles are entirely untranslatable without interaction with the TGB1 protein, suggesting that TGB1 NTPase activity is necessary to promote conformational changes in virion structure (Atabekov *et al*., 2000). This process is found to be ATP-independent (Atabekov *et al*., 2000), indicating that TGB1 ATPase functions are not required for the association of TGB1 with the end of the PVX particle (Atabekov *et al*., 2000; Lough *et al*., 2000; Kiselyova *et al*., 2003; Verchot-Lubicz, 2005; Taliansky *et al*., 2008). It was suggested that the virus moves in the form of fully or partially assembled virions containing a single or multiple TGB1 proteins at one end of the virus particles (Atabekov *et al*., 2000; Rodionova *et al*., 2003; Karpova *et al*., 2006).

An indication of the presence of 'unwound' virions during vRNA transport through PD is the detection of fibrillar material in PD infected with green 'overcoat' PVX (Santa-Cruz *et al*., 1996). It is suggested that binding of unwound vRNA-CP-TGB1 transport complex to the TGB2/TGB3 protein complex allows the linearised vRNA to align along the ER network. This structure then targets plant PD probably via the desmotubule (Epel, 2009). However, no interaction between the TGB1 and the TGB2/TGB3 proteins has been detected in two hybrid assays (Samuels *et al*., 2007). It has been proposed that PVX CP is responsible for the formation of movement complexes with vRNA (Lough *et al*., 1998, 2000; Santa Cruz *et al*., 1998; Atabekov *et al*., 2000). However, the precise role of the viral CP in the movement processes of PVX has not yet been identified. The above data support the hypothesis that virus-encoded MPs and cellular components of the host are involved in the trafficking of the movement complex to PD (Lough *et al*., 1998; Morozov and Solovyev, 2003; Verchot-Lubicz, 2005; reviewed in Lucas, 2006; Verchot-Lubicz *et al*., 2007). However, more *in vivo* experimental evidence of this PVX movement hypothesis is necessary.

It has been proposed in another PVX movement model that mobile vesicles induced by the TGB2 and the TGB3 transport complexes release their cargo into the PD (Ju *et al*.,

2008). This model is based on confocal microscopy studies that showed that PVX GFP-TGB2 or GFP-TGB3 were associated with the ER (Solovyev *et al*., 2000; Mirta *et al*., 2003; Ju *et al*., 2005, 2007; Samuels *et al*., 2007). Moreover, mutational analysis has identified that GFP-TGB2-induced granules are crucial for virus cell-to-cell spread (Ju *et al*., 2007). Other viral factors may have an effect on this movement, but not have yet been determined. The exact nature of viral transport complexes is still unclear (Nelson, 2005).

1.3.5 PVX virions and an 'overcoat' virus

PVX virions are long, flexuous filaments which are composed of coat protein subunits (Smith, 1957). The length of *Potexvirus* virions is about 470-580 nm (reviewed in Verchot-Lubicz *et al*., 2007).

The transport form of PVX has been studied extensively (Kikumoto and Matsui, 1961; Kozar and Sheludko, 1969; Santa Cruz *et al*., 1996, 1998). In early work, particles in fibrous masses associated with PVX infection were found within the cell cytoplasm of *Datura stramonium* L. plants (Kikumoto and Matsui, 1961; Kozar and Sheludko, 1969). These particles resembled those of purified PVX particles in their shape and size. Straight, linearly arranged or variously curved/twisted virus particles, free or associated with cellular components of the host plant were observed (Kozar and Sheludko, 1969). Two types of organisation of virus particles were found (Fig. 1_9). One group had individual particles in loose association with each other, surrounded by a membrane. The second group was observed in a compact, dense bundle or cluster, and no membranous organelles were detected around this particle mass (Kikumoto and Matsui, 1961).

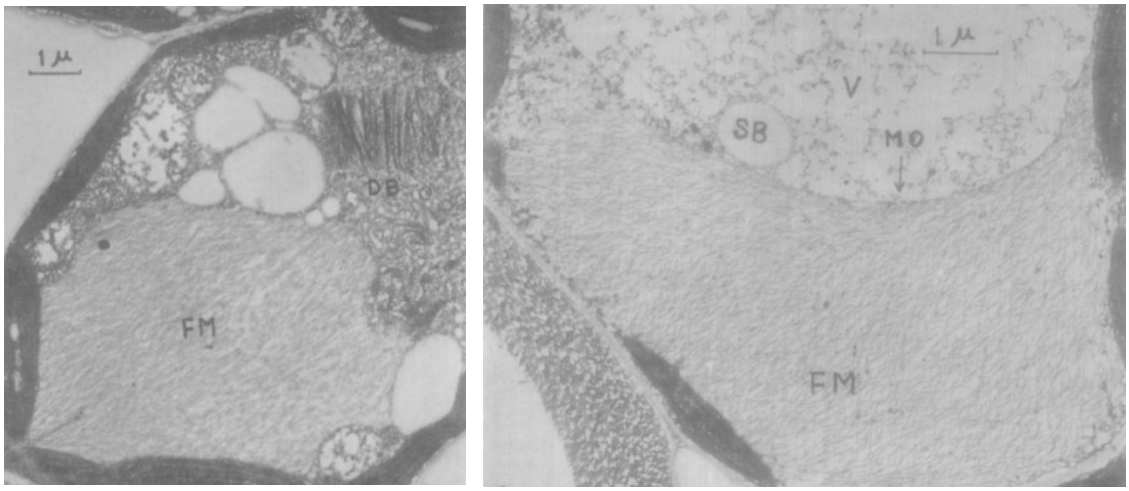

A B

Figure 1_9: A cell of *Datura stramonium* L. plant (Adapted from Kikumoto and Matsui, 1961) containing: A: loosely associated fibrous mass (FM) particles and dense bundles of fibrous particles (DB); B: fibrous mass (FM) surrounded by a membranous organelle (MO); spherical body (SB) was also observed in the PVX-infected plant cell.

PVX has been found to be a beneficial research tool in that its TGB proteins together with its coat protein can be tagged with fluorescent proteins (FPs) for studies of viral infection without affecting the ability of the virus to move both locally and systemically in infected plants. A fluorescent PVX plasmid was constructed by making a modified green fluorescent 'overcoat' virus (pTXS.GFP-2A-CP) by fusing the carboxy-terminus of the 27-kDa GFP to the amino-terminus of the 25-kDa PVX CP gene (Fig. 1_10). PVX GFP fluorescent virions can be then used for studying virus movement in plant cells (Santa Cruz *et al*., 1996).

Figure 1_10: Schematic representation of pTXS.GFP-2A-CP construct (green 'overcoat' PVX)

In work by Santa Cruz *et al*. (1996), it was found that assembly of 'overcoat' PVX into virus particles required the presence of both fused and free CP subunits. In order to supply the virus with mixed pools of fused and unfused CP subunits, a carboxy-terminal 16-amino acid (a.a.) fragment of the 2A peptide from foot-and-mouth-disease virus (FMDV) was inserted between the GFP and N-terminus of the PVX CP gene (GFP-2A-CP fusion) (Santa Cruz *et al*., 1996). 2A 'protease' disrupts formation of peptide bonds during FMDV RNA translation (Lacomme *et al*., 1998). Approximately 50 % cleavage of the viral protein is achieved using this approach, resulting in approximately half of the CP being expressed as free and the other half as a fusion of CP (Lacomme *et al*., 2001).

This 'overcoat' approach allows sub-cellular localisation of PVX virions in plants. In infected plants with pTXS.GFP-2A-CP virus, particles were detected as large, fibrillar aggregates in the cell (Fig. 1_11) (Santa Cruz *et al*., 1996).

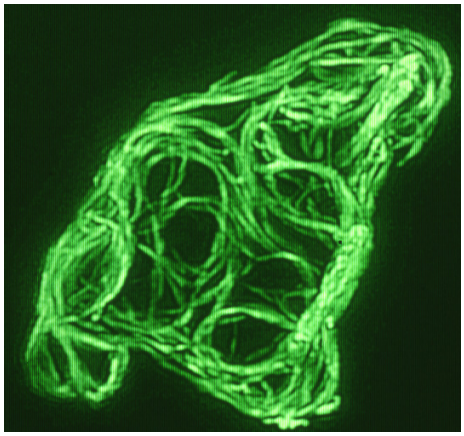

Figure 1_11: Confocal image of pTXS.GFP-2A-CP construct (green 'overcoat' virus) in PVX-infected plant cell

In addition, proteins other than GFP were used for fusions with PVX CP gene. Such fusions were made between PVX CP and chloramphenicol acetyltransferase (26-kDa), PVX CP and neomycin phosphotransferase II (31-kDa). The ability to assemble virions was retained and the function of the protein was not changed. These viruses were able to

move both locally and systemically in plants (Lacomme *et al*., 1998). Thus, generation of the 'overcoat' virus provides a possibility for studying movement of virions in live tissue under the confocal laser scanning microscope (Santa Cruz *et al*., 1996).

1.4 PVX Triple Gene Block (TGB) of Movement Proteins (MPs)

1.4.1 Triple gene block of viral movement proteins

Unlike many other plant viruses (for instance, TMV) which have only one MP gene, the genomes of viruses of *Potex*-, *Beny*-, *Carla-, Fovea*-, *Peclu*-, *Pomo*-, *Hordei*- and *Allexivirus* genera encode three MPs in the overlapping ORFs of a TGB (Fig. 1_12). These are named in order of the positions of their genes in the PVX genome, as TGB1, TGB2 and TGB3, respectively (Skryabin *et al*., 1988; Morozov *et al*., 1989, 1999; Rupasov *et al*., 1989; Koenig *et al*., 1996; Herzog *et al*., 1998; Lough *et al*., 1998; Leisner, 1999; Morozov and Solovyev, 2003). One possible explanation for the overlapping ORFs is that overlaps make it possible to coordinately translate all three ORFs (Davies *et al*., 1993). The positions of the TGB proteins in viruses of different genera can be also different (Morozov *et al*., 1989; Morozov and Solovyev, 1999).

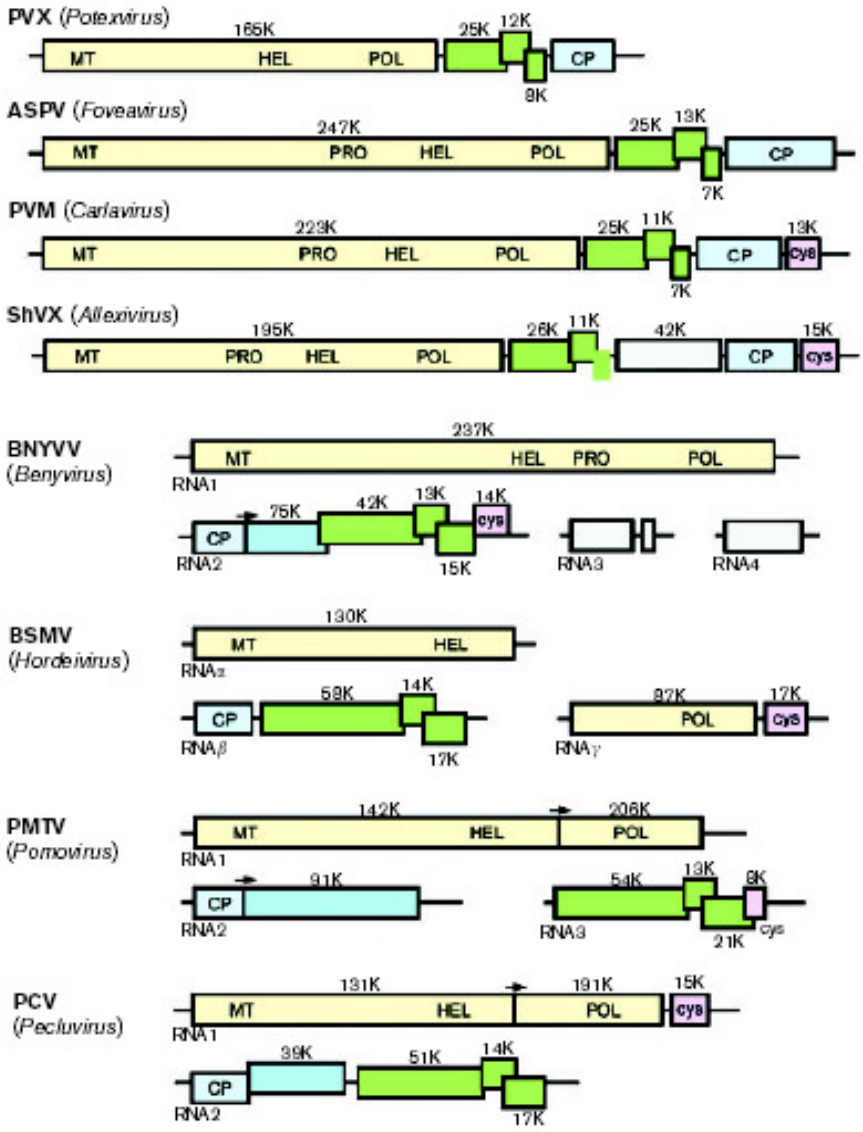

Figure 1_12: Representation of evolutional conservation of the TGB genes of different TGB-containing viruses (Adapted from Morozov and Solovyev, 2003)

Genes are presented as boxes with molecular masses of proteins on top of them. The TGB genes are indicated in green.

MT: methyltransferase; PRO: protease; HEL: helicase; POL: polymerase; CP: coat protein; PVX: Potato virus X; ASPV: Apple stem pitting virus; PVM: Potato virus M; ShVX: Shallot virus X; BNYVV: Beet necrotic yellow vein virus; BSMV: Barley stripe mosaic virus; PMTV: Potato mop-top virus; PCV: Peanut clump virus.

The three PVX TGB proteins are also termed corresponding to their molecular mass, 25K (24548b; TGB1), 12K (12339b; TGB2), and 8K (7623b; TGB3) proteins (Huisman *et al*., 1988). Mutational analysis of the PVX genome showed that all 3 TGBs are required for viral cell-to-cell movement (Huisman *et al*., 1988; reviewed in Koonin and Dolja, 1993; Angell *et al*., 1996; Verchot-Lubicz, 2005). Therefore, it is hypothesised that movement functions that belong to a single MP of TMV are possibly distributed over three TGB proteins in the TGB-carrying viruses (Morozov and Solovyev, 2003). However, the precise function of the triple gene block is not identified. It is likely that these three proteins interact with each other to allow viral intercellular transport, but the nature of these interactions remains poorly understood.

1.4.2 The TGB1 protein

1.4.2.1 TGB1 is a multifunctional protein

The TGB1 ORF is the largest in the PVX genome and codes for a MP of 25-kDa. TGB1 is a multifunctional protein with a number of biological activities. It contains an NTPase/helicase domain (reviewed in Koonin and Dolja, 1993; Morozov and Solovyev, 2003) and possesses ATP/GTPase and RNA-binding activities *in vitro* (Skryabin *et al*., 1988; Gorbalenya and Koonin, 1989; Kalinina *et al*., 1996, 2002; Lough *et al*., 1998; Morozov *et al*., 1999). PVX TGB1 protein, like the TGB1 protein of white clover mosaic virus, induces PD gating by increasing the SEL to enable transfer of virus and other molecules between plant cells, TGB1 moves intercellularly on its own, independently of other PVX-encoded MPs (TGB2, TGB3 and CP) and forms VRCs in neighbouring infected cells (Angell *et al*., 1996; Lough *et al*., 1998, 2000; Yang *et al*., 2000; Howard *et al*., 2004). However, PVX GFP-TGB1 protein did not move cell-to-cell in transgenic tobacco expressing the combined TGB2/TGB3 genes or the CP gene, indicating that intercellular trafficking of TGB1 is inhibited in the presence of other PVX-encoded genes. These data also indicate that non-cell autonomous TGB1 movement can take place early in PVX infection cycle before there is significant amount

of the TGB2 and TGB3 proteins produced in the cell (Yang *et al*., 2000). It was found that PVX TGB1 is cotranslated with the viral gRNA and the viral CP during virus movement (Nelson, 2005).

PVX TGB1 is also a suppressor of RNA silencing and allows virus cell-to-cell movement and systemic infection by inhibiting production or activity of the mobile RNA silencing signal and suppressing RNA silencing-mediated degradation of vRNA. The RNA silencing response from the plant is a protection mechanism against RNA viruses (Voinnet *et al*., 2000; Carrington *et al*., 2001; Baulcombe, 2002; reviewed in Scholthof, 2005).

In addition, TGB1 by itself or in combination with other virus-encoded proteins has an important role in symptom formation in diseased plants. Typical PVX infection symptoms were induced in transgenic TGB1 plants. TGB1 expression caused physiological changes in transgenic plants, including atypical chloroplast functioning and altered metabolite contents. In contrast, tobacco plants transformed with the other PVX-encoded proteins (TGB2, TGB3, viral replicase and CP) showed a normal phenotype compared to control plants (Kobayashi *et al*., 2004).

1.4.2.2 Subcellular localisation and immunogold labeling of the TGB1 protein

Association of PVX TGB1 with cytoplasmic laminate inclusion bodies has been detected in work by Davies *et al*. (Fig. 1_13). It was suggested that this was one of several sub-cellular localisations of TGB1 and represented one of the examples of compartmentalisation of the PVX infection components (Davies *et al*., 1993).

Figure 1_13: Immunogold labelling with anti-TGB1 antibody of systemically infected PVX tobacco leaves at 9 days post-inoculation (Adapted from Davies *et al*., 1993).
The viral replication complex and the TGB1 viral protein in association with the centre are displayed. W: the cell wall; v: aggregates of PVX particles.

In addition, the authors in some cases detected the cytoplasmic inclusion bodies in the cell nucleus (Fig. 1_14).

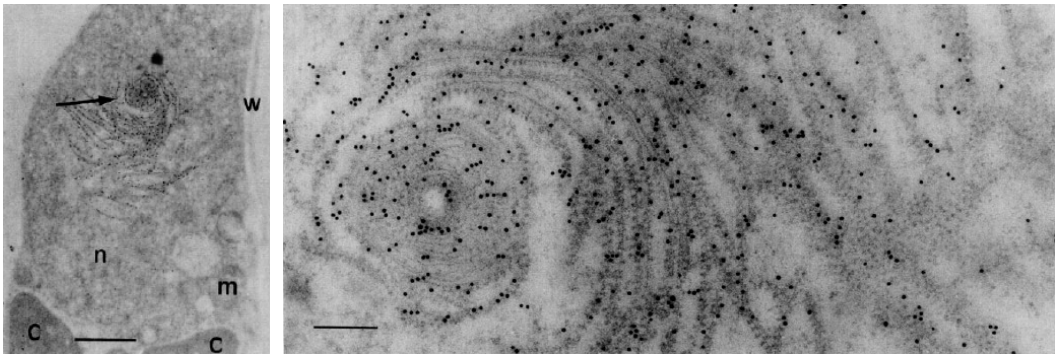

Figure 1_14: Immunogold labelling of TGB1 of the inclusion structures in a PVX-infected cell nucleus at 9 days post-inoculation (Adapted from Davies *et al*., 1993).
N: nucleus; c: chloroplasts; m: mitochondria; w: cell wall.
Right image: a higher magnification area of the arrowed region in the left image. Bars, 1 μm (left image) and 200 nm (right image).

In earlier work, Stols *et al*. (1970) and Shalla and Shepard (1972) found that the laminate inclusion bodies in the cytoplasm of the PVX-infected cells consisted of beaded (Stols *et al*., 1970; Shalla and Shepard, 1972) or smooth sheets in approximately 3 nm wide layers (Shalla and Shepard, 1972). The sheets resembled rough ER but were thinner and destroyed when treated with potassium permanganate, indicating that they were non-membranous structures. The beads were located on both surfaces of the sheets and were morphologically similar to cytoplasmic ribosomes but were usually 11-14 nm in diameter (in contrast, ribosomes are 17-20 nm). The 'beaded sheets' were tightly packed in several layers and contained proteins. No lipids were identified in them. The 'beaded sheets' either contained (Stols *et al*., 1970; Shalla and Shepard, 1972) (Fig. 1_15.5) or did not contain virus particles (Fig. 1_15.4) within their layers. Smooth sheets frequently had virus particles between the sheets (Fig. 1_15.6) (Shalla and Shepard, 1972).

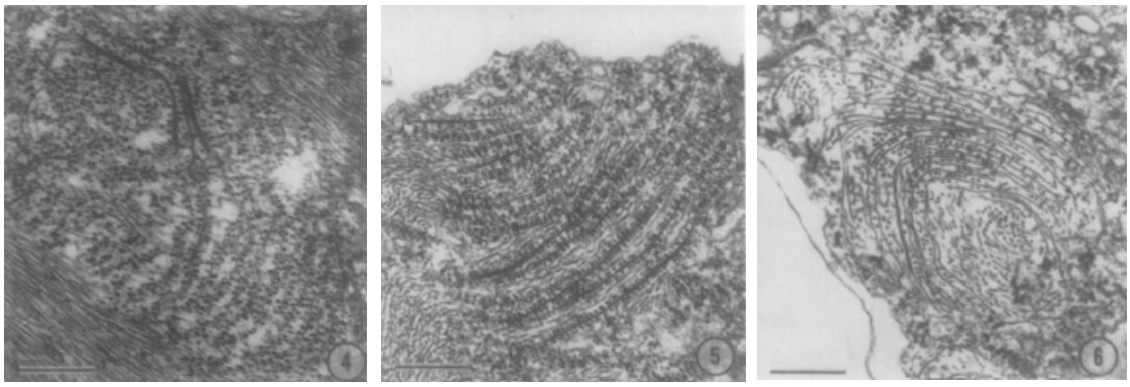

Figure 1_15: Electron micrographs of beads and sheets present in PVX inclusion bodies (Adapted from Shalla and Shepard, 1972)
4: layers of rolled 'beaded sheets' without virus particles; 5: 'beaded sheets' with virus particles between layers of sheets; 6: smooth sheets with virus particles between layers of sheets. Bars, 250 nm.

Due to the fact that these structures were discovered to contain ribosomes (Stols *et al*., 1970), it was considered that the 'beaded sheets' could be sites of active viral protein

synthesis during viral replication process (viral 'factories') (Kozar and Sheludko, 1969; Shalla and Shepard, 1972). However, it was not possible to distinguish whether TGB1 was associated with the beads or with the sheets (Davies *et al*., 1993). Moreover, the biological role of the 'beaded sheets' was not identified and remains to be investigated. Surprisingly, recent work on TGB1 does not refer to the earlier literature described above and does not mention the location of the TGB1 protein within the 'beaded sheet'-like structures in the VRC.

In Samuels *et al*. (2007) work on subcellular localisation of the TGB1 protein, a GFP-TGB1 fusion protein was found in the cell nucleus, cytoplasm, in inclusion bodies, and in the cell wall in PD (Fig. 1_16), suggesting the existence of different localisation patterns of TGB1 in the cell (Samuels *et al*., 2007), similar to Davies *et al*. (1993) findings (Davies *et al*., 1993). However, Davies *et al*. did not detected TGB1 localisation in the cell PD. It is possible that the immunogold labelling method used was unable to detect this localisation of TGB1 (Davies *et al*., 1993). In Samuels *et al*. (2007) data TGB1 often formed elongated rod-like structures in perinuclear inclusion bodies, usually overlapping with each other (Samuels *et al*., 2007).

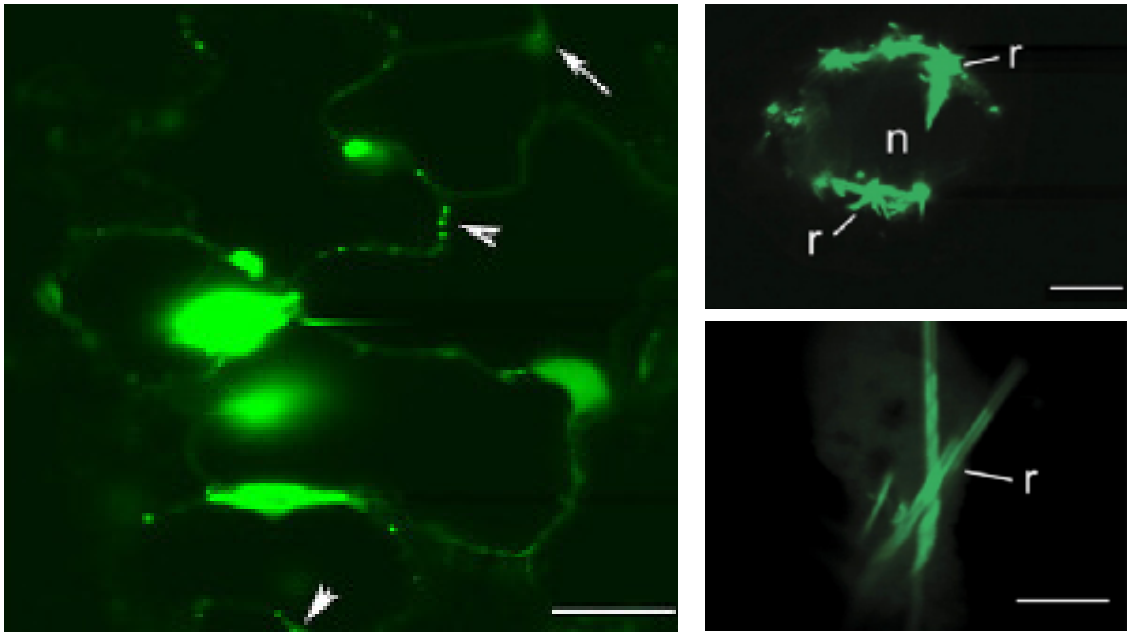

Figure 1_16: Confocal images of plants inoculated with PVX.GFP-TGB1 (Adapted from Samuels *et al*., 2007)
White arrow points to the nucleus; arrowheads point to fluorescent spots of TGB1 in the cell wall (very likely inside PD); n: nucleus; r: rod-like structures.
Bars, 40 μm in the left image; 10 μm in two right images.

1.4.3 TGB2 and TGB3 proteins

1.4.3.1 Molecular organisation of TGB2 and TGB3 proteins and their conservation

The two smaller viral-encoded proteins, TGB2 (12K) and TGB3 (8K), are ER membrane-associated proteins and have been studied extensively (Morozov *et al*., 1989; Hefferon *et al*., 1997; Solovyev *et al*., 2000; Zamyatnin *et al*., 2002; Morozov and Solovyev, 2003).

These PVX proteins have hydrophobic sequences (transmembrane domains) for insertion of these proteins into cellular membranes (Morozov *et al*., 1987, 1989). TGB2

sequence is conserved among all TGB-containing viruses (reviewed in Lucus, 2006). As a result of amino acid sequence analysis in the TGB2 protein, three domains of PVX TGB2 were identified. TGB2 contain two predicted transmembrane segments. Solovyev *et al*. (1996) predicted that these two domains allow the protein to take a U-shaped transmembrane orientation in which N- and C- termini of the domain are predicted to face towards the cytoplasm (Solovyev *et al*., 1996, 2000; Zamyatnin *et al*., 2002). The central domain of TGB2 is located between two transmembrane domains of the protein and is found to localise in the ER lumen (Morozov and Solovyev, 2003). This domain has a segment which is highly evolutionary conserved among the TGB proteins (positions 40 and 64) (Morozov *et al*., 1987; Skryabin *et al*., 1988). Mutations in the conserved residues of the central domain of PVX TGB2 protein affected membrane binding, abolished association of the TGB2 protein with granular vesicles and inhibited virus cell-to-cell trafficking, indicating that the central domain is critical for TGB2-induced formation of granules, and that association of TGB2 with ER membrane and formation of granular-type vesicles is a necessary requirement for PVX movement (Mitra *et al*., 2003; Ju *et al*., 2005, 2007).

Unlike TGB2, which is highly conserved among different TGB-containing viruses, TGB3 proteins of different viruses can have one or two hydrophobic domains (Morozov *et al*., 1991). TGB3 of PVX and other filamentous viruses of *Potex*- (PVX), *Allexi*-, *Carla*- and *Foveavirus* genera is predicted to have two structural domains: one 23-a.a. long N-terminal segment predicted to form a transmembrane hydrophobic domain of PVX TGB3 (potentially in ER lumen), and one 45-a.a. long C-terminal hydrophilic (cytosolic) segment which contains a motif conserved among viruses of the *Flexiviridae* family (Morozov *et al*., 1991; Zamyatnin *et al*., 2002; Krishnamurthy *et al*., 2003; Mitra *et al*., 2003; Morozov and Solovyev, 2003; Adams *et al*., 2004). Mutations in the N-terminal transmembrane domain of PVX TGB3 abolished its association with the ER and affected virus spread from cell-to-cell, indicating that the transmembrane domain is important for PVX movement (Lough *et al*., 2000, Ju *et al*., 2008). A mutation in the transmembrane domain of TGB3 also caused the protein to localise to the cell nucleus,

suggesting that nuclear accumulation of TGB3 is controlled by interactions of this protein with the host ER (Ju *et al*., 2008). It was suggested that the TGB3 hydrophobic segment is required for interaction with cell membranes (Morozov *et al*., 1991; Krishnamurthy *et al*., 2003). Partial and even complete deletion of the C-terminal hydrophilic region of the TGB3 protein did not eliminate its subcellular localisation and did not block the capacity of the mutant virus to move in complementation studies, suggesting that the TGB3 protein functions are mainly associated with its transmembrane hydrophobic sequence (Schepetilnikov *et al*., 2005). Schematic representation of molecular organisation of TGB2 and TGB3 proteins are shown in the Fig. 1_17.

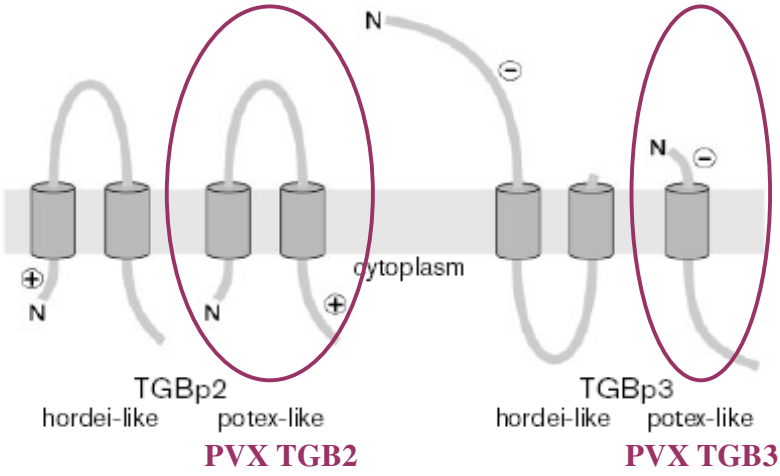

Figure 1_17: Molecular organisation of TGB2 and TGB3 proteins of *Hordei*-like and *Potex*-like (PVX) viruses showing predicted topology of these molecules in the cell membrane (Adapted from Morozov and Solovyev, 2003).
Cylinders: predicted N-terminal transmembrane domains; '+' and '-': the net charge of the C-terminal hydrophilic segment of these proteins.

1.4.3.2 Subcellular localisation of TGB2 and TGB3 proteins

1.4.3.2.1 PVX TGB2 associates with the ER, ER-derived vesicles, but not with Golgi bodies

PVX GFP-TGB2 was found to associate with the ER and ER-derived granular vesicles in the absence of virus in the cell (Ju *et al*., 2007). PVX TGB2 protein induces mobile granular vesicles in early PVX infection. Ribosomes were found in these vesicles (Ju *et al*., 2005). Later during viral infection an increase in cytosolic and nuclear fluorescence has been observed. At the centre of a PVX infection site, GFP-TGB2 is localised both in the ER network and in the ER-derived vesicles that move along the actin cytoskeleton (Fig. 1_18 C), and in perinuclear PVX VRCs (Ju *et al*., 2005; reviewed in Verchot-Lubicz *et al*., 2007). In addition, ER localisation of the TGB2 protein was found to be affected by latrunculin B treatment (Mirta *et al*., 2003). At the leading edge of PVX infection, the GFP-TGB2 signal was identified mainly in the VRCs and the granular vesicles (Fig. 1_18 B). GFP-TGB2 did not colocalise with Golgi bodies (Fig. 1_18 D) (Ju *et al*., 2005, 2007) and was not affected by treatment with brefeldin A, an inhibitor of transport from the ER network to the Golgi apparatus (Mitra *et al*., 2003).

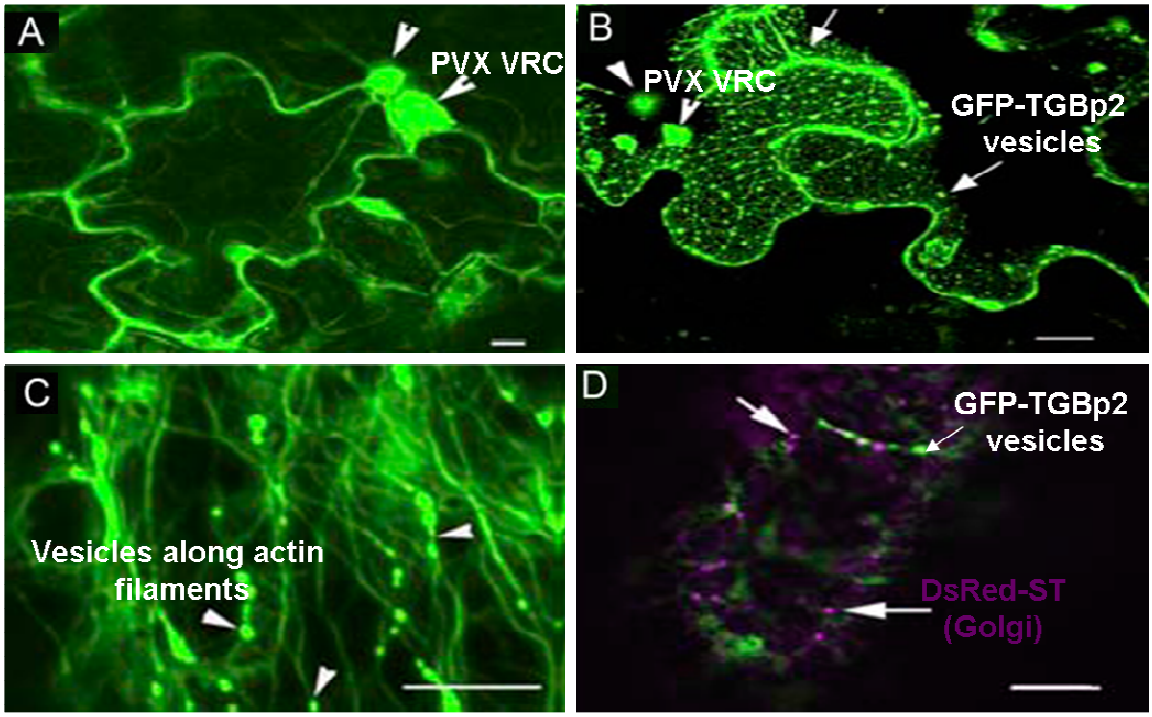

Figure 1_18: Tobacco epidermal cells located at the front (leading edge) of PVX infection (Adapted from Ju *et al*., 2005)

A: PVX.GFP-infected cells at 6 days post-inoculation show green fluorescence in nucleus and in PVX perinuclear VRCs; arrowheads point to both structures;

B: PVX.GFP-TGB2-infected cells at 4 days post-inoculation; arrowheads point to VRCs and arrows position to vesicles;

C: GFP-TGB2 and GFP-Talin-expressing cells (actin marker); arrows point to vesicles along the actin filaments;

D: GFP-TGB2 and DsRed-ST (sialyl-transferase)-expressing cells (Golgi marker); the GFP-TGB2 vesicles (arrowhead) do not colocalise with the DsRed-ST (arrows).

Bars in A,B images represent 20 µm; bars in C,D images represent 10 µm.

1.4.3.2.2 PVX TGB3 associates with the ER, ER-derived vesicles, but not with the Golgi bodies

In the absence of viral infection, PVX TGB3-GFP is found in the cortical ER and nuclear envelope. In the presence of virus infection, TGB3-GFP (when co-expressed with PVX) is, like TGB2, found mainly in the ER network and in the granular vesicles, and perinuclear aggregates associated with the ER (Zamyatnin *et al*., 2002; Krishnamurthy *et al*., 2003; Ju *et al*., 2005, 2007, 2008; Schepetilnikov *et al*., 2005; Samuels *et al*., 2007). PVX TGB3 is also found in the nucleus and nucleoplasm, suggesting that at some stages of virus infection there might be entry to the cell nucleus. However, the nuclear targeting domain has not been identified during mutational analysis of the TGB3 protein. Mutations which eliminated TGB3 association with the ER and affected virus movement did not influence TGB3-GFP localisation in the nucleoplasm. On the basis of fluorescence recovery after photobleaching (FRAP) experiments, it was suggested that TGB3-GFP is either dislocated from the ER and accumulates in the nucleoplasm or is directly transported to the nucleus independently of its accumulation at the ER early in PVX infection. However, further analysis of the TGB3 movement between the ER and nucleus is needed (Ju *et al*., 2008).

Like TGB2, the TGB3 protein was also not found to colocalise with Golgi (Samuels *et al*., 2007). Interestingly, when TGB2 and TGB3 were cobombarded together, localisation of the TGB2 protein was redirected to peripheral bodies in the cell (Fig. 1_19) (Solovyev *et al*., 2000; Schepetilnikov *et al*., 2005).

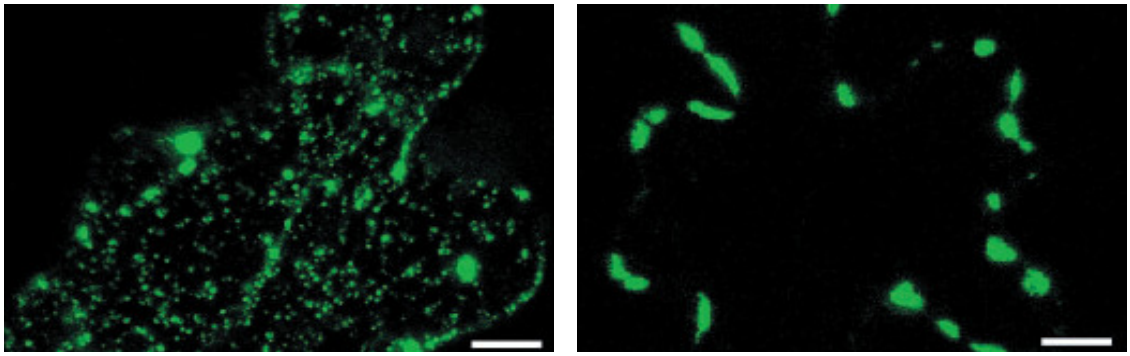

A B

Figure 1_19: Subcellular localisation of bombarded plasmids containing TGB2 and TGB2/TGB3 co-expressed together in *N. benthamiana* leaves (Adapted from Solovyev *et al*., 2000).

A: pRT.GFP-TGB2; B: pRT.GFP-TGB2 + pRT.TGB3. Bars, 10 µm.

The fact that both TGB2 and TGB3 proteins were found in the ER, in granular vesicles, and perinuclear bodies indicates that these two viral proteins act together and have the same subdomains for interaction with the host endomembrane system (Samuels *et al*., 2007). In some studies it was shown that TGB2 and TGB3 can colocalise together in the ER and in the ER-associated vesicles induced by these proteins (Zamyatnin *et al*., 2002; Schepetilnikov *et al*., 2005; Samuels *et al*., 2007). However, there is no experimental evidence as to whether the TGB2/TGB3-related vesicles contain vRNA/CP/TGB1 complex or virions/STPs. It is also yet unclear if TGB2 and TGB3-induced vesicles can traffic from cell-to-cell (Verchot-Lubicz *et al*., 2006). Also, these two proteins have not yet been shown to contribute to the viral replication process (Schepetilnikov *et al*., 2005).

1.5 Plant cell endomembrane system and cytoskeleton

1.5.1 Plant cell endomembrane system

All plant cells are surrounded by a membrane, which divides the cell cytoplasm from the outside environment. The plasma membrane consists of a bilayer of phospholipids with

proteins attached to it and it possesses differential permeability capacity allowing only certain compounds to get into plant cells (Matthews, 1992). Cell organelles are either connected with each other directly or through functional properties, for instance, through the exchange of transport materials (Cheung and de Vries, 2008).

In eukaryotic plant cells the organelles of the endomembrane system include the endoplasmic reticulum, the Golgi apparatus, the nuclear envelope, the plasma membrane, lysosomes, vacuoles and vesicles. The membranes of mitochondria and chloroplasts are not included in the endomembrane system of the cell (Cheung and de Vries, 2008). This introduction will focus on the plant ER, Golgi apparatus and actin cytoskeleton.

1.5.1.1 The ER and the Golgi apparatus

The ER is found in all eukaryotic cells. The ER branches into the cell cytoplasm and takes up to 10 % of the whole plant cell volume. Plant ER forms a mobile network, which consists of sheets (cisternal ER) and branching tubules (tubular ER). Rough ER is so named due to the fact that its surface is covered with ribosomes. Smooth ER does not have ribosomes on its surface (Hepler *et al*., 1990; Vitale and Denecke, 1999). The ER contains different functional domains. At least 16 types of ER domains have been described. As in animal cells, plant ER is continuous with an outer membrane of the nuclear envelope. The outer nuclear membrane is a main microtubule organising centre (MTOC) in plant cells (Staehelin, 1997). The main function of the ER is the synthesis, processing and transport of molecules (proteins and lipids) to cell organelles and the cell exterior. Transitional ER contains ER exit sites from which transport vesicles carrying newly synthesised molecules are taken to the Golgi apparatus (Vitale and Denecke, 1999). The Golgi is connected with the cortical ER network (Fig. 1_20) on its *cis*-face, where molecules enter the Golgi apparatus, while the *trans*-Golgi (where the molecules exit the Golgi stack) is located at the opposite face of the Golgi (reviewed in Neumann *et al*., 2003; DaSilva *et al*., 2004).

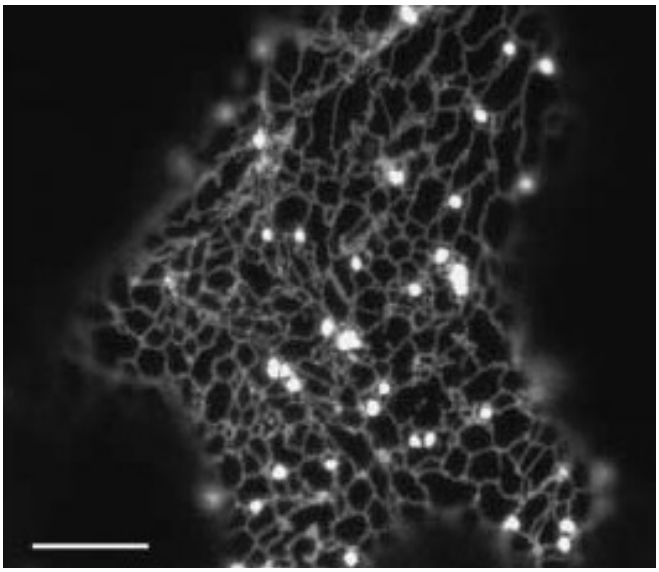

Figure 1_20: Golgi bodies (fluorescent 'blobs') on the cortical ER network (Adapted from Hawes, 2005). Bar, 10 μm.

In contrast to the ER, the Golgi apparatus has dramatic differences in its morphology and behavior between plant and animal cells (Nebenführ *et al*., 1999). Unlike animal Golgi, the higher plant Golgi apparatus (also known as the Golgi complex or the Golgi body) is composed of several organised biosynthetic subunits forming individual stacks of membrane cisternae which are considered to be functionally independent (Staehelin and Moore, 1995). The plant Golgi apparatus is highly mobile and its individual stacks move over the cortical ER network along actin filaments (Boevink *et al*., 1998; Nebenführ *et al*., 1999; Brandizzi *et al*., 2002). In animal cells, the Golgi complex is found in a fairly stationary perinuclear location (Presley *et al*., 1997). In addition, communication between the ER and the Golgi in mammalian cells is dependent on microtubules and cytoskeleton-associated proteins such as dynein and kinesin (Roghi and Allan, 1999; reviewed in Andreeva *et al*., 2000; Sain-Jore *et al*., 2002).

The Golgi is a multifunctional organelle. It receives and modifies protein-containing vesicles from the ER for the packaging of the molecules into transport vesicles for navigation to the correct cell destination. Apart from the processing cargo from the ER, Golgi also synthesises and exports oligo- and polysaccharides and glycolipids (reviewed in Hawes, 2005). Interestingly, not all secretory proteins are passed through the Golgi. Hara-Nishimura *et al*. (1998) and Toyooka *et al*. (2000) suggest that the Golgi may be by-passed and the cargo transported directly from the ER to storage vacuoles (Hara-Nishimura *et al*., 1998; Toyooka *et al*., 2000).

1.5.1.2 Structural association of the ER and the Golgi apparatus with the actin cytoskeleton in plants

On the whole, the plant Golgi apparatus is highly motile and its individual stacks move over the tubules of the cortical ER network on actin filaments (Fig. 1_21). This movement is possibly driven by a myosin motor (Boevink *et al*., 1998; Nebenführ *et al*., 1999; Brandizzi *et al*., 2002).

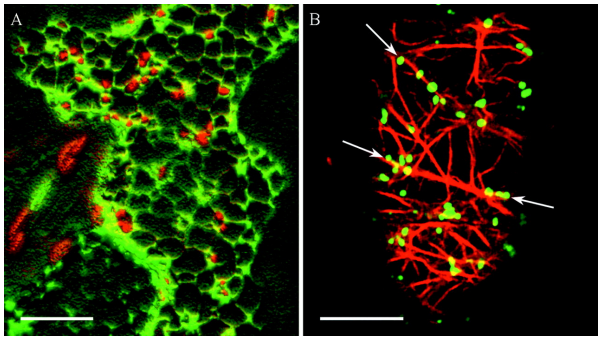

Figure 1_21: Golgi bodies on ER network and actin cables (Adapted from Neumann *et al*., 2003).
Confocal laser scanning images of a tobacco leaf epidermal cell (A) and tobacco BY-2 cell (B) A: Golgi stacks (ST-YFP) in red and cortical ER in green; B: Golgi stacks (ST-GFP) in green and actin filaments (rhodamine-phalloidine labelling of actin) in red; arrows point to the Golgi bodies. Bars, 10 µm.

1.5.2 Plasmodesmata, plant cell endomembrane system and cytoskeleton

Actin microfilaments together with microtubules compose the plant cytoskeleton (reviewed in Takemoto and Hardham, 2004). Microtubules are composed of tubulin and microfilaments are made of actin. F-actin, a primary component of the cytoskeleton, surrounds the cell endomembrane system (Hull, 2002). The plant cytoskeleton is involved in cell growth and development and plays a fundamental role in cell meiosis and mitosis, cytokinesis, cell differentiation and intracellular movement of organelles (Staiger, 2000; Wasteneys and Galway, 2003). In plant cells there is a link between the endomembrane system and the cytoskeleton since the ER is closely associated with actin filaments (cortical ER moves along actin cables) (Allen and Brown, 1988; Quader *et al*., 1987; Boevink *et al*., 1998).

In PD, ER forms the desmotubule (Fig. 1_22), a strand of cortical ER that passes through PD and interconnects the ER of neighbouring cells (Robards and Lucas, 1990; Ding *et al*., 1992a,b; Lucas and Wolf, 1993; Boevink *et al*., 1998; Botha and Cross, 2000; Ehlers and Kollmann, 2001).

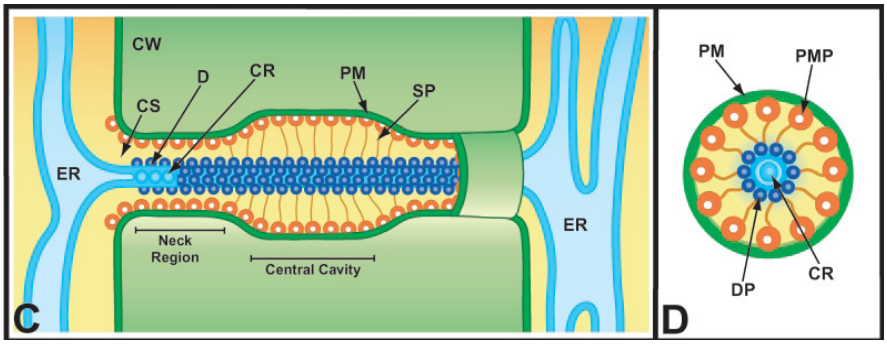

Figure 1_22: Diagrammatic illustration of the substructure of simple plasmodesmata (Adapted from Roberts and Oparka, 2003).
C: PD in longitudinal; D: PD in transverse sections.
ER: endoplasmic reticulum; CW: cell wall; CS: cytoplasmic sleeve; D: desmotubule; CR: central rod; PM: plasma membrane; SP: spoke-like extensions; PMP: plasma membrane-embedded proteins; DP: desmotubule-embedded proteins.

In addition, actin microfilaments are also associated with the plasmodesmal pore (Fig. 1_23) and extend through PD (Blackman and Overall, 1998; White *et al*., 1994).

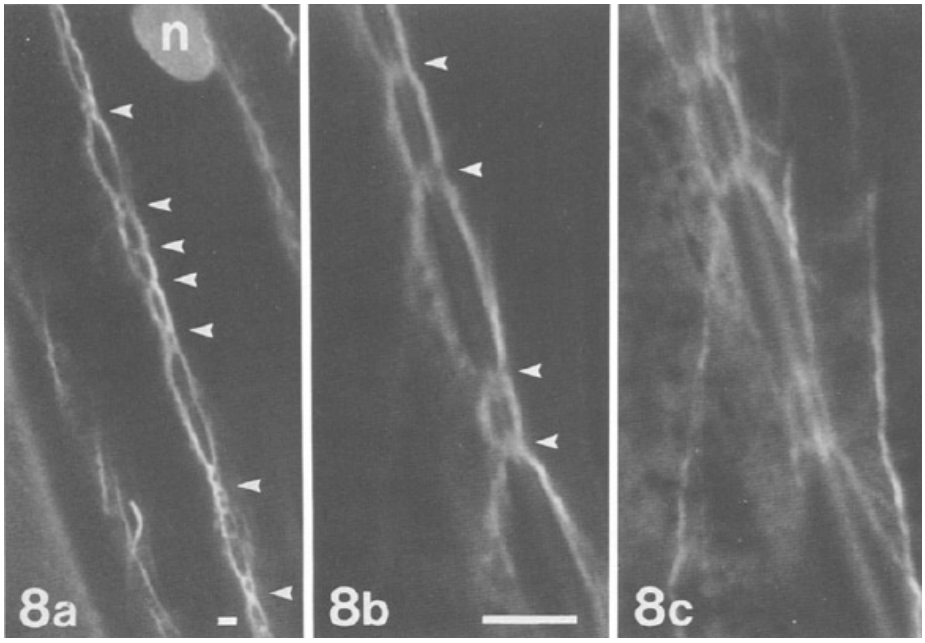

Figure 1_23: Actin is associated with PD (Adapted from White *et al*., 1994)
Confocal laser scanning microscopy of epidermal peels of *H. vulgare* fixed and stained with rhodamine-phalloidin to visualise actin
8a-c: Arrows point to pitfields and show actin microfilaments attached to these pitfields; n: nucleus. Bars, 5 μm.

There are different possible ways of viral transport through PD. It is likely that plant viruses use the cytoplasm between the plasma membrane and desmotubule (cytoplasmic sleeve, CS) for their trafficking to neighboring plant cells (Lucas and Wolf, 1993; Epel, 1994; Kragler *et al*., 1998), possibly assisted by the actin-myosin system of the host (reviewed in Overall and Blackman, 1996). Viral movement is possibly regulated by callose deposition in the cell wall (Maule, 2008), and actin forms a static platform within PD for molecules to move on (White *et al*., 1994).

1.6 Involvement of host organelles in plant virus infection, replication and movement of vRNA

1.6.1 Involvement of host organelles in plant virus infection and replication

Recent data suggests that plant viral replication occurs on specific sites in the cell and these sites are related to the host membrane systems and the plant cytoskeleton (Ploubidou and Way, 2001). It has been reported that distinct types of membranes of different origin can be involved in positive-sense plant and animal RNA virus replication, and the type of host membranes involved depends on the virus (Salonen *et al*., 2005).

This section will provide examples of different host organelles and membrane recruitment (with the focus on the ER and the Golgi apparatus) that is associated with (+)RNA virus replication and movement. The examples of the host membranes associated with plant (+)ssRNA virus replication and spread are listed in the Table 1.1.

Table 1.1: Involvement of the plant organelles in (+)ssRNA virus replication

Membranes derived from:	Virus	Reference
ER/Golgi	AMV	Huang and Zhang (1999)
	BMV	Restrepo-Hartwig and Ahlquist (1996, 1999)
	BYV	Peremyslov *et al*. (1999)
	CPMV	Carette *et al*. (2000)
	GFLV	Ritzenthaler *et al*. (2002)
	PCV	Dunoyer *et al*. (2002)
	PSLV	Zamyatnin *et al*. (2002)
	PVX	Kozar and Sheludko (1969); Stols *et al*. (1970); Hefferon *et al*. (1997); Solovyev *et al*. (2000); Morozov and Solovyev (2003); Schepetilnikov *et al*. (2005); Samuels *et al*. (2007)
	RCNMV	Turner *et al*. (2004)
	TEV	Schaad *et al*. (1997)

	TMV	Esau and Cronshaw (1967); Heinlein *et al*. (1998); Reichel and Beachy (1998); Mas and Beachy (1999)
Nucleus	BYV	Cronshaw *et al*. (1966)
	PEMV	Shikata and Maramorosch (1966); Demler *et al*. (1994)
	PVX	Davies *et al*. (1993); Samuels *et al*. (2007)
	TMV	Goldin (1963); Reddi (1964); Esau and Cronshaw (1967)
Vacuolar membrane	CMV	Hatta and Francki (1981)
	PVX	Kozar and Sheludko (1969); Stols *et al*. (1970)
	TAV	Hatta and Francki (1981)
	TMV	Esau and Cronshaw (1967)
Peroxisome	CymRSV	Russo *et al*. (1983); Lupo *et al*. (1994)
Endosome/lysosome	SFV	Froshauer *et al*. (1988)
Mitochondria	CIRV	Rubino *et al*. (2001); Weber-Lotfi *et al*., 2002)
	PVX	Kozar and Sheludko (1969); Stols *et al*. (1970)
	TRV	Harrison and Roberts (1968)
Chloroplast outer membrane	AMV	de Graaf *at al*. (1993)
	BYV	Leyon (1953); Cronshaw *et al*. (1966)
	ClYMV	Purcifull *et al*. (1966)
	TMV	Zaltlin and Boardman (1958); Matsushita (1965); Esau and Cronshaw (1967); Shalla (1968)
	TYMV	Ralph *et al*. (1966); Hatta *et al*. (1973); Garnier *et al*. (1980, 1986); Prod'homme *et al*. (2001)

AMV – Alfalfa mosaic virus (*Bromoviridae* family)
BMV – Brome mosaic virus (*Bromoviridae* family)
BYV – Beet yellows virus (*Closteroviridae* family)
CIRV – Carnation Italian ringspot virus (*Tombusviridae* family)
ClYMV – Clover yellow mosaic virus (*Flexiviridae* family)
CMV – Cucumber mosaic virus (*Bromoviridae* family)
CPMV – Cowpea mosaic virus (*Comoviridae* family)
CymRSV – Cymbidium ringspot virus (Tombusviridae family)
GFLV – Grapevine fanleaf virus (*Comoviridae* family)
PEMV – Pea enation mosaic virus (*Luteoviridae* family)
PSLV – Poa semilatent virus (*Hordeivirus* genus)
PVC – Peanut clump virus (Furovirus genus)
PVX – Potato virus X (*Flexiviridae* family)
RCNMV – Red clover necrotic mosaic virus (*Tombusviridae* family)
SFV – Semliki forest virus (*Togaviridae* family)
TAV – Tomato aspermy virus (*Bromoviridae* family)
TEV – Tobacco etch virus (*Potyviridae* family)
TMV – Tobacco mosaic virus (*Tobamovirus* genus)

TRV – Tobacco rattle virus (*Tobravirus* genus)
TYMV – Turnip yellow mosaic virus (*Tymoviridae* family)

1.6.1.1 Membranes derived from the ER/Golgi

The membrane for replication of tospoviruses is formed by budding into the Golgi apparatus and takes place in the cytoplasm of the host plant cell (Hull, 2002). A number of plant (+)RNA viruses such as brome mosaic virus (Restrepo-Hartwig and Ahlquist, 1996, 1999; reviewed in Noueiry and Ahlquist, 2003), tobacco etch virus (Schaad *et al*., 1997), TMV (Fig. 1_24) (Esau and Cronshaw, 1967; Heinlein *et al*., 1998; Reichel and Beachy, 1998; Mas and Beachy, 1999), cowpea mosaic virus (CPMV) (Fig. 1_25) (Carette *et al*., 2000), grapevine fanleaf virus (GFLV) (Ritzenthaler *et al*., 2002), peanut clump virus (PCV) (Fig. 1_26) (Dunoyer *et al*., 2002), red clover necrotic mosaic virus (RCNMV) (Turner *et al*., 2004) were shown to use ER-derived membranes for their replication.

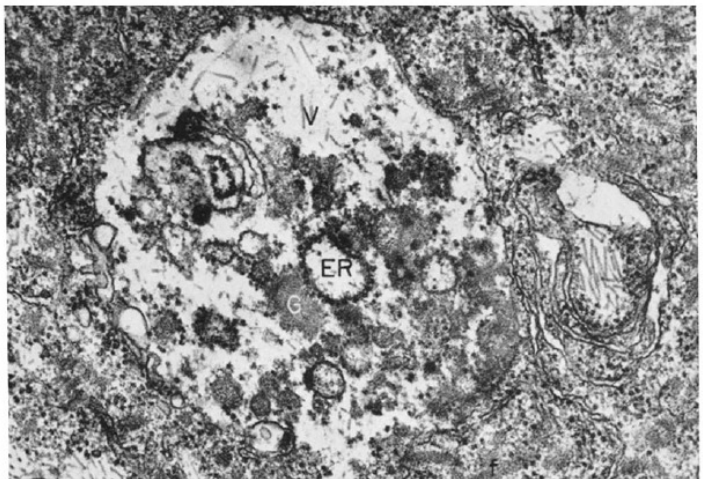

Figure 1_24: Association of TMV with the ER (Adapted from Esau and Cronshaw, 1967)
Electron microscopy (EM) of TMV X-body and its association with cellular components of the host *N. tabacum* plant
V: aggregates of TMV particles; ER: rough ER with ribosomes; G: vacuole containing globules. Magnification: X 52,000.

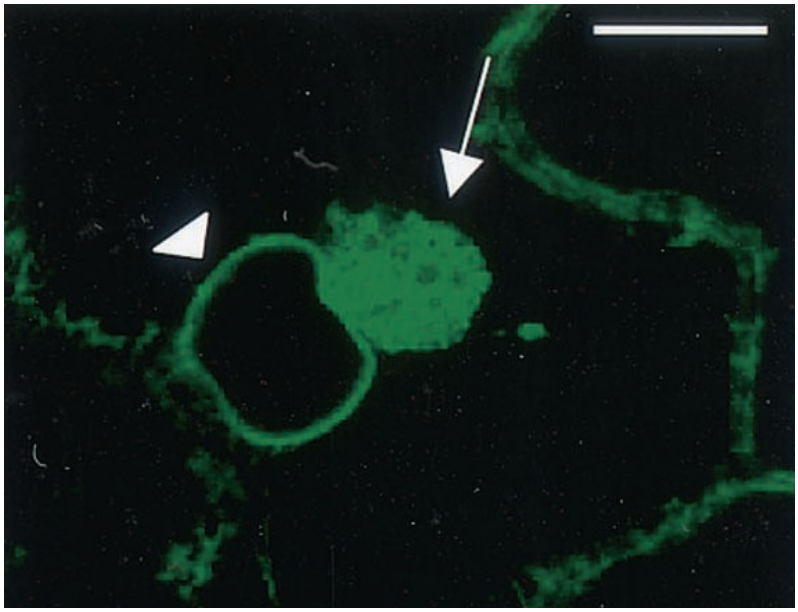

Figure 1_25: Cowpea mosaic virus replication on rearranged ER membranes (Adapted from Carette *et al*., 2000)

Confocal image of *N. benthamiana* transgenic plant with GFP targeted to the lumen of the ER (ER-GFP) infected with CPMV expression vectors to show the effect of expression of different cowpea mosaic virus proteins on ER morphology.

Massive ER proliferation near the nucleus (arrowhead) of a CPMV-infected cell and the CPMV VRC (arrow). Bars, 10 μm.

Replication of peanut clump virus (Fig. 1_26), a member of the *Pecluvirus* genus and the alphavirus-like family, also happens on modified membranes of ER and Golgi apparatus (Dunoyer *et al*., 2002).

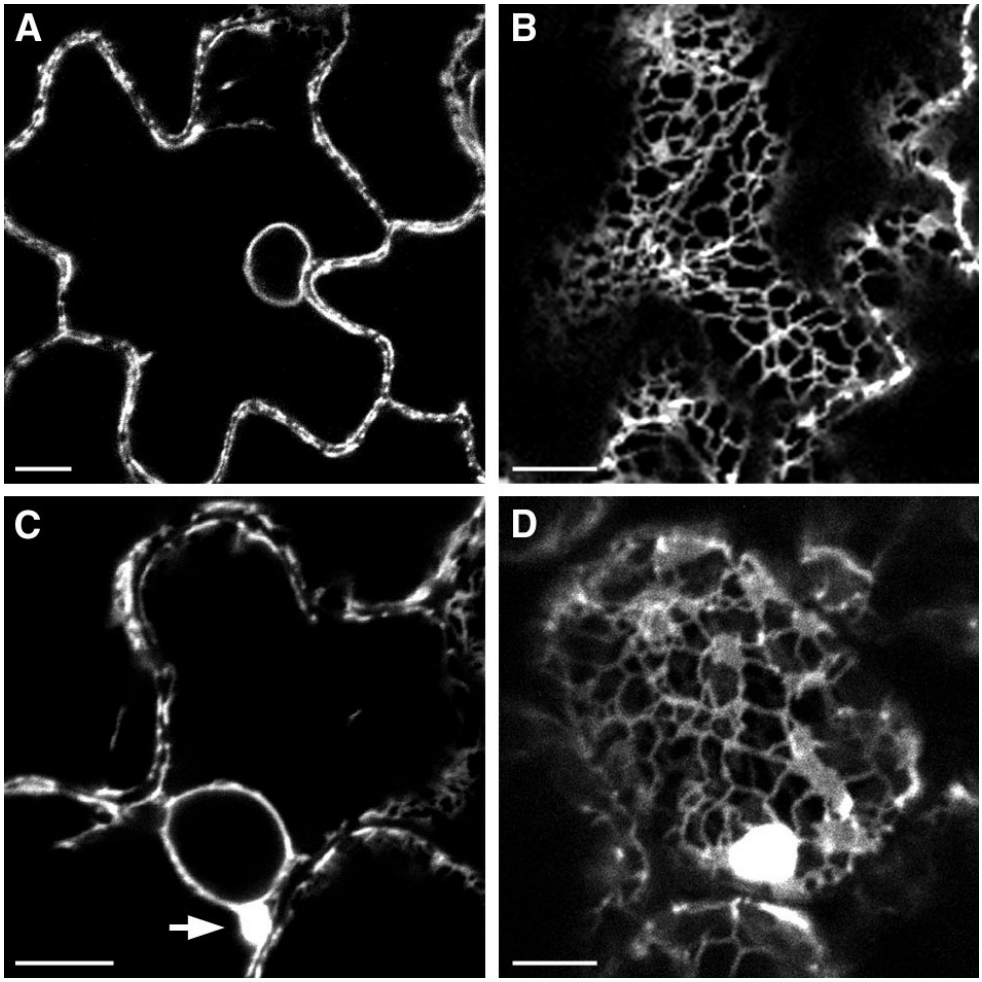

Figure 1_26: Peanut clump virus replication on ER/Golgi membranes (Adapted from Dunoyer *et al*., 2002)

Confocal images of uninfected (A and B) and PCV-infected (C and D) epidermal cells of ER-GFP transgenic *N. benthamiana* plants

A: typical tubular ER network and nuclear envelope in control uninfected plants; B: cortical ER in control uninfected plants; C: perinuclear ER membrane aggregates (arrow) observed in epidermal cells of PCV-infected systemic leaves; D: fluorescent bodies in a cortical ER network in infected cells. Bar, 10 µm.

ER involvement in TMV replication has been studied extensively (Sanfaçon, 2005). Work by Mas and Beachy (1999) found a structural association between vRNA-

replicase complexes, ER membranes and the cytoskeleton (Mas and Beachy, 1999). The labeling of the ER was also found for MPs of beet yellows virus (Peremyslov *et al*., 1999), and alfalfa mosaic virus (Huang and Zhang, 1999), for poa semilatent virus (Solovyev *et al*., 2000; Zamyatnin *et al*., 2002) and for the plant potyvirus replication (Wei and Wang, 2008).

1.6.2 Involvement of the plant cytoskeleton in virus replication and vRNA trafficking

It is shown that some viral MPs (for example, TMV MP and cauliflower mosaic virus P6 protein) interact with the host cytoskeleton systems: with mictrotubules (Heinlein *et al*., 1995) and microfilaments (McLean *et al*., 1995; Boyko *et al*., 2000; Harries *et al*., 2009a). It is very likely that both actin microfilaments and microtubules may act as host elements for vRNA-MP and virion complexes to target PD (Carrington *et al*., 1996; Lazarowitz and Beachy, 1999; Tzfira *et al*., 2000; Heinlein, 2002).

TMV, a single-stranded RNA virus, encodes a 30-kD MP. During TMV infection, this protein binds to vRNA and associates with replicase, ER membranes, microtubules and actin and increases the SEL of PD. It was suggested that TMV MP mediates microtubule-based movement of RNP complexes to and via PD (Wolf *et al*., 1989; Citovsky *et al*., 1992; Heinlein *et al*., 1995, 1998; McLean *et al*., 1995; Reichel and Beachy, 1998; Mas and Beachy, 1999, 2000; Heinlein, 2002; Kawakami *et al*., 2004). There are some contradictory findings for the involvement of actin cytoskeleton in TMV intracellular spread. Some data show that TMV cell-to-cell movement is inhibited by expression of an actin-binding protein (Hofmann *et al*., 2009). Another recent finding showed no influence on TMV spread by latrinculin B applications (Harries *et al*., 2009b). However, the differences in these two results could be due to differences in the experimental approaches, for instance in the duration of inhibitor treatments and in different experimental time-points.

In the work of Kragler *et al*. (2003), MPB2C, a TMV MP-binding protein, was isolated from tobacco and this protein was found to have homologous sequences only in plants. When expressed together, MPB2C colocalised with TMV MP at microtubules but not on the ER. When MPB2C was overexpressed, transport of MP was inhibited, suggesting that a TMV MPB2C is a negative regulator of the TMV transport on microtubules (Kragler *et al*., 2003).

There is also some discussion about the transport of viruses independently of the plant cytoskeleton systems. This theory is supported by the data of Gillespie *et al*. (2002) and Kawakami *et al*. (2004) and includes experiments with a microtubule depolymerisation drug and silencing of the *α*-tubulin gene. Gillespie's data shows that TMV is able to replicate and move in the absence of microtubules (Gillespie *et al*., 2002). Silencing of the *α*-tubulin gene had no major effect on the TMV movement and the MP targeting to PD (Kawakami *et al*., 2004).

MPs of some viruses (for example, tomato spotted wilt virus, cowpea mosaic virus and grapevine fanleaf virus (GFLV)) can form protein tubules. These tubules are needed for the virions to go through PD in infected plant cells (Hull, 1992; Ritzenthaler *et al*., 1995; Storms *et al*., 1995; Lazarowitz and Beachy, 1999; Laporte *et al*., 2003). Interestingly, formation of tubules is inhibited by brefeldin A, a drug that affects protein transport from the ER to the Golgi apparatus and leads to protein accumulation in the ER (Nebenführ *et al*., 2002). However, cytoskeletal inhibitors of actin (cytochalasin D and latrunculin B) did not influence tubule formation or distribution. Application of oryzalin disrupted MP tubule distribution. The authors suggest that tubules of GFLV MP are transported via plant microtubules and propose that the plant secretory pathway has an effect on tubule formation. The authors hypothesise that actin microfilaments are involved in the transport processes if microtubules are depolymerised (Ritzenthaler *et al*., 1995; Lazarowitz and Beachy, 1999; Laporte *et al*., 2003).

1.6.3 Involvement of mammalian host membranes and cytoskeleton in virus infection, replication and movement

Replication of animal viruses has been also shown to occur in close association with cellular membranes of the host (Ploubidou and Way, 2001; Greber and Way, 2006; Radtke *et al*., 2006). The transmembrane domains that are responsible for the anchoring of the virus on host membranes were identified (Echeverri *et al*., 1998; Kusov *et al*., 1998). The replication of togaviruses and coronaviruses takes place on modified membranes of endosomes or lysosomes (Froshauer *et al*., 1988; Peränen *et al*., 1995; Maglianon *et al*., 1998; van der Meer *et al*., 1999). Many animal viruses also use ER as a site of replication (Suhy *et al*., 2000; Mackenzie, 2005). Flavivirus RNA replication has been suggested to take place in vesicles generated from the *trans*-Golgi membranes (Mackenzie *et al*., 1999). Membranes of the ER, the Golgi apparatus, and lysosomes have been identified in the poliovirus-induced vesicles in animal cells (Dales *et al*., 1965; Caliguri and Tamm, 1970; Bienz *et al*., 1987; Schlegel *et al*., 1996). Most of the vesicles induced during viral replication are surrounded by double bilayers of lipids, indicating that it is not just a simple budding process, suggesting a more complex packaging mechanism for vesicle formation (Schlegel *et al*., 1996; Pedersen *et al*., 1999).

Certain animal viruses have been also found to be associated with host cytoskeleton systems during viral entry, replication and translocation within the host mammalian cell (Radtke *et al*., 2006; Lai *et al*., 2008). Viral capsids of herpes simplex virus type 1 and adenovirus type 2 have been found closely associated with microtubules during viral infection. These viruses bind to microtubule-associated motor proteins and utilise host microtubules for movement. Application of a microtubule-depolymerising drug had an effect on intracellular virus transport (Sodeik *et al*., 1997; Suomalainen *et al*., 1999). An interaction of virions with host cell actin has been detected for vaccinia virus, a DNA mammalian virus of the *Poxviridae* family (Cudmore *et al*., 1997; Roper *et al*., 1998). In addition, actin microfilaments and myosin proteins have been shown to be involved in

the transport of endogenous mRNAs within the cell (Sundell and Singer, 1991; Bassel and Singer, 1997). However, little is known about the nature and regulation of animal virus-host cytoskeleton interactions (Stidwill and Greber, 2000).

All in all, the replication of an increasing number of (+)RNA viruses has been discovered to occur on different intracellular membranes of the host plant, and there has been more evidence recently suggesting that plant viral replication and movement complexes could also be related to the plant cytoskeleton (Hull, 2002).

1.7 Current RNA imaging

An increasing number of localised RNA molecules identified over recent years have resulted in a high demand for methods that are suitable to visualise and study RNA dynamics in single cells (reviewed in Neilson and Sharp, 2008). A number of RNA imaging strategies have been designed, ranging from molecular beacons to chemical RNA binding dyes (reviewed in Rodriguez *et al*., 2007). The majority of techniques for viral RNA imaging are based on fluorescence *in situ* hybridisation (Mas and Beachy, 1999; Carette *et al*., 2000) and immunogold EM approaches (Dunoyer *et al*., 2002; Taliansky *et al*., 2003). However, these RNA localisation methods are destructive and do not allow *in vivo* studies of viral RNA dynamics (Tilsner *et al*., 2009).

This section will focus on describing some of the RNA imaging protocols that are most relevant to plant pathogen research to date.

1.7.1 Fluorescent nucleic acid dyes

Fluorescent nucleic acid dyes are another way to label viral genomes. However, the major challenge for their use in plant tissues is their delivery into living plant cells without causing cell death due to toxicity of many fluorescent dyes. Hydrophobic synthetic dyes normally cross the cell barrier passively and easily in animal cell. Getting

the dye in to the plant cell is a challenge due to the hydrophilic cell-wall barrier. Cell-impermeable dyes do not penetrate cellular membranes and require other methods of delivery, for instance, microinjection (reviewed in Jeffrey *et al*., 2008).

There is a broad variety of different nucleic acid dyes, the choice of which depends on the purpose of the experiment and dye properties and characteristics. DAPI (4'-6-diamidino-2-phenylindole; Spence, 2001) is a semi-permanent dye (reviewed in Suzuki *et al*., 2007). This dye forms a blue fluorescent complex when bound to double stranded nucleic acids and therefore it is broadly used for nuclear staining (excitation/emission: 358/461 nm) (reviewed in Kapuscinski, 1995).

When using fluorescent dyes for studies of vRNAs, the dyes have to fulfill a number of requirements, such as their response to RNAs, high detection intensity and low photobleaching level in order to be suitable for successful RNA staining. Brandenburg *et al*. (2007) screened more than 20 RNA-binding dyes available from Molecular Probes (such as acridine orange (AO), RiboGreen, RNA Select, and many different Syto dyes from Syto11-17, 59, 61, 63, 64, 80, 81, 83, 85) for their interaction with poliovirus by the following 5 criteria: 1) membrane permeability of the dye; 2) cytotoxicity; and the requirements for interactivity with the virus, such as 3) dye capacity to bind to the viral RNA to allow single RNA visualisation, 4) absence of interference with RNA incorporation into virions, and 5) virus ability to infect the cells when the dye was applied. As a result of these experiments, the authors identified only one dye, Syto82 (excitation/emission maximum: 541/571 nm), that met all five requirements. Brandenburg *et al*. (2007) used this dye successfully for single poliovirus RNA imaging in living cells. However, rate of photobleaching for Syto82 was high. When applying this dye, extensive photobleaching had to be avoided (Brandenburg *et al*., 2007).

AO is a dual fluorescent nucleic acid dye. This stain is permeable to cell membranes and has green fluorescence with excitation/emission maximum at 500/525 nm when bound to DNA. When this dye associates with RNA, its excitation/emission is shifted towards

the red fluorescence spectrum (460/650 nm), characteristic frame-red signal for AO RNA staining. However, AO is mainly used for staining RNA molecules (Molecular probes web site). Mayor and Diwan (1961) and Mayor and Hill (1961) found that AO dye only interacted with single-stranded nucleic acids by intercalation or possible ionic bonds to the phosphate groups. Weaker van der Waals' forces are probably also involved in the interaction (Mayor and Diwan, 1961; Mayor and Hill, 1961).

In the past AO was broadly used to study viral RNAs of ssRNA viruses, for example, RNA of infectious bursal disease virus (Cho and McDonald, 1980), poliovirus (Mayor and Diwan, 1961) and tobacco mosaic virus (Hirai and Wildman, 1953; Mayor and Diwan, 1961). The authors detected brick red fluorescence when 0.1 % AO was used for staining fixed TMV infected plant hair cells (Hirai and Wildman, 1953). Unlike poliovirus, TMV was discovered to be permeable to AO in the non-fixed condition (Mayor and Diwan, 1961). Hiatt (1960) reported that many viruses (for instance, T3 phage and vaccinia) are also permeable to RNA dyes; however, others (enteroviruses and reoviruses) are totally resistant (Hiatt, 1960).

Mayor and Diwan (1961) performed the so called "vital staining" (Schaffer, 1960; Crowther and Melnick, 1961; Mayor, 1961) in their experiments with TMV, in which they incorporated the dye into forming virions so AO associated with RNA of virus particles. The concentration of the dye (0.01 % AO) in the medium was an important condition in their experiments (Mayor and Diwan, 1961). Schümmelfeder (1958) has shown in experiments on fixed tissue that at high concentration of AO (0.05 %), the change from green to yellow to orange and lastly to red was observed when the pH of the solution was increased. At low concentration of AO (0.01 %) RNA was detected as a red signal (Schümmelfeder, 1958).

In summary, a strong point in using fluorescent nucleic acid dyes is their ability to label RNA molecules in the cells. However, the main problems in fluorescent dye labelling in living cells are no sequence specificity, permeability and toxicity. For instance, even

very low concentration of AO (0.003 %) was found to be extremely toxic to tissue culture cells. AO required fixation of the tissue prior to staining, and therefore was unsuitable for live cell imaging of viral RNAs (Mayor and Diwan, 1961).

1.7.2 New approaches for RNA imaging in living cells

1.7.2.1 Pumilio RNA-binding protein

Ozawa *et al*. (2007) designed an RNA imaging system that allows visualisation of mitochondrial (mtRNA) RNAs in mammalian cells (Ozawa *et al*., 2007) The authors used the RNA-binding Pumilio Homology Domain (PUMHD; Wickens *et al*., 2002) of the human protein Pumilio1 (HsPUM1; a homolog of the *Drosophila melanogaster* Pumilio protein) (Spassov and Jurecic, 2002). HsPUM1 belongs to the Pumilio family (PUF) of RNA-binding proteins. These proteins are unique. The unique conserved PUMHD has a modular structure, consisting of eight imperfect Puf repeats. Each repeat contacts one base of a target RNA molecule creating 8-nt contact sites (Fig. 1_27) (Wang *et al*., 2002). All protein-RNA contacts in each site occur between three amino acid side chains per Puf repeat and the RNA bases, resulting in binding (K_D = 0.05 nM) to its complementary target RNA sequence (Fig. 1_27). Therefore, these characteristics allow the PUMHD to be modified to bind an 8-nt RNA sequence of choice (Cheong and Hall, 2006).

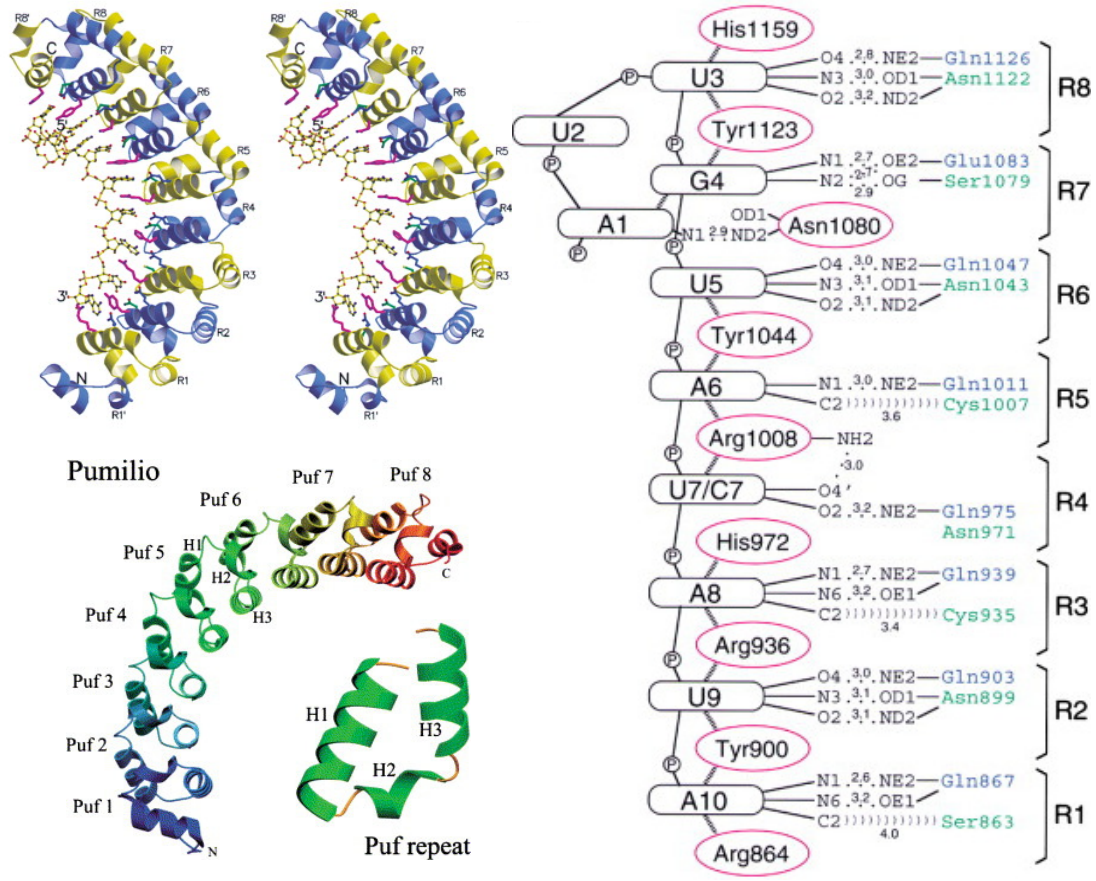

Figure 1_27: Structure of the human HsPUM1 protein (left) and schematic representation of Pumilio protein-target RNA contacts (right) (from Wang *et al*., 2002; Cheong and Hall, 2006; Ozawa *et al*, 2007)

Left: The helical Pumilio protein repeats are labelled R1′ to R8′.

Right: The protein-RNA interactions observed in the structure of the HsPUMHD:NRE2-10 complex.

Hydrogen bonds are shown with dotted lines; stacking interactions are represented with dashed lines; van-der-Waals interactions are indicated with “))))))”; distances between atoms are shown in angstroms under the lines.

Upon binding of two modified PUMHD variants fused to split-FP constructs to the target sites on endogenous mtRNAs in HeLa cells, Ozawa *et al*. visualised mtRNA (Fig. 1_28) (Ozawa *et al*., 2007).

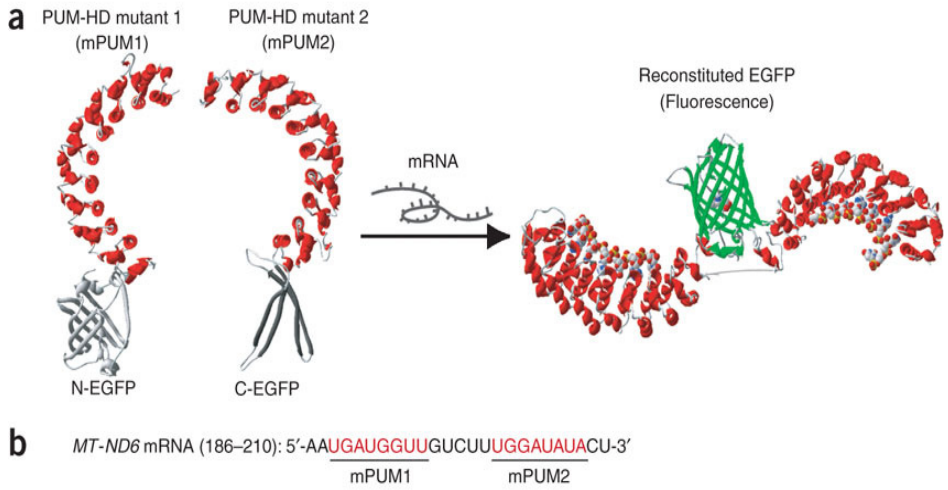

Figure 1_28: Detection of mtRNA molecules by means of the split-FP bimolecular fluorescent complementation (BiFC) approach (Adapted from Ozawa *et al*., 2007)
A: schematic representation of BiFC strategy for mRNA tracking
N-EGFP and C-EGFP: N- and C- terminus of the split-GFP; PUMHD mutant 1 and PUMHD mutant 2: two engineered Pumilio RNA-binding domains for binding to the target RNA sequence.
B: mtRNAs sequences that are recognised by two PUMHD mutant domains.

The difficulties of different RNA labelling methods for viral RNA localisation in living plant cells have been a significant drawback in understanding virus replication and movement in plants. Of specific relevance to this problem is recent work from our lab, in which Dr. Tilsner adapted the Ozawa *et al*. method (Ozawa *et al*., 2007) to study plant viral RNAs, with the focus on their subcellular localisation and movement (Tilsner *et al*. 2009). Tilsner *et al*. (2009) developed a method, in which a Pumilio RNA-binding protein was engineered to interact with the target vRNA in virus-infected living plant

cells (Tilsner *et al*., 2009). This publication is attached in the appendix and will be explained in more details in the corresponding results chapter (see Chapter 5).

1.8 The aims of the project

Despite intense research efforts, the exact mechanism of PVX vRNA transport to and via PD is still poorly understood. The functional significance of PVX VRC, including its biogenesis, structure and the role of viral proteins in vRNA localisation within the VRC remain unclear. Available research data suggests that PVX uses cellular pathways for trafficking its genome; however, there is no clear picture of the molecular details of different stages, including the early stages of viral infection events. The role and involvement of plant host factors during PVX infection remains to be established. To date, it is not known which cellular membrane compartments serve as a centre for PVX replication and movement of viral genomes into adjacent cells. There are several current models of viral cell-to-cell movement with many unanswered questions in these models. The hypothesis of this thesis is that viral movement is dependent on the successful formation of the VRC.

Therefore, the aims of this project are to dissect the PVX VRC in order to:

- analyse the biogenesis and structure of the PVX VRC;

- identify host organelles involved in the formation and establishment of the VRC and to understand their involvement in the viral replication and movement processes;

- explore the localisation of viral proteins in the VRC, their interactions with each other, with vRNA and with the components of the host plant;

- uncover where the viral RNA is located in PVX-infected cells;

- determine which viral gene products recruit host organelles into the VRC;

- establish the link between VRC formation and trafficking of the viral genome to cell PD;

- develop a detailed integrated model of PVX vRNA movement to and through PD.

2. Materials and Methods

2.1 Materials

2.1.1 Plant materials and growth conditions

N. tabacum and *N. benthamiana* plants were grown under the following conditions: 16 h light, 8 h dark (long-day) with the light intensity 1000 µmol m^{-2} sec^{-1} at 25° C (PVX) and at 33° C (TMV).

2.1.1.1 Transgenic plant lines used in this thesis (Table 2.1)

Table 2.1: Transgenic plants

Line #	Transgene	Promoter	Plant host	Source
CB 3	TMV MP-GFP **green secondary PD**	35S	N. tabacum	Roberts *et al*., 2001
CB 13	smRS.GFP-TUA6 **green microtubulin**	35S	N. benth	Ueda *et al*., 1999
CB 28	mGFP5-ER **green ER**	35S	N. benth	Boevink *et al*., 1996
CB 39	ST (sialyl transferase)-GFP **green Golgi**	35S	N. tabacum	Boevink *et al*., 1998
KO 29	FABD2 (fimbrin actin binding domain 2)-GFP **green actin**	35S	N. tabacum	Sheahan *et al*., 2004

2.1.1.2 Plasmids used in this thesis (Table 2.2)

Table 2.2: Constructs and molecular cloning procedures for plasmids constructed and used during this work

Plasmid name	Characte-ristics	Origin
Organelle markers:		
pRTL2-duplicated Cauliflower mosaic virus (CaMV) 35S promoter (*p2x35S*)	3.8 kb; Amp^R	Restrepo *et al*., 1990

pRTL2.ER-tdTomato	5.7 kb; Amp^R; bombardment red ER marker	Dr. Jens Tilsner
pRTL2.Lifeact-tdTomato	5.7 kb; Amp^R; bombardment red actin marker	Dr. Jens Tilsner
pGWB402Ω-*2x35S* promoter and TMV 5' UTR, so-called 'omega sequence' (translational enhancer)	11.7 kb; Spec and Cm^R	Nakagawa *et al*., 2007
pGWB402Ω.Lifeact-TagRFP	12.5 kb; $Spec^R$; binary red actin marker	Dr. Jens Tilsner
PVX-carrying plasmids:		
pGR106	11.1 kb; Kan^R	Jones *et al*., 1999
pGR106.GFP	11.8 kb; Kan^R; binary PVX construct	Prof. David Baulcombe
pGR106.CFP	11.8 kb; Kan^R; binary PVX construct	Dr. Christophe Lacomme
pGR106.mCherry	11.8 kb; Kan^R; binary PVX construct	Dr. Christophe Lacomme
pGR106.pum.CFP	11.8 kb; Kan^R; binary PVX construct	Dr. Christophe Lacomme
pGR106.pum.mCherry	11.8 kb; Kan^R; binary PVX construct	Dr. Christophe Lacomme
pTXS	8.9 kb; Amp^R	Chapman *et al*., 1992
pTXS.CFP	9.6 kb; Amp^R; *in vitro* transcription PVX construct	Dr. Christophe Lacomme
pTXS.GFP-2A-CP	10.4 kb; Amp^R; *in vitro* transcription green 'overcoat' PVX construct	Santa Cruz *et al*., 1996
pRTL2.GFP-2A-CP	11 kb; Amp^R; bombardment green 'overcoat' PVX construct	Dr. Christophe Lacomme
pTXS.mCherry-2A-CP	10.4 kb; Amp^R; *in vitro* transcription PVX construct	Dr. Christophe Lacomme
pTXS.pum.CFP-2A-CP	10.4 kb; Amp^R; *in vitro* transcription	Dr. Christophe Lacomme

	PVX construct	
pTXS.pum.mCherry-2A-CP	10.4 kb; Amp^R; *in vitro* transcription PVX construct	Dr. Christophe Lacomme
	Endogenous PVX TGB1-mCherry:	
pGEMTE.TGB1-mCherry HiFi PCR product (OL29)	4.4 kb; Amp^R	Designed during this thesis by Volha Linnik: The insert was generated from pGR106.mCherry as a template by 2 parallel HiFi PCRs using primer pairs NotI_25K for and Over_25K rev, Over_mCherry for and SacI_mCherry rev to introduce *Not*I site at TGB1 and the *Sac*I site at mCherry. The resulting 2 PCR products were mixed and an overlap HiFi PCR was performed with added primer pairs NotI_25K for and SacI_mCherry rev. The resulting PCR product (an insert) was digested with *Not*I/*Sac*I enzymes and cloned into *Not*I/*Sac*I/CIP-treated OL18 vector (see below). The positive clones were sequenced.
pGR106.TGB1-mCherry HiFi PCR product (OL39)	11.8 kb; Kan^R	Designed during this thesis by Volha Linnik: The insert was generated from pGR106.mCherry as a template by HiFi PCR using primer pairs PmeI_sgp12K for and SacI_AscI rev to introduce the *Pme*I site at the sub-genomic promoter (sgp) of TGB2 and the *Sac*I site at the end of TGB3 next to the *Asc*I site.
pGEMTE.TGB1-mCherry,TGB2,TGB3 (OL40)	5 kb; Amp^R	Designed during this thesis by Volha Linnik: The insert was excised from OL39 (HiFi PCR product) as a *Pme*I/*Sac*I fragment and ligated into *Pme*I/*Sac*I/CIP-treated OL29. The positive clones were sequenced.
pGR106.TGB1-mCherry.GFP (OL41)	12.6 kb; Kan^R	Designed during this thesis by Volha Linnik: The insert (TGB1-mCherry,TGB2,TGB3) was excised from OL40 as an *Apa*I/*Asc*I fragment and ligated into *Apa*I/*Asc*I/CIP-treated pGR106.GFP.
pGR106.TGB1-mCherry.GFP-2A-CP (OL41.2)	12.7 kb; Kan^R	Designed during this thesis by Volha Linnik: The insert GFP-2A-CP was excised from pTXS.GFP-2A-CP as an *Eag*I/Klenow blunted/*Spe*I fragment and ligated into *Asc*I/Klenow blunted/*Spe*I-treated OL41 vector.
pGR106.TGB1-mCherry (OL41.3)	12.7 kb; Kan^R	Designed during this thesis by Volha Linnik: The insert was excited from OL41 vector as an *Asc*I/*Not*I/Klenow fragment and the fragment without GFP was religated.
	Viral gene markers:	
pRTL2.TGB1-mCherry	5.2 kb; Amp^R	Dr. Christophe Lacomme
pRTL2.GFP-TGB2	4.8 kb; Amp^R	Krishnamurthy *et al*., 2002
pRTL2.TGB3-GFP	4.6 kb; Amp^R	Krishnamurthy *et al*., 2002
	PVX mutant constructs:	
pGEMTE.TGBs (OL28)	4.2 kb; Amp^R	Designed during this thesis by Volha Linnik: The insert was generated from pGR106.mCherry as a template by HiFi PCR using primer pairs NotI_25K for and SacI_AscI rev to introduce the *Not*I and the *Sac*I sites. The resulting PCR product

		(the insert with TGBs) was digested with *Not*I/*Sac*I enzymes and cloned into *Not*I/*Sac*I/CIP-treated OL18 vector (see below). The positive clones were sequenced.
pGEMTE.ΔTGB2 (OL30)	4.2 kb; Amp^R	Designed during this thesis by Volha Linnik: The insert was excised from OL28 as a *Xba*I/Klenow fragment (frame-shifting) and religated. The positive clones were sequenced.
pGEMTE.ΔTGB3 (OL31)	4.2 kb; Amp^R	Designed during this thesis by Volha Linnik: The insert was excised from OL28 as an *Eco*NI/Klenow fragment (frame-shifting) and religated. The positive clones were sequenced.
pGEMTE.ΔTGB2-ΔTGB3 (OL32)	4.2 kb; Amp^R	Designed during this thesis by Volha Linnik: The insert was excised from OL30 (ΔTGB2) as an *Eco*NI/Klenow fragment (frame-shifting in TGB3 to generate ΔTGB3) and religated. The positive clones were sequenced.
pGR106.ΔTGB2.GFP (OL35)	11.8 kb; Kan^R	Designed during this thesis by Volha Linnik: The insert (ΔTGB2) was excised from OL30 as an *Apa*I/*Asc*I fragment and ligated into *Apa*I/*Asc*I/CIP-treated pGR106.GFP.
pGR106.ΔTGB3.GFP (OL36)	11.8 kb; Kan^R	Designed during this thesis by Volha Linnik: The insert (ΔTGB3) was excised from OL31 as an *Apa*I/*Asc*I fragment and ligated into *Apa*I/*Asc*I/CIP-treated pGR106.GFP.
pGR106.ΔTGB1.GFP (OL37)	11.8 kb; Kan^R	Designed during this thesis by Volha Linnik: The insert (ΔTGB1) was excised from pGR106.GFP as an *Apa*I/T4 DNA Polymerase fragment (frame-shifting) and religated.
pGR106.pum.mCherry.ΔCP (OL42)	11.1 kb; Kan^R	Designed during this thesis by Volha Linnik: The fragment (ΔCP) was excised from pGR106.pum.mCherry as a *Not*I/*Xho*I/Klenow fragment and the vector without CP was religated.
pGR106.mCherry.ΔCP (OL43)	11.1 kb; Kan^R	Designed during this thesis by Volha Linnik: The fragment (ΔCP) was excised from pGR106.mCherry as a *Not*I/*Xho*I/Klenow fragment and the vector without CP was religated.
pGR106.ΔTGB2-ΔTGB3.GFP (OL44)	11.8 kb; Kan^R	Designed during this thesis by Volha Linnik: The insert (ΔTGB2-ΔTGB3) was excised from OL32 as an *Apa*I/*Asc*I fragment and ligated into *Apa*I/*Asc*I/CIP-treated pGR106.GFP.
pGR106.ΔTGBs.GFP (OL45)	11.8 kb; Kan^R	Designed during this thesis by Volha Linnik: The fragment (ΔTGB2-ΔTGB3) was taken from OL44 as an *Apa*I/T4 DNA Polymerase fragment (frame-shifting in TGB1) and religated.
pGR106.ΔTGB1-ΔTGB2.GFP (OL46)	11.8 kb; Kan^R	Designed during this thesis by Volha Linnik: The insert (ΔTGB1-ΔTGB2) was excised from OL35 as an *Apa*I/T4 DNA Polymerase fragment (frame-shifting) and religated.
pGR106.ΔTGB1-ΔTGB3.GFP (OL47)	11.8 kb; Kan^R	Designed during this thesis by Volha Linnik: The insert (ΔTGB1-ΔTGB3) was excised from OL36 as an *Apa*I/T4 DNA Polymerase fragment (frame-shifting) and religated.
pGR106.ΔTGB1.GFP-2A-CP (OL49)	11.9 kb; Kan^R	Designed during this thesis by Volha Linnik (finished by Dr. Jens Tilsner): The insert (GFP-2A-CP) was excised from pTXS.GFP-2A-CP as an *Eag*I/Klenow

		blunted/*Spe*I fragment and ligated into *Asc*I/Klenow blunted/*Spe*I-treated OL37 vector.
pGR106.ΔTGB2-ΔTGB3.GFP-2A-CP (OL50)	11.9 kb; Kan^R	Designed during this thesis by Volha Linnik: The insert was excited from OL44 vector as an *Asc*I/*Not*I/Klenow fragment and was religated.
pGR106.ΔTGB2.GFP-2A-CP (OL53)	11.9 kb; Kan^R	Designed during this thesis by Volha Linnik (finished by Dr. Jens Tilsner): The insert (GFP-2A-CP) was excised from pTXS.GFP-2A-CP as an *Eag*I/Klenow blunted/*Spe*I fragment and ligated into *Asc*I/Klenow blunted/*Spe*I-treated OL35 vector.
pGR106.ΔTGB3.GFP-2A-CP (OL54)	11.9 kb; Kan^R	Designed during this thesis by Volha Linnik (finished by Dr. Jens Tilsner): The insert (GFP-2A-CP) was excised from pTXS.GFP-2A-CP as an *Eag*I/Klenow blunted/*Spe*I fragment and ligated into *Asc*I/Klenow blunted/*Spe*I-treated OL36 vector.
pGR106.ΔTGB1-ΔTGB2.GFP-2A-CP (OL56)	11.9 kb; Kan^R	Designed during this thesis by Volha Linnik: The insert (GFP-2A-CP) was excised from pTXS.GFP-2A-CP as an *Eag*I/Klenow blunted/*Spe*I fragment and ligated into *Asc*I/Klenow blunted/*Spe*I-treated OL46 vector.
pGR106.ΔTGB1-ΔTGB3.GFP-2A-CP (OL57)	11.9 kb; Kan^R	Designed during this thesis by Volha Linnik: The insert (GFP-2A-CP) was excised from pTXS.GFP-2A-CP as an *Eag*I/Klenow blunted/*Spe*I fragment and ligated into *Asc*I/Klenow blunted/*Spe*I-treated OL47 vector.
	Pumilio/viral RNA imaging constructs:	
pUGW0-single 35S promoter (*p1x35S*)	6 kb; Amp and Cm^R	Nakagawa *et al*., 2007
pRPS5A	6.4 kb; Amp and Cm^R	Weijers *et al*., 2001 (promoter); Tilsner *et at*., 2009 (plasmid)
pUGW0.pRPS5A-a pUGW0-derivative with *p1x35S* replaced by the promoter of the *Arabidopsis* ribosomal *RPS5A* gene (*pRPS5A*) (JT504)	6.7 kb; Amp and Cm^R	Dr. Jens Tilsner (plasmid)
pENTR1A	2.7 kb; Kan^R	Invitrogen
pGEMTE.PUMHD3794-BSEXlinker (JT454)	4.1 kb; Amp^R	Dr. Jens Tilsner
pGEMTE. CitN-PUMHD3794-NLS (without mutation) (OL18) Nuclear localisation signal (NLS)	4.8 kb; Amp^R	Designed during this thesis by Volha Linnik: The insert (PUMHD3794) was excised from JT454 as a *Kpn*I/*Bgl*II fragment and ligated into *Kpn*I/*Bgl*II/CIP-treated pGEMTE-based vector. The positive clones were sequenced.
pGEMTE.PUMHD3809-PUMHD3794-BSEXlinker (JT463)	5.3 kb; Amp^R	Dr. Jens Tilsner
pENTR1A.PUMHD3809-PUMHD3794-BSEXlinker (OL1)	4.4 kb; Kan^R	Designed during this thesis by Volha Linnik: The insert (PUMHD3809-PUMHD3794-BSEXlinker) was excised from JT463 as an *Eco*RI/*Afl*II/Klenow fragment and ligated into *Xmn*I/*Eco*RV/CIP-treated pENTR1A.
pRTL2.DEST-B-//GFPc3	6.4 kb; Cm and	Dr. Jens Tilsner

(JT355)	Amp^R	
pENTR1A.PUMHD3809-PUMHD3794-Δ*Sgr*A-*Eco*RV (OL15Δ)	4.4 kb; Kan^R	Designed during this thesis by Volha Linnik: OL1 vector was digested with *Sgr*AI/*Eco*RV/Klenow in order to cut out the downstream stop codon and phenol-chloroform extracted followed by vector religation.
pRTL2.PUMHD3809-PUMHD3794-GFPc3 (OL27)	6.9 kb; Amp^R; green 'double Pumilio' reporter	Designed during this thesis by Volha Linnik: OL15Δ and JT355 were recombined using Gateway LR Clonase II.
pRTL2.CitN-PUMHD3794 (JT425)	5.5 kb; Amp^R; Pumilio BiFC-based reporter	Dr. Jens Tilsner
pRTL2.PUMHD3809-CitC (JT464)	5.2 kb; Amp^R; Pumilio BiFC-based reporter	Dr. Jens Tilsner
pUGW0.pRPS5A.CitN-PUMHD3794	6.8 kb; Amp and Cm^R; optimised PUMHD-split FP fusion	Dr. Jens Tilsner
pUGW0.PUMHD3809-CitC	5.6 kb; Amp and Cm^R; optimised PUMHD-split FP fusion	Dr. Jens Tilsner

2.2 Methods

2.2.1 Molecular biological methods

2.2.1.1 Preparation of competent cells

2.2.1.1.1 *Escherichia coli* electrocompetent cells preparation

DH5α and XL-1 Blue *E. coli* strains were prepared as follows. To set up overnight cultures, single colonies were picked up from an existing stock plate or from an aliquot of competent cells from the previous batch onto an LB (Luria-Bertani) plate supplemented with the appropriate antibiotic, if any (XL-1 Blue cells were selected against tetracycline 12.5 μg/mL; DH5α were plated on LB media without an antibiotic). The growth of a single colony was performed overnight at 37° C in an orbital shaker. Next day, colonies were inoculated with 5 mL of LB medium. After 24 hours 5 mL of a fresh overnight culture were inoculated with 500 mL of LB media and the flasks were placed in a shaker at 37° C for approximately four hours incubation until the absorbance of the cultures reached 0.8 at OD_{600} (OD, optical density). The range between OD 0.6 and 1.0 was considered acceptable. After the OD was measured, the flasks were placed on ice for 30 minutes to arrest cell growth. To harvest the cells, the cultures were decanted into pre-chilled sterile 250 mL Sorvall bottles, centrifuged at 4,000 rpm for 15 min at 4° C in Beckman centrifuge in a pre-cooled Sorvall SLA-1500 rotor. The supernatant was carefully removed and the pellets were resuspended in 5 mL of chilled 10 % glycerol (in distilled water). Once thoroughly resuspended, the bottles were filled with more glycerol to 250 mL. The next centrifugation step was performed as before. This step was repeated twice more giving three washes in total. For the last wash the resuspensions were pooled into two 250 mL Sorvall bottles, filled with 10 % glycerol and centrifuged as before. The pellets were resuspended in a total volume of 4 mL chilled sterile 10 % glycerol. 50 μL volumes of cells were gently aliquoted into pre-chilled 0.5 mL Eppendorf tubes racked on ice, placed in liquid nitrogen and stored at -80° C.

2.2.1.2 DNA manipulation and analysis

2.2.1.2.1 Electrotransformation of *E. coli* competent cells with plasmid DNA

50 µL aliquots of electrocompetent cells from the -80° C freezer were thawed on ice. 0.2 cm electroporation cuvettes were placed on ice to cool. The electroporator was set to "1800V". 0.5-3 µl of plasmid DNA was added to the aliquot of cells, mixed by pipetting up and down. The cells with DNA were pippeted down the side of the cuvette between the metal plates to get the cells to the bottom of the cuvette and make sure the sample was evenly distributed between the sides of the cuvette (avoiding creating any air bubbles). After 1 min, the sides of the cuvette were dried with a tissue. The cuvette was placed in the electroporation chamber and the electrotransformation was performed. Subsequently, 0.9 mL of LB medium was added to the cuvette with cells. The cells were resuspended by pipetting up and down several times, collected into a new tube and incubated in a shaker at 37° C for 1 hour to allow recovery of cells and for phenotypic expression. After the incubation period a small aliquot of the cells (to get single colonies) was placed on LB agar plate containing appropriate selective antibiotic. Kanamycin (Kan) was used at a final concentration of 50 µg/mL, ampicillin (Amp) and spectinomycin (Spec) were used at a final concentration of 100 µg/mL for both LB agar plates and LB liquid cultures.

2.2.1.2.2 Chemical transformation of *E. coli* competent cells with plasmid DNA

50 µL aliquots of competent DH5α cells (Invitrogen) were thawed on ice. Up to 5 µL of plasmid DNA was added to the aliquot. The mix of competent cells with DNA was incubated on ice for 30 min, followed by 30 sec heat-shock at 42° C in a heating block and then placed immediately on ice to incubate for 2 min. 0.2 mL of room-temperature LB media was added to the cells followed by 1 hour incubation in 37° C. After the incubation period, a small volume of the media with cells was placed on LB plate with an appropriate antibiotic concentration. Following overnight incubation, colonies were picked up individually and inoculated in 4.3 or 50 mL

liquid LB cultures depending on the type of the following plasmid preparation. Liquid media cultures were grown overnight at 37° C.

2.2.1.2.3 Transformation of *Agrobacterium tumefaciens* cells

In this work the following strains of *Agrobacterium* were used: LBA4404, GV3101, AGLI/pSoup, C58. These competent cells were thawed on ice for 1 hour. 1-2 μg of binary plasmid DNA (T-DNA construct containing a gene of interest) was added to 50 μL or 100 μL aliquots of competent cells, mixed by gently flicking the tubes and incubated on ice for about 30 min. The binary plasmids had the left and right T-DNA border sequences, replication origins for both *E. coli* and *A. tumefaciens*, a eukaryotic promoter sequence, selectable antibiotic marker genes and a downstream multiple-cloning site with several restriction sites for the gene of interest (Stougaard, 1995). The virulence genes are located within the plasmid or alternately on a separate helper plasmid (pSoup). The mix of binary DNA and *Agrobacterium* competent cells to be transformed was placed into an electroporator. 0.9 mL of growth medium (yeast extract peptone (YEP) medium: yeast extract, 10 g/L; peptone, 10 g/L; sodium chloride, 5 g/L; pH 7.0) was added to the cells and the mix was incubated for 2-3 hours at 28° C. The cultures were plated out on YEP agar plates with the appropriate concentration of an antibiotic (the antibiotic concentration and the transformation procedure are identical to the ones used for the *E. coli* transformations). The cells were grown for 2-3 days at 28° C.

2.2.1.2.4 Plasmid DNA extraction from *E. coli* and DNA digestion with restriction endonucleases

Once bacterial clones were grown, plasmid DNA was isolated from the cultures of the chosen clone using QIAGEN Mini kit according to the manufacturer's instructions. To get plasmid DNA from the retransformants, QIAGEN Midi kit was used. Restriction digests of plasmid DNA were performed to screen bacterial colonies for the correct insertions. The reaction volume was 20 μL and consisted of 2.5 μL of DNA, 2 μL of buffer supplied with the enzyme, 0.5 μL of restriction

enzyme, 0.2 µL of bovine serum albumin (BSA) (if was required) and distilled water was added to make up 20 µL reaction. Reactions were incubated for 2-4 hours or overnight at 37° C (unless a different temperature was stated by the manufacturer's instructions). For larger quantities of DNA (in case of making a preparative digest), the volumes were increased to 50 µL and consisted of 25 µL of DNA, 5 µL of buffer supplied with the enzyme, 2 µL of restriction enzyme, 0.5 µL of BSA (if required) and distilled water was added to make up 50 µL reaction. These reactions were incubated overnight. Double digests were set up according to the guidelines provided by the manufacturer New England Biolabs (NEB). In case of absence of 100 % enzyme activity in a particular buffer, sequential digestions were performed, in which the restriction enzyme was heat-inactivated after the first digestion and the DNA was spin-dialysed to remove the first buffer.

2.2.1.2.5 Agarose gel electrophoresis and gel extraction

To separate different fragments by size ranging from 100 bp to 10 kb, 1 % gel was prepared by dissolving 1 g of agarose in 100 mL of 0.5 × TBE (Tris/Borate/ ethylenediaminetetraacetic acid (EDTA)) buffer: 4 mM Tris, 4 mM Boric acid, 1 mM EDTA, to keep DNA deprotonated and soluble in water (EDTA protects the nucleic acids against enzymatic degradation). The gel percents varied from 0.7 % to 1 % depending on the type of gel extraction. Ethidium bromide solution (0.5 µg/mL) was added to the melted agarose. This was poured into casts and allowed to solidify at room temperature, then placed into the gel electrophoresis tank with 0.5 × TBE buffer. The loading buffer and samples were run under different voltage depending on the size and separation of the fragments. After running a gel, it was placed on an UV light source, where the digested fragments were visualised (ethidium bromide intercalates into DNA and fluoresces upon UV light activation). To extract DNA from a gel, a QIAquick gel extraction kit was used from QIAGEN. Alternatively, Zymoclean gel DNA recovery kit from ZYMORESEARCH was applied. Both kits give a possibility to recover the purified DNA in a small volume of buffer (7-20 µL), resulting in a higher concentration of DNA of interest. The procedure was followed as per manufacturer's instructions. After the extraction procedure the concentration

of samples was measured using the BioPhotometer from Eppendorf at OD_{260} using the formula: DNA concentration (µg/mL) = (OD_{260}) x (dilution factor).

2.2.1.2.6 Converting 5'-overhang to a blunt ended terminus (Klenow enzyme blunt-end cloning)

Blunting is performed when unable to use the same restriction enzyme for vector and insert DNA. 5'-overhangs were converted into blunt-ended termini by filling in reaction with 1 µL of deoxyribonucleotide triphosphate (dNTP) and 0.5 µL Klenow enzyme. The mix was incubated at 25° C for 15 min. The reaction was terminated by addition of 1 µL 0.5 M EDTA (pH 8), vortexed and incubated at 75° C for 20 min. In such cases, 5'-overhangs were blunted in both insert and vector.

2.2.1.2.7 Converting 3' and 5'-overhang to a blunt ended terminus (T4 DNA polymerase blunt-end cloning)

T4 DNA polymerase, which has both 5'->3' polymerase and 3'->5' exonuclease activity, was used to remove 3' overhangs and fill in 5' overhangs to create blunt ends. The reactions were set up as indicated below: 25 µL DNA, 10 µL 10 x NEB T4 DNA polymerase buffer, 0.5 µL 10 mg/mL BSA and 2 µL 5 mM dNTPs. The reaction was mixed and cooled on ice and 1 µL T4 DNA polymerase was added. The enzyme was added last as in the absence of nucleotides DNA could be rapidly degraded. Keeping the reaction in cold conditions at all times was critical as the exonuclease is more active than the polymerase at higher temperatures. Water was added to a final volume of 50 µL after enzyme addition. The reaction was incubated at 12° C for 1 hour. After the incubation time, the reaction was returned to ice and enzyme was inactivated and removed during phenol-chloroform extraction, followed by chloroform extraction and spin-dialysis.

2.2.1.2.8 Phenol-chloroform extraction

If plasmid DNA was further purified by phenol-chloroform extraction, 1 sample volume of phenol-chloroform-isoamylalcohol was added, mixed and then centrifuged at 13,000 rpm for 5 min. The aqueous phase was transferred to the new tube. 1 volume of chloroform was added to this supernatant, vortexed and centrifuged at 13,000 rpm for 3 more min. Only a clear upper phase (no chloroform was left in the supernatant) was taken out to the new clean tube followed by spin-dialysis.

2.2.1.2.9 Spin-dialysis

The main purpose of spin-dialysis is to remove low molecular weight substances. Sepharose CL-6B, which contains cross-linked agarose beads, was used as a gel matrix. The nominal exclusion size for CL-6B is 194 bp. To purify products of a 20 or 50 µL reaction by spin-dialysis, a column was prepared. A small hole was punched in the bottom of 1.5 mL eppendorf tube. A drop (about 30 µL) of glass beads (0.2 mm; 212-300 µm in sterile water) was added to this tube. Resuspended Sepharose CL-6B (in Tris EDTA (TE) buffer or sterile water, pH 8) was added gently to the glass beads (about six times the sample volume). This column was centrifuged at 2,000 rpm (Centrifuge 5810 R, Eppendorf) for 1 min to remove excess buffer and make sure that the buffer can flow through the column. Then a volume of water equivalent to the sample volume was placed to the centre of the packed column and centrifugation was repeated. Subsequently, the sample was added to the top of the spin column. Finally, a 1.5 mL Eppendorf tube was placed under the column to collect the purified product during the following centrifugation step.

2.2.1.2.10 Dephosphorylation of vectors

Cutting with a single restriction enzyme leads to the linearisation of a vector. To minimise the religation of the linearised vector without incorporation of an insert fragment, the 5' end of the blunted vector was dephosphorylated with 1 µL calf intestinal alkaline phosphatase (CIP) enzyme, which was added to the DNA with 10

x NEB buffer (NEB buffers 2, 3, 4 if added directly to the restriction enzyme digests). This enzyme removes 5' phosphate groups from DNA. The reactions were incubated at 37° C for 1 hour. CIP is difficult to completely heat-inactivate. Therefore, after 1 hour incubation time the samples were phenol-chloroform extracted and further purified by chloroform extraction and spin-dialysis (if desired).

2.2.1.2.11 Ligation reactions

The concentrations of both insert and vector DNA were measured using a BioPhotometer from Eppendorf at optical density OD_{260}. The molar ratio of vector to insert DNA was 1:10. Ligation reactions were set up in 5 to 20 µL (made up to this volume with distilled water) depending on the concentration of total DNA and catalysed with T4 DNA ligase (NEB) overnight at 16° C.

2.2.1.2.12 Gateway LR recombination

The Gateway LR recombination method (L and R restriction sites in the gateway system) was adapted from a Gateway technology with Clonase II manual.

Recombination is a conservative method and does not require DNA synthesis and there is no gain or loss of nucleotides. The gateway cloning technology maintains the orientation and the reading frame. It is based on the site-specific recombination properties of the bacteriophage lambda. The BP recombination reaction (B and P restriction sites in the gateway system) allows transfer of a gene of interest in an *att*B expression clone (or *att*B-PCR product) to an *att*P-containing donor vector to produce an entry clone. Once an entry clone is generated during the BP recombination, the gene of interest is shuttled into a destination vector using the LR recombination reaction. Maximum of 75 ng of entry clone and maximum of 75 ng of gateway destination vector were used for the LR gateway recombination. These two components were mixed up to 4 µL with TE buffer (pH 8) to get the desired concentration. An aliquot of gateway LR Clonase II was thawed on ice (from -80° C freezer) for 2 min, vortexed briefly twice and 1 µL of the enzyme was added to the

reaction (final volume of the reaction was 5 μL). The reaction was gently mixed by flipping the tube bottom and briefly centrifuged. It was then placed to incubate overnight at 25° C. The reaction generated an expression clone and was stopped next day by incubating at 70° C for 30 min. Next day 1 μL of the recombination reaction was transformed and placed on a plate with an appropriate antibiotic, the choice of which was dependent on the destination vector.

2.2.1.2.13 Polymerase Chain Reaction (PCR)

PCR was carried out in a Mastercycler (Eppendorf, Hamburg, Germany). Primers were designed using the vector NTI program (Invitrogen) to amplify target DNA sequences for cloning or for colony PCR screening procedures. All oligonucleotide primers used in this thesis for cloning are listed in table 2.3.

Table 2.3: List of oligonucleotide primers used in this thesis

Primer name	Oligo sequence (5' → 3') and origin
NotI_25K for	TTTGCGGCCGCAATGGATATTCTCATCAGTAG designed during this work in collaboration with Dr. Christophe Lacomme
Over_mCherry for	GTCCGCGCAGGGCCAGTGAGCAA designed during this work in collaboration with Dr. Christophe Lacomme
PmeI_sgp12K for	TTTGTTTAAACGCACCAATAGAGGAAATTG designed during this work in collaboration with Dr. Christophe Lacomme
SacI_mCherry rev	TTGAGCTCGTTTAAACTTACTTGTACAGCTCGTCCAT designed during this work in collaboration with Dr. Christophe Lacomme
Over_25K rev	TTGCTCACTGGCCCTGCGCGGAC designed during this work in collaboration with Dr. Christophe Lacomme
SacI_AscI rev	TTGAGCTCGGCGCGCCAATCGATGCTAG designed during this work in collaboration with Dr. Christophe Lacomme

2.2.1.2.13.1 Standard PCR programs and reactions

To amplify a target DNA sequence by PCR, the following cycling conditions were used:

1. Initial denaturation: 98° C for 30 sec
2. Denaturation of the double-stranded DNA template: 98° C for 10 sec
3. Annealing of the primers for the attachment to their target sequences on the template: 50-60° C for 30 sec

4. Extension: 72° C for 1 min 30 sec (if expected PRC product of a size about 1.3 kb)

   Repeated steps 2-4 for 19 cycles
5. Final extension: 72° C for 10 min
6. 4° C on hold.

The annealing temperature used in the PCRs was primer dependent. The number of cycles used was dependent on the level of amplification required. The duration of the extension time varied according to the expected PCR amplification product size (1 min per 1 kb synthesised) (Santos *et al*., 2008).

The reaction conditions were:
0.5 µL DNA
For 24.5 µL of the master mix:
2.5 µL Promega 10 x thermophilic DNA polymerase buffer
1 µL Promega 50 mM $MgCl_2$
1 µL 5 mM dNTPs
0.5 µL 10 µM 5' primer (forward oligonucleotide primer)
0.5 µL 10 µM 3' primer (reverse oligonucleotide primer)
0.1 µL Promega *Taq* DNA polymerase
18.9 µL sterile water.

2.2.1.2.13.2 High-fidelity (HiFi) PCR

To introduce a new restriction site or new sequence into known DNA plasmid, HiFi PCR reactions were carried out.

All HiFi PCR reactions were prepared in 25 µL total volume as follows:
0.5 µL template
2.5 µL Promega HiFi buffer
1 µL Promega 50mM $MgSO_4$
1 µL 5 mM dNTPs

0.5 µL 10 µM 5' forward primer

0.5 µL 10 µM 3' reverse primer

0.1 µL Promega HiFi *Taq*

18.9 µL water.

Endogenous expression cloning of PVX TGB1-mCherry fusion:

HiFi PCR conditions were:

1. 94° C for 2 min
2. 92° C for 20 sec
3. 60° C for 20 sec
4. 68° C for 1.20 min

   Repeated 2-4 for 4 cycles

5. 92° C for 20 sec
6. 63° C for 20 sec
7. 68° C for 1.20 min

   Repeated 5-7 for 24 cycles

8. 68° C for 5 min
9. 4° C on hold.

Overlap PCR conditions were:

1. 94° C for 2 min
2. 92° C for 20 sec
3. 55° C for 20 sec
4. 68° C for 1 min

   Repeated 2-4 for 9 cycles

Paused and primers NotI_25K for and SacI_mCherry rev were added

5. 92° C for 20 sec
6. 63° C for 20 sec
7. 68° C for 1.40 min

   Repeated 5-7 for 9 cycles

8. 92° C for 20 sec

9. 65° C for 20 sec
10. 68° C for 1.40 min
    Repeated 8-10 for 14 cycles
11. 68° C for 5 min
12. 4° C on hold.

2.2.1.2.13.3 Colony screening PCR

To determine successful *E. coli* transformation, PCR was used to screen for positive clones. A colony screening PCR master mix was prepared according to the following procedure:

For 24.5 µL of the master mix:

2.5 µL Promega 10 x thermophilic DNA polymerase buffer

1 µL Promega 50 mM $MgCl_2$

1 µL 5 mM dNTPs

0.5 µL 10 µM 5' primer (forward oligonucleotide primer)

0.5 µL 10 µM 3' primer (reverse oligonucleotide primer)

0.1 µL Promega *Taq* DNA polymerase

18.9 µL sterile water

24.5 µL aliquots of the master mix were pipetted into 0.2 mL PCR tubes. Single, well-separated, bacterial colonies were picked up from an agar LB plate with an appropriate antibiotic and inoculated in a corresponding colony PCR master mix aliquot using sterile tips and then plated on to a fresh agar plate (the number of a colony on a plate corresponded to the number of the PCR tube with a master mix inoculated with the corresponding clone). The plates were incubated at 37° C for three to six hours while the PCR was running. The PCR tubes were placed into the thermocycler machine and the reaction was carried out as indicated below:

Initial denaturation: 94° C for 4 min

Denaturation: 94° C for 30 sec

Annealing: 50° C for 30 sec

Extension: 72° C for 1 min 50 sec (if expected PRC product size was about 1.5 kb)

    Repeated steps 2-4 for 24 cycles

Final extension: 72° C for 10 min

4° C on hold.

After thermocycling, gel loading buffer was added to the reactions, mixed, and the samples were run on an agarose gel to check the size of the PCR products.

2.2.1.2.14 PCR products purification

To purify PCR products, a QIAquick PCR purification kit (QIAGEN) was used according to the manufacturer's instructions.

2.2.1.2.15 DNA sequencing

All PCR generated clones were confirmed by DNA sequencing. The sequencing reactions were performed by the Edinburgh University Sequencing Service. Chromatograms were analysed in the vector NTI program.

Sanger didesoxyribonucleotide triphosphate (ddNTP) chain termination method shows different ddNTPs labelled with fluorescent dyes in different colours. Separation of DNA fragments is performed by liquid chromatography. Samples that were submitted for sequencing were prepared with an ABI Prism BigDye terminator kit (with reduced BigDye concentration to avoid excess dye peaks) as follows:

2 µL H_2O, 2 µL unquantified DNA, 2 µL BigDye mix, 3 µL ABI buffer (diluted 1:5 in water), 1 µL 3.2 µM primer.

PCR program conditions were:

Lid 105° C, no wait, auto volume

96° C for 10 sec, R = 1° C/sec

50° C for 50 sec, R = 1° C/sec

60° C for 4 min, R = 1° C/sec for 25 cycles

8° C on hold.

2.2.1.2.16 DNA sequence analysis

Vector NTI program from Invitrogen was used for sequence alignments and their following analysis, for planning cloning strategies, constructing plasmid maps, designing primers, planning the performance of preparative and diagnostic restriction digestions.

2.2.1.3 RNA manipulation methods

2.2.1.3.1 *In vitro* transcription, reassembly and inoculation

This method is based on the protocols described by Turner and Foster, 1998; Annamalai and Rao, 2008.

Template plasmid DNA was linearised with an appropriate restriction enzyme downstream of the insert that has to be transcribed (only the *Spe*I site was used during this work). After complete digestion of the plasmid DNA, the reaction mixture was extracted with phenol-chloroform to remove all traces of RNAases, followed by chloroform extraction and spin-dialysis to remove a reaction buffer. The digested plasmid DNA was used for the subsequent *in vitro* transcription.

Biologically active RNA transcripts were synthesised *in vitro* using T7 polymerase promoter. Localisation of the viral sequence downstream of a RNA polymerase promoter is necessary to synthesise infectious RNA transcripts. Any work conducted with RNA required a very careful treatment of the samples and limitation of RNAase contaminations (gloves were changed regularly, new autoclaved tips and tubes were used, the end of pipettes was rinsed with an RNase-inactivating solution; the gel apparatus was treated with 0.5 M NaOH, followed by several rinses with water and then with absolute ethanol).

The commercially available T7 mMESSAGE mMACHINE kit (Ambion, Austin, TX, USA), was used to produce infectious TMV or PVX RNA. The transcription

reactions were set up according to the manufacturer's instructions at 5 µL scale: 2.5 µL 2 x NTP mix, 0.5 µL 10 x buffer, 1.5 µL template (linearised plasmid DNA) and 0.5 µL 10 x enzyme mix. The reactions were assembled at the room temperature in 0.5 µL Eppendorf tubes. When performing multiple transcriptions a master mix was prepared and added to the template. The components were mixed well by gentle pipetting, shortly centrifuged and incubated at 37° C for 2 hours. To check the transcript yield and integrity, a 0.5 µL aliquot of the reaction was taken after 60 min of incubation and electrophoresed on a 0.7 % gel as follows: to the 0.5 µL aliquot 50 µL of RNase-free water and 4.5 µL of Ambion gel loading buffer were added, then vortexed and run on a gel containing ethidium bromide at 75 V. Once the 2 hours incubation period at 37° C was over, 60 µL of diluted TMV CP that had been pre-assembled at 25° C overnight (each 5 µL transcription reaction consisted of 10 µL of 10 mg/mL TMV CP in sodium phosphate buffer and 50 µL of this buffer), was added to the transcription reaction, mixed by gentle pipetting and transferred to be incubated overnight at 25° C. Next day after reassembly the transcripts were stored at 4° C until inoculation.

Uninfected healthy plants (transgenic or non-transgenic) were selected for inoculations. 3 or 4 leaves per plant were marked by puncturing the leaf tips with a pipette tip. These leaves were slightly dusted with aluminium oxide powder. 5-10 µL of reassembled transcript was added to each selected leave to the upper side near the base. The leave was supported below with one hand and then with the other one the inoculum was gently spread across the entire leaf surface (to avoid excessive damage of the leave) in the direction from the main veins towards the periphery (Takahashi and Yoshikawa, 2008). When the inoculation was finished, the leaves were rinsed briefly with water to remove any remaining powder. Inoculated plants were transferred to the 33° C for TMV or to the 25° C for PVX.

2.2.2 Cell biological methods

2.2.2.1 Transient plant transformation by agroinfiltration

The method was adapted from S. N. Chapman and further optimised in the lab (optimisation from the following sources: Neuthaus and Boevink, 2001; Annamalai and Rao, 2008; Haupt *et al*., 2008; Palukaitis *et al*., 2008).

A common method to transiently express the gene of interest in plants is agroinfiltration of the *Agrobacterium tumefaciens* cultures directly into plant leaves. *A. tumefaciens* is a natural plant pathogen, which carries a Ti plasmid (tumour inducing). This plasmid encodes DNA that is integrated into the host plant genome randomly, potentially upon disruption of endogenous genes. This DNA is called the T-DNA (transfer-DNA). Genes within the T-DNA are of eukaryotic type and thus can be expressed in plants. The virulence (vir) genes are present on the Ti plasmids of *Agrobacterium tumefaciens* but not within the T-DNA sequence. They are prokaryotic and encode for proteins expression of which allows the transfer of the DNA from the bacterial cell to the host plant cell. Acetosyringone (4'-hydroxy-3',5'-dimethoxy acetophenone; 3',5'-dimethoxy-4'-hydroxy acetophenone; $C_{10}H_{12}O_4$), a phenolic virulence gene inducer (in very low concentration of acetosyringone), is used as one of the components of the Agromix. Plants generate different phenolic compounds. Acetosyringone is produced naturally in plant wounds (Vaghchhipawala and Mysore, 2008).

Preparation of *Agrobacterium* culture:
Transformed *Agrobacterium* single colonies were picked up from plates incubated at 28° C into tubes containing 5 mL LB or YEP supplemented with an appropriate antibiotic to select for the binary plasmid. Cultures of *A. tumefaciens* carrying recombinant binary plasmids were grown at 28° C for 1-3 days (depending on the strain of *Agrobacterium* used). The bacteria were centrifuged at 2,500 rpm for 15 min at 16° C. The supernatant was removed and the bacterial pellet was resuspended in 1 mL of Agromix. The 1:100 dilutions in water of the resuspensions's aliquots

were prepared and OD_{600} was measured using Eppendorf BioPhotometer. Then the dilutions of the resuspensions were prepared in Agromix to an OD_{600} of between 0.001 and 0.5 (depending on the viral construct's requirements). These diluted cultures were left to stand at room temperature in the dark for 2 to 3 hours.

Preparation of plant materials:
During the incubation period plants (beyond 9-leaf developmental stage) to be inoculated were selected. To mark the leaves for infiltration, a hole was punched into the leaves with a yellow tip in the same way as the procedure described for *in vitro* transcription inoculation. The only difference is that leaves, selected to be infiltrated, had to have a flat surface to allow easier penetration and distribution of the infiltration medium.

Infiltration: (the same procedure as for infiltration of *Agrobacteria* and dyes)
A small spot was punctured on a lower epidermal leaf surface at several sites with a white pipette tip. A 1 mL syringe (without needle) with the bacterial resuspension was placed over the punctured sites on the leaf over the hole and the resuspension was gently infiltrated into the leaf while applying a counter-pressure on the opposite side of the leaf with a finger to facilitate entry of the Agrobacterial resuspension. If the leaf was not infiltrated entirely, the boundary of the infiltrated area was marked with a marker pen. Plants were placed in the controlled growth conditions for 3-4 days (before imaging) with an appropriate temperature required for the virus.

Agromix (infiltration medium in sterile H_2O):
Was prepared fresh from the stock sterile solutions:
0.01 M $MgCl_2$ (from 1M sterile stock)
0.01 M MES (2-(N-Morpholine)-ethane sulfonic acid) buffer (from 0.5 M sterile stock solution, pH adjusted to 5.6 with KOH)
15 μM acetosyringone (from 0.01 M stock).

2.2.2.2 Transient plant transformation by particle bombardment

Genetic transformation by particle bombardment simply involves shooting the gold particles with the DNA of interest into plant cells. When exogeneous DNA enters the nucleus of a cell, it can be incorporated into the plant genome (Haupt *et al*., 2008).

The bombardments in all the experiments were carried out using the Bio-Rad Biolostic PDS-1000/He Particle Delivery System according to the manufacturer's instructions. When the gas is delivered from the cylinder to the gas acceleration tube, it causes an increase in pressure behind the disk at the end of the tube. This disk ruptures and the pulse of gas hits the microcarrier disk. Then the microcarrier hits the stopping screen, the gold particles with DNA are released from a microcarrier disk and shot into the plant tissue.

To make gold for bombardment, a suspension of 50 mg gold particles (1.0 µm) in 1 mL sterile dH_2O was prepared, vortexed vigorously for 1-2 min and centrifuged at 13,000 rpm for 1 min. The supernatant was discarded and the gold particles were washed three times with 100 % ethanol by vortexing and following centrifugation. Then the suspension was washed once with the sterile H_2O, vortexed and centrifuged. The supernatant was discarded. The gold particles were resuspended in 1 mL sterile H_2O and aliquoted with a volume of 25 µL into 1.5 mL eppendorf tubes and stored at 4^{o} C.

To coat the gold particles with plasmid DNA, a 25 µL aliquot of gold particles was resuspended by vortexing or sonicating (a water bath Ultrasonic Cleaning Device). 2-5 µg of plasmid DNA was added to the gold suspension and vortexed or sonicated briefly again. To precipitate DNA on the gold, 25 µL 2.5 M $CaCl_2$ was added and mixed by pipetting up and down 5-10 times (avoiding creating bubbles). To protect the DNA from cellular DNAses, 10 µL of 0.1 M spermidine was added, mixed by pipetting and vortexing at low speed for 2 min. Then the tube was incubated on ice for 5-30 min. The DNA-coated gold particles were pelleted by centrifuging for about 10 sec. To wash the sample, the supernatant was removed and 180 µL of 100 %

ethanol was applied to the tube. The gold particles were resuspended by pipetting up and down followed by sonicating. Then they were pelleted again and the supernatant was removed. Finally, the particles were resuspended in 100 μL 100 % ethanol, mixed and sonicated to fully resuspend. The particles then were ready for bombardment and were stored at -20 ^{o} C for several months (Santos *et al*., 2008; Trutnyeva *et al*., 2008).

The success of transformation by bombardment was dependent on two different parameters, specifically on the pressure at which the gold was shot into the tissue and the distance from the tissue to the stopping screen. If the pressure is too high, or the tissue is too close, the leaves of the plant are damaged extensively and the rate of transformation is very low (Neuthaus and Boevink, 2001).

Parameters for bombarding leaves of *Nicotiana benthamiana* and *Nicotiana tabacum* in all experiments carried out in this thesis:

Tissue: medium size leaves removed from plants (as much of the petiole as possible attached to the leaf).

Position: the leaf was placed on a Petri dish at distance of 6 cm between the leave surface and the stopping grid.

Pressure: 1100 psi.

Plants were bombarded at 3-5 days (local leaves) and 10-15 days (systemic leaves) post-inoculation (d.p.i.). PVX bombarded leaves were kept at 25° C with the petiole of the leaf kept in water, and imaged at 1-5 days post-bombardment (d.p.b.). Leaves bombarded with TMV constructs were kept at 33° C and imaged between 3 and 48 hours after bombardment.

2.2.2.3 Fixation of plant tissue (*N. benthamiana* leaves) and staining with AO

An optimised version of the following fixation protocols (Hawes, 1994; Spence, 2001) was used. Buffer stock of 0.2 M Pipes, pH 6.9 was prepared as follows: to 6.04 g Pipes 50 mL sterile water was added, the powder was dissolved with 8 M NaOH

and pH was adjusted with 0.1 M NaOH to pH 6.9, and then diluted to 100 mL. A 10 % stock solution of paraformaldehyde was prepared from 16 % stock. 25 mL 0.2 M buffer, 4 mL EM grade 25 % glutaraldehyde, 5 mL 10 % paraformaldehyde solutions were mixed together and water was added to make up to 50 mL. The fixation procedure of epidermal peels was performed under the vacuum, then AO was applied to stain RNA in red (0.02 % AO and 0.06 % AO dilutions in phosphate buffer were used). The peels were left for 1.5-2 hours to incubate in a dye, then washed in 0.2 M Pipes at least 3 times and then with 0.1 M phosphate buffer, pH 7 (61.5 mL of 1 M K_2HPO_4 were mixed with 38.5 mL of 1 M KH_2PO_4, pH 7 at 25 ° C to make 0.1 M potassium phosphate buffer).

2.2.2.4 DAPI staining

DAPI stain forms fluorescent complexes with double-stranded nucleic acids. This dye binds to DNA and therefore it is used to stain the cell nucleus (Goodin *et al*., 2008). In this thesis, samples of PVX-infected cells were treated with DAPI dye to differentiate the cell nucleus from PVX VRCs. Leaves infiltrated through abaxial leaf surface with DAPI were suitable for confocal microscopy (405 nm laser) after 1-2 h. Stock solution of DAPI in DMSO (dimethyl sulfoxide) was at the concentration of 14.3 mM. Working solution was used at the concentration of 300 nM and was prepared as a dilution of the stock DAPI in sterile water.

2.2.2.5 Infectious sap collection

To collect PVX infectious sap, leaves of *N. benthamiana* and *N. tabacum* carrying virus construct (preferably inoculated non-systemic leaves) were cut and weighted. They were then grinded with a pestle in a mortar with 2 volumes of 10 mM Sorensens buffer (adjusted with NaOH to pH 7.2). For example, to 35 g of leaves 70 mL of the buffer was added. The homogenate was equally transferred into new tubes and centrifuged at 4,000 rpm at 4° C for 25 min to pellet debris. The supernatant was filtered through Miracloth into a falcon tube standing on ice and then aliquoted into 0.5 mL tubes and stored at -20° C. For the pTXS.GFP-2A-CP ‘overcoat’ PVX

construct the centrifugation step was skipped and the homogenate containing PVX virions was collected into new tubes and stored at -20° C.

2.2.2.6 Confocal microscopy of *N. benthamiana* and *N. tabacum* leaves

Experimental leaves were imaged on a Leica SP2 laser scanning confocal microscope (LSCM). Confocal microscopy eliminates out-of-focus light and provides the ability to collect serial optical sections from thick specimens (Shaw, 2001; Trutnyeva *et al*., 2008). Double sided tape was used to hold the leaves on the glass slides. Leaves were imaged on the confocal microscope with the 63 x water dipping lenses or 100 x oil immersion lenses.

The following excitation wavelengths were used (Goodin *et al*., 2008):
GFP fluorescence was visualised using an Ar 488 laser; mCherry was excited using 594 nm; cyan fluorescent protein (CFP) and DAPI, 405 nm; mCitrine for BiFC assay, 514 nm; dsRed/tdTomato, 561 nm; monomeric red fluorescent protein (mRFP), Ar/Kr 568 nm laser.

Visualisation of GFP and CFP, GFP and mRFP signals was performed by sequential scanning to minimise signal bleed-through (a cross-talk between two channels). Microscope settings were adjusted to optimise contrast for each individual experiment. The gain was kept as low as possible to improve image quality and to keep the background signal low. Images were acquired at a pixel resolution of 1024 x 1024. To find expressing cells, an appropriate filter set for a particular fluorescent protein was used. Projections were saved as individual files with file type “TIFF”.

3. Analysis of PVX VRC formation – involvement of host organelles

3.1 Aim

Recent data suggest that positive-sense RNA replication and movement occur for both plant and animal viruses on specific sites in the cell, and these sites are related to the host intracellular membrane systems and the plant cytoskeleton (Ploubidou and Way, 2001; Hull, 2002; Salonen *et al*., 2005; Greber and Way, 2006; Radtke *et al*., 2006). Despite intense research efforts on PVX, to date it is not known which cellular membrane compartments serve as a centre for PVX replication and which cytoskeleton components are involved in trafficking of the viral genome from a VRC through PD into adjacent cells. The hypothesis is that viral spread in the host plant is dependent on successful replication and formation of the viral replication and movement complex. Therefore, the aim of this results chapter is to analyse the structure of the PVX VRC and to identify host organelles involved in the formation of this viral structure and to understand their involvement in PVX replication and viral cell-to-cell movement. Thus, the recruitment of plant host organelles into the VRC and its role for the virus during PVX infection was investigated. The possible reasons for redirection of host organelles into the developing VRC are discussed.

3.2 Results

3.2.1 Plasmids used in this study (Table 3.1, Fig. 3_1)

Plasmids used in this results chapter can be divided into two groups which are listed below in Table 3.1

1) <u>According to the method of plasmid delivery</u>:

i) Bombardment plasmids for transient plant transformation by biolistic bombardment:
pRTL2 (Restrepo *et al*., 1990)

ii) Plasmids containing T7 polymerase promoter for synthesis of infectious PVX RNA transcripts for *in vitro* transcription, reassembly and inoculation:
pTXS (Chapman *et al*., 1992)

2) According to the expressed marker or gene:

Plasmid name	Expressed marker or gene	Figure number
Organelle markers:		
pRTL2.Lifeact-tdTomato	red actin marker	Fig. 3_1 A
Transgenic Nicotiana plants that stably express:		
mGFP5-ER	green reporter for ER	see Table 2.1 in Chapter 2 for more details
ST-GFP	green reporter for Golgi	
FABD2-GFP	green reporter for actin	
GFP-TUA6	green reporter for microtubulin	
PVX-carrying plasmids:		
pTXS.CFP	PVX with cyan fluorescent protein	Fig. 3_1 B
pTXS.mCherry-2A-CP	PVX with red (monomeric Cherry) fluorescent protein fused to coat protein	Fig. 3_1 C

Leaves of transgenic plants that express a 27-kDa monomeric green fluorescent protein (mGFP) isolated from the jellyfish *Aequorea victoria*, targeted to either the ER, Golgi, actin or microtubules were infected with PVX (Fig. 3_1 B; Fig. 3_1 C). GFP is a very bright and easy to locate in plant cells once it is expressed. It is very stable and non-toxic to plant cells (Prasher *et al*., 1992; Chalfie *et al*., 1994; Oparka *et al*., 1997b; Takahashi and Yoshikawa, 2008). GFP-visualised organelles allow an opportunity to study virus-induced changes in the host components of the infected plant during PVX infection. Morphological changes in the host organelles were studied in the centre of PVX infection where the virus has already moved into adjacent cells. The annotation d.p.i. (days post-inoculation of plant local leaves with the viral construct) is used in this thesis. This annotation is an approximate way to show for how long the viral infection has been present but does not indicate accurately the stage of infection in any given cell.

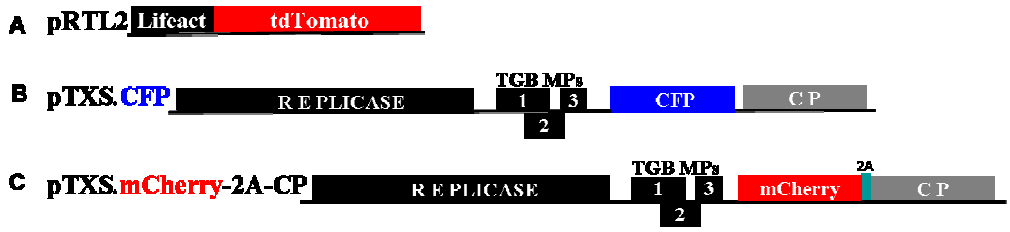

Figure 3_1: Schematic representation of plasmids used in this results chapter
TGB: triple gene block, MP: movement protein; CP: coat protein.

3.2.2 PVX reorganises the ER network during VRC establishment (Fig. 3_2)

The PVX TGB2 and TGB3 proteins are known to associate with the ER membrane (Zamyatnin *et al*., 2002; Krishnamurthy *et al*., 2003; Ju *et al*., 2005, 2007, 2008; Schepetilnikov *et al*., 2005; Samuels *et al*., 2007) and the association of PVX VRCs with cellular organelles (ER, Golgi, vacuoles and mitochondria) was identified in early EM studies by a number of authors (Kozar and Sheludko, 1969; Stols *et al*., 1970). It was also shown that the ER was rearranged during the replication of a range of other viruses, including TMV (Esau and Cronshaw, 1967; Heinlein *et al*., 1998; Reichel and Beachy, 1998; Mas and Beachy, 1999; Carette *et al*., 2000; Dunoyer *et al*., 2002; Ritzenthaler *et al*., 2002; reviewed in Noueiry and Ahlquist, 2003). Thus, the ER structure in PVX-infected cells was the first focus of this thesis.

To determine the effect of PVX infection on ER morphology, transgenic *Nicotiana* plants that stably expressed a reporter for ER were infected with PVX (Fig. 3_1 C). In transgenic *Nicotiana benthamiana* plants expressing an ER-localised GFP fusion (mGFP5-ER) (Boevink *et al*., 1996), GFP is fused to an N-terminal cleavable ER-targeting and C-terminal HDEL ER luminal retention signal sequence (Haseloff *et al*., 1997), both of which are responsible for targeting of GFP to the ER, resulting in accumulation and retention of GFP within the ER lumen and nuclear envelope (Zamyatnin *et al*., 2002; Krishnamurthy *et al*., 2003; Ju *et al*., 2005). The ER lumen contains isomerases and chaperones that help folding of the protein (Haseloff *et al*., 1997). Application of membrane potential-sensitive fluorescent stains verified that the GFP had been retained in the ER (Boevink *et al*., 1996). Therefore, a

characteristic reticular green fluorescent network of cytoplasmic interconnected tubules that are continuous with the nuclear envelope sheets is seen in the transgenic control plants (Fig. 3_2 A,E) (see also Staehelin, 1997; Boevink *et al*., 1998).

PVX-infected transgenic mGFP5-ER *N. benthamiana* leaves were observed under the confocal laser scanning microscope. Infected epidermal cells were identified by the presence of numerous PVX-induced VRCs in the cell cytoplasm. These infected plants were compared with the uninfected controls. The ER was found to be involved in PVX VRC formation and the morphology of the ER was intensively altered by the viral infection. Green fluorescence associated with the plant ER was no longer uniformly distributed in the cytoplasm highlighting the ER network, but was instead drawn into the VRC (Fig. 3_2 B-D,F). During early infection, the recruited ER was highly mobile (Movie 3.1a,b) and moved in and out of the VRC (Fig. 3_2 B). In addition, at the early infection events, the ER strands formed circular rings in the VRC (Fig. 3_2 C), suggesting that the ER membranes surrounded additional sub-compartments of the VRC. During later infection events, the GFP-ER signal in the VRC became gradually more disperse. ER became trapped within the VRC (and formed a large 'cluster' within which intact individual tubules of the ER were almost undetectable and the ER was concentrated in those structures forming large, perinuclear membrane aggregates (Fig. 3_2 D). Interestingly, the cortical ER network was also detected and was not affected by PVX infection. However, cortical ER was found to be continuous with the ER in the VRC (Fig. 3_2 F). This pattern of green fluorescence was observed in all repeated experiments with different ER markers. No ER aggregates were detected in uninfected control plants, strongly implying that these observed morphological changes in the ER structure are the results of PVX presence in these plant cells.

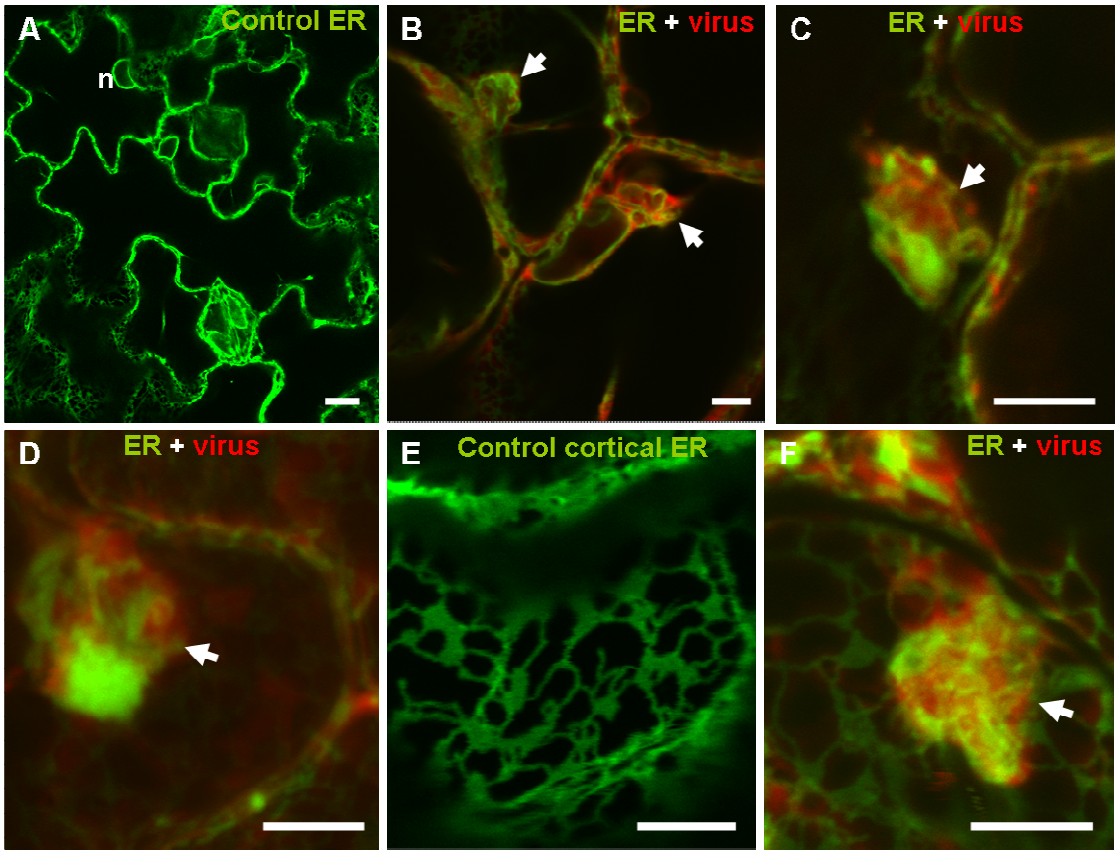

Figure 3_2: PVX on mGFP5-ER *N. benthamiana* transgenic plants
Confocal laser scanning images of control uninfected (ER in green; A,E) and PVX-infected (ER in green, PVX in red; B,C,D,F) epidermal cells of mGFP5-ER transgenic *N. benthamiana* plants to show the effect of PVX on ER morphology
A: Typical tubular ER network and nuclear envelope in control uninfected plants; B: strand of ER going into the PVX VRC (4 d.p.i.); C: ER ring in PVX VRC (4 d.p.i.); D: ER membrane aggregates observed in epidermal cells of PVX-infected leaves (7 d.p.i.); E: typical cortical ER network in control uninfected plants; F: fluorescent ER bodies in the cortical ER network in PVX-infected epidermal cells (4 d.p.i.).
d.p.i. – days of post-inoculation of the leaf tissue with PVX; n – nucleus; arrows point to PVX VRCs.
Bars, 10 µm (A) and 5 µm (B-F).

3.2.3 PVX rearranges the Golgi apparatus during VRC formation (Fig. 3_3)

Plant ER is continuous with the Golgi apparatus through transport vesicles (Boevink *et al*., 1998; Vitale and Denecke, 1999). To find out if Golgi is also involved in PVX VRC formation and establishment, transgenic *Nicotiana* plants that stably expressed a reporter for Golgi stacks (a transmembrane domain with the N-terminal signal anchor sequence of a rat sialyl transferase) (Munro, 1995) fused to GFP (ST-GFP) (Boevink *et al*., 1998; Wee *et al*., 1998), were infected with PVX (Fig. 3_1 B; Fig. 3_1 C). This protein fusion is transported from the ER to the Golgi apparatus through the COPII pathway (Boevink *et al*., 1998; Saint-Jore *et al*., 2002). The ST-GFP fusion allowed Golgi visualisation in leaf epidermal *Nicotiana tabacum* cells. The Golgi stacks in uninfected control plants (Fig. 3_3 A) were observed to be highly mobile within the cytoplasm of the epidermal cells as described in previous studies (Boevink *et al*., 1998; reviewed in Hawes, 2005).

PVX-infected ST-GFP *N. tabacum* leaves were studied under the confocal laser scanning microscope. The infected plants were compared with the uninfected control transgenic Golgi plants (Fig. 3_3 A). The Golgi membranes were discovered to be involved in PVX VRC formation (Fig. 3_3 B-E), suggesting substantial modifications in the host endomembrane system (e.g. ER and Golgi are in the VRC). The number and size of VRCs varied from cell to cell (Fig. 3_3 B). During early viral infection, the ST-GFP started to accumulate in the PVX VRC (Movie 3.2; 10 days post-inoculation) and were found to be distributed relatively uniformly within this viral structure (Fig. 3_3 B,C). In the sites of late PVX infection (at 24 days post-inoculation), the Golgi bodies formed ‘clusters’ in the VRC but the integrity of the VRC was retained (Fig. 3_3 D,E). With progressive infection, several small VRCs (less than 5 μm in size) at the cell periphery and large VRCs (over 25 μm in size) next to the cell nucleus were formed with the increased number of Golgi ‘clusters’ per infected plant cell (Fig. 3_3 E). This fluorescence pattern was observed in all repeated experiments, and no remodelling of the Golgi apparatus was detected in uninfected control plants, proving evidence that observed above morphological changes in Golgi membranes are the results of PVX infection of these plant cells.

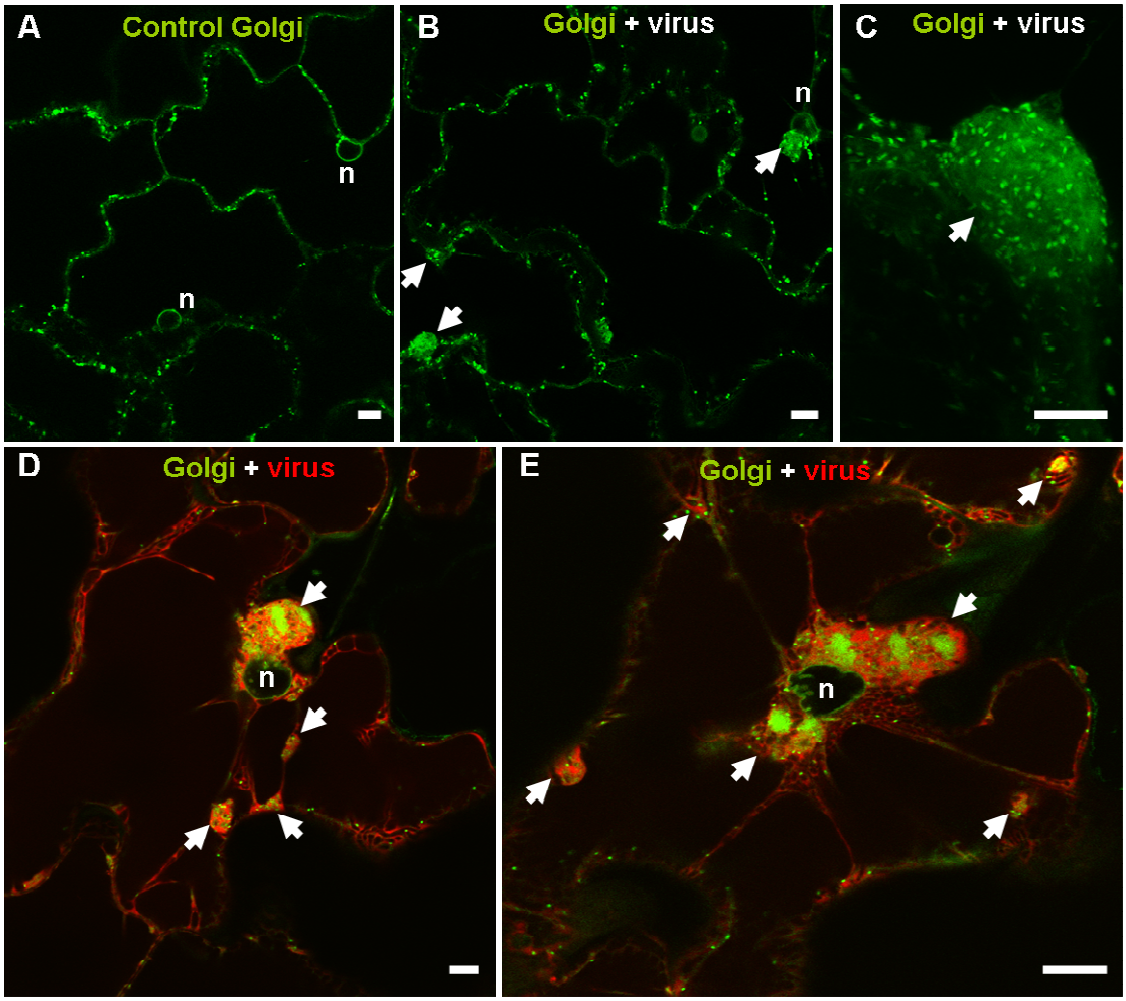

Figure 3_3: PVX on ST-GFP *N. tabacum* transgenic plants
Confocal laser scanning images of control uninfected (Golgi in green; A) and PVX-infected (Golgi in green, PVX is either unlabelled (B,C) or PVX in red (D,E)) epidermal cells of ST-GFP transgenic *N. tabacum* plants to show the effect of PVX on Golgi morphology
A: Typical Golgi apparatus in control uninfected plants; B: Golgi bodies in PVX VRCs in close association with the nucleus of virus-infected epidermal cells (10 d.p.i.); C: closer magnification showing Golgi accumulating on the VRC (10 d.p.i.); D,E: PVX-infected epidermal cells showing developed perinuclear VRCs (24 d.p.i.) with Golgi clusters in them.
d.p.i. – days post-inoculation of PVX; n – nucleus; arrows point to PVX VRCs.
Bars, 10 µm.

3.2.4 PVX recruits actin microfilaments during VRC establishment (Fig. 3_4)

Plant cortical ER moves along actin cables (Quader *et al*., 1987; Boevink *et al*., 1998) and it is also continuous with actin in plasmodesmata that provide continuity of ER between neighbouring cells (Roberts and Lucas, 1990; Ding *et al*., 1992; Lucas and Wolf, 1993; White *et al*., 1994; Boevink *et al*., 1998; Botha and Cross, 2000). To find out if actin is also involved in PVX VRC formation and establishment, transgenic *Nicotiana* plants expressing a reporter for actin, fimbrin actin binding domain 2 fused to GFP (FABD2-GFP) (Sheahan *et al*., 2004), were infected with PVX (Fig. 3_1 B; Fig. 3_1 C).

As above, the infected *N. tabacum* leaves were examined under the confocal laser scanning microscope and compared with uninfected control plants (Fig. 3_4 A). Unpolymerised actin was found to be recruited to the VRC during the formation of the PVX infection site (Fig. 3_4 B-E). These are the first data showing that F-actin is recruited to the PVX replication complex. Recruited host actin was found to be internalised into the VRC with the formation of 'spider web'-like arrays of actin microfilaments (Fig. 3_4 B,C). In addition, actin was found around specific sub-compartments of the PVX VRC (Fig. 3_4 D,E). The circular rings of actin microfilaments around the VRC sub-compartments provide additional evidence that the PVX VRC is a complex compartmentalised structure containing domains with specific, defined function. Some 'empty' sub-compartments (Fig. 3_4 D,E) were identified in actin-PVX localisation studies, suggesting that these 'empty' spaces could be the sites of the recruitment of the plant host endomembrane system or the viral components of PVX. Actin strands were also detected around the whole VRC (Fig. 3_4 E). However, these host cytoskeleton elements associated with the VRC not only surrounded this viral structure but, in addition, actin cables were found to be continuous with radiating cortical actin strands that exited the VRC towards the cell periphery (Fig. 3_4 B,C,E), suggesting that virus may employ this route for movement of its genome from the VRC to and through PD.

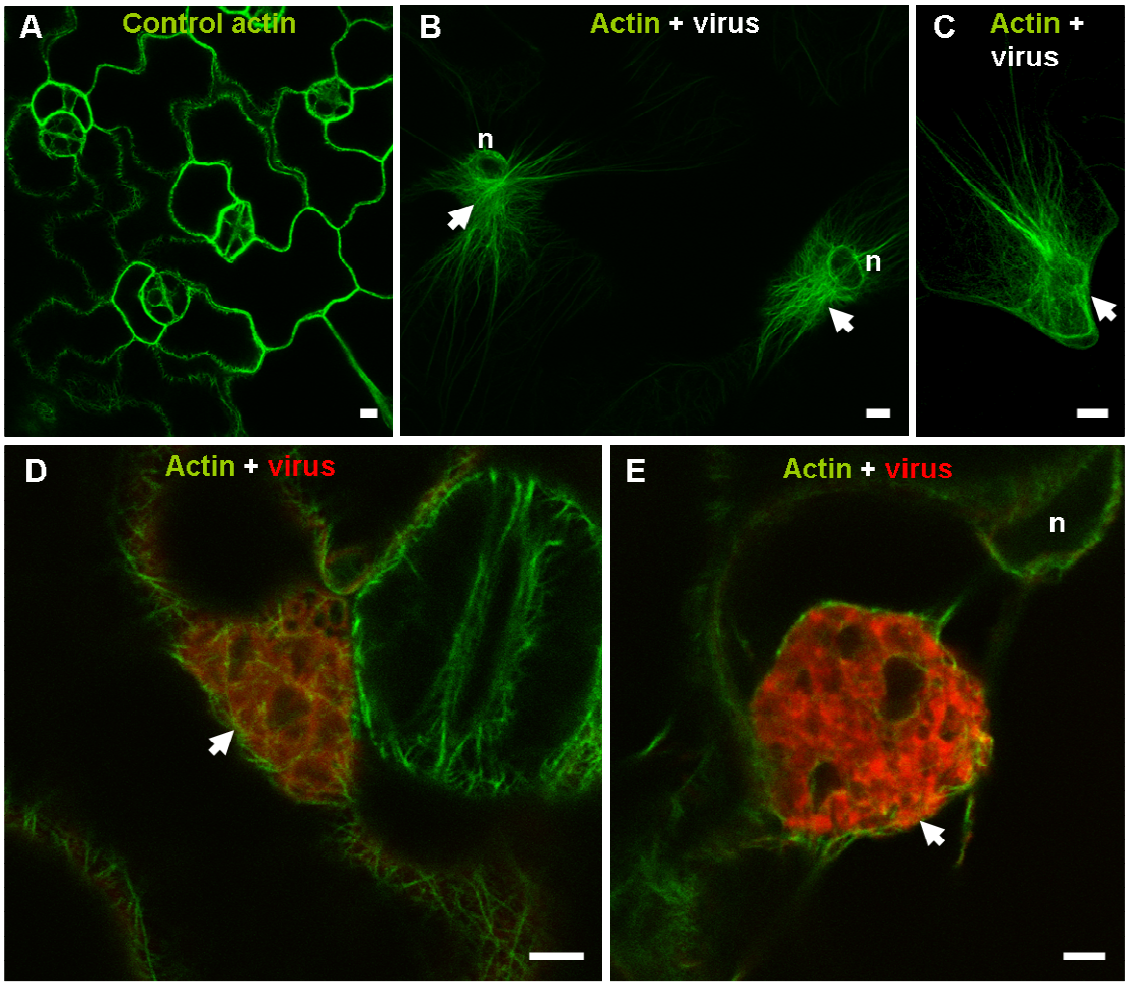

Figure 3_4: PVX on FABD2-GFP *N. tabacum* transgenic plants
Confocal laser scanning images of control uninfected (actin in green; A) and PVX-infected (actin in green, PVX is either unlabelled (B,C) or PVX in red (D,E)) epidermal cells of FABD2-GFP transgenic *N. tabacum* plants to show the effect of PVX on actin morphology
A: Typical actin microfilaments in control uninfected plants; B: PVX-infected epidermal cell with actin recruited into the VRC (due to low gain the cortical actin is not visualised in this image); B,C: 'spider web'-like actin in PVX VRCs (14 d.p.i.) in close association with the nucleus of virus-infected epidermal cells; D: actin microfilaments in the VRC (6 d.p.i.); E: actin surrounds the PVX VRC and forms rings around the VRC sub-compartments (12 d.p.i.).
d.p.i. – days post-inoculation of PVX; n – nucleus; arrows point to PVX VRCs.
Bars, 10 µm (A-C), 5 µm (D,E).

3.2.5 PVX does not recruit intact microtubules into the VRC (Fig. 3_5)

Actin microfilaments together with microtubules compose the plant cytoskeleton (reviewed in Takemoto and Hardham, 2004). To examine whether microtubules are involved in PVX VRC formation, transgenic *Nicotiana* plants that stably express a reporter fused to tubulin (GFP-TUA6) (Ueda *et al*., 1999) were infected with PVX (Fig. 3_1 C). PVX-infected GFP-TUA6 *N. benthamiana* leaves were studied under the confocal laser scanning microscope and were compared with the uninfected control plants (Fig. 3_5 A). Microtubules were abundant in both infected and uninfected cells but tubulin was unpolymerised within the VRC (Fig. 3_5 B-E). However, the host tubulin was found to be diffuse in the VRC (Fig. 3_5 B,E), and unlike actin microfilaments, no 'spider web'-like arrays of tubulin were detected in the infected cells. No obvious compartmentation of tubulin was found within the VRC structure. Also, no 'unbroken' microtubules were seen around the viral replication complex. The host tubulin in the VRC was not detected to be continuous with intact microtubules of the cell. Intact microtubules were not found to exit the VRC, suggesting that virus may disrupt microtubule assembly during PVX infection and indicates that intact microtubules are not involved in PVX VRC establishment, and consequently in viral replication and spread.

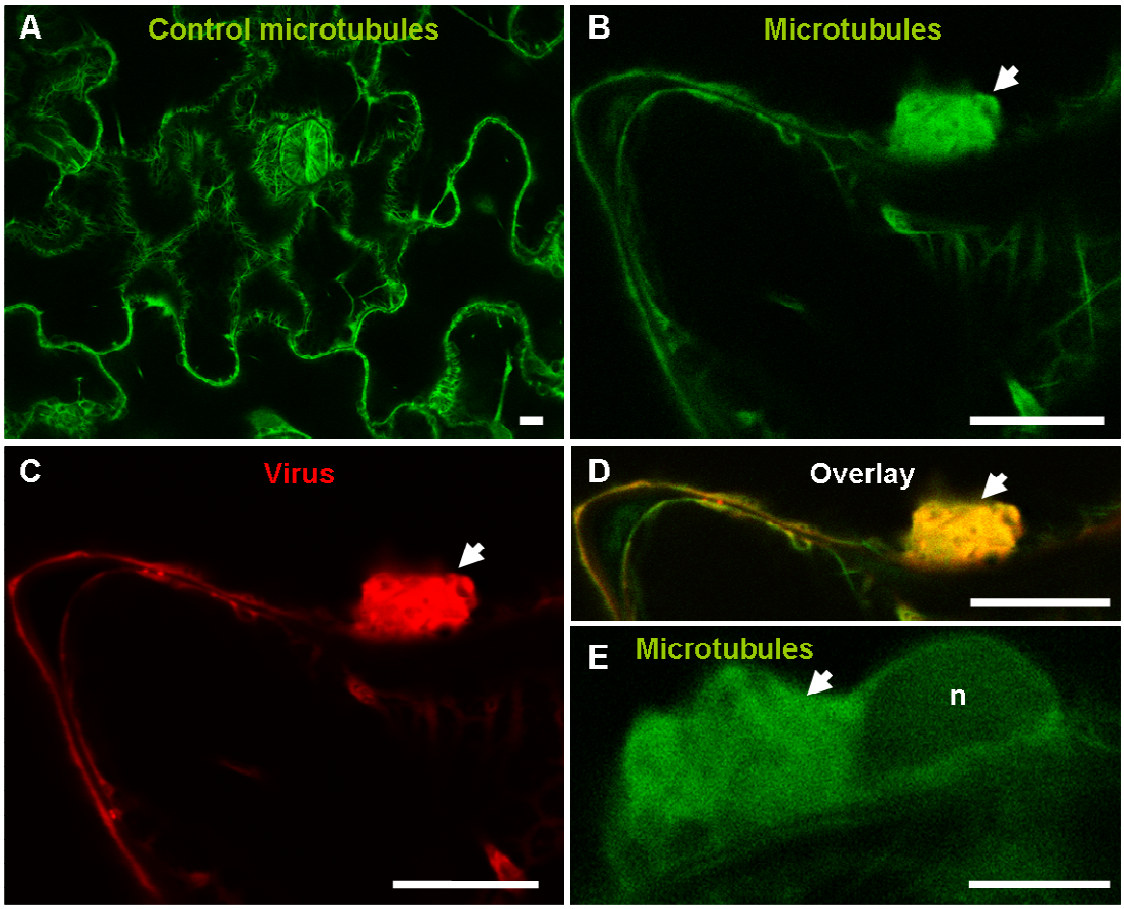

Figure 3_5: PVX on GFP-TUA6 *N. benthamiana* transgenic plants
Confocal laser scanning images of control uninfected (microtubules in green; A) and PVX-infected (microtubules in green; PVX in red (B-D)) epidermal cells of GFP-TUA6 transgenic *N. benthamiana* plants to show the effect of PVX on microtubules morphology
A: Typical microtubules in control uninfected plants; B, E: microtubules (green channel) in the PVX VRC of a virus-infected epidermal cell (5 d.p.i.); C: PVX VRC (red channel) in the epidermal cell (5 d.p.i.); D: overlay image of B and C (microtubules + PVX) showing a PVX VRC (5 d.p.i.).
d.p.i. – days post-inoculation of PVX; arrows point to PVX VRCs; n – nucleus.
Bars, 10 µm.

3.2.6 Colocalisation of ER and actin in PVX-infected cells (Fig. 3_6)

To examine how the VRC is structured in relation to different organelles, transgenic *Nicotiana* plants expressing mGFP5-ER were infected with PVX (Fig. 3_1 B). An actin marker (Fig. 3_1 A) was subsequently bombarded into the PVX infection. Infected *N. benthamiana* leaves were studied under the confocal laser scanning microscope. As before, the ER membranes were detected in the VRC (Fig. 3_6 A). Actin microfilaments were also found to be internalised into this viral structure (Fig. 3_6 B). In addition, when the two signals were overlaid, actin cables were observed around the VRC and in specific sub-domains of the VRC (Fig. 3_6 C). The individual sub-compartments of the ER were found to be interconnected by intact actin filaments, as well as surrounded by actin from the outside edges of these ER sub-domains (Fig. 3_6 D). ER and actin host organelles colocalised in discrete areas within the VRC (Fig. 3_6 E), suggesting that each of these components is recruited into the same sub-compartment of the VRC. ER-/actin-free sub-compartments were also identified within the VRC, and separate domains, containing only ER or only actin were also found (Fig. 3_6 C,E). These results indicate that there are other sub-domains within the VRC, occupied by other viral or host components.

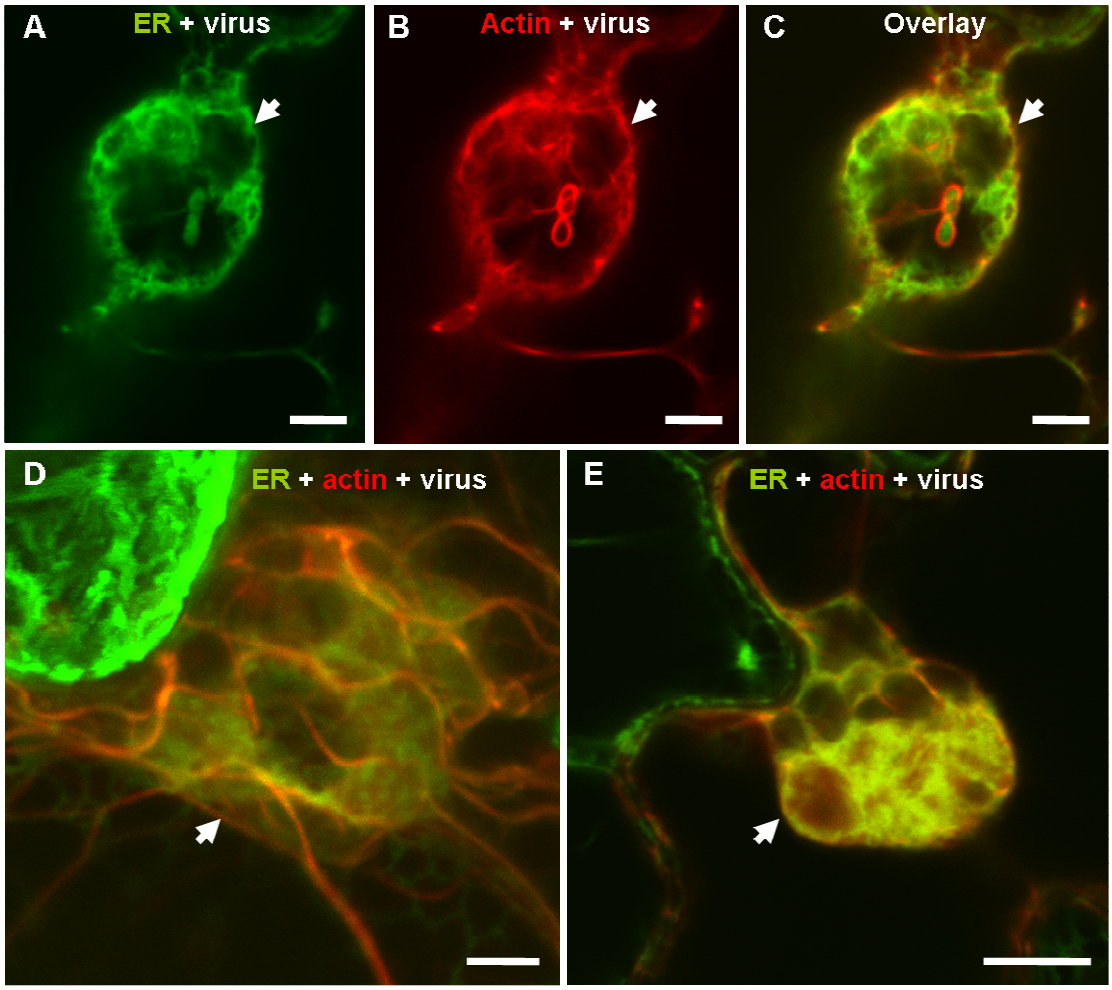

Figure 3_6: PVX on mGFP5-ER *N. benthamiana* transgenic plants + actin marker

Confocal laser scanning images of PVX-infected (PVX is unlabelled) epidermal cells of mGFP5-ER transgenic *N. benthamiana* plants (ER in green) cobombarded with actin marker (actin in red)

A: ER (green channel) and B: actin (red channel) in the PVX VRC of a virus-infected epidermal cell; C: overlay image of A and B (ER + actin) (13 d.p.i. + 1 d.p.b.); D,E: overlay images (ER + actin) showing PVX VRCs; D: 15 d.p.i. + 9 d.p.b. E: 15 d.p.i. + 1 d.p.b.

d.p.i. – days post-inoculation of PVX; d.p.b. – days post-bombardment of actin marker; arrows point to PVX VRCs.

Bars, 5 µm.

3.2.7 Colocalisation of Golgi and actin in PVX-infected cells (Fig. 3_7)

Next, transgenic *Nicotiana* plants stably expressing ST-GFP were infected with PVX (Fig. 3_1 B) followed by bombardment of an actin marker (Fig. 3_1 A) into the infection sites. As above, PVX-infected ST-GFP *N. tabacum* leaves were studied under the confocal laser scanning microscope. As expected, the Golgi membranes were detected in the VRC (Fig. 3_7 A,D). The actin microfilaments were also found to be internalised into this viral structure, as well as detected around the VRC (Fig. 3_7 B,E). In addition, when the two signals were overlaid, the Golgi bodies completely colocalised with the host actin, appearing superimposed on the actin strands (see also Boevink *et al*., 1998) within the VRC and between the VRC and the cell cortex (Fig. 3_7 C,F). The actin cables with the Golgi bodies moving on them (Movie 3.3a,b; 10 days post-inoculation) were found to be continuous with radiating cortical actin strands that exited the VRC towards the cell periphery (Fig. 3_7 C,F). The Golgi stacks together with the actin network formed VRCs resembling a 'birds nest'-like structure in the infected cell (Fig. 3_7). In addition, different sized (smaller Fig. 3_7 C; and bigger Fig. 3_7 F) actin- and Golgi-free sub-compartments were identified within the VRC. These data show that actin and Golgi colocalise in the VRCs and that there are Golgi-/actin-free sub-compartments probably occupied by additional organelles or by PVX-encoded proteins.

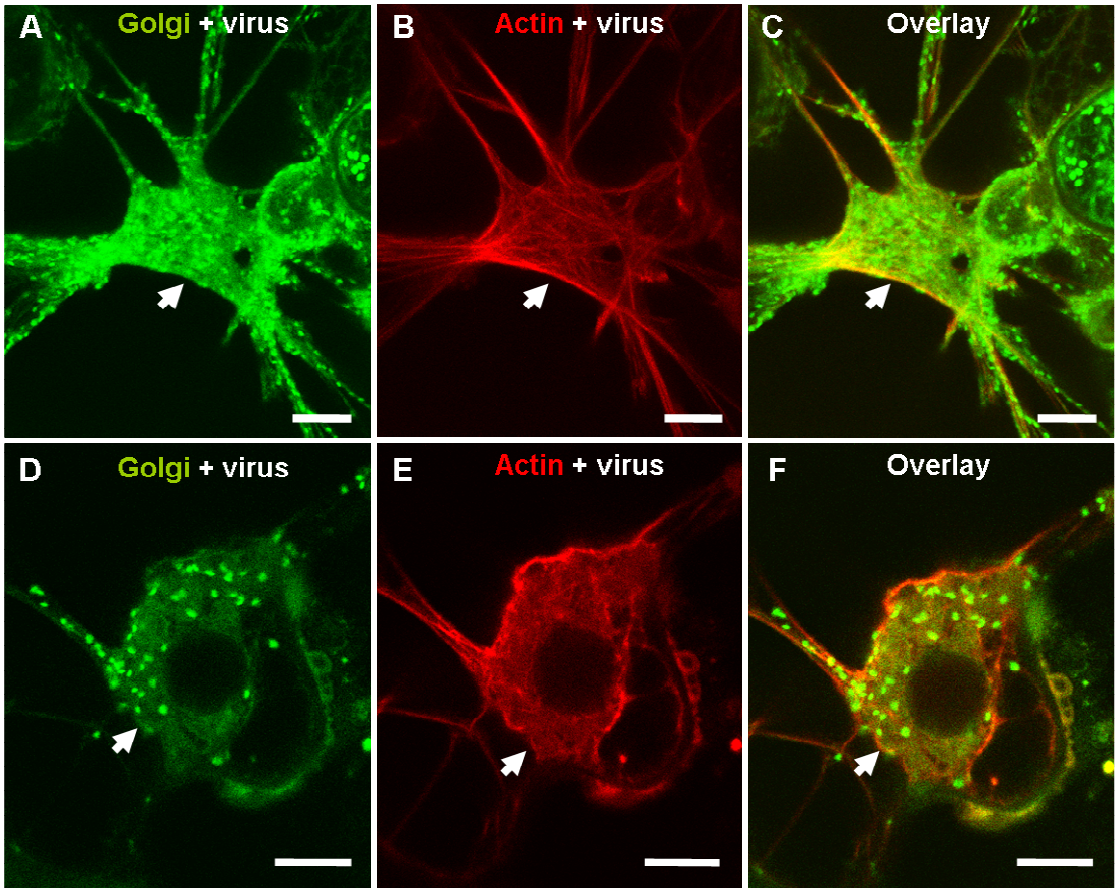

Figure 3_7: PVX on ST-GFP *N. tabacum* transgenic plants + actin marker
Confocal laser scanning images of PVX-infected (PVX is unlabelled) epidermal cells of ST-GFP transgenic *N. tabacum* plants (Golgi in green) cobombarded with actin marker (actin in red)
A,D: Golgi (green channel) and B,E: actin (red channel) in the PVX VRC of a virus-infected epidermal cell; C: overlay image of A and B (Golgi + actin); F: overlay image of D and E (Golgi + actin) showing PVX VRCs.
A-C: 10 d.p.i. + 1 d.p.b.; D-F: 10 d.p.i. + 2 d.p.b.
d.p.i. – days post-inoculation of PVX; d.p.b. – days post-bombardment of actin marker; arrows point to PVX VRCs.
Bars, 10 µm.

3.3 Discussion

3.3.1 ER remodelling during PVX infection

My data show that PVX reorganises the host ER network during the VRC establishment. The ER modifications triggered by PVX infection resemble those induced by a wide range of viruses. Many animal (+)RNA viruses are known to use the ER as a site of replication (Suny *et al*., 2000; Mackenzie, 2005). A variety of plant (+)RNA viruses such as tobacco mosaic virus (Esau and Cronshaw, 1967; Heinlein *et al*., 1998; Reichel and Beachy, 1998; Mas and Beachy, 1999; Sanfaçon, 2005), tobacco etch virus (Schaad *et al*., 1997), brome mosaic virus (Restrepo-Hartwig and Ahlquist, 1996, 1999; reviewed in Noueiry and Ahlquist, 2003), cowpea mosaic virus (Carette *et al*., 2000), peanut clump virus (Dunoyer *et al*., 2002), poa semilatent virus (Solovyev *et al*., 2000; Zamyatnin *et al*., 2002), grapevine fanleaf virus (Ritzenthaler *et al*., 2002), red clover necrotic mosaic virus (Turner *et al*., 2004), beet yellows closterovirus and alfalfa mosaic virus (Huang and Zhang, 1999; Peremyslov *et al*., 1999) also use ER-derived membranes for their replication processes. For instance, replication of peanut clump virus takes place on modified membranes of the ER and the Golgi apparatus (Dunoyer *et al*., 2002) while cowpea mosaic virus forms large ER perinuclear fluorescent aggregates (Carette *et al*., 2000) similar to those induced by PVX infection (Fig. 3_2 D). Association of the PVX TGB2 and TGB3 proteins with the ER membrane has been under extensive study (Zamyatnin *et al*., 2002; Krishnamurthy *et al*., 2003; Ju *et al*., 2005, 2007, 2008; Schepetilnikov *et al*., 2005; Samuels *et al*., 2007). In addition, association of PVX VRCs with different cellular components, including the ER was identified in early EM studies (Kozar and Sheludko, 1969; Stols *et al*., 1970). These data have been largely ignored in recent reports of PVX infection. In this study, remodelling and redistribution of the host ER into the developing VRC is presented for the first time. In this work, the degree of ER incorporation into the VRC was found to correlate with the stage of viral infection. These data highlight that the ER morphology and mobility changes once the infection progresses. This begins with a highly mobile ER component moving in and out of the VRC (Movie 3.1a,b) (Fig. 3_2 B) and, over

time, results in formation of the large, perinuclear ER membrane aggregations within the VRC (Fig. 3_2 D). The mobile ER network moving in and out of the VRC indicates that during early infection PVX extensively recruits these host membranes into the forming VRC. Over time, the ER membranes appear to become trapped within the VRC and may serve as centres for active viral RNA synthesis and PVX replication. Large fluorescent ER aggregates at later stages of viral infection may form due to the increased reorganisation of the ER network with developing infection, suggesting that a general redistribution of host membranes in the infected cell may also take place. Large perinuclear ER 'clusters' may derive from existing tubular ER elements or perhaps from *de novo* membrane synthesis. Additionally, the PVX VRC was found to be continuous with the cortical ER network in this study (Fig. 3_2 F). Unlike grapevine fanleaf virus (Ritzenthaler *et al*., 2002), peanut clump virus (Dunoyer *et al*., 2002), cowpea mosaic virus (Carette *et al*., 2000) and tobacco mosaic virus (Reichel and Beachy, 1998), the morphology of the cortical ER was not disrupted by the presence of PVX. My hypothesis is that, unlike these viruses, PVX may utilise unmodified cortical ER network for movement of its genome through PD. Differences in the morphology of the host cortical ER induced by different plant virus groups, and even viruses within the same family, suggest that these viruses may use dissimilar mechanisms when recruiting cellular organelles into the VRC and establishing a movement pathway to PD.

3.3.2 Golgi redistribution during PVX infection

My data also show that PVX rearranges the Golgi apparatus during VRC formation. Golgi membranes were also found to be involved in the establishment of the VRC (Fig. 3_3 B-E) together with the ER, indicating that ER is not the only contributor to the morphogenesis of the VRC. Like PVX, a number of animal and plant viruses have been found to replicate in close association with Golgi-derived membranes. For example, flavivirus RNA replication has been suggested to take place in vesicles generated from the *trans*-Golgi membranes (Mackenzie *et al*., 1999). Membranes of the ER, Golgi apparatus and lysosomes have been identified in the poliovirus-induced vesicles in animal cells (Dales *et al*., 1965; Caliguri and Tamm, 1970; Bienz

et al., 1987; Schlegel *et al*., 1996). These data suggest that sub-cellular Golgi redistribution is a common event during a wide range of infections of both (+)RNA mammalian and plant viruses. Like ER, the Golgi apparatus was found to undergo different changes in its organisation during PVX infection. At the beginning of PVX infection, the Golgi bodies were observed to accumulate within the developing VRC (Fig. 3_3 B,C). This is probably achieved by Golgi bodies moving on the actin filaments targeted to the developing VRC. The Golgi 'clusters' formed at the later PVX infection events (Fig. 3_3 D,E) are probably due to reabsorption of the Golgi membranes into the VRC, forming an endomembrane sub-compartment. As virus infection progresses, PVX may reorganise host membranes, and the amorphous Golgi 'clusters' observed at later stages of infection are likely to be comprised of disassembled lipids and proteins. The mechanism of such cellular changes is unknown (Takemoto and Hardham, 2004). Such a dramatic structural reorganisation of host organelles is likely a product of interactions between the host components of the infected cell and the virally-encoded proteins. The Golgi and the ER membranes may not be the only contributors to the morphogenesis of the VRC as the association of PVX VRCs with vacuoles and mitochondria was also identified in early EM studies (Kozar and Sheludko, 1969; Stols *et al*., 1970). These results indicate that other host membranes can potentially make a contribution towards the VRC structure and could also be possible sites for PVX replication.

3.3.3 Origin of the modification of cellular membranes

The modifications in cellular membrane structure could involve proliferation and invaginations of host membranes, and possibly vesiculation to expand the surface of infection. One possible explanation of the virus-induced aggregates formed in PVX-infected cells is a clustering of vesicles derived from the ER or Golgi. A number of viruses have been also shown to induce vesiculation during replication processes, among them comoviruses (Eggen and van Kammen, 1988), potyviruses (Lesemann, 1988), polioviruses (Semler *et al*., 1988) and tombusviruses (Burgyan *et al*, 1996; Rubino and Russo, 1998; Rubino *et al*., 2001; Weber-Lotfi *et al*., 2002). Most of the vesicles induced during replication of animal viruses are surrounded by double

bilayers of lipids, indicating that modification of cellular membrane structure requires a more complex packaging mechanism for vesicle formation than a simple membrane budding process (Schlegel *et al*., 1996; Pedersen *et al*., 1999).

3.3.4 Potential involvement of the plant cytoskeleton in PVX replication and movement

This is the first report that demonstrates recruitment of unpolymerised actin microfilaments into the PVX VRC during the formation of the infection site (Fig. 3_4 B-E). Actin was found to form 'spider web'-like arrays of microfilaments within the VRC (Fig. 3_4 B,C). In addition, actin was detected around the VRC (Fig. 3_4 E) and around specific sub-compartments within this structure (Fig. 3_4 D,E), supporting a hypothesis that the PVX VRC is highly compartmentalised and contains a series of spatially functioning sub-domains of undefined viral function. Some 'empty' sub-compartments (Fig. 3_4 D,E) were also identified, indicating and these 'vacant' regions may be the sites of recruitment of the plant host endomembrane system or the PVX gene products produced during infection. Importantly, actin cables were found to be continuous with radiating cortical actin strands that exited the VRC towards the cell periphery (Fig. 3_4 B,C,E), suggesting that PVX is very likely to take this pathway for movement of its genome from a VRC to and through PD.

Certain animal viruses have been found to be associated with host cytoskeleton systems, both microtubules (Sodeik *et al*., 1997; Suomalainen *et al*., 1999) and actin microfilaments (Sundell and Singer 1991; Bassel and Singer 1997; Cudmore *et al*., 1997; Roper *et al*., 1998) during viral entry, replication and translocation within the host cell (Radtke *et al*., 2006; Lai *et al*., 2008). The plant cytoskeleton has been also implicated in replication and movement of different viruses (see Chapter 1). It has been also shown that some movement proteins of plant viruses (for example, TMV MP) may interact with mictrotubules (Heinlein *et al*., 1995) and with microfilaments (McLean *et al*., 1995; Liu *et al*., 2005). It has also been proposed that both actin microfilaments and microtubules may act as host channels for vRNA-MP and/or

virion complexes to target cell PD (Carrington *et al*., 1996; Lazarowitz and Beachy, 1999; Tzfira *et al*., 2000; Heinlein, 2002), possibly involving host myosin motors (Liebe and Quader, 1994; Prokhnevsky *et al*., 2005; Harries *et al*., 2009b). However, little is known about the nature and regulation of virus-host cytoskeleton interactions (Stidwill and Greber, 2000).

The data of this chapter support the hypothesis that host actin is involved in trafficking of PVX genome to PD. These data also support recent findings showing that the intercellular movement of PVX is influenced by disruption of actin microfilaments, suggesting that the intercellular trafficking of this plant virus is dependent on the host actin cytoskeleton. Like PVX, intercellular spread of TMV and tomato bushy stunt virus was also found to be influenced by disruption of actin microfilaments, suggesting that the intercellular movement of these viruses is also dependent on actin. Movement of turnip vein-clearing virus (a tobamovirus that is closely related to TMV) was not arrested by application of the actin inhibitor, latrunculin B, indicating that viruses even from the same group may differ in their utilisation of the plant cytoskeleton elements (Harries *et al*., 2009b).

My data also illustrate that intact microtubules are not recruited into the PVX VRC. In stead, a pool of diffuse unpolymerised tubulin was observed within the VRC (Fig. 3_5 B,E). Unlike actin microfilaments, no 'spider web'-like arrays of tubulin were detected in the infected cells and no intact microtubules were found to exit the VRC. These data suggest that PVX may disrupt microtubule organisation during infection, and that this host organelle is not involved in PVX VRC establishment. My data also imply that PVX may use host actin for translocation between the VRC and the cell periphery. This hypothesis is supported by various studies showing that actin microfilaments are involved in viral transport processes when microtubules are depolymerised (Ritzenthaler *et al*., 1995; Lazarowitz and Beachy, 1999; Laporte *et al*., 2003). Microtubule depolymerisation has been also reported for vaccinia virus infection (Ploubidou *et al*., 2000), suggesting that this event also takes place during infection of animal viruses. In the future studies it would be interesting to examine if treatment with mictrotubule-depolymerising agents (oryzalin, nocodazole), and the

application of a microtubule-stabilising drug (taxol) during PVX infection interfere with viral replication and spread. Although myosins are suggested to be involved in transport of organelles and ER along actin microfilaments (Liebe and Quader, 1994), an involvement of myosins as candidate motor proteins for facilitating movement of different animal (Sasaki *et al*., 1995; Forest *et al*., 2005; Greber and Way, 2006) and plant viruses (Harries *et al*., 2009b) has also been documented. It is also possible that some viruses may make use of the energy released during depolymerisation of tubulin (Molodtsov *et al*., 2005).

The data of this chapter suggest that both plant actin cytoskeleton and endomembrane system are associated with PVX VRC. The presence of actin and cortical ER within PD supports the hypothesis that the cytoskeleton is required for virus movement (White *et al*., 1994; Nelson, 2005), and one possible pathway for plant viruses to spread through plasmodesmata is via the desmotubule (Cantrill *et al*., 1999; reviewed in Roberts and Oparka, 2003).

3.3.5 Colocalisation of ER, actin and Golgi in PVX-infected cells

Colocalisation data support the idea that PVX VRCs are complex compartmentalised structures within which host organelles are spatially separated. These data help to build a structural VRC model, in which intact actin filaments surround the individual sub-compartments of the ER within the VRC (Fig. 3_6 C,D; Fig. 3_7 B,E). Within VRCs, ER and actin were also colocalised in the same sub-compartments (Fig. 3_6 E). ER/actin-free sub-domains were also identified within the VRC, as well as separate domains that were free of ER or free of actin (Fig. 3_6 C,E). These results suggest that there are other sub-compartments within PVX VRCs, probably taken up by other viral or host components. The Golgi membranes were found to colocalise with actin cables within the PVX VRC and on the exit from this viral structure towards the cell cortex through radiating cortical actin strands (Fig. 3_7 C,F). Such an organisation of recruited host organelles in the VRC is likely to have an important role for the compartmentation of vRNA and viral proteins synthesised during infection.

3.3.6 Potential roles of host organelles within the PVX VRC

Remodeling and recruitment of host membranes and cytoskeleton elements is likely to be a critical event in the PVX infection process in order to sustain viral replication, and is also a potentially crucial step for viral spread between cells. Various reasons are possible for the recruitment of cellular membranes and cytoskeleton into the VRC (Salonen *et al*., 2005). One possible reason is that these viral structures are formed to enlarge the surface area for viral RNA synthesis and replication. This would lead to an increase in the local concentration of the essential RNA replication machinery components. In addition, recruited host membranes may help to protect the replicating virus from defense systems of the host plant. If the virus is wrapped in host membranes, it is more difficult for the plant to recognise it as its pathogen. Therefore, alterations in membrane structure potentially create isolated compartments for replication within the VRC protecting the newly synthesised vRNA molecules from degradation and RNA silencing (Dunoyer *et al*., 2002; Schwartz *et al*., 2002, 2004; Sanfaçon, 2005). To achieve this protection, and to successfully replicate and move to adjacent cells, it is important for the virus to have the required plant components in the correct amounts, at the right time, and in the right place within the host cell (Sanfaçon, 2005). Importantly, the virus may not only direct host functions, it may also coordinate its own replication and movement machinery to avoid irreversible damage to the host plant (Salonen *et al*., 2005; Sanfaçon, 2005). Finally, an established VRC is not just a static anchoring site for essential components of the replication complex (Schwartz *et al*., 2002, 2004; Sanfaçon, 2005). By recruiting plant cytoskeleton to the VRC, the virus generates a transport pathway for its movement to infect healthy adjacent plant cells. Therefore, the successful formation of PVX VRCs determines the success of viral cell-to-cell movement in the host plant.

3.3.7 Conclusions

In general, PVX infection caused a complex remodeling of the ER network, a redistribution of the Golgi bodies in the cell and an extensive recruitment of actin

microfilaments into the forming VRC. The host components within the VRC were found to be continuous with the cortical ER/actin network located close to the cell periphery. This involvement of host plant organelles in the VRC has not previously been reported for PVX. All of these morphological modifications to host organelles may generate a PVX VRC structure that facilitates successful viral replication and determines the success of viral movement between cells.

4. Analysis of PVX VRC formation in relation to viral gene products

4.1 Aim

The functional significance of PVX VRC and the role of viral proteins for replication and movement remain poorly understood. For example, TGB2 and TGB3 have not yet been shown to contribute to the viral replication process, although they are required for movement (Schepetilnikov *et al*., 2005). Available research data suggest that PVX uses cellular pathways for translocation of its genome. However, there is no clear picture of the early stages of viral infection events. Furthermore, there is no experimental evidence to show whether the TGB2/TGB3-related vesicles contain vRNA/CP/TGB1 or virions/STPs for PVX movement. It is also yet unclear if TGB2 and TGB3-induced vesicles can traffic from cell-to-cell. Mutational analysis of the PVX genome shows that all 3 TGBs (and viral CP) are required for cell-to-cell movement (Huisman *et al*., 1988; reviewed in Koonin and Dolja, 1993; Angell *et al*., 1996; Verchot-Lubicz, 2005). It is likely that these viral proteins interact with each other to allow intercellular transport, but the nature of these interactions and the precise function of the TGB proteins and viral CP in the movement processes of PVX has not yet been established. The hypothesis I suggest is that PVX transport is dependent on successful viral replication and the formation of the VRC.

The previous chapter examined the recruitment of host organelles into the PVX VRC. The aim of this chapter was to pinpoint the location of the TGB proteins and the CP of PVX during infection. While TGBs have been studied extensively in the past (see Chapter 1), there is confusion as to their location and function. In this chapter, the sub-cellular localisation of PVX TGB proteins and CP during the infection process was examined using both red and green fluorescent reporter constructs. PVX TGB proteins were investigated in relation to the formation of the PVX VRC, both in the absence and presence of viral infection. The structure of the PVX VRC was also explored by colocalisation of viral proteins with components of the host plant. Mutational analysis

was used to determine which viral gene products are required for the VRC formation and for the recruitment of host organelles into the VRC.

4.2 Results

4.2.1 Plasmids used in this study (Table 4.1, Fig. 4_1)

To carry out *in vivo* plant cell imaging, PVX and a variety of reporters of cellular or viral components were introduced into the same epidermal plant cell using different approaches: PVX was inoculated onto (pTXS), agroinfiltrated into (pGR106), or bombarded into (pRTL2) non-transgenic plants or transgenic plants expressing ER, Golgi, actin and secondary PD markers.

To express PVX proteins in a plant cell, constructs were used in which the proteins of interest were expressed either (i) transiently from a non-viral pRTL2 expression vector as fusions to fluorescent proteins under the control of CaMV 35S promoter or (ii) from a PVX-based pGR106 vector under the control of the CaMV 35S promoter. To express endogenous TGB1 from a virus-based vector, a PVX pGR106 endogenous TGB1-mCherry construct was designed in which the TGB1 coding sequence was tagged with mCherry (mCherry fluorescent protein was fused in frame to the 3' end of the PVX TGB1 gene) and was expressed in the viral pGR106 construct. In this construct the TGB1 protein was expressed from its own subgenomic promoter within the PVX genome. Two endogenous TGB1 constructs were generated (Fig. 4_1 J; Fig. 4_1 K). The first construct (Fig. 4_1 J) was found to be infectious in the host plant. The second construct, which contained the GFP-2A-CP insertion (Fig. 4_1 K), was not infectious. Many viruses are known to be limited by the size of the insert (Neuthaus and Boevink, 2001). It is very likely that this virus did not tolerate insertion of additional gene sequences (GFP-2A-CP) into its genome.

The biolistic bombardment assay leads to transient gene expression restricted to single epidermal plant cells. The sites of bombardment (small rings of tissue on the leaf) were normally seen after 1 day post-bombardment. The time of appearance of bombarded sites on the leaf was usually dependent on different factors, such as plant condition, pressure of bombardment and the amount of gold used for the bombardment (Neuthaus and Boevink, 2001). Usually two, but not more than three, bombardments were made per individual plant leaf in order to minimise plant tissue damage and the data were collected the day after bombardment.

The centre of the infection events was studied in this chapter, apart of the localisation of the CP and the TGB1 protein experiments in which both the leading edge of infection site and the centre of infection were examined.

Plasmids used in this results chapter can be divided into two groups which are listed in Table 4.1

1) According to the method of plasmid delivery:

i) Binary plasmids for transient plant transformation by agroinfiltration:
pGR106 (Jones *et al*., 1999)
pGWB402Ω (Nakagawa *et al*., 2007)
ii) Bombardment plasmids for transient plant transformation by biolistic bombardment:
pRTL2 (Restrepo *et al*., 1990)
iii) Plasmids containing T7 polymerase promoter for synthesis of infectious PVX RNA transcripts for *in vitro* transcription, reassembly and inoculation:
pTXS (Chapman *et al*., 1992)

2) According to the expressed marker or gene:

Plasmid name	Expressed marker or gene	Figure number
Viral gene markers:		
pRTL2.TGB1-mCherry	red TGB1 viral movement protein reporter	Fig. 4_1 A

pRTL2.GFP-TGB2	green TGB2 viral movement protein reporter	Fig. 4_1 B
pRTL2.TGB3-GFP	green TGB3 viral movement protein reporter	Fig. 4_1 C
Organelle markers:		
pRTL2.ER-tdTomato	red ER marker	Fig. 4_1 D
pRTL2.Lifeact-tdTomato	red actin marker	Fig. 4_1 E
pGWB402Ω.Lifeact-TagRFP	red actin marker	Fig. 4_1 F
Transgenic Nicotiana plants that stably express:		
TMV MP-GFP	green reporter for secondary PD	see Table 2.1 in Chapter 2 for more details
mGFP5-ER	green reporter for ER	
ST-GFP	green reporter for Golgi	
FABD2-GFP	green reporter for actin	
PVX-carrying plasmids:		
pTXS.GFP-2A-CP 'overcoat' virus	PVX with green fluorescent protein fused to coat protein, *in vitro* transcription vector	Fig. 4_1 G
pRTL2.GFP-2A-CP 'overcoat' virus	PVX with green fluorescent protein fused to coat protein, bombardment vector	Fig. 4_1 H
pGR106.CFP	PVX with cyan fluorescent protein, binary vector	Fig. 4_1 I
pGR106.TGB1-mCherry	PVX with endogenous TGB1 fusion to red FP (mCherry); no FP fusion to coat protein	Fig. 4_1 J
pGR106.TGB1-mCherry, GFP-2A-CP 'overcoat' virus	PVX with endogenous TGB1 fusion to red FP (mCherry) and with green fluorescent protein fused to coat protein	Fig. 4_1 K
PVX mutant constructs:		
1) PVX mutant constructs cloned during this thesis:		
pGR106.a-g.GFP a. ΔTGB1 b. ΔTGB2 c. ΔTGB3 d. ΔTGB1-ΔTGB2 e. ΔTGB1-ΔTGB3 f. ΔTGB2-ΔTGB3 g. ΔTGBs	PVX with mutated viral proteins and with green fluorescent protein	Fig. 4_1 L
h. pGR106.mCherry.ΔCP i. pGR106.pum.mCherry.ΔCP	PVX with deleted viral coat protein and with red fluorescent protein	
pGR106.j-l.GFP-2A-CP	PVX with mutated viral proteins	

j. ΔTGB1-ΔTGB2 k. ΔTGB1-ΔTGB3 l. ΔTGB2-ΔTGB3	and with green fluorescent protein fused to coat protein	
2) PVX mutant constructs subcloned from 1) by Dr. Jens Tilsner:		
pGR106.ΔTGB1.GFP-2A-CP 'overcoat' virus	PVX with mutated TGB1 protein and with green fluorescent protein fused to coat protein	Fig. 4_1 M
pGR106.ΔTGB2.GFP-2A-CP 'overcoat' virus	PVX with mutated TGB2 protein and with green fluorescent protein fused to coat protein	Fig. 4_1 N
pGR106.ΔTGB3.GFP-2A-CP 'overcoat' virus	PVX with mutated TGB3 protein and with green fluorescent protein fused to coat protein	Fig. 4_1 O

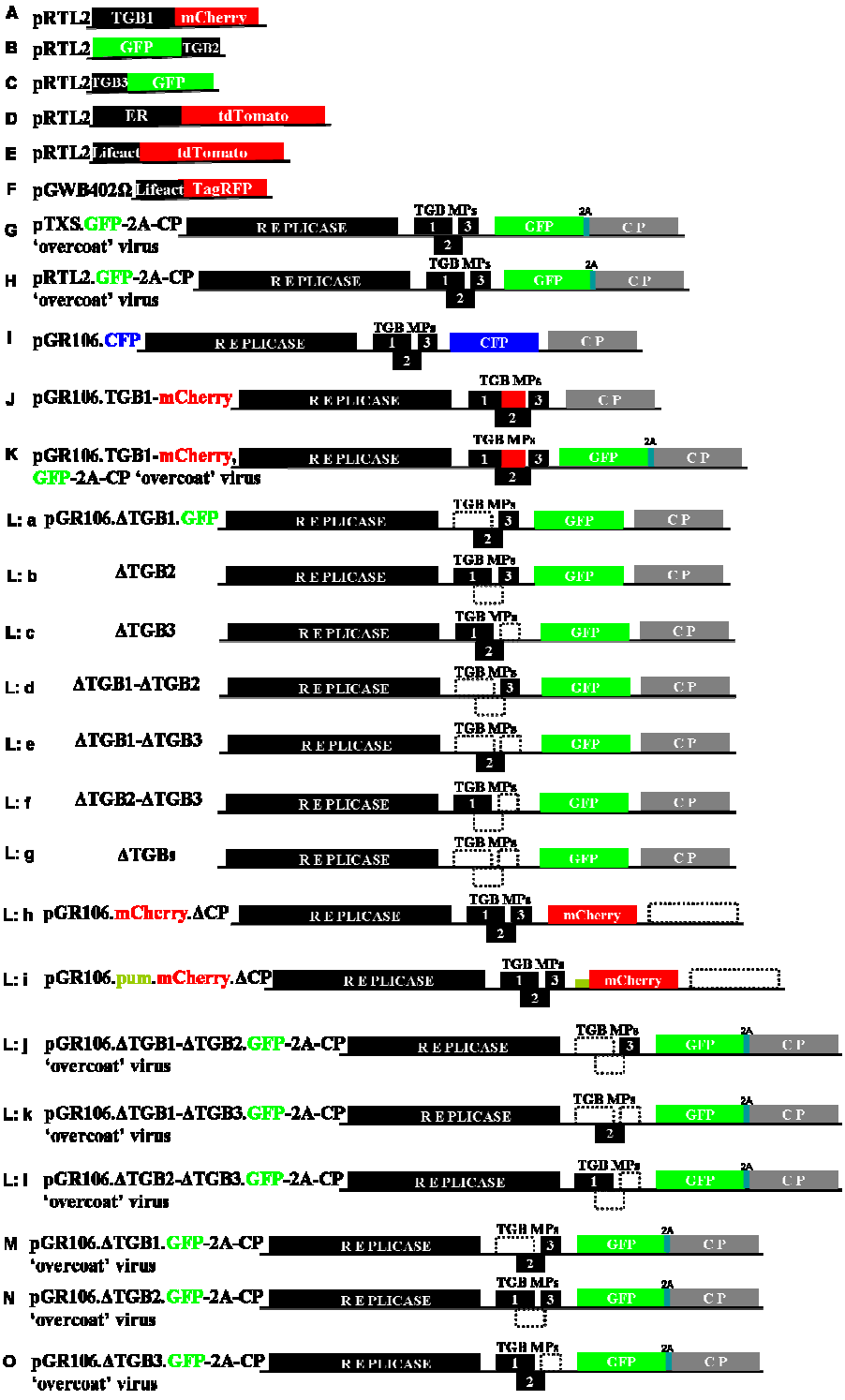

Figure 4_1: Schematic representation of plasmids used in this results chapter

TGB: triple gene block, MP: movement protein; CP: coat protein.

4.2.2 Localisation of viral TGB movement proteins individually and in combination

4.2.2.1 The TGB1 protein labels PD in the absence of viral infection (Fig. 4_2)

Due to the fact that the TGB1 protein is a multifunctional protein able to move cell-to-cell (Angell *et al*., 1996; Lough *et al*., 1998, 2000; Yang *et al*., 2000; Howard *et al*., 2004), my first interest was to find out whether TGB1 associates with PD in the absence of virus. To test this hypothesis, transgenic *N. tabacum* plants that stably expressed the MP of TMV fused to GFP (MP-GFP; Roberts *et al*., 2001), were used to locate branched secondary PD (Faulkner *et al*., 2008). These plants were then bombarded with the TGB1 fluorescent fusion protein (Fig. 4_1 A).

Transgenic, uninfected *N. tabacum* leaf epidermal cells were examined under the confocal laser scanning microscope. PD labeling of the epidermal cells was identified by the presence of numerous GFP-expressing dots in the cell periphery (Fig. 4_2 A,D). These epidermal cells were then compared with the cells bombarded with TGB1 (Fig. 4_2 B,E). It was found that the TGB1 signal colocalised precisely with the green signal in the central cavities of branched PD (Fig. 4_2 C,F), indicating that TGB1 is targeted to PD in the absence of virus infection. The TGB1 signal was also found at the cell periphery in the spots, free of secondary PD marker, presumably in simple PD (Fig. 4_2 F).

It is highly unlikely that MP of TMV facilities association of TGB1 with PD due to the fact that in a different experiment TGB1, when this protein was expressed in the cell along, was able to localise to PD, traffic to adjacent cells and establish the VRCs in uninfected neighbouring cells in the complete absence of other viral gene products (unpublished data from our lab).

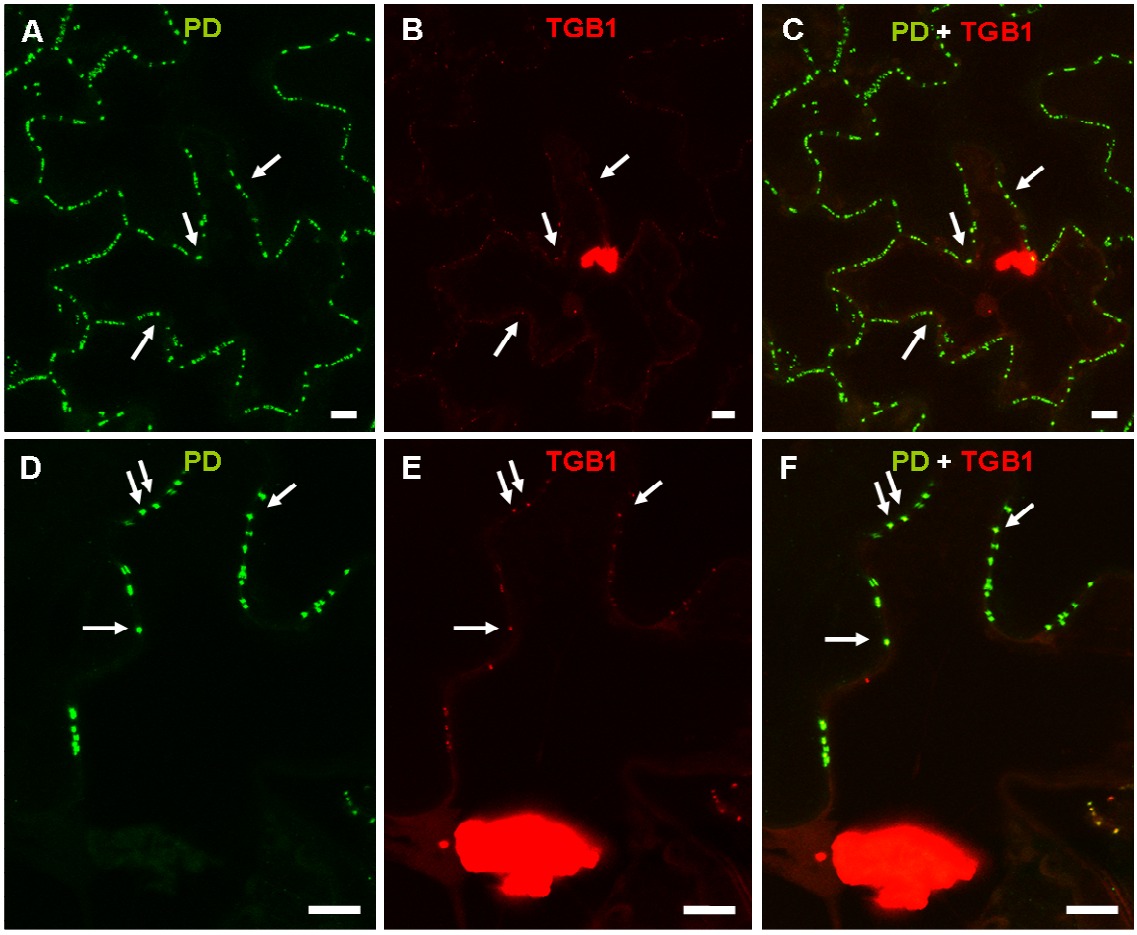

Figure 4_2: TGB1 on TMV MP-GFP *N. tabacum* transgenic plants
Confocal laser scanning images of epidermal cells of uninfected TMV MP-GFP transgenic *N. tabacum* leaves bombarded with the TGB1 viral protein to show TGB1 (red) in the cell secondary PD (green) in the absence of viral infection
A,D: PD (green channel); B,E: TGB1 (red channel); C,F: overlay of green and red channel (PD + TGB1) at 1 d.p.b.
d.p.b. – days post-bombardment of TGB1; thin arrows point to the colocalisation of green PD labelling with red TGB1 signal at the cell periphery; the large red structure presents the 'VRC'.
Bars, 20 µm.

4.2.2.2 The TGB1 protein and PVX 'overcoat' are present in small particles in PVX-infected cells (Fig. 4_3 – Fig. 4_8)

To test if TGB1 within PD colocalised with 'overcoat' particles, the TGB1 construct (Fig. 4_1 A) was bombarded into plants infected with PVX 'overcoat' (Fig. 4_1 G).

4.2.2.2.1 Sub-cellular localisation of PVX 'overcoat' virions and motile CP particles

A genetically modified virus that expressed CP tagged to GFP (PVX 'overcoat'; Fig. 4_1 G) was used as a strategy to locate assembled virions in the living plant cells, and as a non-destructive method for visualisation of virus movement *in vivo*. This viral construct was shown previously to replicate, encapsidate and move cell-to-cell (Santa Cruz *et al*., 1996). Non-transgenic *N. benthamiana* plants were infected with PVX 'overcoat' (Fig. 4_1 G). GFP-expressing viral lesions were detected under UV illumination as small fluorescent dots at 3 days post-inoculation (d.p.i.) of PVX. An increase in size of fluorescent rings indicated that the virus was successfully replicating and spreading within the inoculated leaf. Long-distance movement from a local, inoculated leaf into uninfected leaf tissue occurred after 5-6 days post-inoculation (data not shown).

The leading edge and the centre of the infection sites, respectively, were monitored. The leading edge of an infection site represents the earliest detectable stage in which the virus has entered new cells. Therefore, examination of the leading edge provides information on where viral proteins first accumulate in the cell. The centre of the PVX infection is characterised as a late stage of infection in which significant levels of virus have already accumulated. The centre of an infection thus provides information on the distribution of proteins after the virus has invaded adjoining cells.

At the centre of viral infection large, fibrillar aggregates of PVX virions were present in the perinuclear VRCs of infected cells (Fig. 4_3 A; see also Santa Cruz *et al*., 1996).

During closer examination of the VRC, PVX CP was found to form cages of fibrillar masses with central cores unlabeled by GFP (Fig. 4_3 B). At the leading edge of a PVX 'overcoat' infection, characteristic fibrillar VRCs and small virus-like particles containing PVX CP were observed (Fig. 4_3 C,D). These 'packets' of particles were found to be highly mobile (Movie 4.1a,b). They were observed to move in and out of the PVX VRC (Movie 4.2) and they were found statically localised to PD (Fig. 4_3 E). From the leading edge towards the centre of infection, more fibrillar virions that localised to VRCs were detected and less GFP signal in motile particles was seen (Fig. 4_3 C).

4.2.2.2.2 Motile particles of PVX contain both TGB1 and CP

Based on the fact that PVX requires its CP for trafficking between cells (see Chapter 1) and TGB1 is detected in PD, colocalision studies of TGB1 with the 'overcoat' virus were carried out. The TGB1 protein (Fig. 4_1 A) was co-expressed transiently with PVX 'overcoat' (Fig. 4_1 H) (Fig. 4_4 A-F, Fig. 4_7) and, in a different experimental approach, the TGB1 protein (Fig. 4_1 A) was bombarded into leaves infected with PVX 'overcoat' (Fig. 4_1 G) of non-transgenic *N. benthamiana* plants (Fig. 4_4 G-I; Fig. 4_5; Fig. 4_6; Fig. 4_8 C,D). Biolistic bombardment was used to visualise TGB1 and viral CP in the same cell and to follow movement from bombarded cells to neighbouring non-bombarded cells. The TGB1 particles were found to be moving together with 'overcoat' particles in the cell cytoplasm (Movie 4.3a,b; arrows in the cell cytoplasm Fig. 4_4 A-F), indicating that TGB1 and CP are present in the same motile particles.

4.2.2.2.3 TGB1 and CP signals colocalise in PD

TGB1-mCherry signal also localised to the cell wall of the bombarded cells (stationary punctate spots of red fluorescence) together with the green PVX particles (Fig. 4_4 G-I). Most of these populations of particles (TGB1 and CP) were targeted to numerous PD (Fig. 4_5). In addition, the TGB1 and CP particles were detected in pitfields of

plasmodesmata (arrowheads in Fig. 4_5; Fig. 4_6 A-C). Interestingly, structures in which the two signals (mCherry and GFP) were separated were also observed. These structures resembled single-tailed particles (STPs) of PVX with one end of the particle (TGB1) located within PD and the other end (CP) protruding into the cytoplasm (Fig. 4_6 D-F). The TGB1 and CP particles were also found outside of the bombarded cells in the cell cytoplasm of neighbouring cells (Movie 4.4; motile population; Fig. 4_7 A-C) and in PD located at the cell periphery of adjacent cells (Fig. 4_7 D-F).

4.2.2.2.4 TGB1-mCherry expression from a virus-based vector reveals circular 'walnut-like' TGB1 inclusions in the PVX VRC

To confirm that the observed sub-cellular localisation of bombarded TGB1 protein is a true biological component of the PVX infection, an infectious virus was constructed to express a TGB1-mCherry fusion (Fig. 4_1 J). This endogenous TGB1 construct gave more details of TGB1 structure in the VRC (Fig. 4_8 A,B) compared to the bombarded TGB1 construct (Fig. 4_4 B,E,H; Fig. 4_7 B,E). In the bombarded TGB1 construct, possibly due to protein overexpression, it was more difficult to obtain a clear image of the TGB1 protein in the VRC. At the infection centre, however, endogenous TGB1 formed circular 'walnut-like' inclusions in the VRC, sometimes forming rod-like elongated structures in the cell cytoplasm (arrowheads in Fig. 4_8 A). This was also observed in earlier studies using an EM approach (Davies *et al*., 1993; Samuels *et al*., 2007).

4.2.2.2.5 Dual imaging of the PVX VRC reveals different localisation patterns of TGB1 and CP

Although TGB1 and CP colocalised in PD, these proteins were found to be spatially separated from one another in the VRC. TGB1 was located at the centre of PVX VRC and CP was observed around the TGB1 protein, localised towards the periphery of the VRC, outside the TGB1-containing sub-compartments (Fig. 4_8 C,D).

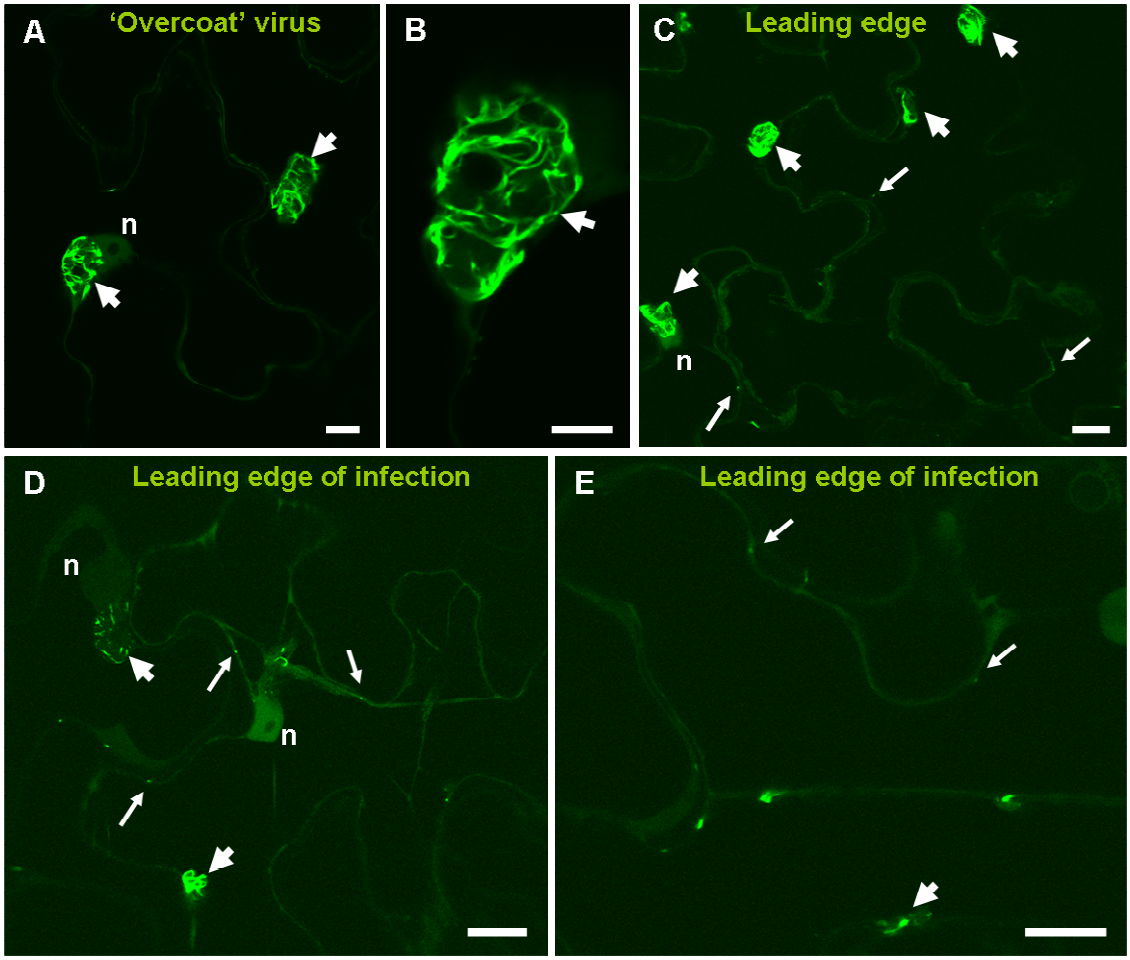

Figure 4_3: PVX 'overcoat' on non-transgenic *N. benthamiana* plants
Confocal laser scanning images of PVX 'overcoat'-infected (green) epidermal cells of non-transgenic *N. benthamiana* leaves
A: PVX-infected epidermal cells with developed perinuclear 'overcoat' VRCs; B: a higher magnification image of the PVX 'overcoat' VRC; C-E: a leading edge of a PVX 'overcoat' infection with PVX VRCs and PVX mobile particles at 5 d.p.i. (local leaves).
d.p.i. – days post-inoculation of PVX; thick arrows point to PVX VRCs; thin arrows point to PVX 'overcoat' mobile particles; n – nucleus.
Bars, 10 µm (B), 20 µm (A, C-E).

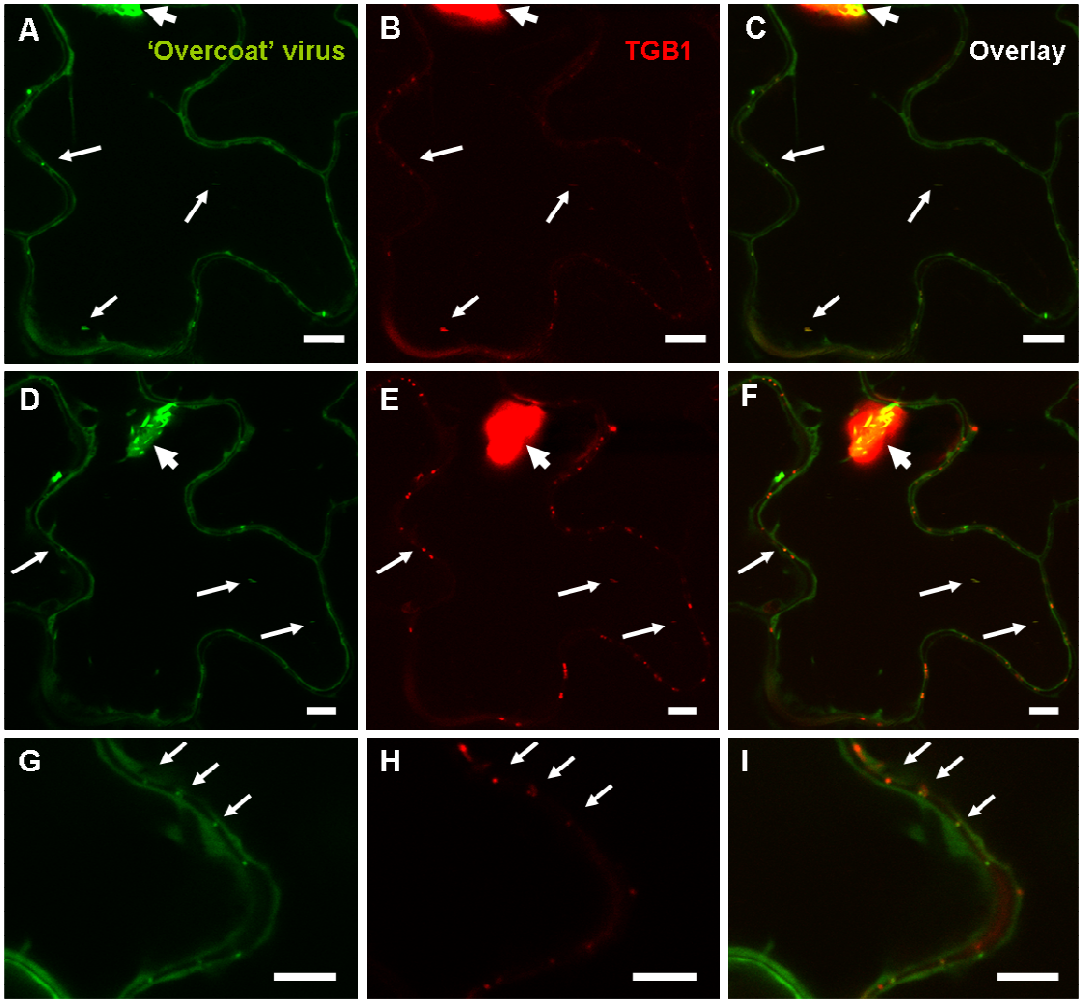

Figure 4_4: PVX 'overcoat' and TGB1 on non-transgenic *N. benthamiana* plants
1) Confocal laser scanning images of epidermal cells of non-transgenic *N. benthamiana* leaves cobombarded with PVX 'overcoat' (green) and TGB1 (red) (A-F).
2) Confocal laser scanning images of PVX 'overcoat'-infected (green) non-transgenic *N. benthamiana* leaves bombarded with TGB1 (red) (G-I).
A,D,G: PVX 'overcoat' (green channel): PVX VRCs and PVX particles; B,E,H: TGB1 (red channel): TGB1 in PVX VRCs and TGB1 particles; C,F,I: overlay of green and red channel (PVX 'overcoat' + TGB1).
A-F: 2 d.p.b.; G-I: 12 d.p.i. (systemic leaves) + 1 d.p.b.
d.p.i. – days post-inoculation of PVX; d.p.b. – days post-bombardment; thick arrows point to PVX VRCs; thin arrows point to the colocalisation of green and red particles in the cell cytoplasm (mobile population) and in PD (stationary population).
Bars, 10 µm.

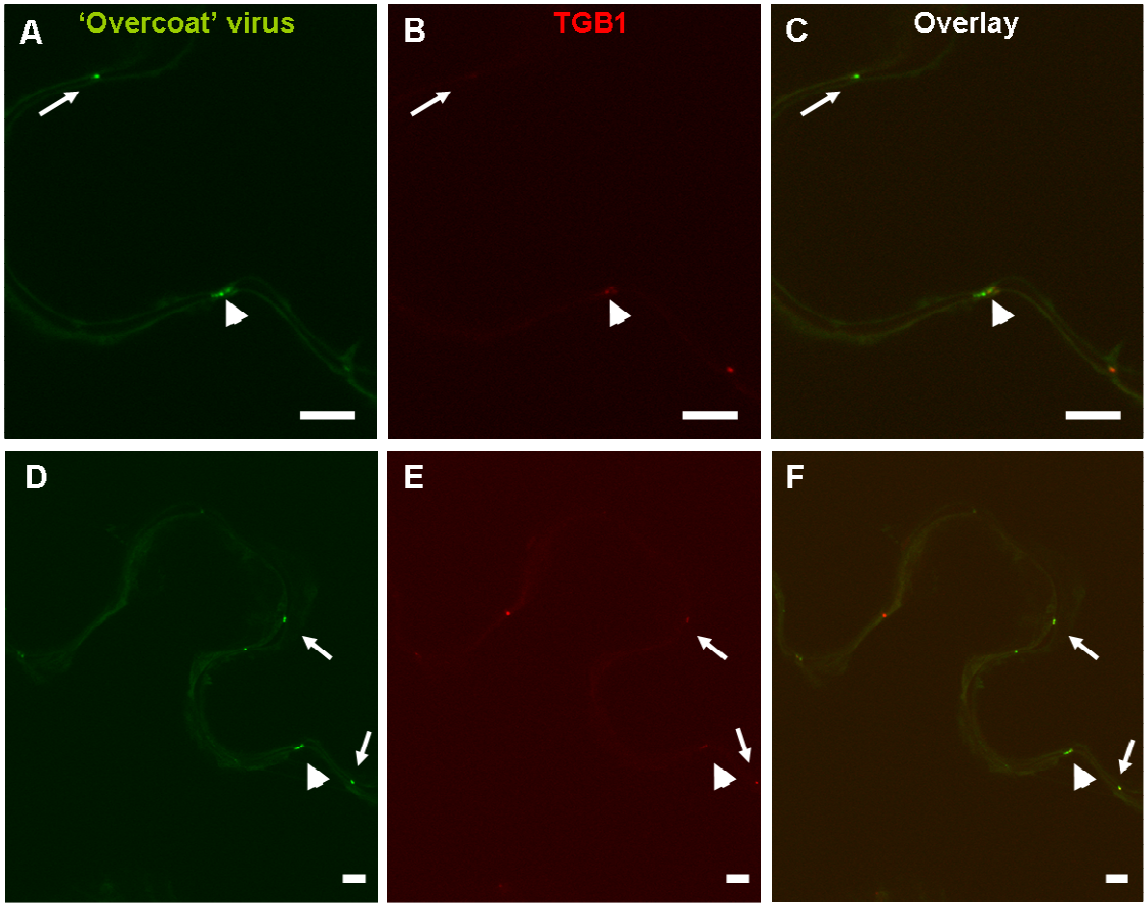

Figure 4_5: PVX 'overcoat' and TGB1 on non-transgenic *N. benthamiana* plants
Confocal laser scanning images of epidermal cells of PVX 'overcoat'-infected (green) non-transgenic *N. benthamiana* leaves bombarded with TGB1 (red)
A,D: PVX 'overcoat' particles (green channel); B,E: TGB1 particles (red channel); C,F: overlay of green and red channel (PVX 'overcoat' + TGB1) at 5 d.p.i. (local leaves) + 1 d.p.b.
d.p.i. – days post-inoculation of PVX; d.p.b. – days post-bombardment of TGB1; arrowheads point to pitfields; thin arrows point to the colocalisation of green and red particles in PD (stationary population).
Bars, 10 µm.

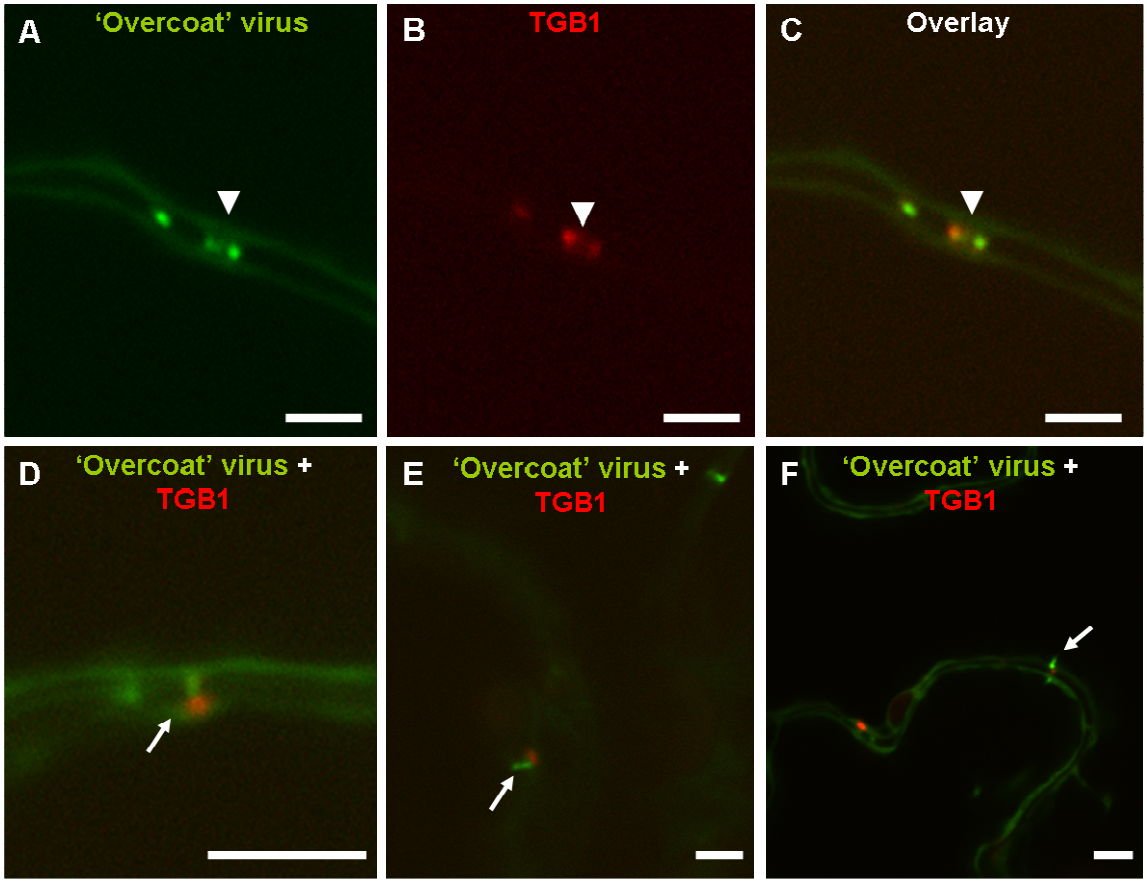

Figure 4_6: PVX 'overcoat' and TGB1 on non-transgenic *N. benthamiana* plants
Confocal laser scanning images of epidermal cells of PVX 'overcoat'-infected (green) non-transgenic *N. benthamiana* leaves bombarded with TGB1 (red)
A: PVX 'overcoat' particles (green channel); B: TGB1 particles (red channel); C: overlay of A and B images (PVX 'overcoat' + TGB1 in PD pitfields); D-F: overlay of green and red channel (STPs of PVX 'overcoat' (green) attached to TGB1 (red)).
A-E: 5 d.p.i. (local leaves) + 1 d.p.b.; F: 12 d.p.i. (systemic leaves) + 1 d.p.b.
d.p.i. – days post-inoculation of PVX; d.p.b. – days post-bombardment of TGB1; arrowheads point to pitfields; thin arrows point to PVX STPs.
Bars, 5 µm.

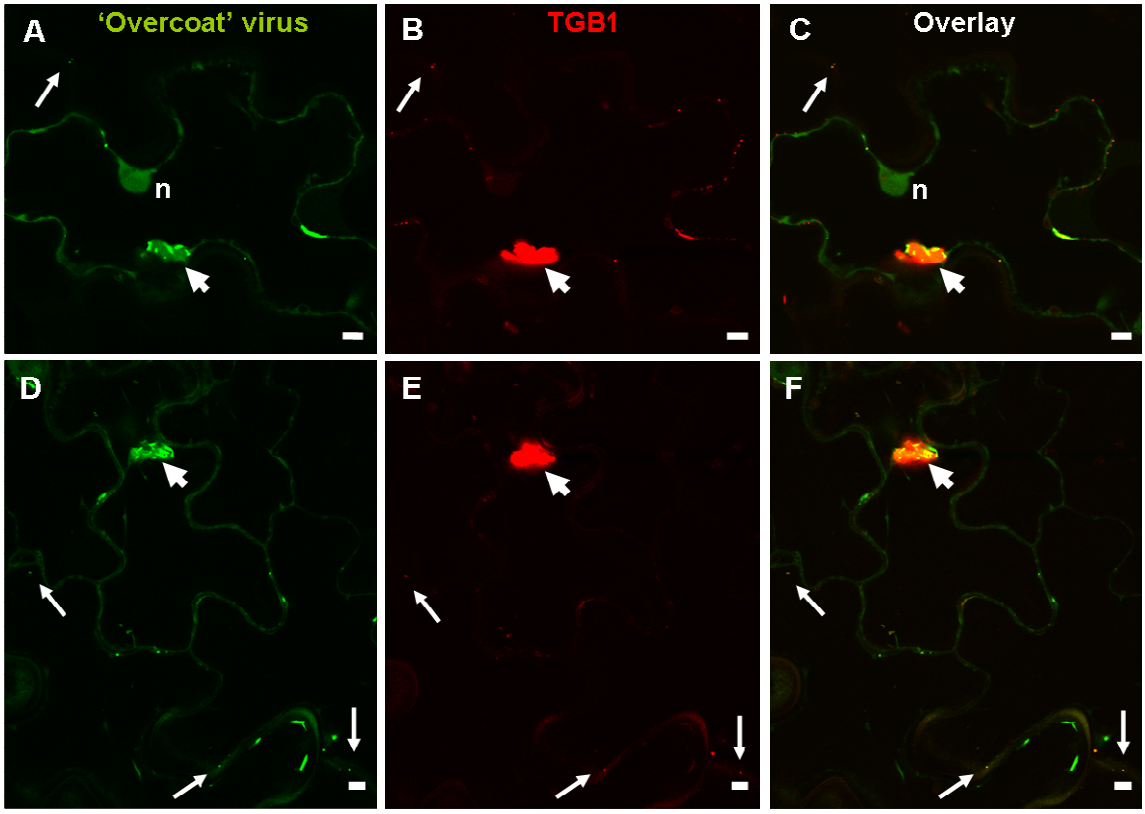

Figure 4_7: PVX 'overcoat' and TGB1 on non-transgenic *N. benthamiana* plants
Confocal laser scanning images of epidermal cells of non-transgenic *N. benthamiana* leaves cobombarded with PVX 'overcoat' (green) and TGB1 (red)
A,D: PVX 'overcoat' (green channel): PVX VRCs and PVX particles; B,E: the TGB1 protein (red channel): TGB1 in PVX VRCs and TGB1 particles; C,F: overlay of green and red channel (PVX 'overcoat' + TGB1) at 2 d.p.b.
d.p.b. – days post-bombardment; thick arrows point to PVX VRCs; thin arrows point to the colocalisation of green and red particles outside of the bombarded cells in the cytoplasm (mobile population) (A-F) and in PD (stationary population) (D-F); n – nucleus.
Bars, 10 µm.

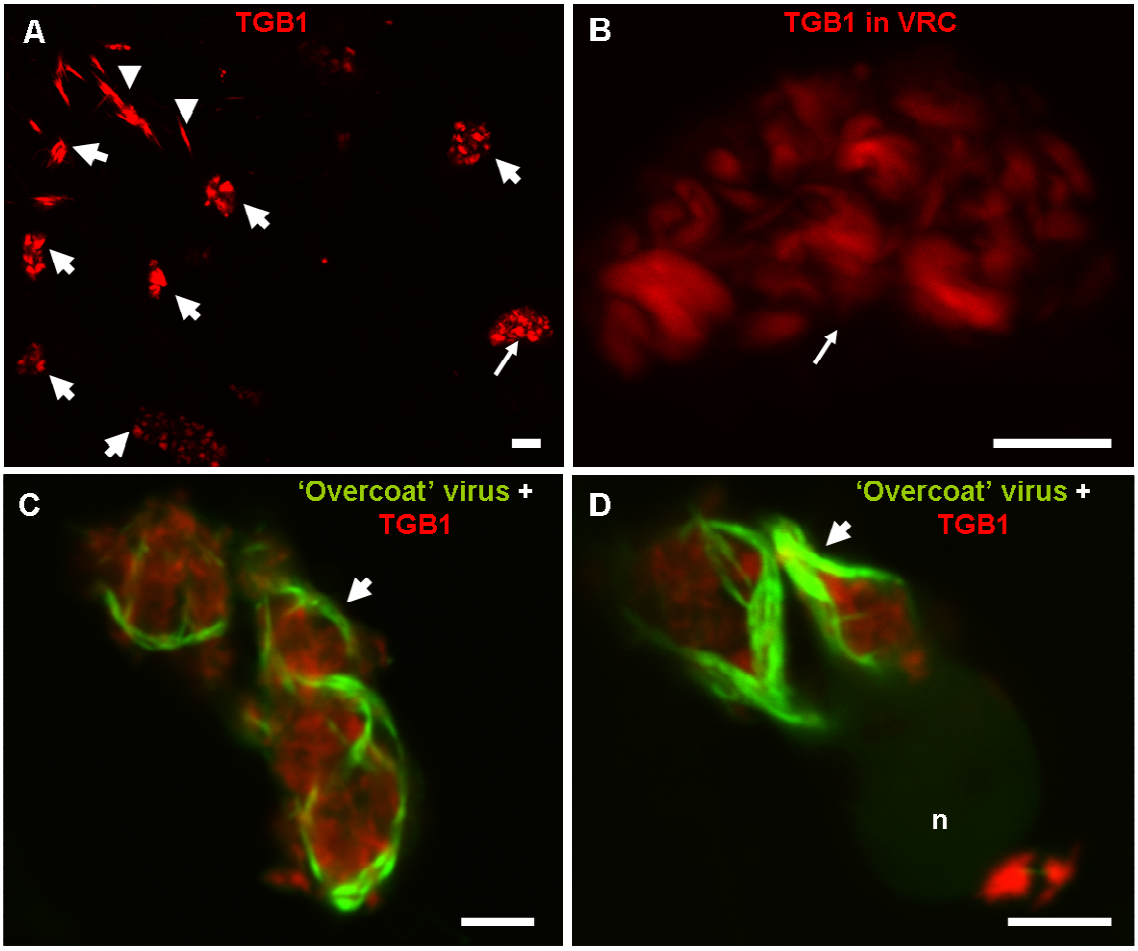

Figure 4_8: Endogenous TGB1 expressed from a viral construct (A,B) + PVX 'overcoat' and TGB1 (C,D) on non-transgenic PVX-infected *N. benthamiana* plants
1) Confocal laser scanning images of epidermal cells infected with endogenous TGB1 (red) expressed from a viral construct (A,B).
2) Confocal laser scanning images of epidermal cells infected with PVX 'overcoat' (green) and bombarded with TGB1 (red) (C,D).
A: Sub-cellular localisation of endogenous TGB1 (red); B: a higher magnification image of TGB1 localised in the PVX VRC in image A (thin arrow); C,D: localisation of PVX 'overcoat' (green) and TGB1 (red) in the cell perinuclear VRC.
A,B: 7 d.p.i. (local leaves); C,D: 5 d.p.i. (local leaves) + 1 d.p.b.
d.p.i. – days post-inoculation of PVX; d.p.b. – days post-bombardment of TGB1 (C-D); thick arrows point to PVX VRCs; thin arrows point to the sub-cellular localisation of TGB1 in the PVX VRC and a higher magnification image of a single VRC with TGB1 (B); arrowheads point to the rod-like TGB1 structures in the cell cytoplasm; n – nucleus. Bars, 10 µm (B-D), 20 µm (A).

4.2.2.3 TGB2 and TGB1 localise to separate sub-compartments within the VRC and also accumulate in PD (Fig. 4_9 – Fig. 4_11)

The expression of virus-encoded movement proteins individually cannot provide a full picture about the localisation of these proteins in VRCs nor about their normal interactions during virus replication and spread. To determine the sub-cellular distribution of the TGB proteins in relationship to one other, and to find out whether TGB2 and TGB1 have different localisations in uninfected versus infected epidermal cells, the TGB2 protein (Fig. 4_1 B) was cobombarded with the TGB1 protein (Fig. 4_1 A) into uninfected (Fig. 4_9) and PVX-infected (Fig. 4_1 I) *N. benthamiana* plants (Fig. 4_10-11).

TGB2 in the presence of TGB1 induced abundant vesicles at the cell periphery and in the cell cytoplasm without (Fig. 4_9 A-C) and with viral infection (Fig. 4_10 A-B). Importantly, that only in the presence of TGB1 some of the TGB2-induced vesicles clearly localised at PD in the absence (Fig. 4_9 C) and presence of virus (Fig. 4_10 D-F), suggesting that mutual accumulation of TGB1 and TGB2 may occur in PD. As always, VRCs were found to be larger in the infected cells (Fig. 4_10-11) when compared to the uninfected tissue (Fig. 4_9), indicating that in infected tissue VRCs become larger over time as a result of the accumulation of viral proteins in the VRCs. TGB2 and TGB1 localised to the 'VRCs' next to the cell nucleus in the absence of PVX (Fig. 4_9 A-C) and also in PVX-infected cells (Fig. 4_10). TGB1 was not found in the TGB2-induced vesicle both in the absence (Fig. 4_9 B) and presence of infection (data not shown).

Optical confocal sectioning through the VRC revealed that these two proteins had a different localisation pattern to each other in the absence (Fig. 4_9 D-F) and in the presence of viral infection (Fig. 4_10 B-C): TGB1 was central in the VRC, while TGB2 surrounded the TGB1 sub-compartment of the VRC. In addition, TGB1 expressed in the initial bombarded cells was found in the VRCs of surrounding non-bombarded infected

cells and also accumulated at the centre of established VRCs (Fig. 4_11; labelling by TGB1 up to 10 VRCs around the bombarded cell was identified), indicating that the TGB1-mCherry fusion moved extensively from cell to cell into the VRCs of neighbouring infected cells. Unlike TGB1, the TGB2 viral protein was not found outside of the bombarded cells.

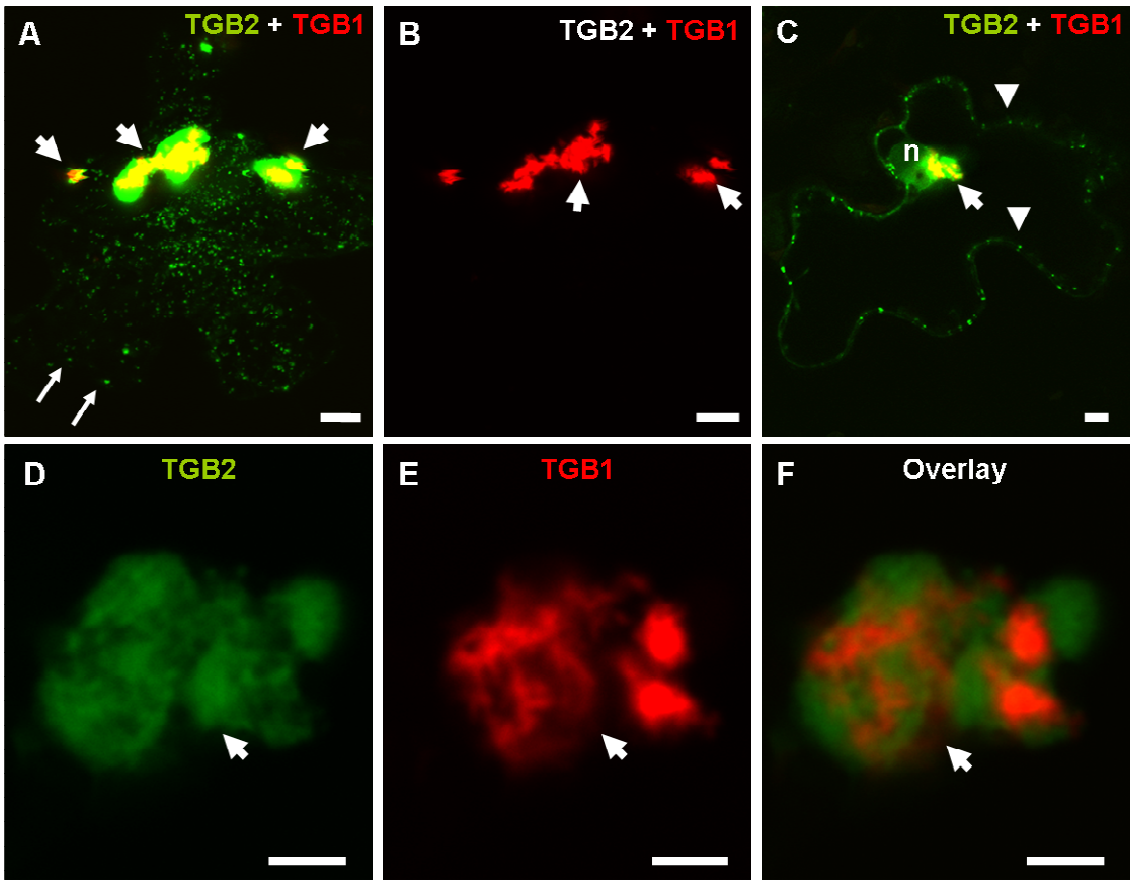

Figure 4_9: TGB2 and TGB1 on uninfected non-transgenic *N. benthamiana* plants
Confocal laser scanning images of non-transgenic *N. benthamiana* epidermal leaves cobombarded with TGB2 (green) and TGB1 (red)
A-C: Cellular localisation of TGB2 (green) and TGB1 (red); B: TGB1 (red channel); C: TGB2 (green) in PD (arrowheads); D-F: TGB2 and TGB1 in the perinuclear 'VRC'; D: TGB2 (green channel); E: TGB1 (red channel); F: overlay of green and red channel (TGB2 + TGB1) in the 'VRC'.
A-F: 1 d.p.b.
d.p.b. – days post-bombardment of TGBs; thick arrows point to the 'VRCs'; thin arrows point to the TGB2-induced vesicles; arrowheads point to TGB2 in PD (C); n – nucleus.
Bars, 5 µm (D-F), 10 µm (A-C).

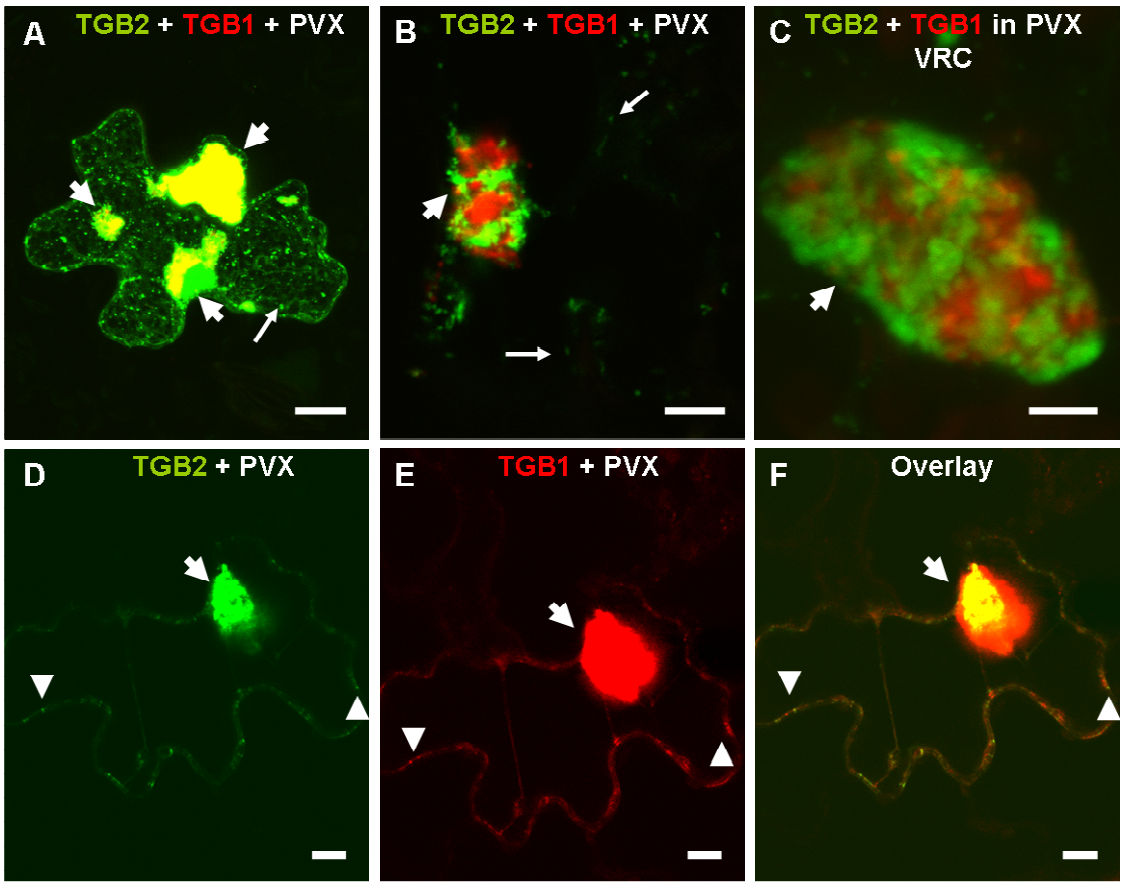

Figure 4_10: TGB2 and TGB1 on PVX-infected non-transgenic *N. benthamiana* plants

Confocal laser scanning images of PVX-infected (PVX is unlabelled) non-transgenic *N. benthamiana* epidermal leaves cobombarded with TGB2 (green) and TGB1 (red)

A,B: Cellular localisation of TGB2 (green) and TGB1 (red) in PVX-infected epidermal cells; C: TGB2 (green) and TGB1 (red) in the PVX VRC; D: TGB2 (green) in PD (arrowheads); E: TGB1 (red) in PD (arrowheads); F: overlay of D and E (TGB2 + TGB1).

A,D-F: 2 d.p.b.; B,C: 1 d.p.b.

d.p.b. – days post-bombardment of TGBs; thick arrows point to PVX VRCs; thin arrows point to the TGB2-induced vesicles; arrowheads point to TGB2 and TGB1 in PD (D-F).

Bars, 5 µm (C), 10 µm (B,D-F), 20 µm (A).

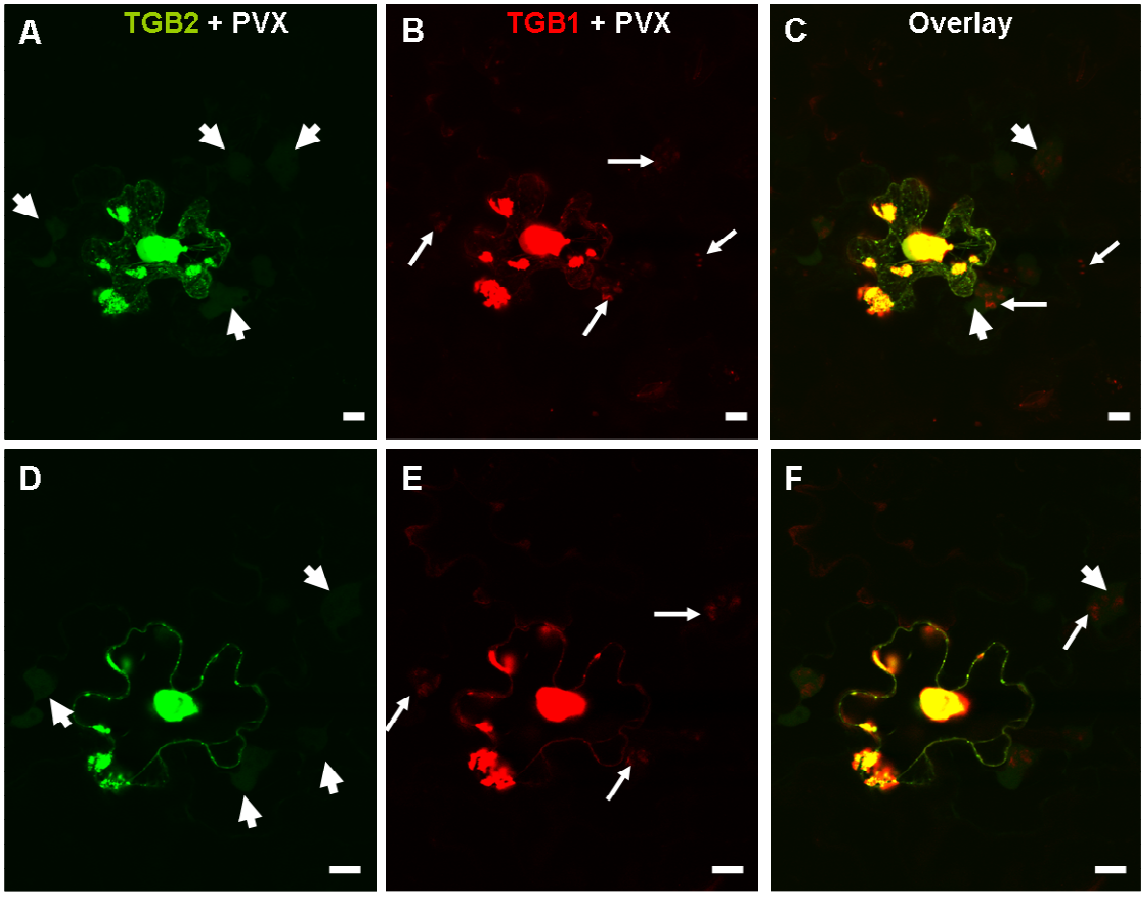

Figure 4_11: TGB2 and TGB1 on PVX-infected non-transgenic *N. benthamiana* plants
Confocal laser scanning images of PVX-infected (PVX is unlabelled) non-transgenic *N. benthamiana* epidermal leaves cobombarded with TGB2 (green) and TGB1 (red)
A,D: Cellular localisation of TGB2 (green channel); B,E: cellular localisation of TGB1 (red channel); C,F: overlay of green and red channel (TGB2 + TGB1).
A-F: 2 d.p.b.
d.p.b. – days post-bombardment of TGBs; thick arrows point to PVX VRCs; thin arrows point to TGB1 in the VRCs of neighbouring non-bombarded cells.
Bars, 20 µm.

4.2.2.4 TGB3 and TGB1 localise to distinct VRC sub-compartments (Fig. 4_12)

To answer the question whether TGB3 and TGB1 have different locations in the VRC of uninfected and infected epidermal cells, and whether TGB3, like TGB2, also localises to PD in the presence of TGB1, the TGB3 protein (Fig. 4_1 C) was cobombarded in combination with the TGB1 protein (Fig. 4_1 A) into uninfected (Fig. 4_12 A-C) and infected (Fig. 4_1 I) *N. benthamiana* plants (Fig. 4_12 D-F).

TGB3 in the presence of TGB1 also stimulated appearance of numerous characteristic ER-derived vesicles in the absence (Fig. 4_12 A-B) and presence of viral infection (Fig. 4_12 D-E). In this study, TGB3-vesicles in the presence of TGB1 were not convincingly identified in PD. VRCs were also found to be larger in the infected cells (Fig. 4_12 F) when compared to the structures resembling VRCs in the uninfected tissue (Fig. 4_12 C). TGB3 and TGB1 localised to the VRCs in the absence (Fig. 4_12 A-C) and presence of virus (Fig. 4_12 D-F). However, these two proteins had a different localisation pattern to each other in the VRC in the absence (Fig. 4_12 C) or presence of viral infection (Fig. 4_12 F). The TGB1 protein was central in the VRC while TGB3, like TGB2, surrounded the TGB1 sub-compartment (Fig. 4_12 C,F). The fluorescent pattern in the VRC observed for TGB2- and TGB3-GFP-expressing cells was qualitatively different; TGB3 formed grape-like clusters around the TGB1 protein (Fig. 4_12 C,F), while TGB2 was more uniformly dispersed throughout the VRC (Fig. 4_9 F, Fig. 4_10 C).

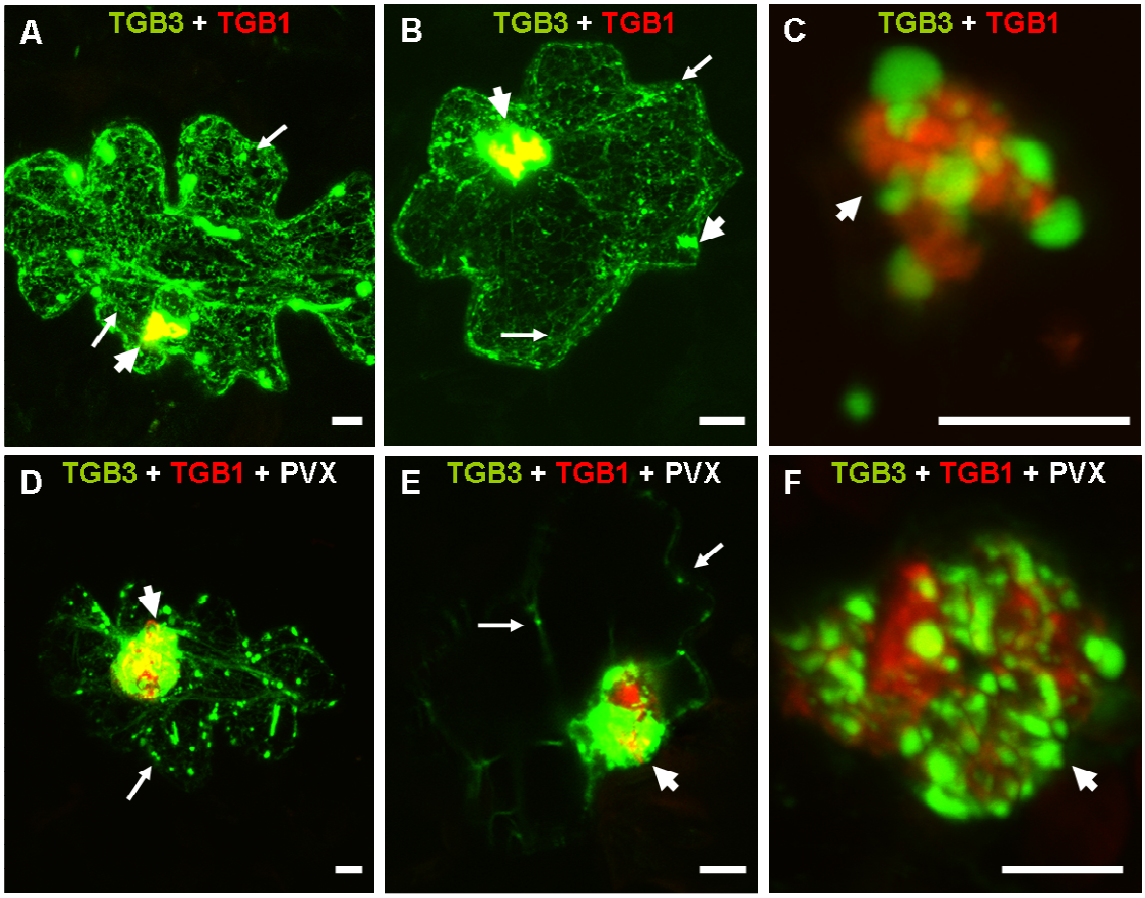

Figure 4_12: TGB3 and TGB1 on uninfected (A-C) and on PVX-infected (D-F) non-transgenic *N. benthamiana* plants

Confocal laser scanning images of non-transgenic *N. benthamiana* epidermal leaves of uninfected (A-C) or PVX-infected (PVX is unlabelled) (D-F) plants and cobombarded with TGB3 (green) and TGB1 (red) (A-F)

A,B: Cellular localisation of TGB3 (green) and TGB1 (red) in uninfected epidermal cells; C: a higher magnification image of TGB3 (green) and TGB1 (red) in 'VRC'; D,E: cellular localisation of TGB3 (green) and TGB1 (red) in PVX-infected epidermal cells; F: TGB3 (green) and TGB1 (red) in the PVX VRC.

A-F: 1 d.p.b.

d.p.b. – days post-bombardment of TGBs; thick arrows point to perinuclear VRCs; thin arrows point to the TGB3-induced vesicles.

Bars, 10 µm.

4.2.2.5 TGB2/TGB3 and TGB1 localise to separate VRC sub-compartments (Fig. 4_13 – Fig. 4_14)

To find out how the VRC is structured in relationship to three TGB proteins, TGB2 (Fig. 4_1 B), TGB3 (Fig. 4_1 C) and TGB1 (Fig. 4_1 A) were cobombarded into non-transgenic, uninfected (Fig. 4_13) and PVX-infected (Fig. 4_14) *N. benthamiana* plants. Sub-cellular localisation of TGB2, TGB3 and TGB1 was compared in uninfected epidermal cells (Fig. 4_13) and in PVX-infected tissues (Fig. 4_1 I) (Fig. 4_14).

The TGB2- and TGB3-related vesicles were observed in the presence of TGB1 at the cell periphery and in the cell cytoplasm in the absence (Fig. 4_13 A,B) and presence of viral infection (Fig. 4_14 A,D). As predicted, TGB2/TGB3 had a different localisation pattern to TGB1 in the VRC both in the absence (Fig. 4_13 C-E) and in the presence of viral infection (Fig. 4_14 E). The TGB1 protein was concentrated in the centre of the VRC, separately from the other two TGB proteins, while the TGB2/TGB3 sub-compartment of the VRC was peripheral to the TGB1 protein. TGB1 was also discovered in the VRC of neighbouring, non-bombarded cells infected with PVX and also localised at the centre of the viral replication complex (Fig. 4_14 A-C).

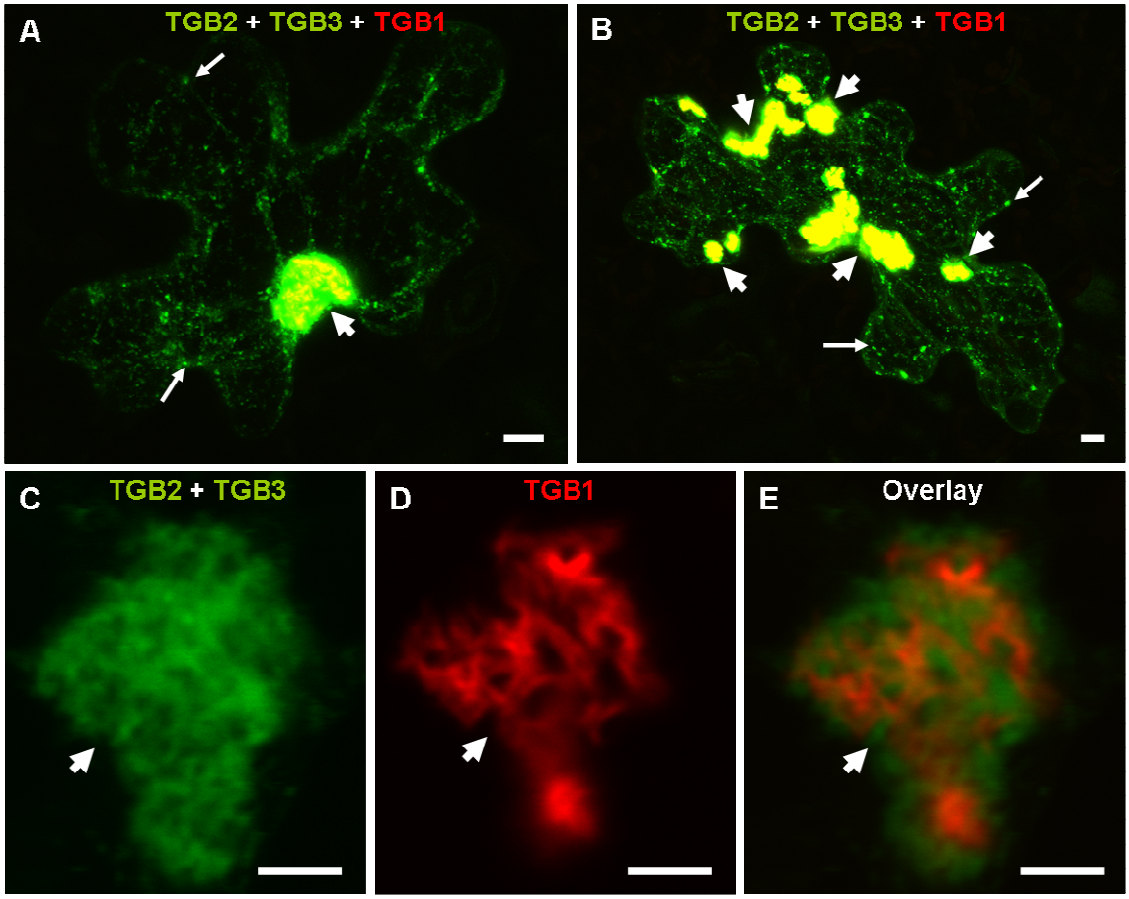

Figure 4_13: TGB2 and TGB3 and TGB1 on non-transgenic *N. benthamiana* plants
Confocal laser scanning images of non-transgenic *N. benthamiana* epidermal leaves cobombarded with TGB2 and TGB3 (both in green) and TGB1 (red)
A,B: Cellular localisation of TGB2 and TGB3 (both in green) and TGB1 (red) in uninfected epidermal cells; C-E: a higher magnification image of TGB2/TGB3 and TGB1 in the perinuclar 'VRC'; C: TGB2/TGB3 (green channel); D: TGB1 (red channel); E: overlay of C and D images (TGB2/TGB3 + TGB1 in the 'VRC').
A-E: 1 d.p.b.
d.p.b. – days post-bombardment of TGBs; thick arrows point to perinuclear 'VRCs'; thin arrows point to the TGB2/TGB3-induced vesicles.
Bars, 5 µm (C-E), 10 µm (A,B).

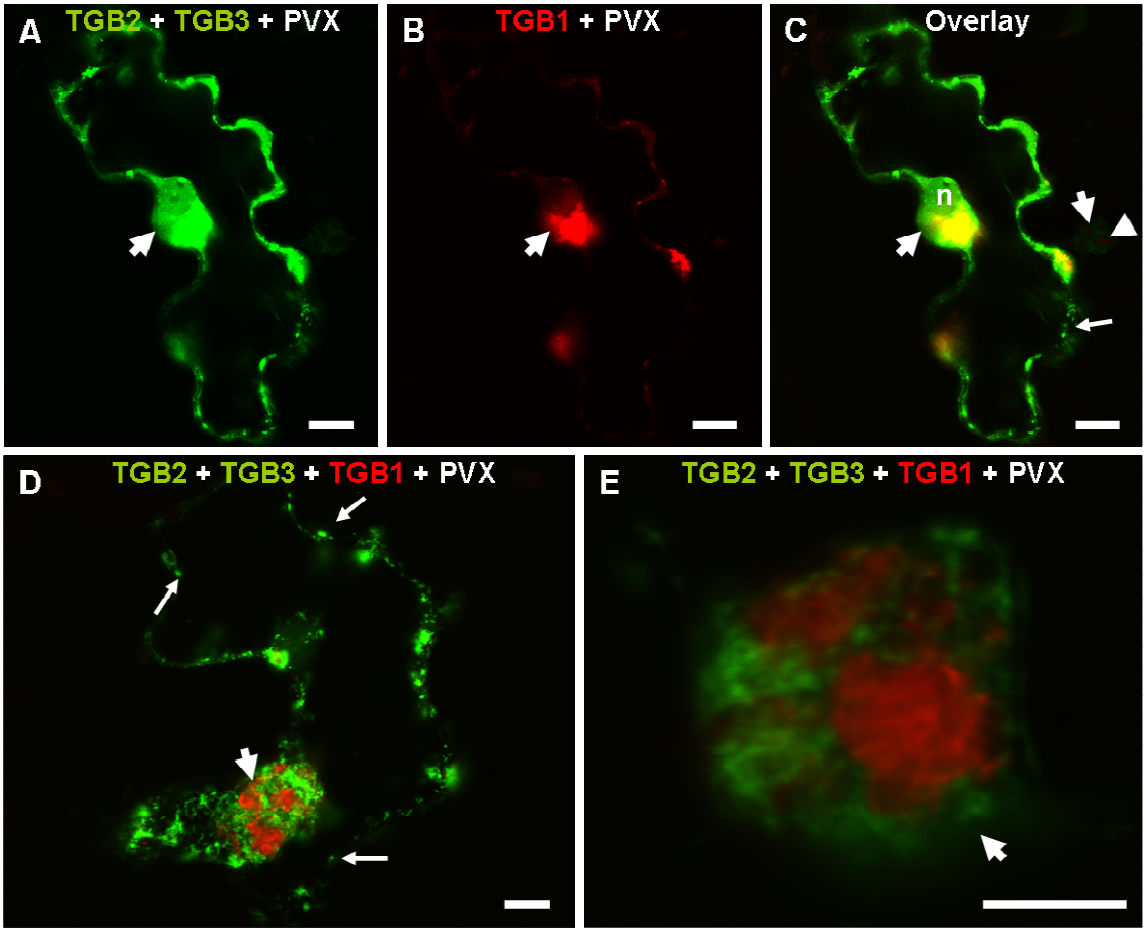

Figure 4_14: TGB2 and TGB3 and TGB1 on PVX-infected non-transgenic *N. benthamiana* plants

Confocal laser scanning images of non-transgenic PVX-infected (PVX is unlabelled) *N. benthamiana* epidermal leaves cobombarded with TGB2 and TGB3 (both in green) and TGB1 (red)

A-D: Cellular localisation of TGB2 and TGB3 (both in green) and TGB1 (red) in PVX-infected epidermal cells; A: TGB2/TGB3 (green channel); B: TGB1 (red channel); C: overlay of A and B images (TGB2/TGB3 + TGB1); E: a higher magnification image of TGB2/TGB3 and TGB1 in PVX VRCs.

A-E: 1 d.p.b.

d.p.b. – days post-bombardment of TGBs; thick arrows point to PVX VRCs; thin arrows point to the TGB2/TGB3-induced vesicles; arrowheads point to TGB1 in the PVX VRC of neighbouring non-bombarded cell; n – nucleus.

Bars, 10 µm (D,E), 20 µm (A-C).

4.2.3 Localisation of viral TGB movement proteins with host organelles

4.2.3.1 The TGB1 protein alone recruits ER into the VRC in the absence of viral infection (Fig. 4_15 – Fig. 4_16)

Due to the fact that TGB1 is a key movement protein of PVX, colocalisation experiments of this protein with host organelles were performed. To determine whether the presence of TGB1 alone was sufficient to induce host organelle association with the VRC, the TGB1 protein was introduced into transgenic plants stably expressing markers for ER, Golgi and actin. Uninfected transgenic mGFP5-ER *N. benthamiana* epidermal cells expressing TGB1 (Fig. 4_1 A) (Fig. 4_15 A-C) were compared with PVX-inoculated plants (Fig. 4_1 I) (Fig. 4_15 D-F) or cells infected with the endogenous TGB1 viral construct (Fig. 4_1 J) (Fig. 4_16).

It was found that the TGB1 viral protein could recruit host ER into the VRC and induce membrane modifications in the complete absence of viral infection (Fig. 4_15 A-C). No difference in the structure of the VRC was detected between uninfected (Fig. 4_15 A-C) and infected cells (Fig. 4_15 D-F; Fig. 4_16) in the presence of TGB1. These results demonstrate that the TGB1 protein, on its own, is able to induce major ER reorganisation in the plant cell. ER tubules were detected closely around the TGB1 inclusions in both uninfected (Fig. 4_15 A-C) and infected (Fig. 4_15 D-F; Fig. 4_16) *N. benthamiana* epidermal cells. Rearranged ER tubules were found to be incorporated into the VRC and were continuous with the cortical ER network (Fig. 4_16 B).

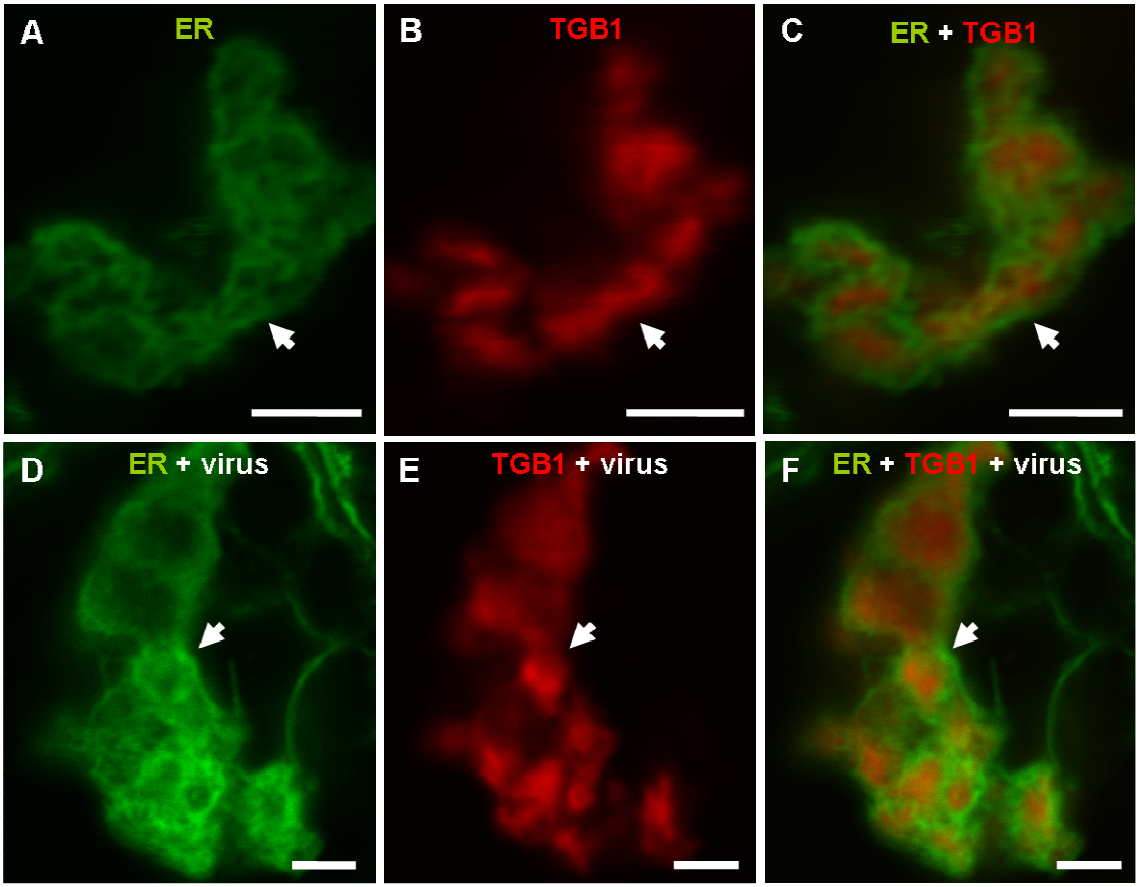

Figure 4_15: TGB1 on uninfected (A-C) and PVX-infected (D-F) transgenic mGFP5-ER *N. benthamiana* plants
Confocal laser scanning images of mGFP5-ER (green) transgenic *N. benthamiana* leaves bombarded with TGB1 (red)
A,D: ER (green channel); B,E: TGB1 (red channel); C,F: overlay of green and red channel (ER + TGB1) in the VRC.
A-C: 1 d.p.b.
D-F: 16 d.p.i. + 1 d.p.b.
d.p.i. – days post-inoculation of PVX; d.p.b. – days post-bombardment of TGB1; thick arrows point to PVX VRCs.
Bars, 5 µm.

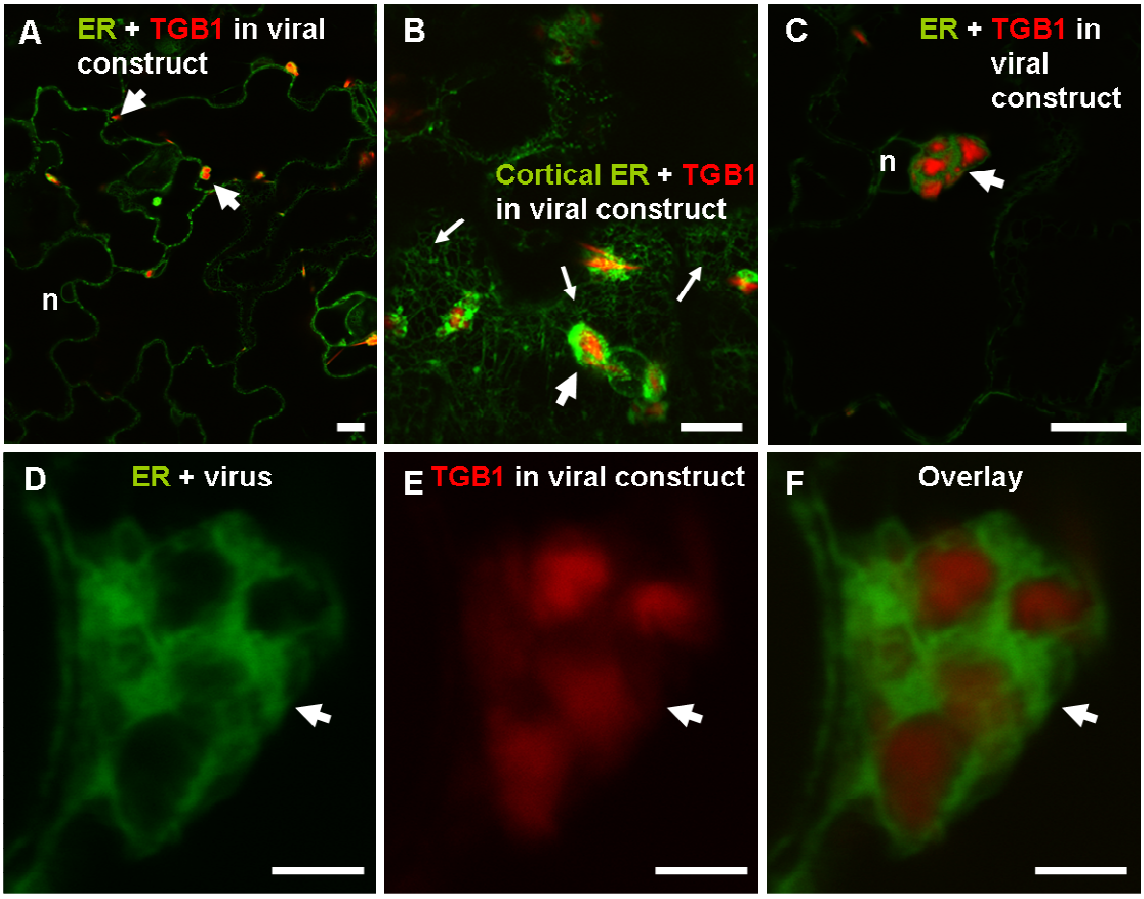

Figure 4_16: Endogenous TGB1 expressed from a viral construct on transgenic mGFP5-ER *N. benthamiana* plants

Confocal laser scanning images of epidermal cells of mGFP5-ER (green) transgenic *N. benthamiana* leaves infected with endogenous TGB1 (red)

A: A leading edge of PVX infection with TGB1 in the centre of PVX VRCs; B: cortical ER network in infected cells; C: a single epidermal cell with TGB1 in the centre of PVX VRCs; D: ER (green channel) in PVX VRC; E: TGB1 (red channel) in PVX VRC; F: overlay of green and red channel (ER + TGB1) in PVX VRC.

A-F: 4 d.p.i. (systemic leaves)

d.p.i. – days post-inoculation of PVX; thick arrows point to PVX VRCs; thin arrows point to the cortical ER network.

Bars, 5 µm (D-F); 20 µm (A-C).

4.2.3.2 The TGB1 protein alone recruits Golgi bodies into the VRC (Fig. 4_17)

Next, to examine whether the TGB1 protein alone induces host Golgi redistribution in the absence of virus infection, the TGB1 protein was introduced into transgenic plants stably expressing Golgi marker. Uninfected transgenic ST-GFP *N. tabacum* epidermal cells expressing TGB1 (Fig. 4_1 A) (Fig. 4_18 A) were compared with cells infected with the endogenous TGB1 viral construct (Fig. 4_1 J) (Fig. 4_17 B-D) or PVX-inoculated plants (Fig. 4_1 I) (Fig. 4_17 E-I).

It was found that TGB1 alone was able to recruit host Golgi into the VRC (Fig. 4_17 A). Uninfected ST-GFP transgenic leaf epidermal cells in the presence of TGB1 (Fig. 4_17 A) displayed a fluorescence pattern in the VRC similar to that of infected cells (Fig. 4_17 B-I). These results illustrate that the TGB1 protein alone is able to recruit the Golgi apparatus into the VRC in the absence of virus. TGB1 and Golgi were found to occupy separate localisations within the VRC in uninfected (Fig. 4_17 A) and infected (Fig. 4_17 B-I) epidermal cells. At the early stages of viral infection (3 d.p.i.), individual Golgi bodies clustered around the TGB1 VRC inclusions (Fig. 4_17 B-D). At the later stages of viral infection (10 d.p.i.), Golgi bodies were incorporated into a distinct sub-compartment of the VRC. (Fig. 4_17 E-I).

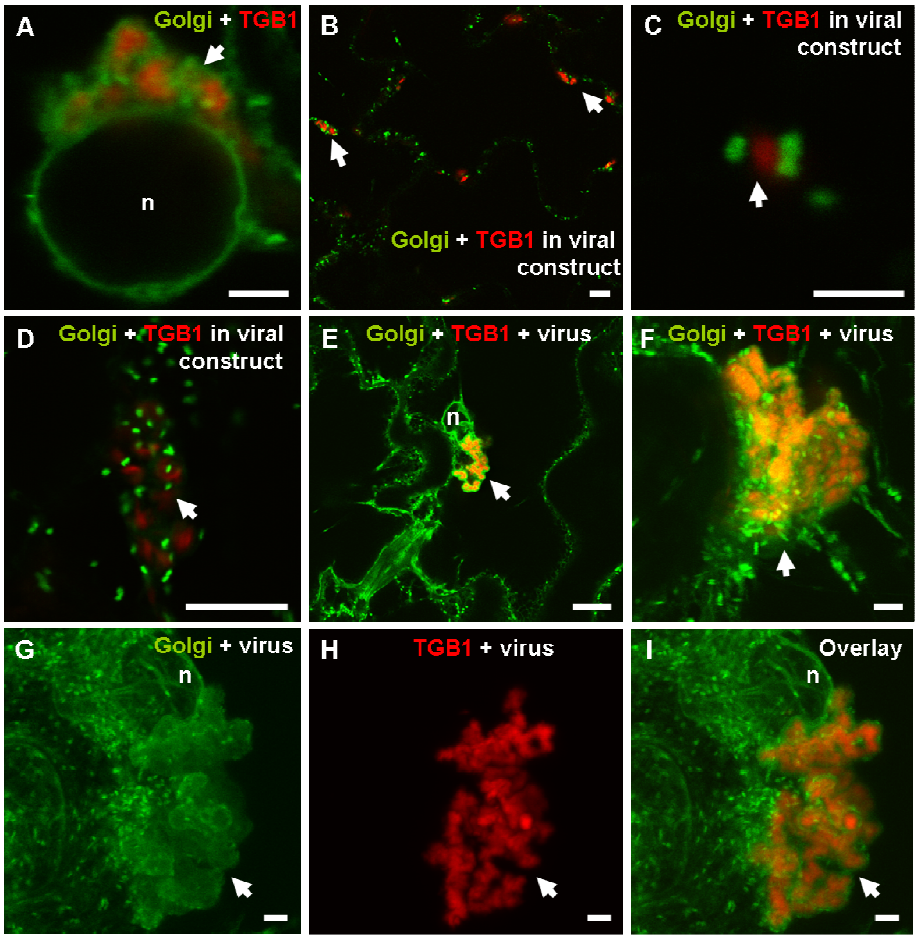

Figure 4_17: TGB1 on uninfected transgenic ST-GFP *N. tabacum* plants (A), endogenous TGB1 expressed from a viral construct on transgenic ST-GFP *N. tabacum* plants (B-D) and TGB1 on PVX-infected transgenic ST-GFP *N. tabacum* plants (E-I)

Confocal laser scanning images of epidermal cells of ST-GFP (green) transgenic *N. tabacum* leaves uninfected (A) or infected with endogenous TGB1 viral construct (B-D) or PVX (PVX is unlabelled) (E-I) (TGB1 in red)

A: A perinuclear 'VRC' with Golgi bodes accumulated around TGB1 in the absence of viral infection; B: epidermal cells of ST-GFP transgenic plants infected with endogenous TGB1 viral construct; C: a higher magnification image of a small forming VRC at early infection events (3 d.p.i.); D: a higher magnification image of a larger PVX VRC at an early infection time-point (3 d.p.i.); E: a single epidermal PVX-infected cell with bombarded TGB1 (10 d.p.i.); F: a higher magnification image of PVX VRC (10 d.p.i.); G: Golgi (green channel) in PVX VRC; H: TGB1 (red channel) in PVX VRC; I: overlay of green and red channel (Golgi + TGB1) in PVX VRC (10 d.p.i.).

A: 1 d.p.b.; B-D: 3 d.p.i. (local leaves); E-I: 10 d.p.i. + 1 d.p.b.; d.p.i. – days post-inoculation of PVX; d.p.b. – days post-bombardment of TGB1; thick arrows point to PVX VRCs; n – nucleus. Bars, 5 µm (A,C,F-I); 20 µm (B,D,E).

4.2.3.3 The TGB1 protein alone recruits host actin into the developing VRC (Fig. 4_18)

Next, to examine whether the TGB1 protein alone is capable of recruiting host actin into the VRC in the absence of virus infection, the TGB1 protein was introduced into transgenic plants stably expressing FABD2-GFP as an actin marker. Uninfected transgenic FABD2-GFP *N. tabacum* epidermal cells expressing TGB1 (Fig. 4_1 A) (Fig. 4_18 A,B) were compared with PVX-inoculated plants (Fig. 4_1 I) (Fig. 4_18 C) or cells infected with the endogenous TGB1 viral construct (Fig. 4_1 J) (Fig. 4_18 D-H).

The results show that the TGB1 protein was able to recruit host actin cytoskeleton into the VRC in the absence of infection (Fig. 4_18 A,B), as it does in a natural PVX infection. The structure of VRCs and the actin fluorescent pattern was nearly identical in uninfected (Fig. 4_18 A,B) and infected cells (Fig. 4_18 C-H). These results suggest that TGB1 on its own can redirect actin into the VRC in the complete absence of virus infection. Actin was identified inside the VRC and around the VRC structure in both uninfected (Fig. 4_18 A,B) and infected (Fig. 4_18 C-H) epidermal cells. As in PVX-infected cells (Fig. 4_18 C-H), actin cables within the VRC were continuous with the cortical actin strands radiating out to the cell cortex (Fig. 4_18 A,B). TGB1 particles were also observed to be moving on actin filaments both in the VRC (Movie 4.5) and in the cytoplasm (Movie 4.6) of the plant cell (Fig. 4_18 D-H).

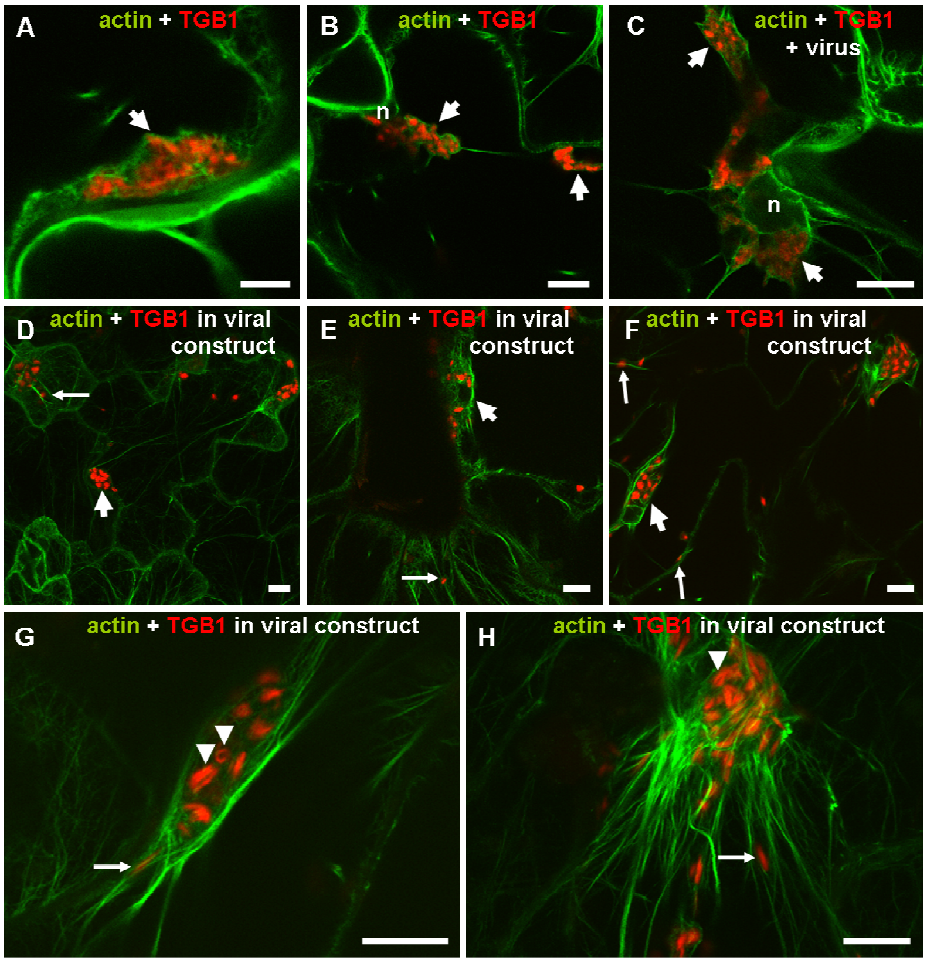

Figure 4_18: TGB1 on uninfected transgenic FABD2-GFP *N. tabacum* plants (A,B), TGB1 on PVX-infected transgenic FABD2-GFP *N. tabacum* plants (C) and endogenous TGB1 expressed from a viral construct on transgenic FABD2-GFP *N. tabacum* plants (D-H)

Confocal laser scanning images of epidermal cells of FABD2-GFP (green) transgenic *N. tabacum* leaves uninfected (A,B) or infected with PVX (PVX is unlabelled) (C) or endogenous TGB1 viral construct (D-H) (TGB1 in red)

A,B: a peripheral (A) and perinuclear (B) the TGB1-induced 'VRC' with actin recruited into the 'VRC' and around this structure in the absence of viral infection; C: a perinuclar PVX VRC at late infection events (19 d.p.i.); D-H: epidermal cells of FABD2-GFP transgenic plants infected with endogenous TGB1 viral construct showing PVX VRCs with 'walnut-like' TGB1 in the centre of VRCs; G-H: a higher magnification image of PVX VRC. A,B: 1 d.p.b.; C: 19 d.p.i. + 1 d.p.b.; D,E: 5 d.p.i. (local leaves); F-H: 6 d.p.i. (local leaves); d.p.i. – days post-inoculation of PVX; d.p.b. – days post-bombardment of TGB1; thick arrows point to PVX VRCs; thin arrows point to TGB1 on actin network; arrowheads point to 'walnut-like' structures of TGB1; n – nucleus.

Bars, 10 μm (A); 20 μm (B-H).

4.2.3.4 The TGB2 and TGB3 proteins induce ER vesicles in the absence and presence of virus infection (Fig. 4_19 – Fig. 4_22)

The TGB2 (Fig. 4_1 B) and the TGB3 (Fig. 4_1 C) proteins were co-expressed together with organelle markers for ER (Fig. 4_1 D) and actin (Fig. 4_1 E) and were found to induce the formation of the abundant small membranous vesicles in the cell cytoplasm and at the cell periphery in the absence (TGB2: Fig. 4_19, TGB3: Fig. 4_21) and presence of PVX (TGB2: Fig. 4_20, TGB3: Fig. 4_22). TGB2 and TGB3 in the VRC and TGB2/TGB3-induced vesicles were found to colocalise with the ER network in the absence (TGB2: Fig. 4_19, TGB3: Fig. 4_21) and presence of PVX infection (TGB2: Fig. 4_20, TGB3: Fig. 4_22). These data indicate that these viral proteins accumulate either in the ER or on these aggregates of the ER. In the presence of infection, it was also observed that some of the ER-induced vesicles did not completely colocalise with TGB2-originated vesicles (Fig. 4_20 C,F) probably due to the disruption of the ER network as a consequence of TGB2 bombardment into the plant cell.

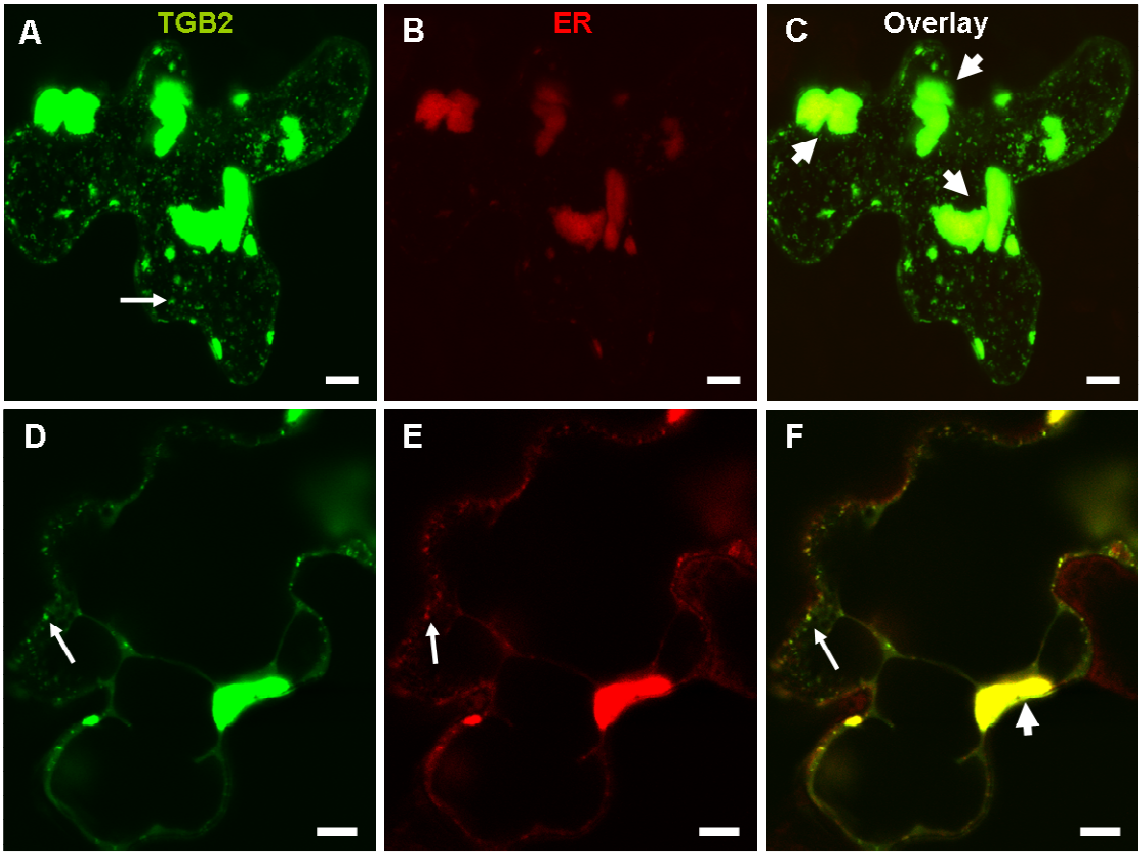

Figure 4_19: Cobombarded TGB2 and ER marker into uninfected non-transgenic *N. benthamiana* plants

Confocal laser scanning images of non-transgenic *N. benthamiana* leaves cobombarded with TGB2 (green) and ER marker (red)

A,D: TGB2 (green channel); B,E: ER marker (red channel); C,F: overlay of green and red channel (TGB2 + ER).

A-F: 1 d.p.b.

d.p.b. – days post-bombardment of TGB2 and ER marker; thick arrows point to 'VRCs'; thin arrows point to the TGB2-induced vesicles.

Bars, 10 µm.

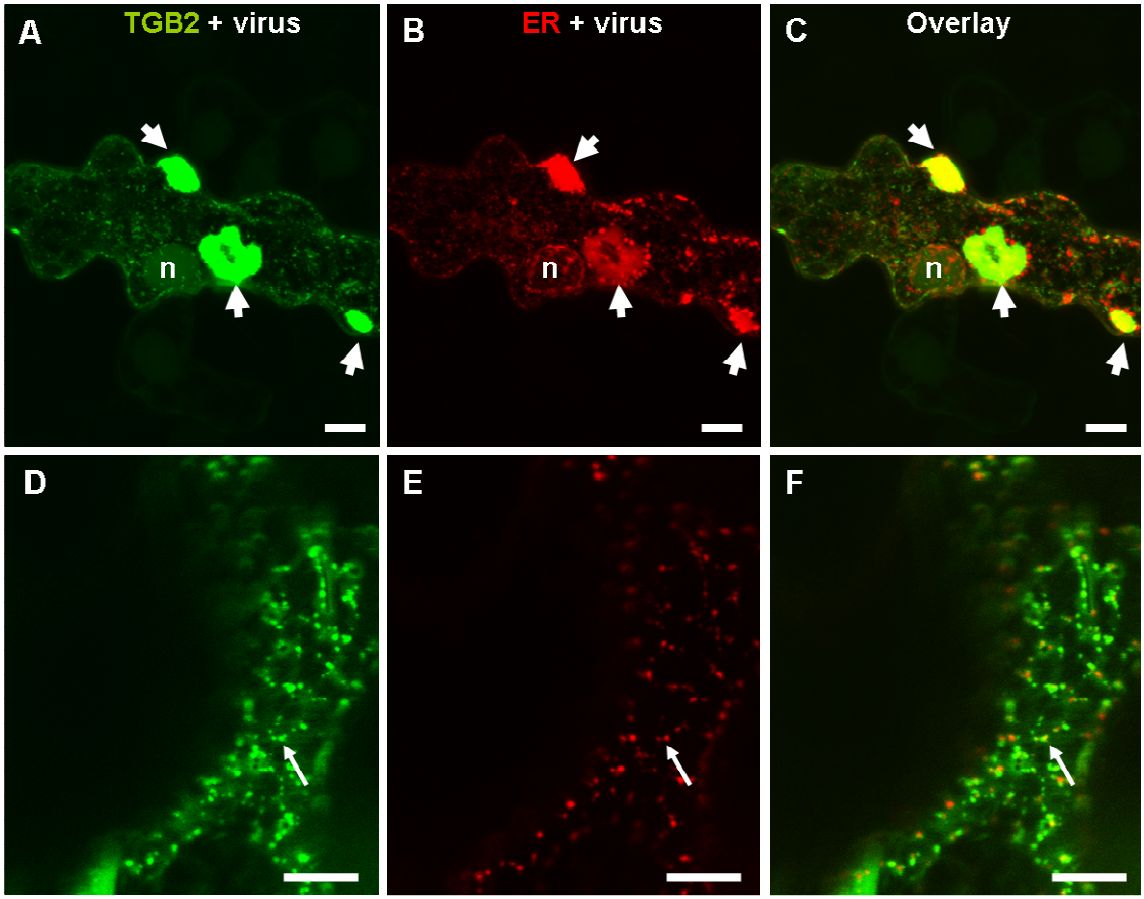

Figure 4_20: Cobombarded TGB2 and ER marker into PVX-infected non-transgenic *N. benthamiana* plants
Confocal laser scanning images of non-transgenic PVX-infected (PVX is unlabelled) *N. benthamiana* leaves cobombarded with TGB2 (green) and ER marker (red)
A,D: TGB2 (green channel); B,E: ER marker (red channel); C,F: overlay of green and red channel (TGB2 + ER); A-C: a single epidermal cell; D-F: a higher magnification image of the cell periphery.
A-F: 1 d.p.b.
d.p.b. – days post-bombardment of TGB2 and ER marker; thick arrows point to PVX VRCs; thin arrows point to the TGB2-induced vesicles; n – nucleus.
Bars, 10 µm.

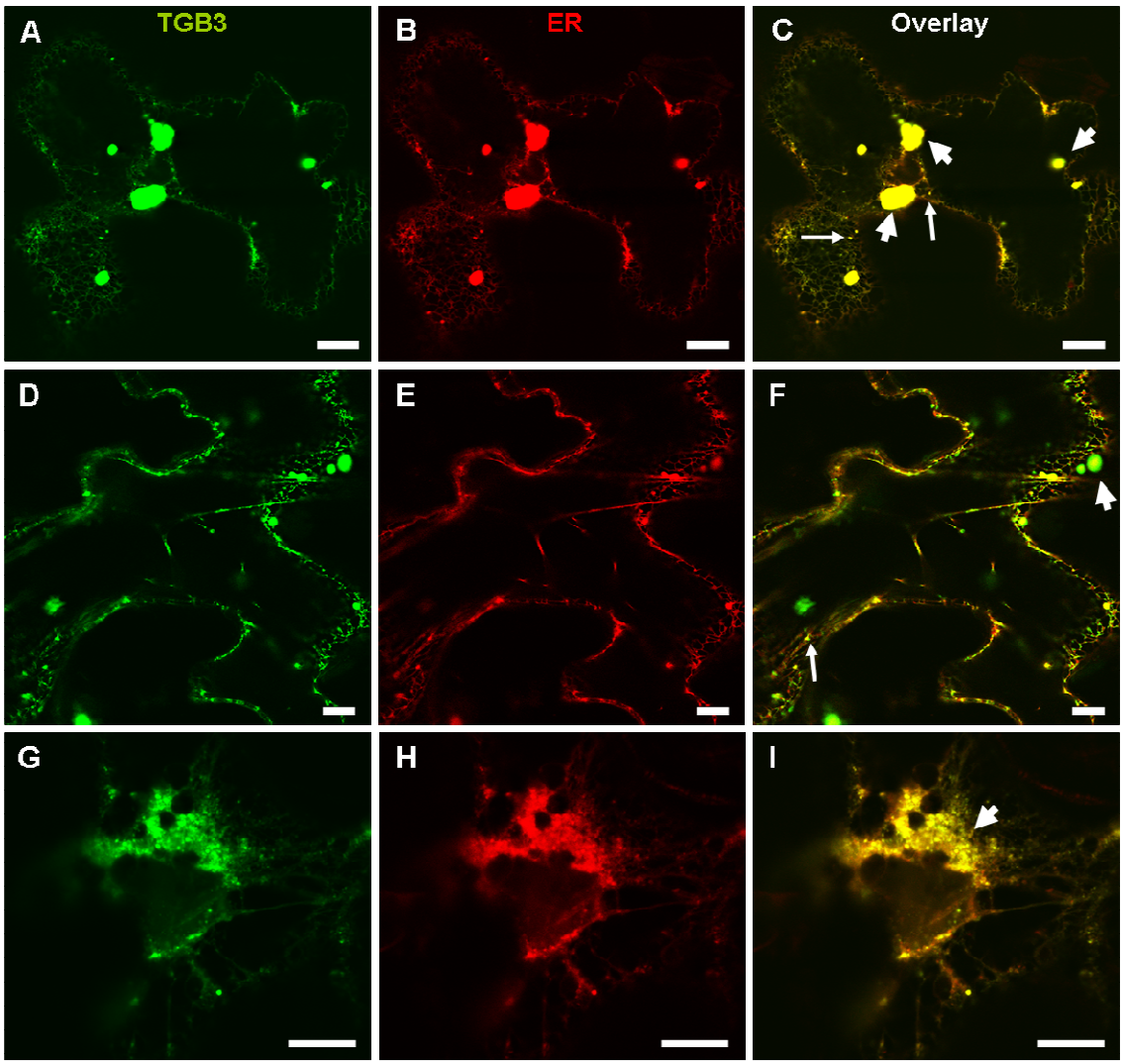

Figure 4_21: Cobombarded TGB3 and ER marker into uninfected non-transgenic *N. benthamiana* plants
Confocal laser scanning images of non-transgenic *N. benthamiana* leaves cobombarded with TGB3 (green) and ER marker (red)
A,D,G: TGB3 (green channel); B,E,H: ER marker (red channel); C,F,I: overlay of green and red channel (TGB3 + ER).
A-I: 1 d.p.b.
d.p.b. – days post-bombardment of TGB3 and ER marker; thick arrows point to 'VRCs'; thin arrows point to the TGB3-induced vesicles.
Bars, 20 µm.

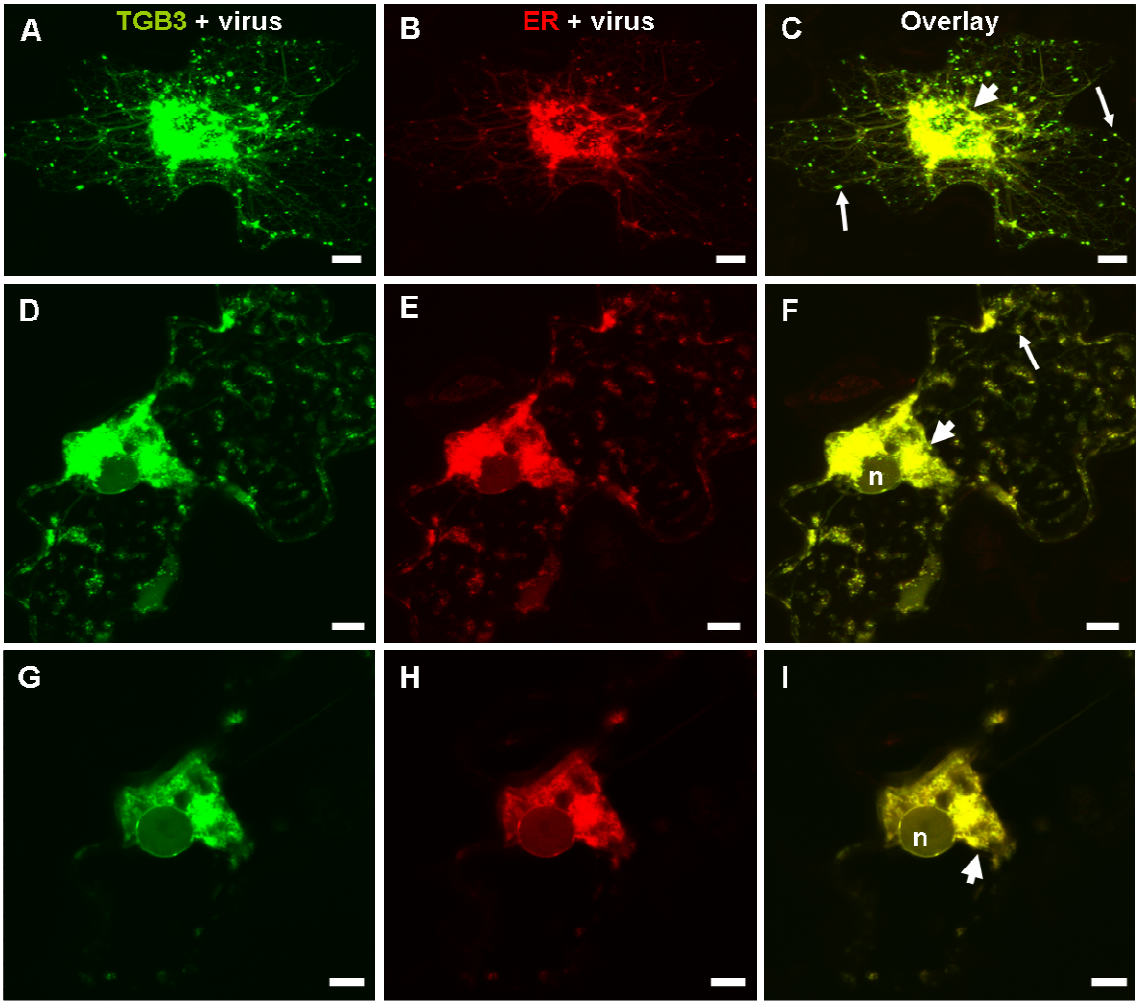

Figure 4_22: Cobombarded TGB3 and ER marker into PVX-infected non-transgenic *N. benthamiana* plants

Confocal laser scanning images of non-transgenic PVX-infected (PVX is unlabelled) *N. benthamiana* leaves cobombarded with TGB3 (green) and ER marker (red)

A,D,G: TGB3 (green channel); B,E,H: ER marker (red channel); C,F,I: overlay of green and red channel (TGB3 + ER); A-F: a single epidermal cell; G-I: a higher magnification image of PVX VRC.

A-I: 1 d.p.b.

d.p.b. – days post-bombardment of TGB3 and ER marker; thick arrows point to PVX VRCs; thin arrows point to the TGB3-induced vesicles; n – nucleus.

Bars, 10 µm.

4.2.3.5 TGB2- and TGB3-derived vesicles move on actin cables (Fig. 4_23 – Fig. 4_26)

Next, uninfected and infected plants were cobombarded with either TGB2 (Fig. 4_1 B) or TGB3 (Fig. 4_1 C) together with the actin marker (Fig. 4_1 E). As before, uninfected control plants were compared with infected plants. TGB2 and TGB3 were also shown to induce numerous green fluorescent vesicles in the cell cytoplasm and at the cell periphery in the absence (TGB2: Fig. 4_23, TGB3: Fig. 4_25) and presence of PVX (TGB2: Fig. 4_24, TGB3: Fig. 4_26). The TGB2- and TGB3-derived vesicles were found to be moving on actin filaments (TGB2: Movie 4.7-4.8, TGB3: Movie 4.9) (also thin arrows in Fig. 4_23, 4_24 C; Fig. 4_25 C, 4_26 F). These results confirm earlier findings that TGB2-induced vesicles move on actin (Ju *et al*., 2005; reviewed in Verchot-Lubicz *et al*., 2007). Actin was also detected around vesicle aggregates of TGB2, and especially of TGB3, in the absence (TGB2: Fig. 4_23 B, TGB3: Fig. 4_25 H) and presence of infection (TGB2: Fig. 4_24 B, TGB3: arrowheads in Fig. 4_26 B).

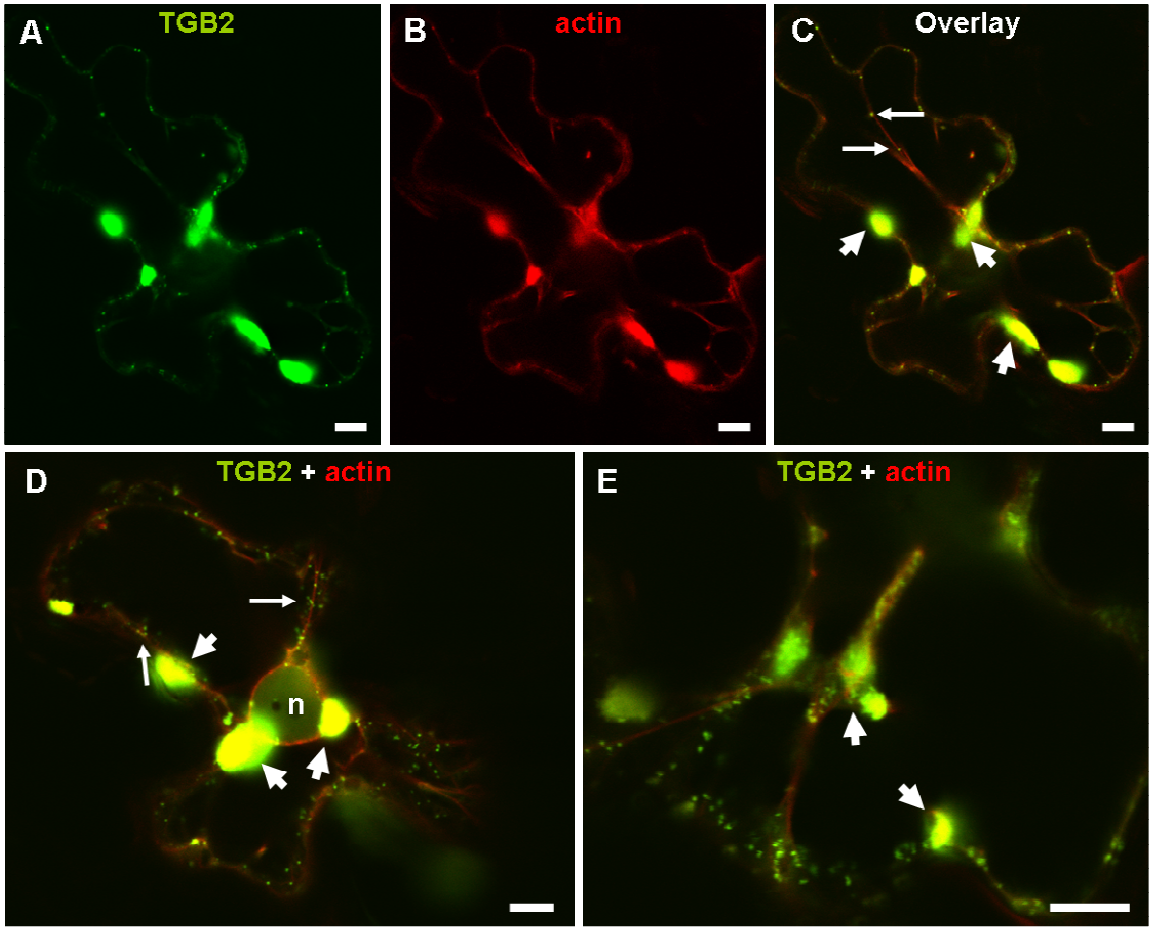

Figure 4_23: Cobombarded TGB2 and actin marker into uninfected non-transgenic *N. benthamiana* plants
Confocal laser scanning images of non-transgenic *N. benthamiana* leaves cobombarded with TGB2 (green) and actin marker (red)
A: TGB2 (green channel); B: actin marker (red channel); C-E: overlay of green and red channel (TGB2 + actin).
A-E: 1 d.p.b.
d.p.b. – days post-bombardment of TGB2 and actin marker; thick arrows point to 'VRCs'; thin arrows point to the TGB2-induced vesicles moving on actin cables.
Bars, 10 µm.

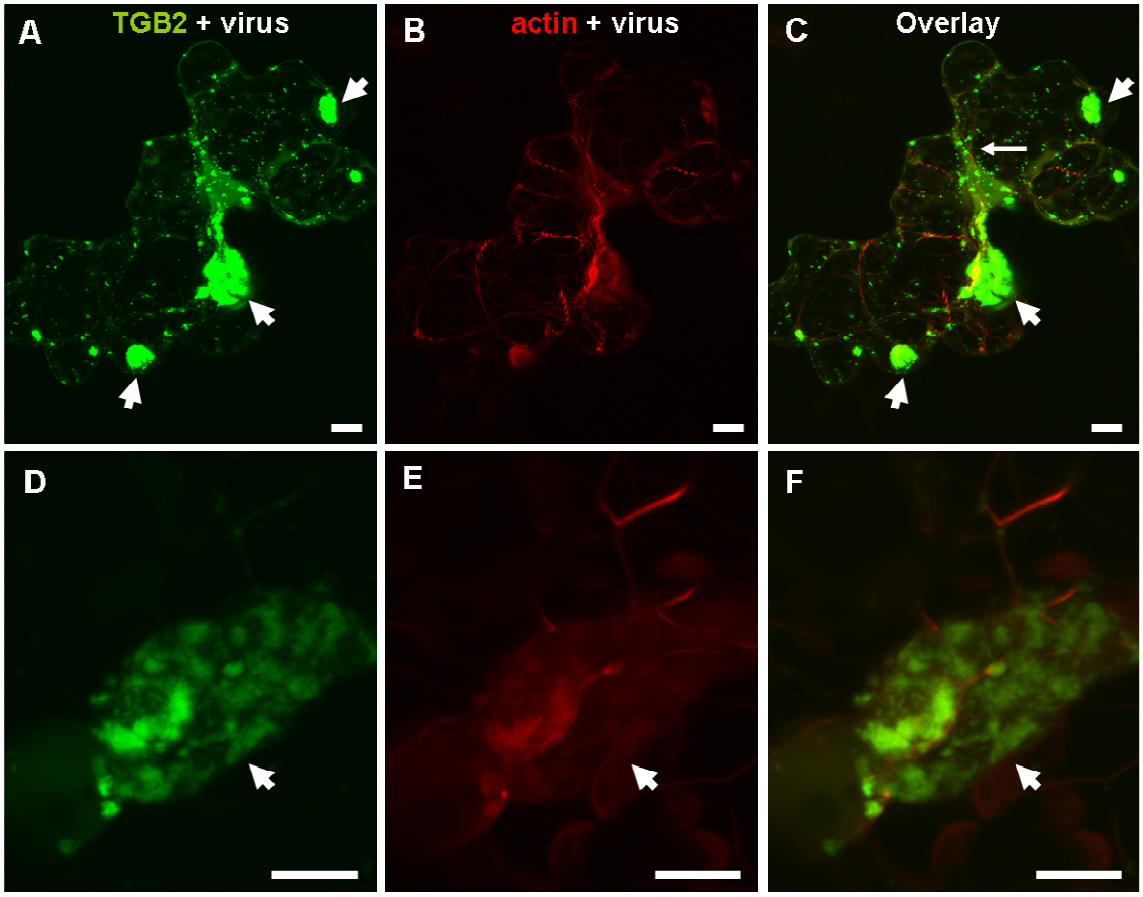

Figure 4_24: Cobombarded TGB2 and actin marker into PVX-infected non-transgenic *N. benthamiana* plants
Confocal laser scanning images of non-transgenic PVX-infected (PVX is unlabelled) *N. benthamiana* leaves cobombarded with TGB2 (green) and actin marker (red)
A,D: TGB2 (green channel); B,E: actin marker (red channel); C,F: overlay of green and red channel (TGB2 + actin); A-C: a single epidermal cell; D-F: a higher magnification image of PVX VRC.
A-F: 1 d.p.b.
d.p.b. – days post-bombardment of TGB2 and actin marker; thick arrows point to PVX VRCs; thin arrows point to the TGB2-induced vesicles moving on actin cables.
Bars, 10 µm.

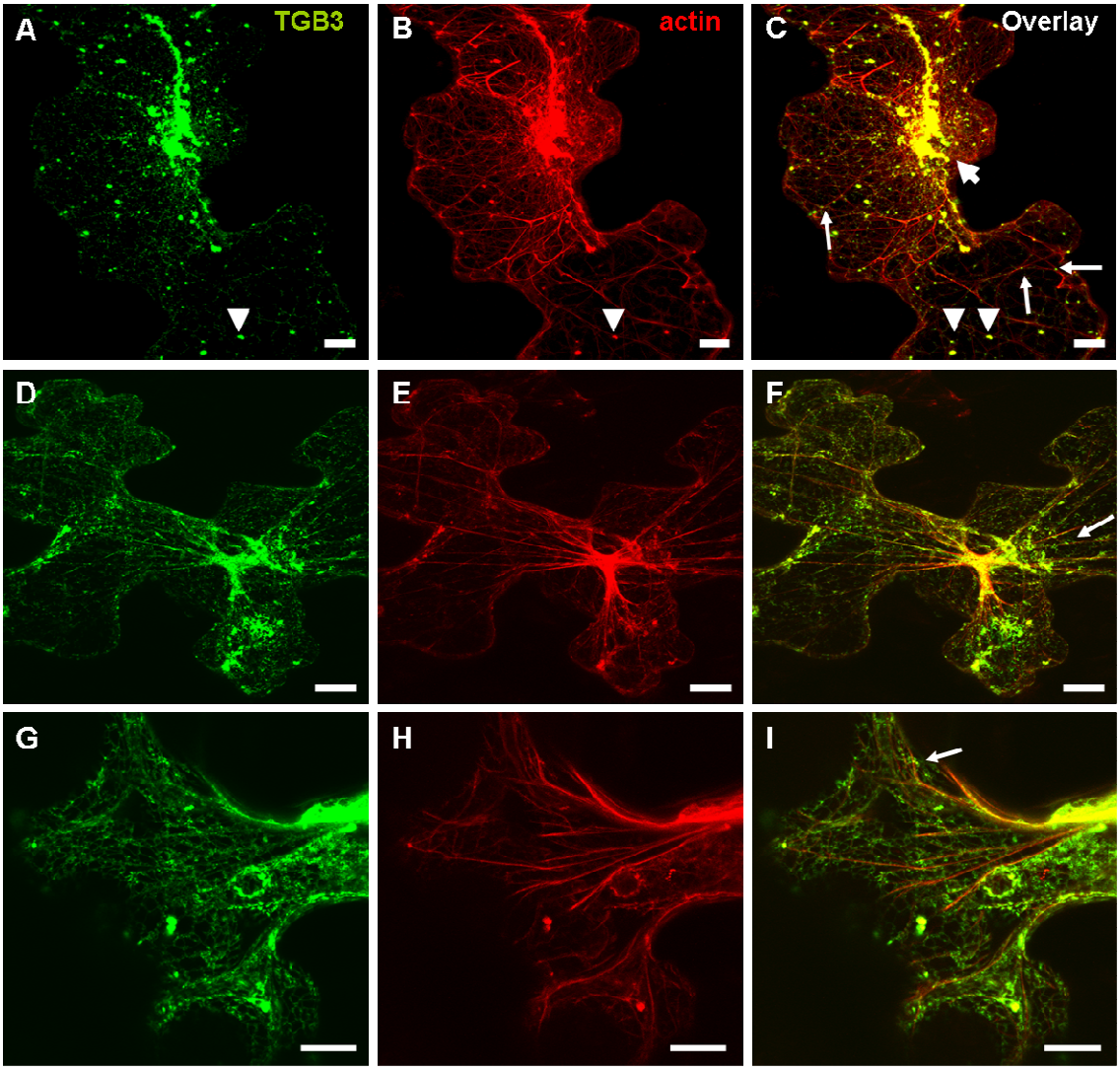

Figure 4_25: Cobombarded TGB3 and actin marker into uninfected non-transgenic *N. benthamiana* plants

Confocal laser scanning images of non-transgenic *N. benthamiana* leaves cobombarded with TGB3 (green) and actin marker (red)

A,D,G: TGB3 (green channel); B,E,H: actin marker (red channel); C,F,I: overlay of green and red channel (TGB3 + actin).

A-I: 1 d.p.b.

d.p.b. – days post-bombardment of TGB3 and actin marker; thick arrows point to 'VRCs'; thin arrows point to the TGB3-induced vesicles moving on actin cables; arrowheads point to the TGB3-induced vesicles and colocalised actin clusters around these vesicles.

Bars, 20 µm.

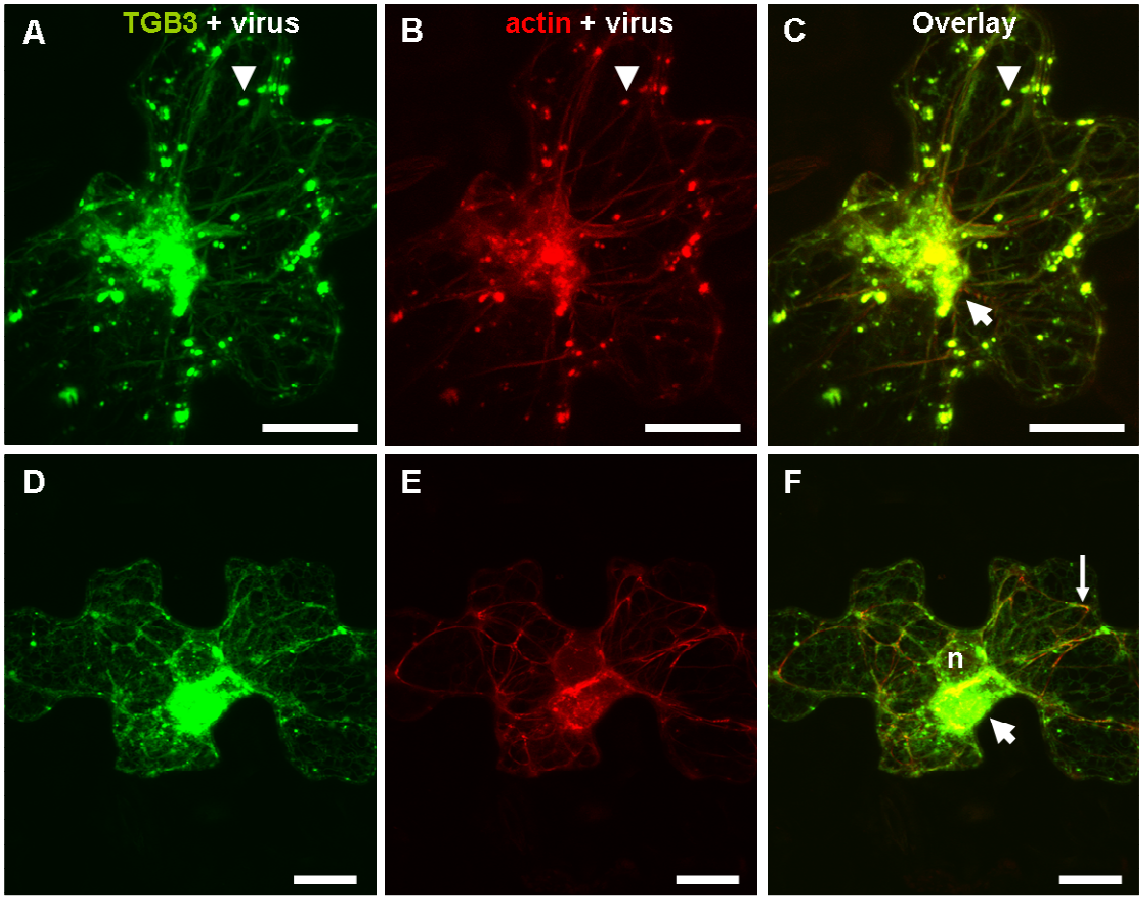

Figure 4_26: Cobombarded TGB3 and actin marker into PVX-infected non-transgenic *N. benthamiana* plants
Confocal laser scanning images of non-transgenic PVX-infected (PVX is unlabelled) *N. benthamiana* leaves cobombarded with TGB3 (green) and actin marker (red)
A,D: TGB3 (green channel); B,E: actin marker (red channel); C,F: overlay of green and red channel (TGB3 + actin).
A-F: 1 d.p.b.
d.p.b. – days post-bombardment of TGB3 and actin marker; thick arrows point to PVX VRCs; thin arrows point to the TGB3-induced vesicles moving on actin cables; arrowheads point to the TGB3-induced vesicles and colocalised actin clusters around these vesicles; n – nucleus.
Bars, 20 µm.

4.2.4 Mutational analysis of PVX constructs

To answer the question which viral gene products are required to construct a VRC, and to find out which viral proteins are essential for the attachment of the transport complex to PD, PVX mutant constructs were generated using a reverse genetics approach. Frameshift mutations in the individual TGB genes and deletions of the CP gene were constructed. Mutant constructs lacking a combination of two and/or all three TGB proteins were generated (Fig. 4_1 L). In this approach the mutated gene of interest becomes non-functional leading to an altered infection phenotype (Dietrich, 2000). However, due to time constraints, some of the mutational analyses were done by Dr. Jens Tilsner.

The biogenesis and structure of the PVX VRC was investigated in the absence of specific viral gene products (ΔTGB1, Fig. 4_27 A,B; ΔTGB2, Fig. 4_27 C; ΔTGB3, Fig. 4_27 D,E). To answer the question which of TGB1, TGB2 and/or TGB3 are required for VRC formation, non-transgenic plants were agroinfiltrated with PVX 'overcoat' mutant constructs lacking TGB1 (Fig. 4_1 M), TGB2 (Fig. 4_1 N) and TGB3 (Fig. 4_1 O) genes, respectively. Single infected plant cells were examined under the confocal laser scanning microscope due to the fact that the deletion of TGB movement proteins leads to a loss of PVX transport function.

4.2.4.1 Mutation of the TGB1 gene affects VRC formation (Fig. 4_27)

ΔTGB1 mutation abolished PVX VRC formation, and only weak cytosolic and nuclear GFP signals were detected in the single infected cells (Fig. 4_27 A). However, brighter spots of GFP fluorescence were also found in some cells (arrowheads in Fig. 4_27 B) which were likely to be small aggregates of PVX 'overcoat' particles.

4.2.4.2 Mutation of the TGB2 and TGB3 genes does not influence VRC formation (Fig. 4_27)

ΔTGB2 and ΔTGB3 mutations failed to abolish VRC formation, and normal VRCs (ΔTGB2, Fig. 4_27 C; ΔTGB3, Fig. 4_27 D,E) developed in the cell cytoplasm for up to 5 days post-inoculation. The VRCs resembled the 'native' VRCs observed previously (see Fig. 4_3 A,B). However, 'overcoat' virus particles were detected only in ΔTGB2-infected plant cells (Fig. 4_27 C), not in ΔTGB3-infected cells, indicating that mutation in the TGB2 protein does not completely inhibit the formation of PVX 'overcoat' particles.

4.2.4.3 TGB1, but not TGB2/TGB3, is essential for actin recruitment into the VRC (Fig. 4_27)

To verify which TGB proteins are required for actin recruitment into the VRC, Dr. Jens Tilsner coinfiltrated non-transgenic *N. benthamiana* plants with mutated viral constructs lacking the TGB1 protein (Fig. 4_1 M), the TGB2 protein (Fig. 4_1 N) and the TGB3 protein (Fig. 4_1 O) together with an actin marker (Fig. 4_1 F).

The results show that mutation of the TGB1 gene (Fig. 4_1 M) leads to abolishment of actin association with the VRC as only very weak GFP nuclear signal was detected in PVX-infected cells (Fig. 4_27 F). These results verified that PVX TGB1 plays a central function in the rearrangement of host actin into the VRC. In contrast, agroinfiltrated ΔTGB2 (Fig. 4_1 N) and ΔTGB3 (Fig. 4_1 O) viruses did not influence actin organisation, and actin recruitment into the VRC was detected (data not shown), suggesting that these two viral proteins are unlikely to play a significant role in actin recruitment into the VRC.

The summary of the results of the studied mutations described above is represented in Table 4.2.

Table 4.2: Summary of the outcome of the mutations studied

Mutation	**PVX VRC formation**	**Viral CP localisation**		**Actin association with the VRC**
		in the perinuclear VRC	**in the cell cytoplasm**	
ΔTGB1	Abolished	None	Some aggregates of PVX 'overcoat' virus-like particles	None
ΔTGB2	Normal VRCs	Large, fibrillar aggregates of PVX virions	Small PVX 'overcoat' virus-like particles	Present
ΔTGB3	Normal VRCs	Large, fibrillar aggregates of PVX virions	None	Present

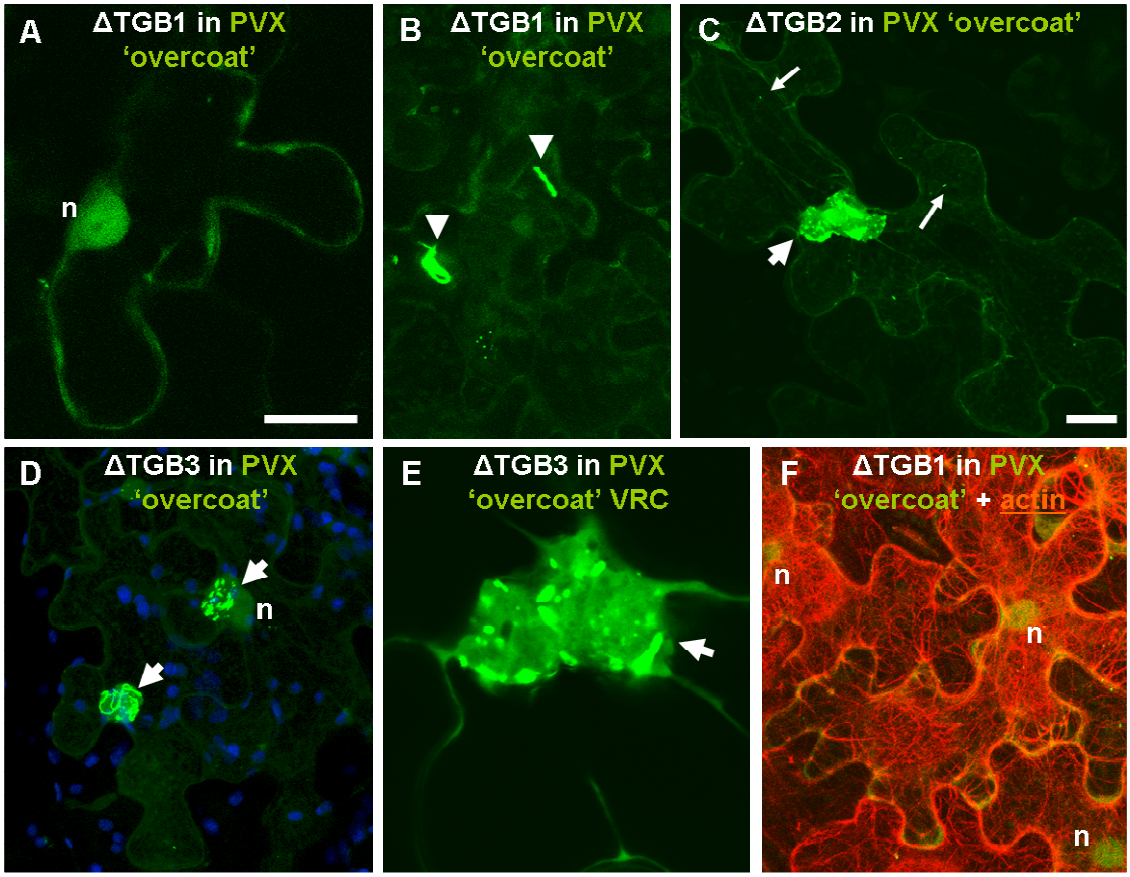

Figure 4_27: ΔTGB1 (A,B), ΔTGB2 (C), ΔTGB3 (D,E) PVX 'overcoat' mutant constructs, ΔTGB1 PVX 'overcoat' mutant construct + actin marker (F) on non-transgenic *N. benthamiana* plants

Confocal laser scanning images of non-transgenic *N. benthamiana* leaves infected with PVX 'overcoat' mutant constructs (green) (A-F) and coinfiltrated with an actin marker (red) (F)

A,B: ΔTGB1 PVX 'overcoat' mutant construct (CP in green); C: ΔTGB2 PVX 'overcoat' mutant construct (CP in green); D,E: ΔTGB3 PVX 'overcoat' mutant construct (CP in green); D: overview of the infected cells: ΔTGB3 PVX CP (green), chloroplasts (blue); E: a higher magnification image of the ΔTGB3 PVX 'overcoat' VRC; F: ΔTGB1 PVX 'overcoat' mutant construct (CP in green) + actin marker (actin in red).

A-E: 5 d.p.i., F: 4 d.p.i. + 1 d.p.a.

d.p.i. – days post-inoculation of PVX; d.p.a. – days post-agroinfiltration of actin marker; thick arrows point to PVX VRCs; thin arrows point to the PVX 'overcoat' particles; arrowheads point to the pockets of virions; n – nucleus.

Bars, 20 µm.

All images represented in Fig. 4_27 were adapted from Dr. Jens Tilsner.

4.3 Discussion

4.3.1 The TGB1 protein associates with PD in the absence of virus infection

The results of this thesis identified that PVX TGB1 accumulated in PD in the absence of virus infection (Fig. 4_2). Importantly, PVX TGB1 protein has not previously been reported in PD in the absence of infection (Samuels *et al*., 2007). It has been shown that the TGB1 MP of beet necrotic yellow vein virus (BNYVV) localises to PD of virus-infected plant cells by means of immunogold studies (Erhardt *et al*., 2000; 2005). However, the TGB1 protein of BNYVV was not identified in PD in the absence of virus infection (Erhardt *et al*., 2005).

The mechanism of targeting of PVX TGB1 protein to PD is speculative. Samuels *et al*. hypothesised that the CP is the most important candidate for TGB1 targeting to PD (Samuels *et al*., 2007) due to the fact that PVX CP is known to associate with PD of infected cells (Oparka *et al*., 1996). They hypothesised that a TGB1-PD association may happen independently of other TGB MPs (Samuels *et al*., 2007). My results and results from our lab indicate that TGB1 does not require other viral gene products to accumulate in PD (Fig. 4_2 C,F).

4.3.2 Colocalisation studies of PVX TGB MPs and CP in PD

4.3.2.1 Colocalisation of TGB1 and CP signals in PD

An indication of the presence of virions during vRNA transport through PD is the detection of fibrillar material in PD infected with green 'overcoat' PVX (Santa-Cruz *et al*., 1996). In the experiments here, localisation of PVX CP in infected plant cells was confirmed by detection of characteristic large, fibrillar aggregates of PVX virions in the perinuclear VRCs (Fig. 4_3 A,B). In addition, a highly mobile population of small virus-like particles containing PVX CP was detected, and CP was found in numerous PD (Fig.

4_3 C,E; arrowheads in Fig. 4_5; Fig. 4_6 A-C). Significantly, the TGB1 protein was found in the same motile particles as viral CP (Fig. 4_4; Fig. 4_5; Fig. 4_6 A-C). The TGB1 and CP particles were also observed to be moving together in the cytoplasm of bombarded cells (Fig. 4_4 A-F), and were detected outside the bombarded area in the cytoplasm of the neighbouring cells (Fig. 4_7). These results provide evidence that the TGB1 and CP may be part of the movement complex that traffics the viral genome from the VRC through PD. These results also support the proposed model of PVX cell-to-cell movement, in which the PVX genome can move in a the form of a virion-like ribonucleoprotein complex consisting of vRNA, CP and TGB1 (Oparka *et al*., 1996; Lough *et al*., 1998; Santa Cruz *et al*., 1998; Solovyev *et al*., 2000; Rodionova *et al*., 2003; Karpova *et al*., 2006; reviewed in Verchot-Lubicz *et al*., 2007).

Early *in vitro* experiments on PVX viral particle assembly discovered STPs consisting of vRNA, CP and TGB1 (Lough *et al*., 1998, 2000; Atabekov *et al*., 2000, 2001; Rodionova *et al*., 2003; Karpova *et al*., 2006). In these experiments STPs assemble by CP interaction with the 5' region of the vRNA. Once TGB1 binds to this assembled CP-vRNA complex, the vRNA is converted into a translatable form (Karpova *et al*., 2006). The data of this thesis also identified structures at the cell periphery of PVX-infected cells resembling partially coated STPs with one end attached to the TGB1 protein (Fig. 4_6 D-F). However, STPs of TGB1 associated with PVX 'overcoat' particles were not found outside of cells bombarded with TGB1.

In a different experiment, it was shown that TGB1 alone can traffic from uninfected to surrounding, non-bombarded cells. However, TGB1 moves more extensively when coexpressed during a PVX infection, and accumulates in the centre of VRCs in adjacent cells (Fig. 4_11; Fig. 4_14 A-C), suggesting that the TGB1 protein is non-cell autonomous. These results also indicate that interaction of TGB1 with viral CP or/and vRNA of PVX may be necessary to facilitate expansive cell-to-cell movement of TGB1. In addition, these data are in agreement with prior reports in which the PVX TGB1 protein, like the TGB1 protein of white clover mosaic virus (Wong *et al*., 1998), induced

PD gating by increasing the SEL of plasmodesmata to enable the transfer of virus and other molecules between plant cells. This intercellular movement of TGB1, independently of other PVX-encoded MPs (TGB2, TGB3 and CP), was also recorded in earlier reports (Angell *et al*., 1996; Lough *et al*., 1998, 2000; Yang *et al*., 2000; Howard *et al*., 2004). The data on TGB1 trafficking from infected into uninfected tissue is also consistent with the role of this protein in suppressing host viral RNA silencing (Voinnet *et al*., 2000; Carrington *et al*., 2001; Baulcombe, 2002; reviewed in Scholthof, 2005). The TGB1 protein may be sequestered away from PD when the role of this protein in PD gating is no longer necessary for the virus (Yang *et al*., 2000). In addition, despite the negative results of the two yeast hybrid screen (Samuels *et al*., 2007), the results of this thesis indicate that there is an interaction between the TGB1 and TGB2 protein as the TGB2 association with PD was only detected in the presence of TGB1 (see the following section for more details).

4.3.2.2 Colocalisation of TGB2, TGB3 and CP signals in PD

Very recently our lab has shown that the TGB2 protein also localises in the motile packets of 'overcoat' particles at the leading edge of infection, and that TGB2 and 'overcoat' particles also colocalise in PD (unpublished data from Dr. Jens Tilsner). These results are also consistent with reports in which PVX TGB2 was shown to increase PD SEL, allowing the passage of a free GFP between PVX-infected cells (Tamai and Meshi, 2001). In addition, it was found that PVX TGB2 could associate with TIP, a host factor that interacts with β-1,3-glucanase, resulting in increased callose degradation (Fridborg *et al*., 2003). This could be a possible mechanism of regulating the size exclusion limit of PD during PVX infection (reviewed in Boevink and Oparka, 2005). However, TGB2 PD targeting is probably achieved through association with the TGB1 viral protein, as accumulation of TGB2 in PD was only observed when TGB1 was present. It is likely that TGB1 interacts with components in the cytoplasmic sleeve or/and the desmotubule of PD. The association of TGB2 with host factors in the membrane or lumen of the cortical ER strand in PD is also possible. Also, due to the fact

that no or limited non-cell autonomous movement of TGB2 has been reported (this study, see also Lough *et al*., 2000, Krishnamurthy *et al*., 2002, 2003, Mitra *et al*., 2003), TGB2 may act as the main PD gating protein for PVX genome translocation from one cell to another (Tamai and Meshi, 2001).

In contrast, the TGB3-induced vesicles were not convincingly identified in PD either in the absence (Fig. 4_12 A-B) or presence of virus infection (Fig. 4_12 D-E). However, like TGB2, an attempt to colocalise TGB3 with the CP-expressing particles has now been successful. The TGB3 protein was found in the same motile particles together with the viral CP in the cell cytoplasm (motile population) and TGB3 was also colocalised with the virus-like particles in the cell PD (stationary population of TGB3 and virus-like particles) (unpublished data from Dr. Jens Tilsner). Our failed efforts to detect TGB3 in PD may be the result of the very low expression of TGB3 in natural PVX infections (Yang *et al*., 2000). The amounts of TGB2 and TGB3 are regulated in the cell relative to the other viral proteins, and the TGB2 and TGB3 proteins are found at much lower amounts in the infected cells compared to other viral proteins (Yang *et al*., 2000). The TGB3 protein is particularly expressed in very low amounts, probably due to a leaky ribosome scanning translation mechanism (Guilford and Forster, 1986; Dolja *et al*., 1987; Zhou and Jackson, 1996; Morozov and Solovyev, 2003). For example, the transcript ratio of TGB1/TGB2/TGB3 for the potexvirus barley strip mosaic virus is 100/10/1, respectively (Lim *et al*., 2008). Based on our knowledge of barley stripe mosaic virus and other TGB-containing viruses with similar expression strategies to PVX, the TGB2/TGB3 ratio for PVX is expected to be about 10/1. Therefore, if the TGB2 protein was barely detected in PD using immuno-transmission electron microscopy approach, TGB3 would be very likely to be undetectable using confocal scanning methods. This idea is consistent with other experiments in which PVX TGB3 could not be detected in infected cells (Gorshkova *et al*., 2003). In addition, is has been also noted in earlier studies (Ju *et al*., 2008), and confirmed in our laboratory (unpublished data from Dr. Jens Tilsner), that PVX infection initiates the degradation of the TGB3 viral protein, explaining the fact the TGB3 particles were found to be

dispersed at the periphery of PVX 'overcoat'-infected cells (unpublished data from Dr. Jens Tilsner). Unlike TGB3, viral CP, TGB1 and TGB2 proteins were all detected in the PD of infected cells.

4.3.3 PVX TGBs and CP occupy different locations within the VRC

4.3.3.1 Different localisation patterns of TGB1 and 'overcoat' virions in the PVX VRC

The TGB1 and PVX 'overcoat' signals were spatially separated from one another in the VRC (Fig. 4_8 C,D). Similar to PVX, the TGB1 protein inclusions of foxtail mosaic potexvirus (FMV) were also described in close proximity to virion 'packets' in the study of Rouleau *et al*. (1994). However, the morphology of FMV TGB1 inclusions was found to be different to that of PVX TGB1. FMV TGB1 forms elaborate potexvirus crystals, possibly associated with particle processing before viral movement (Rouleau *et al*., 1994).

The data on TGB1 and PVX 'overcoat' colocalisation studies is consistent with EM data that show viral replication complexes containing PVX CP particles in a regularly stacked form at the outer edges of the PVX VRC or sometimes distributed randomly throughout the VRC (Kozar and Sheludko, 1969; Shalla and Shepard, 1972; Tilsner *et al*., 2009).

When the CP is synthesised, the coating of newly produced (+)RNA is initiated, resulting in the generation of fully-coated viral particles (Hillman, 1998; Ring and Blair, 2001) that are probably sequestered towards the outer edges of the VRC. This would explain the arrangement of PVX virions on the periphery of the VRC. The location of viral CP at the outer edges of the VRC also indicates that the formation of a transport complex with vRNA, TGB1 and CP may take place at the outside edge of the VRC,

after vRNA and TGB1 have been through a 'production line' consisting of a series of spatially defined PVX VRC sub-compartments.

4.3.3.2 Circular 'walnut-like' TGB1 inclusions in the PVX VRC are the 'beaded sheets' shown in EM studies

It was found that at the infection centre, endogenous mCherry-tagged TGB1 protein expressed from a virus-based vector (Fig. 4_1 J) formed circular 'walnut-like' inclusions in the VRC (Fig. 4_8 A,B). This observation is consistent with the early literature in which rounded 'beaded sheets' of PVX TGB1 protein were found in the perinuclear X-bodies (Kozar and Sheludko, 1969; Stols *et al*., 1970; Shalla and Shepard, 1972; Allison and Shalla 1974; Davies *et al*., 1993; see Fig. 1_13-15 in Chapter 1). Moreover, the 'beaded sheet-like' structures of the TGB1 protein disappear in the absence of TGB1 (unpublished data from our lab), proving an additional support that TGB1 is the main component of this viral structure.

The TGB1-induced rod-shaped elongated inclusions in the cytoplasm of infected cells were first identified in early EM studies (Davies *et al*., 1993; Rouleau *et al*., 1994) and were also reported in Samuels *et al*. work (Samuels *et al*., 2007). These structures were also seen in my study and are probably the same TGB1 inclusions in the VRC (Fig. 4_8 A,B) when viewed in a confocal laser scanning microscope. It is possible that this 'needle-like' arrangement of the TGB1 protein is due to the protein aligning along actin microfilaments.

4.3.4 Compartmentation of PVX TGBs in the VRC

In all combinations of TGB proteins, TGB1, TGB2 and TGB3 were found to localise in separate, spatially distinct sub-compartments within the VRC both in the absence (Fig. 4_9 D-F; Fig. 4_12 C; Fig. 4_13 E) and presence of viral infection (Fig. 4_11 B-C; Fig. 4_12 F; Fig. 4_14 D,E). The TGB1 protein was central in the VRC, while TGB2/3

compartments surrounded the TGB1 sub-compartment. The spatial separation of TGB2/3 from TGB1 is consistent with the fact that TGB1 was not shown to interact with TGB2 and TGB3 (Samuels *et al*., 2007).

However, the fluorescent pattern in the VRC observed for TGB2 and TGB3 was found to be different: TGB3 formed 'grape-like' clusters around the TGB1 protein (Fig. 4_12 C,F) while TGB2 was observed to be more dispersed in the VRC (Fig. 4_9 F, Fig. 4_10 C), suggesting that TGB2 and TGB3 may not be completely colocalised in the VRC. These data are also consistent with earlier findings showing that in infected tissues TGB2 labels the ER more generally and is dispersed in the reticular network in the form of vesicles, while TGB3 is concentrated in discrete round cytoplasmic aggregates that when concentrated together form 'grape-like' structures in the VRC (Ju *et al*., 2005, 2007). In addition, it has been suggested that in early infection TGB2 and TGB3 proteins are likely to target separate sub-domains of the endomembrane system and at the later stages of viral infection become colocalised in the same sub-compartments of the VRC (Samuels *et al*., 2007).

Mutational analysis of PVX constructs showed that TGB1 (Fig. 4_27 A,B), but not TGB2 (Fig. 4_27 C) or TGB3 (Fig. 4_27 D,E), is required for VRC formation. ΔTGB2 and ΔTGB3 mutations failed to abolish PVX VRC formation. The results also indicate that the TGB1 protein is a main player in encapsidation of viral RNA due to the fact that mutation of the TGB1 gene led to the reduction of the 'overcoat' virion accumulation in infected cells (Fig. 4_27 B). It is likely that TGB1 RNA helicase activity may be involved in the process of assembly of virions at the outer edges of the VRC.

4.3.5 Colocalisation studies of PVX TGB MPs with host organelles

4.3.5.1 TGB1 recruits host endomembranes and actin to the VRC in the absence of virus infection

TGB1 alone was also found to redirect the host ER, Golgi and actin filaments into the VRC. The mutational analysis verified that TGB1 is essential for actin recruitment into the PVX VRC due to the fact that the deletion in the TGB1 gene led to abolishment of actin association with the VRC. All this suggests that TGB1 is the main PVX protein required for rearrangement and recruitment of host organelles into the developing VRC.

TGB1 was surrounded by endomembranes and cortical actin, providing further evidence for strong compartmentation of the PVX VRC. TGB1 was also found to move along actin microfilaments in the cell cytoplasm (Fig. 4_18 D-H). Like the PVX TGB1, the TMV replicase, a 126-kDa protein, is also a central component of the TMV VRC. Significantly, this protein also traffics on actin filaments (dos Figueira *et al*., 2002; Liu *et al*., 2005). In agreement with these data, very recently, it has been shown that actin is required for both PVX and TMV movement (Harries *et al*., 2009b). Nevertheless, it is still unknown how the virus is transported on actin to PD. My data suggest that the TGB1 protein, by arranging the VRC structure, may establish a functional pathway for genome targeting from the VRC to PD. However, the mechanism of actin recruitment to the VRC by the TGB1 protein has not yet established. It is likely that binding of actin to TGB1 occurs at the N-terminal part of TGB1 due to the fact that this viral protein contains an NTPase/helicase domain and possesses ATP/GTPase and RNA-binding activities *in vitro* (see Chapter 1). It could be hypothesised that actin reorganisation could be achieved by an interaction of TGB1 with actin nucleation factors (for example, the Arp2/3 complex and/or the formin family of proteins), or by a deformation of bound actin filaments through self-oligomerisation of the TGB1 protein (Leshchiner *et al*., 2008).

The mechanism of ER and Golgi recruitment to the VRC is also unclear since the TGB1 protein of PVX, unlike the MP of TMV (Fujiki *et al*., 2006), has no transmembrane domains. Therefore, the link from TGB1 to the ER is more likely to be indirect through the close structural association of the ER with the actin cytoskeleton (Quader *et al*., 1987; Boevink *et al*., 1998). Cortical ER and actin filaments are also known to be components of PD. In PD, the ER forms the desmotubule, a strand of cortical ER that passes through PD and interconnects the ER of neighbouring cells (Robards and Lucas, 1990; Ding *et al*., 1992; Lucas and Wolf, 1993; Boevink *et al*., 1998; Botha and Cross, 2000). Actin microfilaments are also associated with the plasmodesmal pore and extend through PD (White *et al*., 1994). Therefore, the recruitment of host organelles into the VRC by TGB1 may provide the first direct connection to the actin cytoskeleton. To verify if ER redirection by TGB1 is actin-dependent, application of actin-depolymerising drugs, such as latrunculin B and cytochalasin D needs to be tested.

4.3.5.2 Association of TGB2- and TGB3-related vesicles with the ER membrane

The two smaller viral-encoded proteins, TGB2 and TGB3, are ER membrane-associated proteins that have been studied extensively (see Chapter 1). These PVX proteins have hydrophobic region (transmembrane domains) for insertion into cellular membranes (Morozov *et al*., 1987, 1989). PVX TGB2 and TGB3 proteins induced formation of numerous vesicle clusters in the absence and presence of virus infection, resembling the effects of brefeldin A in plant cells (Ritzenthaler *et al*., 2002). Like the TGB2/TGB3 proteins of PVX, a 6-kDa protein of the tobacco etch virus also associates with the ER by its central 19-a.a. hydrophobic sequence. This virus also forms numerous ER membrane-derived vesicles in the cell (Schaad *et al*., 1997).

Both fusion proteins (TGB2 and TGB3) localise to the ER network in the form of motile vesicles. The precise nature and the mechanism of the formation of the numerous motile vesicles are unclear. It has been suggested that these vesicles can be formed by invaginations of the ER network (Ju *et al*., 2005). During replication, other viruses have

also been reported to induce spherular invaginations of intracellular membranes (Salonen *et al*., 2005). For example, replication of brome mosaic virus is associated with membrane vesiculation (Schwartz *et al*., 2004) and some tombusviruses (for example, carnation italian ringspot virus and cymbidium ringspot virus) establish vesicular structures derived from mitochondria or peroxisomes (Burgyan *et al*, 1996; Rubino and Russo, 1998; Rubino *et al*., 2001; Weber-Lotfi *et al*., 2002). The TGB2-originated vesicles are either targeted to the ER, or TGB2 triggers reorganisation of the ER. It is also likely that TGB2 is unstable and is redirected for degradation by the 26S proteosome (Ju *et al*., 2005; 2007). In addition, the TGB3-contaning granular aggregates have been suggested to be the replication sites of the virus since TGB3-related vesicles immuno-colocalise with the viral 165-kDa protein, a viral replicase (Bamunusinghe *et al*., 2009).

4.3.5.3 Movement of TGB2- and TGB3-originated vesicles on actin cytoskeleton and detection of actin around these vesicles

TGB2- (Fig. 4_23; Fig. 4_24) and TGB3-originated vesicles (Fig. 4_25; Fig. 4_26) were found moving on actin filaments in the absence and presence of viral infection, providing more evidence in support of the hypothesis that these two proteins are very likely to be part of the viral movement complex. Among TGB proteins, only TGB2-derived vesicles were previously reported to be moving along the actin cytoskeleton (Ju *et al*., 2005; reviewed in Verchot-Lubicz *et al*., 2007). Actin was also detected in smaller and larger green fluorescent vesicle aggregates of the TGB2 protein and especially of the TGB3 protein. A diverse number of proteins of plant viruses have been found to associate with actin microfilaments. Among these viral proteins are TMV 126-kDa protein, the Hsp70h homolog of cellular heat shock proteins of beet yellows virus, PVX TGB2, TGB2/TGB3 proteins of potato mop-top virus, and the P6 of cauliflower mosaic virus (Haupt *et al*., 2005; Ju *et al*., 2005; Prokhnevsky *et al*., 2005; Harries *et al*., 2009b). However, disruption of actin with the formation of small aggregates in the cell cytoplasm was recorded in PVX-infected cells (Fig. 4_25 B). In addition, an actin

marker (Fig. 4_1 E) used in this work was found to form some aggregates in the cell when bombarded into uninfected control non-transgenic plants (unpublished data from Dr. Jens Tilsner). Therefore, there is a possibility of experimental artifacts that have to be taken into consideration when dealing with proteins expressed at higher levels due to biolistic bombardment (Brandizzi *et al*., 2002). However, despite the possibilities of an overexpression artifact of the marker protein fusion with a risk if its mistargeting and misfolding, localisation of actin around the TGB2- and particularly TGB3-induced vesicles implies a functional relevance of host actin in PVX infection processes. To further prove this relevance more experimental data are needed.

The discovery that both TGB2 and TGB3 locate to PD (this thesis; unpublished data of Dr. Jens Tilsner) suggests that TGB2 and TGB3 are very likely to be a part of the movement complex that traffics from the VRC to PD. These two proteins probably provide a link to the cortical ER/actin network for attachment of the vRNA/CP/TGB1 complex. My data also imply that TGB2 and TGB3 interact with the transport complex at the outside edges of the VRC due to the fact that these two proteins were found to the exterior of the TGB1 sub-compartment.

4.3.6 Conclusions

The current data suggest that PVX VRCs are not only the centres of viral replication, but also centres for preparing the virus to move between cells. It is hypothesised that movement functions belonging to the single MP of TMV are possibly distributed over three TGB proteins in the TGB-carrying viruses (Morozov and Solovyev, 2003), including PVX. TGB1 plays the most important role in establishing the structure of the VRC by recruiting the host organelles required for cell-to-cell transport of PVX. The TGB2 and TGB3 proteins localise to the endomembrane sub-compartment of the VRC and are likely also to be part of the viral movement complex, possibly by providing a direct link onto the cortical ER/actin network for intracellular trafficking of the viral genome to PD.

5. Analysis of PVX VRC formation in relation to viral RNA

5.1 Aim

The growing number of sub-cellularly localised RNA molecules identified over recent years (reviewed in Neilson and Sharp, 2008) has created a high demand for development of methods that are suitable for visualising RNA dynamics in single infected cells. Therefore, a wide number of RNA imaging strategies have been designed (reviewed in Rodriguez *et al*., 2007); however, the majority of these techniques for viral RNA tracking are based on fluorescence *in situ* hybridisation (Mas and Beachy, 1999; Carette *et al*., 2000) and immunogold EM methods (Dunoyer *et al*., 2002; Taliansky *et al*., 2003). These RNA localisation approaches are destructive and do not allow *in vivo* studies of viral RNA dynamics (Tilsner *et al*., 2009). In this thesis chapter RNA-binding dyes and a novel RNA imaging Pumilio reporter system adopted in our lab for plant virus RNA imaging in living cells were successfully used. This chapter will cover the advantages and disadvantages of these RNA imaging methods.

Despite intense research on PVX, there are still many unanswered questions and uncertainties in terms of viral RNA localisation, distribution and movement in infected cells. The exact mechanism of PVX RNA transport to and via PD is poorly understood. My hypothesis is that the success of PVX RNA movement from a VRC to PD, and through PD from one cell to another, is dependent on the successful formation and establishment of the viral replication complex. Therefore, the aim of this chapter is to uncover where the viral RNA is located in PVX-infected cells and to establish the link between VRC formation and trafficking of the viral genome to PD. Thus, sub-cellular localisation and distribution of vRNA was investigated and a model of PVX RNA movement to and through PD is proposed.

5.2 Results

5.2.1 Plasmids used in this study (Table 5.1, Fig. 5_1)

Plasmids used in this results chapter can be divided into two groups which are listed in Table 5.1

1) According to the method of plasmid delivery:

i) Binary plasmids for transient plant transformation by agroinfiltration:
pGR106 (Jones *et al*., 1999)
ii) Bombardment plasmids for transient plant transformation by biolistic bombardment:
pRTL2 (Restrepo *et al*., 1990) pUGW0 (Nakagawa *et al*., 2007) pRPS5A (promoter, Weijers *et al*., 2001) pUGW0.pRPS5A (plasmid, Tilsner *et al*., 2009)
iii) Plasmids containing T7 polymerase promoter for synthesis of infectious PVX RNA transcripts for *in vitro* transcription, reassembly and inoculation:
pTXS (Chapman *et al*., 1992)

2) According to the expressed marker or gene:

Plasmid name	Expressed marker or gene	Figure number
	Viral gene markers:	
pRTL2.TGB1-mCherry	red TGB1 viral movement protein reporter	Fig. 5_1 A
	Organelle markers:	
pRTL2.ER-tdTomato	red ER marker	Fig. 5_1 B
pRTL2.Lifeact-tdTomato	red actin marker	Fig. 5_1 C
	Pumilio constructs:	
pRTL2.PUMHD3809-PUMHD3794-GFPc3	green 'double Pumilio' reporter	Fig. 5_1 D
pRTL2.CitN-PUMHD3794 + pRTL2.PUMHD3809-CitC	Pumilio BiFC-based reporter system based on pRTL2 plasmids (PUMHD-split FP fusions)	Fig. 5_1 E

pUGW0.pRPS5A.CitN-PUMHD3794 + pUGW0.PUMHD3809-CitC	optimised PUMHD-split FP fusions	Fig. 5_1 F
PVX-carrying plasmids:		
pTXS	PVX without a FP marker	Fig. 5_1 G
pTXS.pum	PVX with Pumilio-binding sequence	Fig. 5_1 H
pTXS.pum.FP	PVX with Pumilio-binding sequence and fluorescent protein	Fig. 5_1 I
pTXS.pum.mCherry-2A-CP	PVX with Pumilio-binding sequence and red fluorescent protein (mCherry) fused to coat protein	Fig. 5_1 J
pTXS.pum.CFP-2A-CP	PVX with Pumilio-binding sequence and cyan fluorescent protein fused to coat protein	Fig. 5_1 K
pGR106.pum.CFP	PVX with Pumilio-binding sequence and cyan fluorescent protein	Fig. 5_1 L
pTXS.GFP-2A-CP green 'overcoat' virus	PVX with green fluorescent protein fused to coat protein	Fig. 5_1 M

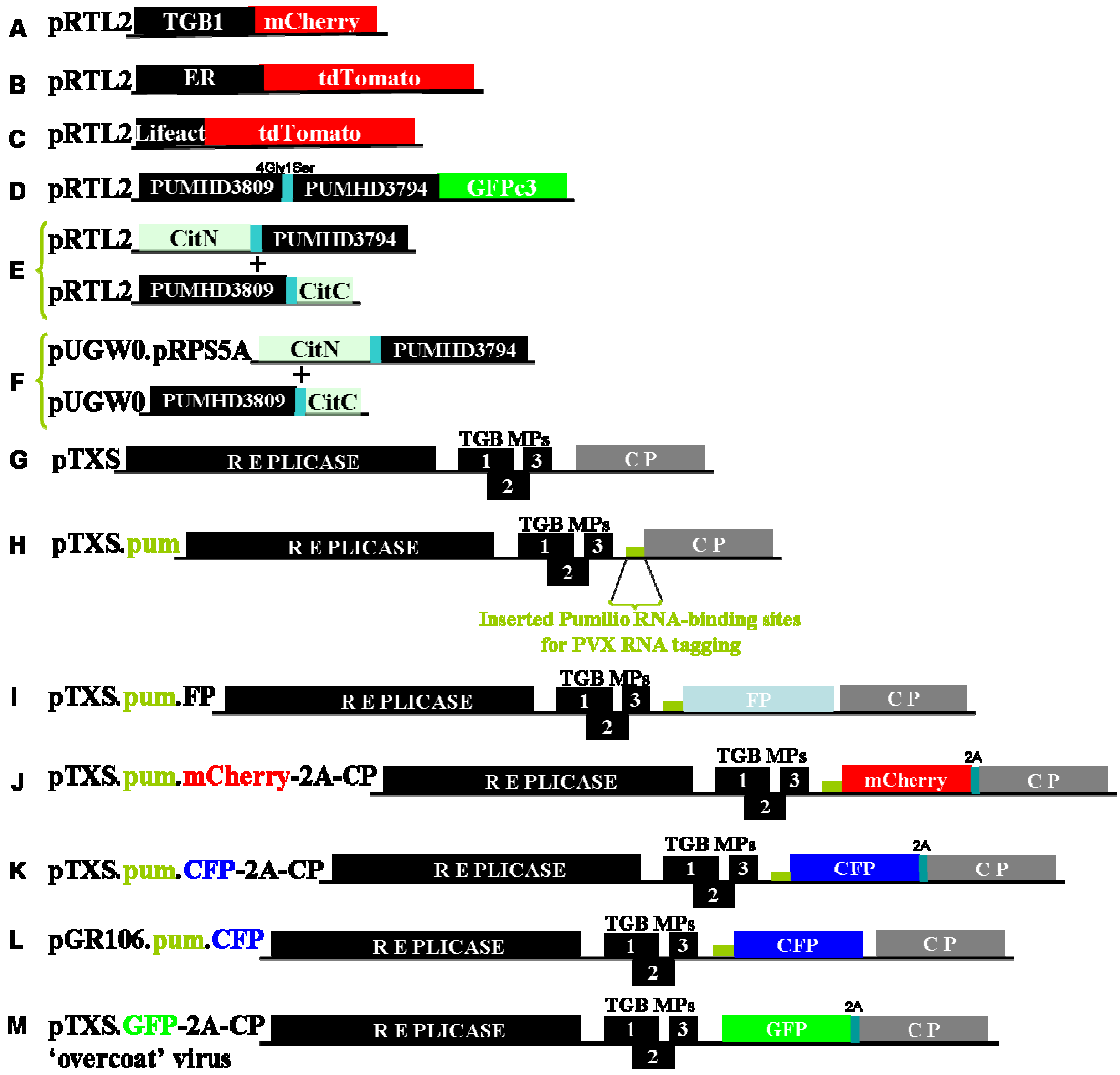

Figure 5_1: Schematic representation of plasmids used in this results chapter

TGB: triple gene block, MP: movement protein; CP: coat protein; FP: fluorescent protein; PUMHD: Pumilio Homology Domain.

5.2.2 Pumilio as a BiFC-based reporter system to image the genomes of RNA viruses in living plant cells

Recently we modified Pumilio as a BiFC-based reporter system for imaging of plant viral RNAs in living plant cells (Tilsner *et al*., 2009). This publication is attached in the appendix to this thesis.

5.2.2.1 Pumilio RNA-binding protein reporter as a novel approach for imaging viral RNA in living plant cells (Fig. 5_2)

The difficulties of traditional methods for viral RNA localisation in living plant cells have been a significant drawback in understanding of virus replication and movement in plants. To circumvent this limitation Dr. Jens Tilsner in our lab adapted the Pumilio method (Ozawa *et al*., 2007) to study plant viral RNAs (Tilsner *et al*. 2009). An RNA-binding protein with distinctive RNA-binding Pumilio Homology Domain (PUMHD; Wickens *et al*., 2002) of the human protein Pumilio1 (HsPUM1) (Spassov and Jurecic, 2002) (for more detailed explanation of the unique features of the Pumilio RNA-binding protein see Chapter 1) was engineered to interact with the vRNA of tobacco mosaic virus in virus-infected living plant cells (Tilsner *et al*., 2009). The unique characteristics of the PUMHD allowed this protein to be modified (Cheong and Hall, 2006) to recognise and bind to two adjoining 8-nt RNA sequences of choice in the TMV genome (Tilsner *et al*., 2009).

Two native 8-nt sequences were selected in the TMV genome, thus the TMV RNA was not modified. The first sequence was named 3794 (nucleotides from 3794 to 3801 in the RNA molecule: UGUAGAUA). The second sequence was termed 3809 (nucleotides from 3809 to 3816 were selected: UGAUAGUU) (in green in Fig. 5_2 A). PUMHD polypeptides were engineered to bind to these two sequences on the viral RNA. Each modified PUMHD protein was fused to N- or C-terminal half of a split mCitrine (Griesbeck *et al*., 2001), monomeric yellow fluorescent protein (PUMHD-split FP

fusions) (Fig. 5_2 B). Split mCitrine fragments are referred to as CitN and CitC hereafter. The C-terminal part of CitN was fused to PUMHD3794 peptide (CitN-PUMHD3794). The N-terminal part of CitC was fused to PUMHD3809 (PUMHD3809-CitC). A flexible 5 amino acids (Gly_4Ser) linker was inserted between each half of a FP and a PUMHD peptide. Therefore, when two modified PUMHD fusion proteins are bound to the 8-nt target sites on the vRNA, the C-terminus of PUMHD3809 and the N-terminus of PUMHD3794 are positioned towards each other, leading to close contact between the split FP parts fused to these PUMHD polypeptides, resulting in restoration of the complete FP and initiation of bimolecular fluorescence complementation (BiFC; Hu *et al*., 2002) and vRNA visualisation in living infected plant cells (Fig. 5_2 C) (Tilsner *et al*., 2009).

The Pumilio RNA imaging reporter system was first successfully applied to target the RNA of tobacco mosaic virus (Fig. 5_2 D). To image vRNA of PVX with the Pumilio reporter system, the TMV-derived sequence recognised by the engineered PUMHD variants was transferred and inserted into PVX RNA as a tag (PVX.pum: Fig. 5_1 H) downstream of the subgenomic CP promoter in order to incorporate the PUMHD tag into both genomic and subgenomic RNAs (Fig. 5_2 E). However, this Pumilio BiFC-based reporter system was found to have background fluorescence and a nucleoplasmic and cytosolic fluorescent signal was detected in uninfected control plant cells (Tilsner *et al*., 2009).

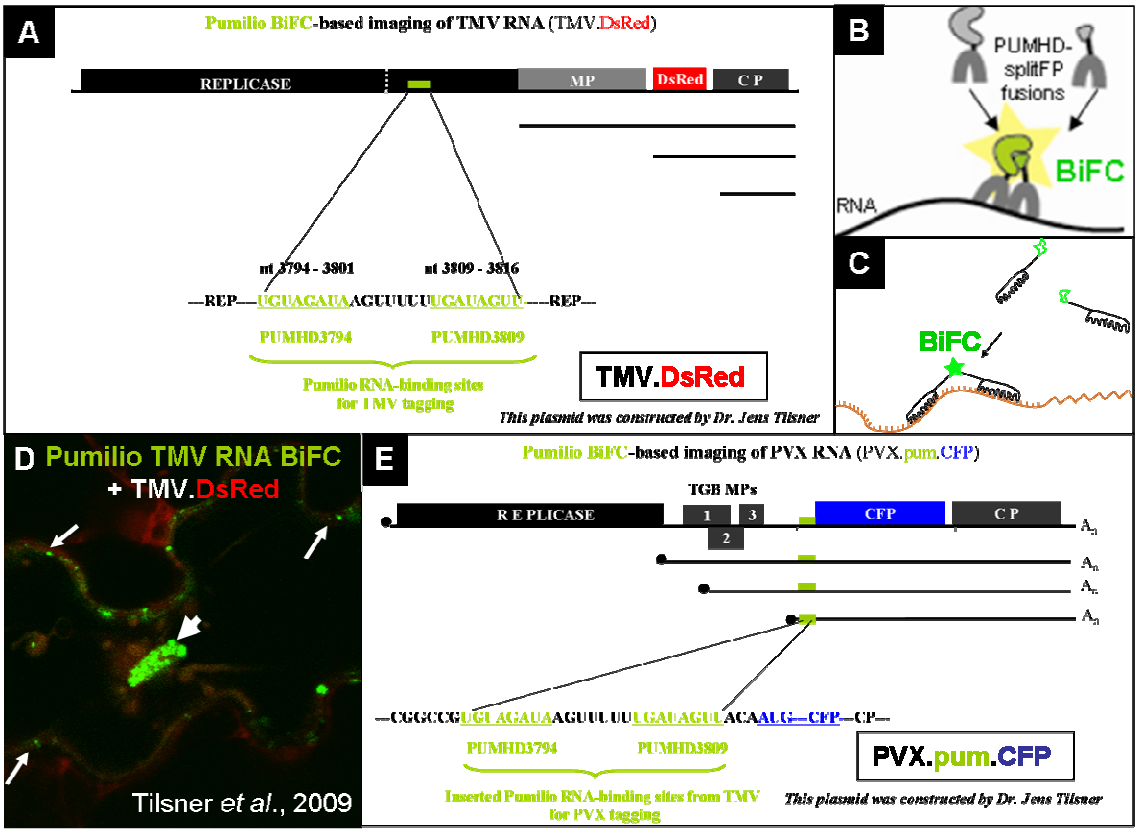

Figure 5_2: Pumilio BiFC-based reporter system as a novel approach to image the genomes of RNA viruses in living plant cells

A: Construction of Pumilio BiFC-based reporter system for imaging of TMV RNA
MP: movement protein; CP: coat protein; PUMHD: Pumilio Homology Domain.
Two 8-nt sequences on TMV RNA (green) (A) are recognised by the engineered PUMHD-split fluorescent protein (FP) constructs (B).
B: Split FP Pumilio constructs used in bimolecular fluorescence complementation (BiFC) assay for detection of viral RNA in living plant cells.
C: Schematic representation of restoration of complete FP, leading to BiFC.
D: Engineered PUMHD-split FP constructs bombarded into DsRed-expressing TMV (TMV.DsRed)-infected *Nicotiana* epidermal cells. Pumilio labels TMV RNA (green) in a perinuclear VRC (thick arrow) and in viral RNA particles at the cell periphery (thin arrows).
Data adapted from Tilsner *et al.*, 2009.
E: Construction of Pumilio BiFC-based reporter system for imaging of PVX RNA
TGB: Triple Gene Block.
Two 8-nt sequences on PVX RNA (green) (E) are recognised by the engineered PUMHD-split FP constructs (B).

5.2.2.2 Generation of 'double-Pumilio' constructs (Fig. 5_3)

In a different experimental strategy of using the Pumilio-RNA binding protein for vRNA localisation in the infected cell, I tested the feasibility of using a 'double Pumilio' approach. Pumilio split FP-based pRTL2 plasmids (Fig. 5_1 E) use a BiFC assay for detection of viral RNA when these plasmids are cobombarded into PVX-infected tissue with a virus carrying a Pumilio-recognition sequence and a FP as an infection marker (Fig. 5_1 H-L). Each Pumilio BiFC-based construct contains one Pumilio domain fused to a split mCitrine half (Fig. 5_1 E): mCitN-PUMHD3794 + PUMHD3809-mCitC (Fig. 5_3 A). The 'double Pumilio' technique was also designed for delivery into PVX-infected tissue with a virus carrying a Pumilio-recognition sequence (Fig. 5_1 H). However, unlike the BiFC approach, 'double Pumilio' expressing pRTL2 plasmid contains two Pumilio domains in the same bombardment construct fused to a complete FP (Fig. 5_1 D): pRTL2.PUMHD3809-PUMHD3794-GFPc3 (Fig. 5_3 B).

The 'double Pumilio' fusion approach was thought to be advantageous due to the fact that the position of the Pumilio domains was fixed in the plasmid and a BiFC assay was not required. However, when this 'double Pumilio' construct (Fig. 5_1 D) was expressed in the plant cell, an aggregation of a 'double Pumilio' protein was found. My data showed that the 'double Pumilio' construct forms many aggregates in the cell (Fig. 5_3 C,D). This protein fusion to GFP was observed to aggregate even very early after biolistic bombardment (after 2 hours post-bombardment of this construct) with the formation of a large green aggregate and a number of smaller green aggregates in the plant cell (Fig. 5_3 C). After 4 hours, the number of fluorescent masses increased and the fluorescent aggregates were found to be distributed throughout the cytoplasm (Fig. 5_3 D). Due to this aggregation problem, a further viral RNA analysis was carried out by using Pumilio BiFC-based imaging of PVX RNA (Fig. 5_3 A).

In order to solve the unspecific fluorescence background problem of Pumilio BiFC, a number of transient expression plasmids with different strength of promoters were tested

(this thesis work and also in Tilsner *et al*., 2009). pRTL2 with a duplicated CaMV 35S promoter (Restrepo *et al*., 1990) was found to be the strongest. pUGW0 with a single 35S promoter (Nakagawa *et al*., 2007) resulted in some background signal. pUGW0.pRPS5A, a plasmid engineered by Dr. Tilsner which originated from the pUGW0 vector by replacing the single 35S promoter in pUGW0 (Nakagawa *et al*., 2007) with the promoter of the *Arabidopsis* ribosomal RPS5A gene (Weijers *et al*., 2001), had the lowest unspecific fluorescence background. An optimal signal-to-noise ratio in bimolecular fluorescence complementation assay of PUMHD-split FP fusions in viral RNA imaging was achieved when combinations of plasmids with lower strength promoters (pUGW0.pRPS5A.CitN-PUMHD3794 and pUGW0.PUMHD3809-CitC: Fig. 5_1 F) were co-expressed in the same PVX-infected plant cell (Tilsner *et al*., 2009).

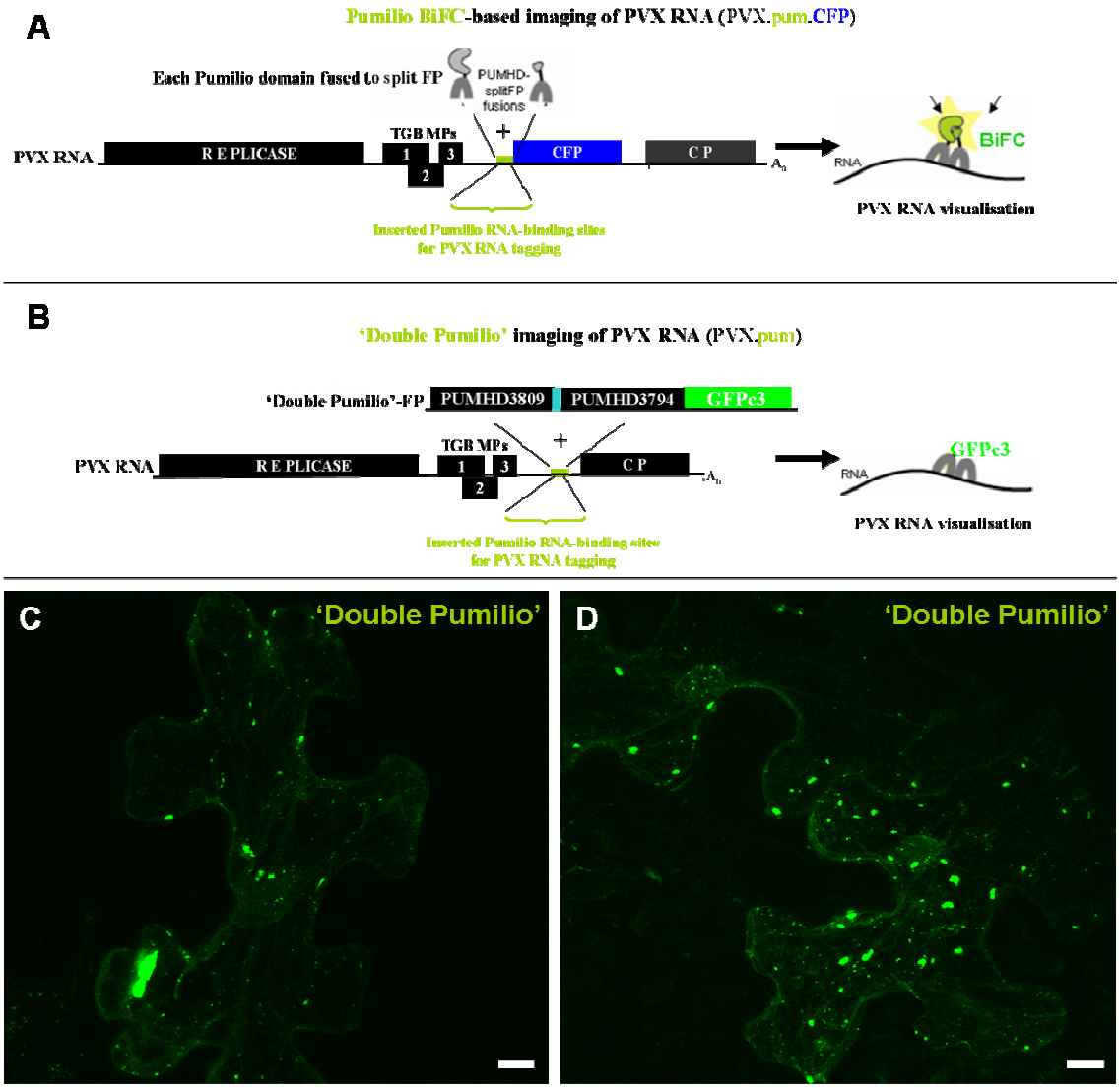

Figure 5_3: 'Double Pumilio' approach to targeting PVX RNA

A: A schematic representation of Pumilio BiFC-based imaging of PVX RNA in comparison to B: 'Double Pumilio' imaging of PVX RNA.

C-D: 'Double Pumilio'-GFP on non-transgenic *N. benthamiana* plants

Confocal laser scanning images of epidermal cells of uninfected non-transgenic *N. benthamiana* leaves cobombarded with 'double Pumilio'-GFP (green)

C: 2 h.p.b.; D: 6 h.p.b.

h.p.b. – hours post-bombardment.

Bars, 20 µm.

5.2.3 Imaging vRNA and replication sites in PVX-infected cells

5.2.3.1 Pumilio BiFC allows simultaneous visualisation of vRNA and the TGB1 viral movement protein in PVX-infected plant cells (Fig. 5_4)

To find out where the viral RNA is located in infected plant cells, an optimised Pumilio BiFC-based reporter approach (Fig. 5_1 F) was used. Due to the fact that the TGB1 protein is a multifunctional protein and has already been shown to recruit plant host organelles to the viral replication complex in the complete absence of viral infection and to target several distinct localisations in the infected cell (see Chapter 4), I examined whether the vRNA and TGB1 colocalised in the infected cell. Colocalisation of vRNA with TGB1 was achieved by cobombarding PVX-infected (Fig. 5_1 L) non-transgenic *N. benthamiana* plants with the TGB1 fluorescent fusion protein (Fig. 5_1 A) along with the optimised Pumilio BiFC-based reporter system (Fig. 5_1 F). PVX-infected leaf epidermal cells were examined under the confocal laser scanning microscope.

5.2.3.1.1 PVX RNA localises around the TGB1 inclusions in the VRC and colocalises with the TGB1 particles in PD

In addition to the TGB1 protein in the infected cell, two populations of the vRNA were recognised by the Pumilio system. The first pool of vRNA was found in the VRC. Unencapsidated vRNA of PVX was visualised in discrete circular 'whorls' within the VRC (Fig. 5_4 A,D; see also Tilsner *et al*., 2009). These data revealed that circularly arranged RNA 'whorls' contained amorphous regions unlabelled by the Pumilio BiFC signal in the central cavity of these 'whorls' (Fig. 5_4 A,D). The TGB1 protein was found in the centre of the VRC, in the central cores of the PVX RNA unlabeled by the Pumilio BiFC (Fig. 5_4 B,E). PVX RNA was localised around the TGB1 sub-compartments of the VRC (Fig. 5_4 C,F), indicating spatial separation of viral RNA and TGB1 within the VRC. A second population of vRNA was localised in small particles at the cell periphery presumably associated with PD (thin arrows in Fig. 5_4 A,D).

Significantly, introduction of PVX constructs without the Pumilio-recognition sequence (Fig. 5_1 G) did not lead to labelling of viral RNA in PVX VRCs (Tilsner *et al*., 2009), indicating that only viral constructs tagged with an engineered Pumilio-binding sequence are recognised by the modified Pumilio BiFC-based reporter system (Fig. 5_1 F). In addition, combinations of unfused CitN and PUMHD-CitC did not result in labelling of TMV RNA (Tilsner *et al*., 2009), suggesting that both fusions of Pumilio domains to split FP halves (Fig. 5_1 F) are required for BiFC and successful viral RNA imaging. Unexpectedly, application of the native, unmodified PUMHD sequence into plant cells infected with PVX.pum constructs (Fig. 5_1 H) resulted in the same labelling of PVX VRCs described above (Fig. 5_4). When the PVX genome was searched for potential Pumilio-binding sites, a site that had only 1 nucleotide difference between the 'native' PUMHD and PVX sequence was identified. This suggests that native, unmodified PUMHD sequence carries an adequate affinity for detection of PVX RNA molecules in the infected plant cell (Tilsner *et al*., 2009).

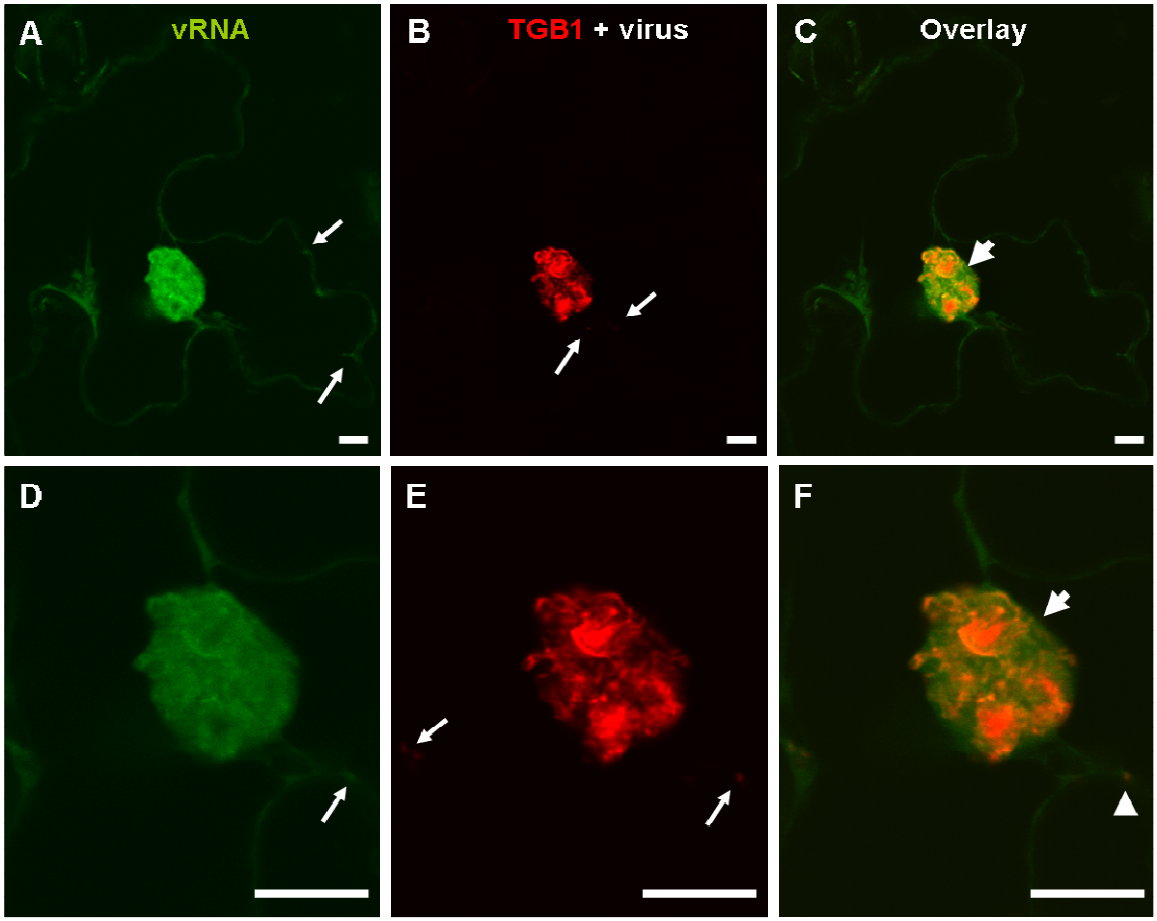

Figure 5_4: vRNA and TGB1 on PVX-infected non-transgenic *N. benthamiana* plants

Confocal laser scanning images of epidermal cells of PVX-infected (PVX is unlabelled) non-transgenic *N. benthamiana* leaves cobombarded with Pumilio BiFC reporter (vRNA in green) and TGB1 (red).

A,D: vRNA (green channel); B,E: TGB1 (red channel); C,F: overlay of green and red channel (vRNA + TGB1 in PVX-infected cell); A-C: a lower magnification image of PVX-infected epidermal cell; D-F: a higher magnification image of the PVX VRC and a part of the cell periphery.

A-F: 1 d.p.b.

d.p.b. – days post-bombardment; thick arrows point to PVX VRCs; thin arrows point to the TGB1 particles and vRNA at the cell periphery (A,B,D,E); arrowhead points to colocalisation of TGB1 and vRNA (F).

Bars, 10 µm.

5.2.3.2 The Pumilio BiFC-based reporter system allows visualisation of vRNA localisation with host organelles (ER and actin) in PVX-infected plant cells (Fig. 5_5)

Due to the fact that host organelles were found to be involved in PVX VRC formation (see Chapter 3), I examined the relationship between vRNA and recruited plant organelles within the VRC. PVX-infected (Fig. 5_1 L) non-transgenic *N. benthamiana* plants were cobombarded with an ER marker (Fig. 5_1 B) or an actin marker (Fig. 5_1 C) together with the optimised Pumilio BiFC-based reporter constructs (Fig. 5_1 F). PVX-infected leaf epidermal cells were examined under the confocal laser scanning microscope.

5.2.3.2.1 PVX RNA colocalises with the endoplasmic reticulum and is surrounded by actin microfilaments in the VRC

The vRNA was found to colocalise with the ER sub-compartments of the viral replication complex, with small vRNA fractions located independently of the ER (Fig. 5_5 A-C). In addition, vRNA was scattered in ER fluorescent aggregates within the VRC (Fig. 5_5 C). These data are in agreement with published results showing that PVX RNA synthesis and replication takes place in close association with cellular membranes and the ER membranes are likely sites of viral replication (Doronin and Hemenway, 1996). Moreover, the vRNA was found to be closely associated with actin filaments that were recruited into the VRC during PVX infection (Fig. 5_5 D-F). Actin strands were observed to surround the VRC, and also were found around the circular vRNA 'whorls' within the VRC (Fig. 5_5 F). These data indicate that PVX RNA transport to and via PD may take place on actin elements of the infected cell.

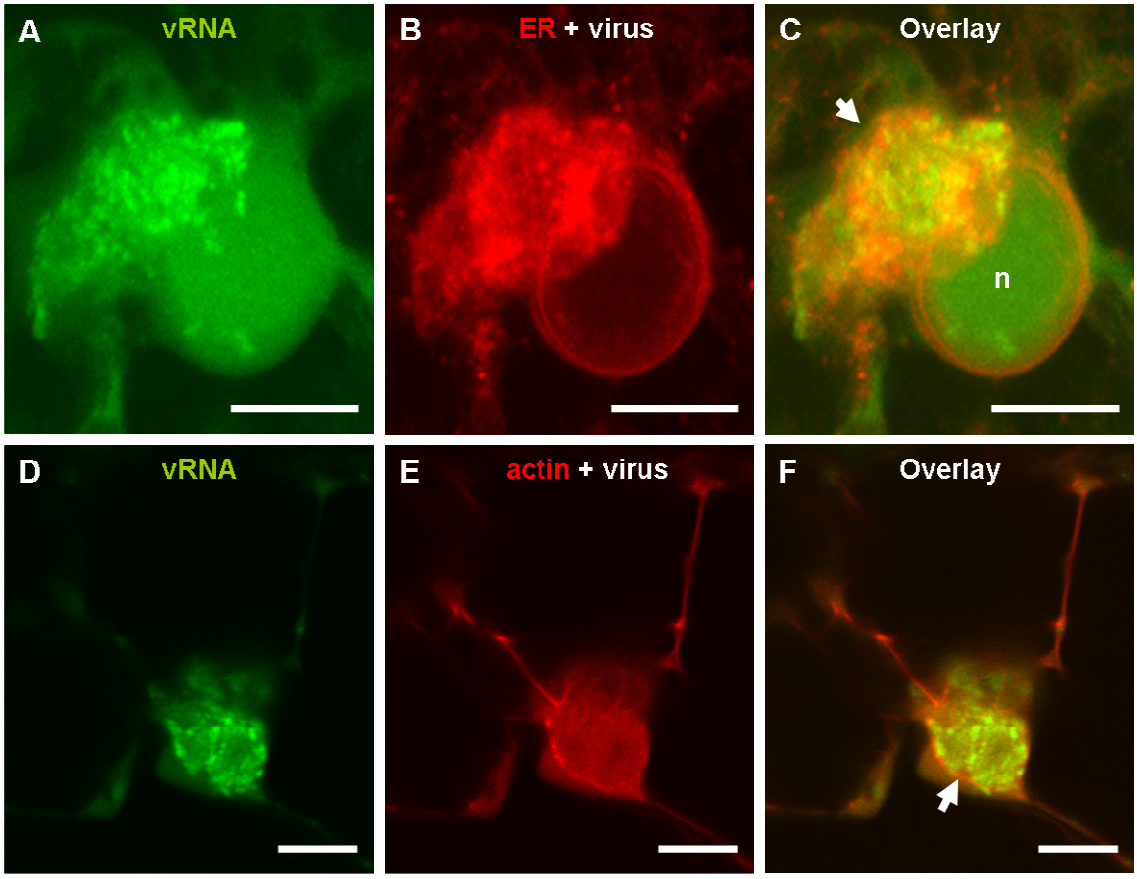

Figure 5_5: vRNA and ER (A-C) or actin (D-F) on PVX-infected non-transgenic *N. benthamiana* plants
Confocal laser scanning images of epidermal cells of PVX-infected (PVX is unlabelled) non-transgenic *N. benthamiana* leaves cobombarded with Pumilio BiFC reporter (vRNA in green) and ER (red) (A-C) or actin (red) (D-F)
A,D: vRNA (green channel); B: ER (red channel); E: actin (red channel); C,F: overlay of green and red channel (vRNA + ER or vRNA + actin in PVX-infected cell).
A-F: 1 d.p.b.
d.p.b. – days post-bombardment; thick arrows point to PVX VRCs; n – nucleus.
Bars, 10 µm.

5.2.3.3 Application of RNA-binding dyes to image vRNA in PVX-infected plant cells (Fig. 5_6)

The Pumilio-BiFC assay is limited to the detection of single-stranded RNA forms (ssRNA) in the infected tissue. However, during viral replication double-stranded RNA molecules (dsRNA) are generated as replication intermediates. Therefore, to build up a more comprehensive picture of viral RNA distribution and the site of replication within the PVX VRC, RNA-binding dyes were tested in addition to the Pumilio BiFC-based reporter system. Two different RNA-binding stains were used in this study, acridine orange (AO) and Syto82. PVX-infected (Fig. 5_1 M) non-transgenic *N. benthamiana* tissue was fixed and stained with AO (Fig. 5_6 A-C) known to preferentially label ssRNA molecules (Mayor and Diwan, 1961; Mayor and Hill, 1961). The second stain, Syto82, was infiltrated into PVX-infected plants (Fig. 5_1 M) by Dr. Nynne Christensen in our lab (Fig. 5_6 D,E). Syto82 RNA dye was shown previously to preferentially label dsRNA forms (Brandenburg *et al*., 2007).

5.2.3.3.1 PVX RNA localises in the centre of the VRC (AO staining) and in smaller punctate pattern (Syto82 staining)

AO stained the vRNA of PVX in the central regions of the VRCs (Fig. 5_6 A), the same region detected using Pumilio BiFC-based reporter (Fig. 5_1 F). Unencapsidated vRNA of PVX is surrounded by the viral CP (Fig. 5_6 A; see also Tilsner *et al*., 2009). DAPI, a double-stranded nucleic acids-specific dye know to form a blue fluorescent complex when bound to double-stranded nucleic acids (reviewed in Kapuscinski, 1995), was used to stain the infected tissue segments (Fig. 5_6 B) in order to distinguish vRNA within the VRCs from DNA in the cell nucleus. However, some blue staining in the VRC was also detected due to the fact that the double-stranded RNA forms are produced as a result of viral replication in the infected cell. Therefore, DAPI stained these double-stranded nucleic acids within the VRC. A closer examination of PVX VRCs revealed discrete circular ‘whorls’ of vRNA stained by AO within the VRC (thick arrows in Fig.

5_6 C), similar to the labelling of PVX RNA found using Pumilio BiFC. A second population of vRNA stained by AO was also identified in small particles at the cell periphery associated with PD (thin arrows in Fig. 5_6 C). Syto82 staining gave a smaller punctate pattern in the VRC (thick arrows in Fig. 5_6 D,E; see also Tilsner *et al*., 2009), and also detected a second RNA pool targeted to PD (thin arrows in Fig. 5_6 E). These data indicate that PVX VRC contains 'hot spots' of RNA localisation as well as RNA-free sub-compartments.

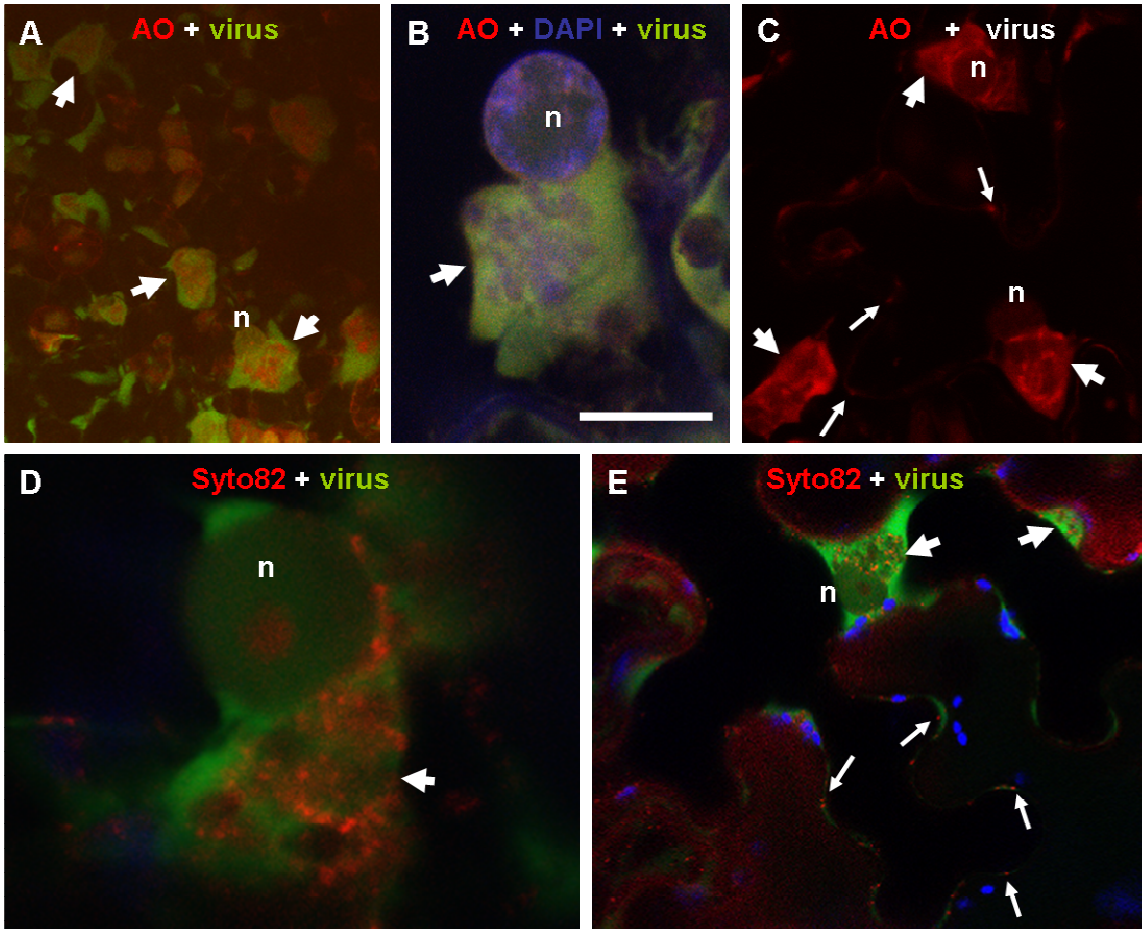

Figure 5_6: PVX 'overcoat' and AO (A-C) or Syto82 (D-E) on non-transgenic *N. benthamiana* plants

Confocal laser scanning images of epidermal cells of PVX 'overcoat'-infected (PVX in green) non-transgenic *N. benthamiana* leaves fixed and stained with 0.06 % AO (red) (A-C) or infiltrated with 1.25 µm Syto82 (red) (D-E)

A: Overview of several PVX 'overcoat'-infected (CP in green) epidermal cells with AO staining vRNA (red) in the central regions of PVX VRCs; B: a higher magnification image of the PVX VRC double stained with AO (red, RNA) and DAPI (blue, DNA); C: AO staining vRNA (red) in PVX VRCs and in PD; D: vRNA in the PVX VRC stained with Syto82; E: a single epidermal cell in which Syto82 labels dsRNA in the PVX VRC (thick arrows) and at the cell periphery in PD (thin arrows).

Thick arrows point to PVX VRCs; thin arrows point to vRNA in PD stained with AO (C) and Syto82 (E); n – nucleus.

Bars, 20 µm.

5.3 Discussion

5.3.1 Pumilio protein as a novel approach for viral RNA imaging in living plant cells

The Pumilio BiFC-based reporter system was successfully used in two different ways in our lab. The first approach involved the engineering of the PUMHD variants to target an RNA sequence of choice in an unmodified viral genome of TMV. The second strategy involved modification of the genomic RNA of a plant virus by inserting a TMV-derived tag for PUMHD peptides to recognise and bind to this sequence on the viral RNA of PVX (Tilsner *et al*., 2009).

5.3.1.1 Advantages of the Pumilio vRNA labelling system

The Pumilio BiFC-mediated viral RNA labelling was found to have advantages among the limited number of *in vivo* RNA imaging systems reported to date. Pumilio BiFC-based RNA imaging is less disruptive to the RNA secondary structure than other available non-invasive RNA imaging systems, like phage MS2 CP-mediated RNA labelling (Bertrand *et al*., 1998; Hamada *et al*., 2003; Zhang and Simon, 2003; Zimyanin *et al*., 2008) and the λ N22 peptide-based RNA imaging system (Daigle and Ellenberg, 2007). Also, both these methods require permanent fluorescent reporters due to the fact that they do not utilise BiFC. In addition, MS2 CP, like the λ N22 peptide, depends on the CP binding to stem-loop structures. Therefore, the secondary structure introduced into the RNA molecule can have a potential effect on RNA function (Dreher and Miller, 2006, Miller and White, 2006) and sub-cellular localisation (Lange *et al*., 2008). Moreover, to enable efficient recognition and reasonable detection levels, both MS2 and λ N22 peptide are used in several tandem repeats. Up to 96 RNA binding motifs for MS2 peptide (Bertrand *et al*., 1998; Fusco *et al*., 2003; Zhang and Simon, 2003) and up to 12 repeats for λ N22 (Daigle and Ellenberg, 2007; Lange *et al*., 2008, reviewed in Schifferer and Griesbeck, 2009) have been used for optimal signal-to-noise ratio, adding up to >2 kb of additional sequence. Therefore, this particularly long tag is not only a

potential cloning problem, but also has a high possibility to influence the dynamics of RNA, and therefore interfere with RNA functions. This may be especially problematic for viral RNA tracking also as large insertions of non-viral fragments are likely to result in alteration of viral function. In contrast, Pumilio has an advantage over these two RNA labeling systems due to the fact that the vRNA can either be left unmodified or, if tagged, the tag with the Pumilio-recognision sites on the viral RNA is very small (two 8-nt sequences and a 4-7-a.a. linker between them; Ozawa *et al*., 2007; Tilsner *et al*., 2009) and is potentially easy to engineer and subclone. In addition, the likelihood of disturbing the RNA function with such a small tag is significantly lower than for long tandem repeats of RNA hairpins. Moreover, the Pumilio approach allows real-time RNA imaging and can be used to study early events at the leading edge of infection when Pumilio BiFC is bombarded or agroinfiltrated into the viral infection site.

5.3.1.2 Disadvantages of the Pumilio vRNA labelling system

There are a number of potential reasons for nonspecific Pumilio BiFC signal. When working with fluorescent protein fusions, different problems can occur, such as weak, hardly detectible fluorescent signals, incorrect sub-cellular localisation of the protein fusion, cytoplasmic aggregation and loss of protein function (Dixit *et al*., 2006; Millar *et al*., 2009). The 'double Pumilio' protein was found to cause aggregation artifacts that possibly lead to mistargeting and loss of function of the Pumilio fusion and made it unfeasible. This protein aggregation may have occurred as a result of self-aggregation of the protein or as a result of overexpression during biolistic bombardment. Therefore, all PVX RNA localisation was carried out using the modified Pumilio BiFC approach with optimised promoters. However, the main drawback of Pumilio BiFC is an unspecific BiFC signal in uninfected cells that could not be completely eliminated regardless of optimisation strategies and efforts. The fact that co-expression of unfused CitN and CitC did not result in any fluorescence suggests that Pumilio fusions to split FP halves can potentially alter the stability or folding of the fluorescent protein fragments (reviewed in Lalonde *et al*., 2008; Tilsner *et al*., 2009).

The nonspecific background fluorescence detected with unmodified PUMHD BiFC fusions could be due to a number of reasons. The first is potential 'looping' of the RNA as a result of long-distance interactions between RNA molecules during transcription and translation (Gallie, 1996; Dreher and Miller, 2006; Miller and White, 2006). The second possible reason is a 'tandem' interaction between closely adjoining strands of viral RNA. Finally, BiFC may have occurred on RNA molecules that are 'stacked' and therefore brought into close proximity within the viral replication complex (see Fig. 3i in Tilsner *et al*., 2009). In addition, Gupta *et al*. (2008) have shown very recently that the HsPUM1 RNA-binding protein has a potential to bind to noncognate RNAs as not all Pumilio RNA-binding protein repeats are absolutely base-specific and binding of a 9-nt RNA target is also possible (Gupta *et al*., 2008). These findings may explain the fact that the unmodified PUMHD peptides were able to induce unspecific fluorescence in control experiments (Tilsner *et al*., 2009). One more possible drawback of using split FP-based imaging of vRNA is FP reconstitution which can take up to several hours to occur (reviewed in Schifferer and Griesbeck, 2009).

Despite the fact that Pumilio BiFC is not an entirely background-free system (Tilsner *et al*., 2009), it has proven to be a valuable tool for tracking RNA in live cells since it allows successful viral RNA localisation and distribution studies *in vivo*. As the structural knowledge of the Pumilio RNA-binding protein and its interactions with the RNA molecules gradually expands, further optimisations to restrict unspecific background fluorescence signal will become possible (Tilsner *et al*., 2009). To increase sensitivity of the RNA labelling methods, choosing the brightest (but non-toxic and photo-stable) available FP variants will be essential (Shaner *et al*., 2005). Successful RNA labelling based on optimal protein-to-RNA ratio is also dependent on the balance between a fluorescent protein fusion and an RNA-binding protein and its target endogenous RNA level in the cell (reviewed in Schifferer and Griesbeck, 2009). Additional optimisations are necessary for any viral RNA under study and for further improvement of the Pumilio method. For instance, the sequence of every RNA under

study has to be searched for possible natural binding sites of the Pumilio BiFC-based reporter system.

5.3.2 Pumilio BiFC-based reporter system for imaging vRNA localisation and distribution in PVX-infected cells

In this study the Pumilio system has been successfully applied for localisation studies of PVX RNA in the infected cell and colocalisation of vRNA with the TGB1 viral MP, viral CP and also with the host organelles of the infected cell.

5.3.2.1 PVX RNA is localised around the TGB1 inclusions in the VRC and also localised in PD of PVX-infected cells

Pumilio BiFC reporter detected discrete circular vRNA 'whorls' within the PVX VRC (Fig. 5_4 A,D). The TGB1 protein was located in the centre of these RNA 'whorls' (Fig. 5_4 B,E) and PVX unencapsidated 'naked' RNA surrounded the central TGB1 sub-compartment of the viral replication complex (Fig. 5_4 C,F). This localisation of vRNA and TGB1 in the VRC provides additional support for a model of the PVX VRC in which the TGB1 viral protein takes a central localisation in this complex and acts as key viral protein for PVX replication and movement. The distribution of viral RNA and PVX TGB1 in the VRC also suggests that the synthesis of RNA and the accumulation of the TGB1 viral protein take place in closely located sites within the VRC. In comparison to TMV, PVX RNA was found to have a different localisation pattern at its replication site, since TMV RNA was detected in punctate spots, rather than circular 'whorls' within the TMV VRC (Tilsner *et al*., 2009).

Additionally, application of AO allowed detection of PVX RNA (thin arrows in Fig. 5_6 C) in PD of PVX-infected cells. TGB1 and viral CP were also found in PD (see Chapter 4). These data are consistent with *in vitro* experiments on PVX viral particle assembly that discovered that CP is most likely associated with the 5' region of vRNA (Atabekov

et al., 2000; Rodionova *et al*., 2003; Karpova *et al*., 2006). TGB1 binding to this assembled CP-vRNA complex results in the destabilisation of PVX virions and conversion of vRNA into a translatable form (Atabekov *et al*., 2000). However, in contrast to TMV, the stability of this binding of PVX TGB1 to vRNA *in vitro* is found to be lower than in the 30K MP of TMV (Kalinina *et al*., 1996, 1998; Lough *et al*., 1998).

I suggest that the first population of PVX 'naked' RNA detected in the VRC does not traffic from one cell to another. Rather, it is a later progeny pool of encapsidated RNA that moves from the VRC during the development of the infection site. Detection of PVX RNA in PD suggests that newly synthesised RNA molecules may move to and through PD to infect the whole plant. However, visualisation of vRNA in PD by the Pumilio system was less common and could be associated with the very low amounts of vRNA in these intracellular channels. In addition, the detection of vRNA in PD is almost beyond the sensitivity of the Pumilio BiFC-baser reporter system due to the fact that Pumilio approach is designed to visualise unencapsidated vRNA. During infection, the Pumilio target sites on the genomic PVX RNA may be covered by CP subunits and therefore inaccessible to Pumilio BiFC once the vRNA is fully coated (Tilsner *et al*., 2009). However, detection of PVX RNA in PD by the Pumilio system suggests that the virus may replicate at PD. Additionally, these data implies that partially coated transport particles containing vRNA and TGB1 may be present in PD of infected plant cells. This is consistent with the view that PVX transport complex may contain single-tailed particles in which there are large regions of unencapsidated vRNA (Atabekov *et al*., 2000, 2001; Rodionova *et al*., 2003; Karpova *et al*., 2006).

The data on detection of PVX CP around the unencapsidated vRNA (Fig. 5_6 A; see also Tilsner *et al*., 2009) suggest that vRNA assembly occurs at the centre of the VRC while encapsidation occurs at the periphery for formation of transport particles/complexes to spread the infection to neighboring cells. Separate localisations of TGB1 and CP in the VRC also indicate that these viral proteins are synthesised in distinct compartments within the viral complex or are quickly transported to these

separate destinations. In addition, due to the fact that TGB1 was found to destabilise PVX virions *in vitro* (Atabekov *et al*., 2000), this explains a distinct accumulation of the viral CP away from the TGB1 protein in the VRC *in vivo*.

5.3.2.2 PVX RNA colocalises with the endoplasmic reticulum and actin microfilaments in the VRC

The data of this chapter demonstrate that vRNA colocalises with the ER by associating with scattered ER bodies within the VRC (Fig. 5_5 C). In this study, PVX RNA was found in close association with not only ER membranes (Fig. 5_5 A-C), but also with the actin cytoskeleton in the VRC (Fig. 5_5 D-F), suggesting that PVX RNA synthesis and replication may take place on the ER and the viral RNA transport from infected cells to adjacent healthy cells may occur on actin microfilaments. Similar to PVX, TMV MP and TMV RNA are also closely associated with the host cytoskeleton: with mictrotubules (Heinlein *et al*., 1995) and microfilaments (McLean *et al*., 1995). Therefore, the host cytoskeleton may provide the 'tracks' required for moving viral transport complexes to PD (Carrington *et al*., 1996; Lazarowitz and Beachy, 1999; Tzfira *et al*., 2000; Heinlein, 2002). Very recently it has been shown that intercellular spread of TMV and also PVX is influenced by disruption of actin microfilaments, suggesting that the intercellular trafficking of these viruses is dependent on the host actin cytoskeleton (Harries *et al*., 2009b).

5.3.3 Application of RNA-binding dyes for tracking vRNA localisation in PVX-infected cells

Fluorescent nucleic acid dyes provide a different approach for labelling viral genomes. In this thesis, application of RNA-binding dyes, AO and Syto82, confirmed the existence of two populations of PVX RNA detected by Pumilio BiFC reporter in infected cells. These experiments have shown that the first pool of unencapsidated 'naked' PVX RNA is concentrated in discrete central compartments within the VRC

(Fig. 5_4 A,D; Fig. 5_6 A,C). The second pool of PVX RNA was detected in PD using the three different RNA detection approaches, suggesting that there are several populations of viral RNAs in infected cells. One pool is localised in the VRC and does not traffic between cells. The second pool may be part of the viral transport complex to PD, perhaps responsible for initiating virus cell-to-cell movement.

Both Pumilio BiFC and AO RNA detection were limited to single-stranded RNA forms and these methods labelled PVX RNA in a discrete circular pattern ('whorls' of vRNA) within the VRC. As in other experiments using AO for studying viral RNAs of single-stranded RNA viruses (Hirai and Wildman, 1953; Mayor and Diwan, 1961; Cho and McDonald, 1980), AO staining of PVX RNA required fixation of tissue as due to the high toxicity of this RNA dye it can cause cell death. Therefore, it was unsuitable for live-cell imaging of viral RNA. The Syto82 stain was found to have a lower toxicity effect on plant cells and therefore could be infiltrated into live plant tissue. In contrast to AO and Pumilio BiFC reporter, Syto82 dye was suitable for detecting the double-stranded RNA forms that are generated during viral replication. Application of this dye led to the appearance of a punctate staining pattern in PVX VRCs (thick arrows in Fig. 5_6 D,E; also in Tilsner *et al*., 2009), indicating that the PVX VRC may contains 'hot spots' of dsRNA localisation. It is conceivable that PVX replication takes place in these distinct regions within the ssRNA 'whorls' of the VRC.

5.3.4 Conclusions

Despite unspecific background fluorescence, Pumilio BiFC was found to be a powerful novel tool for localising RNA of plant viruses in living cells. The Pumilio BiFC reporter enabled localisation of unencapsidated vRNA and TGB1 in the VRC and colocalisation of vRNA with the TGB1 particles in PD of infected cells, as well as colocalisation of vRNA with CP in the PVX VRC. PVX RNA was also found in close association with the ER membranes and actin cytoskeleton elements of the host cell. Application of RNA-binding dyes confirmed the existence of two populations of viral RNA detected by

the Pumilio BiFC-based method in infected cells. Finally, Pumilio BiFC demonstrated a central function of the PVX VRC in harbouring unencapsidated viral RNA during infection.

6. General discussion, future work and final conclusions

6.1 Current model of PVX vRNA replication and movement

An experimental model of the VRC as a viral replication and movement complex was gradually built up during this thesis. Based on the findings of tagged PVX protein studies and the ability to image viral RNA with the Pumilio BiFC-based assay and RNA-binding dyes, it is possible to establish a model of PVX infection, replication and movement. The experimental data of this thesis support the model proposed in Fig. 6_1 (Fig. 6_1).

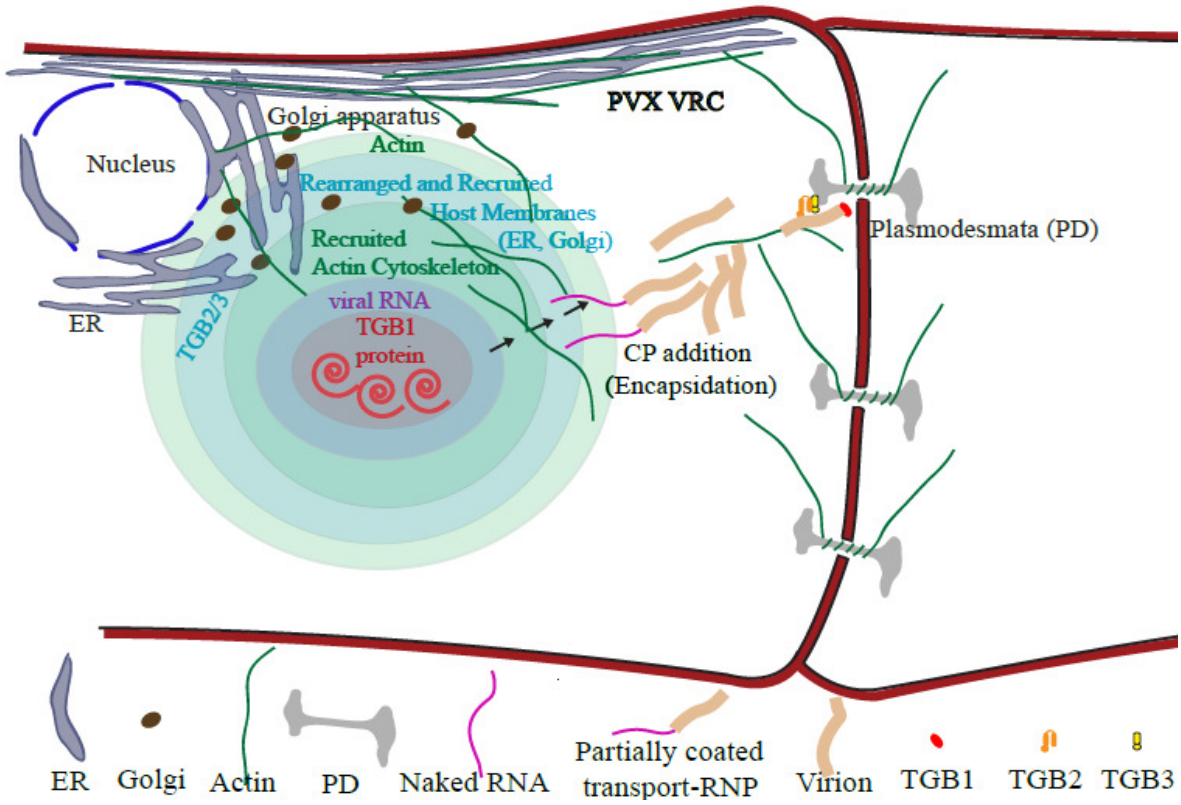

Figure 6_1: Schematic illustration of PVX viral RNA replication and movement

Once the virus enters a plant cell, it forms VRCs. Minute PVX VRCs are first detected about 3 days post viral infection throughout of the cytoplasm of the infected cell. As the viral infection progresses, VRCs become larger (up to twice the size of the cell nucleus) and usually are located near the cell nuclear envelope. The increase in the size of the VRCs could be a result of the fusion of small VRCs or the result of extensive viral protein synthesis and recruitment of the host components into the

developing VRC during the viral infection cycle. First, the viral RNA has to be translated and the viral genome to be replicated. The genomic and subgenomic RNAs have to be produced, which are then translated into the TGB proteins and CP and possibly remain associated with the replication site. In this proposed model the TGB1 protein plays a key role in viral infection by its capacity to recruit host endomembranes and actin into the forming VRC. TGB1 can perform this function in the complete absence of viral infection in the cell (Fig. 4_15 A-C; Fig. 4_17 A; Fig. 4_18 A,B). The recruitment of host organelles into the VRC is believed to be an essential process in establishing the VRC for replication and for virus movement to PD.

The TGB1 viral protein is capable of movement ahead of infection (unpublished data from our lab), gates PD and localises in the centre of VRCs in neighboring cells (Fig. 4_11 B,E; Fig. 4_14 B; see also Angell *et al*., 1996; Lough *et al*., 1998, 2000; Yang *et al*., 2000; Howard *et al*., 2004). The TGB1 viral protein interacts with the viral RNA and upon its binding activates viral RNA translation in neighboring cells (Karpova *et al*., 2006). PVX TGB1 occupies a central localisation in the VRC (Fig. 5_4 B,E). The circular structure of the TGB1 inclusions, in the form of 'beaded sheets', is surrounded by discrete circular vRNA 'whorls' within the VRC (Fig. 5_4 C,F; see also Tilsner *et al*. 2009). This special arrangement of the viral RNA and the TGB1 protein in close proximity indicates that PVX RNA replication may take place in the central region of the VRC. Unencapsidated ('naked') vRNA of PVX is surrounded by actin microfilaments (Fig. 5_5 F) and host endomembranes (Fig. 5_5 D) to which are attached the TGB2 and TGB3 viral movement proteins (Fig. 4_19-4_26). TGB2 and TGB3 exit these host endomembrane compartments in the form of motile granules and may play a regulatory function in coordinating PVX replication due to their association with the host cellular membranes. The CP is added to this complex at the periphery of this viral structure (Fig. 5_6 A,D; see also Tilsner *et al*. 2009) in order to pack the viral genome into transport particles by encapsidating the 'naked' vRNA pool into progeny virions. The transport particles first become visible as motile 'packets' detected at the leading edge of a PVX 'overcoat' infection (Fig. 4_3 C-E).

Presumably, the VRC also recruits host molecular motors to traffic the movement complex along the cortical actin cytoskeleton. Recently, such molecular motors, (myosins) were shown to be involved in PVX movement between cells (Harries *et al*., 2009b). The transport complex then becomes anchored at PD, in which the first partially or fully encapsidated progeny RNA molecules are 'inserted' into the PD pore (detection of vRNA in PD: Fig. 5_6 C,E). In the model, these RNA molecules represent a secondary, progeny population of vRNA.

Importantly, viral movement from infected to neighbouring cells does not simply involve translocation of virus particles through the PD. The hypothesis is that the PVX VRC is not only the site of virus replication, but also the origin of the viral movement complex as it contains virus-encoded movement proteins and the coat protein needed for the viral spread. Moreover, it is suggested that viral RNA will not traffic from one cell to another until a complete viral replication cycle has occurred. This idea was experimentally proven in our lab for TMV during microinjection studies. These experiments showed that injected TMV RNA did not move through PD until a cycle of replication had happened (Christensen *et al*., 2009). Therefore, once the complex is ready for the movement, vRNA is transported from the site of synthesis to PD.

The model presented in this thesis for PVX infection opposes the model based on TGB2/TGB3-derived vesicles as the transport form of the virus (Ju *et al*., 2007). This vesicle-based transport model implies that PVX TGB1 is not needed for vRNA movement towards PD, but suggests that TGB1 plays a role in trafficking vRNA through PD once vRNA is released from the transport vesicles (Verchot-Lubicz *et al*., 2007). According to a different hypothesis, vRNA, CP and TGB1 complex, either through an interaction with TGB2 and TGB3, or alone, is targeted to PD (Oparka *et al*., 1996; Lough *et al*., 1998; Santa Cruz *et al*., 1998; Solovyev *et al*., 2000; Rodionova *et al*., 2003; Karpova *et al*., 2006). This thesis does not completely support any of the available proposed models, but offers an integrated model that shows that the transport complex contains all three TGB proteins, viral CP and the vRNA. The viral CP has been shown to accumulate in PD but does not gate PD (Oparka *et al*., 1996) and was detected together with TGB1 in PD in this work (Fig. 4_4 F,I; Fig. 4_5; Fig. 4_6). The TGB1 and TGB2 viral proteins have been found to gate PD (see

Chapter 1). TGB2 and TGB3 have also been shown to interact with each other (Samuels *et al*., 2007) and TGB2 has been found to associate with PD in the presence of TGB1 (Fig. 4_9 C; Fig. 4_10 F). The vRNA was also detected in PD during these studies (Fig. 5_6 C,E). This indicates that these viral proteins act together to transport the viral genome through PD, and that TGB2 and TGB3 are likely to be involved in attachment of the transport complex to the ER network through their putative transmembrane domains for insertion of these proteins into cellular membranes (Morozov *et al*., 1987, 1989).

6.2 Compartmentation of PVX VRC

PVX VRCs are highly organised replication 'factories' with a series of spatially arranged and defined units working in a close coordination to 'prepare' the virus for transport to and through PD. In the proposed model, the vRNA has to go through an ordered series of compartments, acting as a viral 'factory' in which all required host and viral components are sequentially added to the vRNA. In the model, there is no difference in the structure of small and large VRCs of PVX, and their functional significance for viral replication and movement remains the same during infection. The large VRCs formed in older infected cells carry out the same roles as smaller VRCs in earlier infected tissue, resulting in continuous synthesis of vRNA and accumulation of viral proteins and a massive reorganisation of the host endomembrane system (Fig. 3_2-3_3) and actin cytoskeleton (Fig. 3_4). By incorporating ER and Golgi membranes and actin microfilaments into the VRC, the virus not only replicates on host membranes and protects its genome, but also establishes a transport pathway for movement of its vRNA to and through PD. Collectively, formation of the PVX VRC includes: compartmentation of vRNA synthesis and replication, synthesis of viral proteins, and establishment of the viral transport complex destined for PD. In the future, additional experiments will be necessary to better define the nature of the host organelle recruitment during PVX infection, to further determine the role of the viral gene products in the VRC formation and to establish the origin of replication sites in the VRC. Additional data is also needed to connect the TGB2/TGB3-induced vesicles to the viral transport complex that targets PD.

6.3 Future work

6.3.1 Cellular inhibitor studies of PVX VRCs

To find out if the VRC formation is dependent on the host cell organelles, and to test which host factors contribute to virus replication and movement, an inhibitor study is required. If host endomembranes are the sites of PVX replication and the plant cytoskeleton provides the bridge between the VRC and PD then their integrity will be affected by the following inhibitors: brefeldin A (inhibiting protein transport from the ER to the Golgi apparatus), cerulenin (influence on *de novo* phospholipid biosynthesis), latrunculin B and cytochalasin D (actin-depolymerising drugs), oryzalin and nocodazole (mictrotubule-depolymerising agents) and taxol (a microtubule-stabilising drug). For example, if brefeldin A has no effect on a VRC structure then COPII vesicles that transport proteins from the ER to Golgi are unlikely to play a significant role in VRC formation. If treatment with cerulenin does not alter VRC structure, this will suggests that *de novo* lipid biosynthesis is not required for VRC formation and viral replication. Cytochalasin D and latrunculin B might inhibit actin microfilament recruitment into the VRC. These actin depolymerising drugs should also have an effect on the ER/Golgi remodelling and redistribution within the VRC as it is known that ER, Golgi and actin are structurally connected in plants (Quader *et al*., 1987; Boevink *et al*., 1998; Neumann *et al*., 2003), and an actinomyosin system is involved in the dynamics of these organelles (Liebe and Quader, 1994). To verify whether actin determines the pattern of the TGB1 inclusions in the VRC, actin inhibitors could be co-introduced with TGB1 into the same epidermal cell. Oryzalin and nocodazole are predicted to have no effect on PVX VRC structure due to the fact that intact microtubules were not found to be present in VRCs (this thesis) and the fact that PVX cell-to-cell movement occurs in the absence of microtubules (Harries *et al*., 2009b).

6.3.2 Mutational analysis of the PVX TGB proteins and viral CP

In order to answer fully which viral gene products are required to establish a VRC, PVX genomes lacking individual TGBs, or a combination of two or all three TGB proteins, require to be analysed. Such deletion mutants were constructed during this

thesis (Fig. 4_1 L) and are ready to be used for a complete analysis of PVX replication and movement. It has been shown that the deletion in the TGB1 viral gene has a significant effect on host actin recruitment into the VRC (Fig. 4_27 A,B). This thesis has also shown that TGB1 alone can redirect host organelles into the developing VRC (Fig. 4_15 A-C; Fig. 4_17 A; Fig. 4_18 A,B). However, other viral genes may also contribute to this recruitment of host factors into the VRC. Moreover, the precise role of the viral CP in PVX infection has yet to be established. Additionally, to identify the precise role of the TGB proteins in vRNA sub-cellular localisation and distribution in the infected cell, vRNA localisation in the complete absence of TGB proteins should also be investigated. Finally, due to the fact that TGB1 is a key viral protein, it would be interesting to test if this viral protein determines the localisation of other TGB proteins to the VRC.

6.3.3 Replication sites studies

To date, no experimental proof exists to show which cellular membrane compartments serve as the centre for PVX replication. In particular, experiments are required to determine if the replicase is associated with the endomembranes recruited into the VRC.

6.3.4 Reconstruction of the components of the PD transport pathway

Our group has shown that PVX TGB proteins, together with the viral RNA and CP, accumulate in PD of PVX-infected plant epidermal cells. These data imply that all of these viral proteins may be components of the PVX movement complex. However, there is no experimental evidence as yet to show whether the putative movement complex is located on the TGB2/TGB3-induced vesicles. To determine if TGB2/TGB3-related vesicles are connected to the viral transport complex, co-localisation experiments of green ‘overcoat’ PVX with red TGB2 and TGB3 proteins should be carried out. In order to distinguish between possible overexpression artefacts and true biological infection events, a close study of the timing of the appearance of TGB2- and TGB3-related vesicles is needed. For instance, if these vesicles appear immediately after the bombardment of these two viral proteins, this would indicate that TGB2/3 vesicles are real. If the vesicles are detected a few days

after bombardment, this result implies that overexpression artefacts may contribute to their appearance. Further experiments will also be necessary to verify that TGB2 and TGB3 associate with the viral RNA, a feature not yet tested. Colocalisation studies of TGB2/TGB3 with Syto82 labelling of dsRNA at the leading edge of infection events may verify this.

6.4 Final conclusions

This research project studied the relationship between potato virus X and its host plants, *Nicotiana benthamiana* and *Nicotiana tabacum*. PVX was found to be a beneficial research tool. Its TGB proteins together with its CP could be tagged with fluorescent proteins for studies of viral infection without affecting the ability of the virus to move and replicate in infected host plants. This project focused on an exploration of the structural and functional significance of the PVX VRC. During the work the aims laid out at the beginning of this project were gradually, but not completely, fulfilled. The thesis analysed the biogenesis of the VRC a largely ignored structure in the literature, explored the distribution of viral proteins during infection, and pinpointed the location of the vRNA for the first time. A direct link between VRC formation and trafficking of the viral genome to cell PD was suggested, and an integrative model of PVX vRNA replication and movement proposed. In this model, the VRC is presented as a highly compartmentalised structure in which TGB1 functions as a key component for the recruitment of host organelles into the VRC to enable successful viral replication and spread.

7. References

ABOUHAIDAR, M. G., XU, H. & HEFFERON, K. L. (1998) Potexvirus isolation and RNA extraction. IN FOSTER, G. D. & TAYLOR, S. C. (Eds.) *Methods in Molecular Biology. Volume 81. Plant virology protocols: from virus isolation to transgenic resistance.* Totowa, NJ, Humana Press.

ADAMS, M. J., ANTONIW, J. F., BAR-JOSEPH, M., BRUNT, A. A., CANDRESSE, T., FOSTER, G. D., MARTELLI, G. P., MILNE, R. G., ZAVRIEV, S. K. & FAUQUET, C. M. (2004) The new plant virus family Flexiviridae and assessment of molecular criteria for species demarcation. *Arch. Virol.,* 149**,** 1045-1060.

AGRANOVSKY, A. A. & MOROZOV, S. Y. (1999) Gene expression in positive strand RNA viruses: conventional and aberrant strategies. IN MANDAHAR, C. L. (Ed.) *Molecular biology of plant viruses.* Boston/Dordrecht/London, Kluwer.

ALLEN, N. S. & BROWN, D. T. (1988) Dynamics of the endoplasmic reticulum in living onion epidermal cells in relation to microtubules, microfilaments, and intracellular particle movement. *Cell. Motil. Cytoskelet.,* 10**,** 153-163.

ALLISON, A. V. & SHALLA, T. A. (1974) The ultrastructure of local lesions induced by potato virus X: a sequence of cytological events in the course of infection. *Phytopathology,* 64**,** 784-793.

ANDREEVA, A. V., ZHENG, H., SAINT-JORE, C. M., KUTUZOV, M. A., EVANS, D. E. & HAWES, C. R. (2000) Organization of transport from endoplasmic reticulum to Golgi in higher plants. *Biochemical Society Transactions,* 28**,** 505-512.

ANGELL, S. M. & BAULCOMBE, D. C. (1995) Cell-to-cell movement of potato virus X revealed by microinjection of a viral vector tagged with the beta-glucuronidase gene. *The Plant Journal,* 7**,** 135-140.

ANGEL, S. M., DAVIES, C. & BAULCOMBE, D. C. (1996) Cell-to-cell movement of potato virus X is associated with a change in the size exclusion limit of plasmodesmata in trichome cells of Nicotiana clevelandii. *Virology,* 216**,** 197-201.

ANNAMALAI, P. & RAO, A. L. N. (2008) RNA encapsidation assay. IN FOSTER, G. D., JOHANSEN, I. E., HONG, Y. & NAGY, P. D. (Eds.) *Methods in Molecular Biology. 451. Plant Virology protocols: From viral sequence to protein function. 2nd edition.* Totowa, USA, Humana Press.

ASURMENDI, S., BERG, R. H., KOO, J. C. & BEACHY, R. N. (2004) Coat protein regulates formation of replication complexes during tobacco mosaic virus infection. *PNAS,* 101**,** 1415-1420.

ATABEKOV, J. C., DOBROV, E., KARPOVA, O. & PODIONOVA, N. (2007) Potato virus X: structure, disassembly and reconstitution. *Molecular Plant Pathology,* 8**,** 667-675.

ATABEKOV, J. G., RODIONOVA, N. P., KARPOVA, O. V., KOZLOVSKY, S. V., NOVIKOV, V. K. & ARKHIPENKO, M. V. (2001) Translational activation of

encapsidated potato virus X RNA by coat protein phosphorylation. *Virology,* 286**,** 466-474.

ATABEKOV, J. G., RODIONOVA, N. P., KARPOVA, O. V., KOZLOVSKY, S. V. & POLJAKOV, V. Y. (2000) The movement protein-triggered in situ conversion of potato virus X virion RNA from a nontranslatable into a translatable form. *Virology,* 271**,** 259-263.

BAMUNUSINGHE, D., HEMENWAY, C. L., NELSON, R. S., SANDERFOOT, A. A., YE, C. M., SILVA, M. A. T., PAYTON, M. & VERCHOT-LUBICZ, J. (2009) Analysis of potato virus X replicase and TGBp3 subcellular locations. *Virology,* 393**,** 272-285.

BARRY, J. K. & MILLER, W. A. (2002) A–1 ribosomal frameshift element that requires base pairing across four kilobases suggests a mechanism of regulating ribosome and replicase traffic on a viral RNA. *PNAS,* 99**,** 11133-11138.

BASSELL, G. & SINGER, R. H. (1997) mRNA and cytoskeletal filaments. *Current Opinion in Cell Biology,* 9**,** 109-115.

BAULCOMBE, D. (2002) Viral suppression of systemic silencing. *Trends in Microbiology,* 10**,** 306-308.

BAULCOMBE, D. C., CHAPMAN, S. & SANTA CRUZ, S. (1995) Jellyfish green fluorescent protein as a reporter for virus infections. *The Plant Journal,* 7(6)**,** 1045-1053.

BEFFA, R. S., HOFER, R. M., THOMAS, M. & MEINS, J. F. (1996) Decreased susceptibility to viral disease of [beta]-1,3-glucanase-deficient plants generated by antisense transformation. *Plant Cell,* 8**,** 1001-1011.

BERTRAND, E., CHARTR, P., SCHAEFER, M., SHENOY, S. M., SINGER, R. H. & LONG, R. M. (1998) Localization of ASH1 mRNA particles in living yeast. *Mol. Cell,* 2**,** 437-445.

BIENZ, K., EGGER, D. & PASAMONTES, L. (1987) Association of polioviral proteins of the P2 genomic region with the viral replication complex and virus-induced membrane synthesis as visualized by electron microscopic immunocytochemistry and autoradiography. *Virology,* 160**,** 220-226.

BLACKMAN, L. M. & OVERALL, R. L. (1998) Immunolocalisation of the cytoskeleton to plasmodesmata of Chara corallina. *The Plant Journal,* 14**,** 733-741.

BLEYKASTEN-GROSSHANS, C., GUILLEY, H., BOUZOUBAA, S., RICHARDS, K. E. & JONARD, G. (1997) Independent expression of the first two triple gene block proteins of beet necrotic yellow vein virus complements virus defective in the corresponding gene but expression of the third protein inhibits viral cell-to-cell movement. *Molecular Plant-Microbe Interactions,* 10**,** 240-246.

BOEVINK, P., OPARKA, K., SANTA CRUZ, S., MARTIN, B., BETTERIDGE, A. & HAWES, C. (1998) Stacks on tracks: the plant Golgi apparatus traffics on an actin/ER network. *The Plant Journal,* 15**,** 441-447.

BOEVINK, P. & OPARKA, K. J. (2005) Virus-host interactions during movement processes. *Plant Physiololgy,* 138**,** 1815-1821.

BOEVINK, P., SANTA CRUZ, S., HAWES, C., HARRIS, N. & OPARKA, K. J. (1996) Virus-mediated delivery of the green fluorescent protein to the endoplasmic reticulum of plant cells. *The Plant Journal,* 10(5)**,** 935-941.

BOTHA, C. E. J. & CROSS, R. H. M. (2000) Towards reconciliation of structure with function in plasmodesmata - who is the gatekeeper? *Micron,* 31**,** 713-721.

BOYKO, V., FERRALLI, J., ASHBY, J., SCHELLENBAUM, P. & HEINLEIN, M. (2000) Function of microtubules in intercellular transport of plant virus RNA. *Nature Cell Biology,* 2**,** 826-832.

BRANDENBURG, B., LEE, L. Y., LAKADAMYALI, M., RUST, M. J., ZHUANG, X. & HOGLE, J. M. (2007) Imaging poliovirus entry in live cells. *PLoS Biology,* 5**,** e183.

BRANDIZZI, F., SNAPP, E. L., ROBERTS, A. G., LIPPINCOTT-SCHWARTZ, J. & HAWES, C. (2002) Membrane protein transport between the endoplasmic reticulum and the Golgi in tobacco leaves is energy dependent but cytoskeleton independent: evidence from selective photobleaching. *Plant Cell,* 14**,** 1293-1309.

BROWNING, K. S. (2004) Plant translation initiation factors: it is not easy to be green. *Biochemical Society Transactions,* 32**,** 589-591.

BURGYAN, J., RUBINO, L. & RUSSO, M. (1996) The 5'-terminal region of a tombusvirus genome determines the origin of multivesicular bodies. *J. Gen. Virol.,* 77**,** 1967-1974.

CALIGURI, L. A. & TAMM, I. (1970) The role of cytoplasmic membranes in poliovirus biosynthesis. *Virology,* 42**,** 100-111.

CARETTE, J. E., STUIVER, M., VAN LENT, J., WELLINK, J. & VAN KAMMEN, A. (2000) Cowpea mosaic virus infection induces a massive proliferation of endoplasmic reticulum but not Golgi membranes and is dependent on de novo membrane synthesis. *Journal of Virology,* 74**,** 6556-6563.

CARETTE, J. E., VAN LENT, J., MACFARLANE, S. A., WELLINK, J. & VAN KAMMEN, A. (2002) Cowpea mosaic virus 32- and 60-kilodalton replication proteins target and change the morphology of endoplasmic reticulum membranes. *Journal of Virology,* 76**,** 6293-6301.

CARRINGTON, J. C., KASSCHAU, K. D. & JOHANSEN, L. K. (2001) Activation and suppression of RNA silencing by plant viruses. *Virology,* 281**,** 1-5.

CARRINGTON, J. C., KASSCHAU, K. D., MAHAJAN, S. K. & SCHAAD, M. C. (1996) Cell-to-cell and long distance transport of viruses in plants. *Plant Cell,* 8**,** 1669-1681.

CHALFIE, M., TU, Y., EUSKIRCHEN, G., WARD, W. W. & PRASHER, D. C. (1994) Green fluorescent protein as a marker for gene expression. *Science,* 263**,** 802-805.

CHAPMAN, S., KAVANAGH, T. & BAULCOMBE, D. (1992) Potato virus X as a vector for gene expression in plants. *The Plant Journal,* 2(4)**,** 549-557.

CHEONG, C. G. & TANAKA HALL, T. M. (2006) Engineering RNA sequence specificity of Pumilio repeats. *PNAS,* 103**,** 13635-13639.

CHEUNG, A. Y. & DE VRIES, S. C. (2008) Membrane trafficking: intracellular highways and country roads. *Plant Physiology,* 147**,** 1451-1453.

CHO, B. R. & MCDONALD, T. L. (1980) Infectious bursal disease virus: further characterization with evidence for a single-stranded RNA virus. *Avian Diseases,* 24**,** 423-434.

CHOI, C. W. (1999) Modified plasmodesmata in Sorghum (Sorghum bicolor L. Moench) leaf tissues infected by maize dwarf mosaic virus. *Journal of Plant Biology,* 42**,** 63-70.

CHRISTENSEN, N., TILSNER, J., BELL, K., HAMMANN, P., PARTON, R., LACOMME, C. & OPARKA, K. (2009) The 5' cap of Tobacco Mosaic Virus (TMV) is required for virion attachment to the actin/ER network during early infection. *Traffic,* 10**,** 536-551.

CITOVSKY, V., MCLEAN, B. G., ZUPAN, J. R. & ZAMBRYSKI, P. (1993) Phosphorylation of tobacco mosaic virus cell-to-cell movement protein by a developmentally regulated plant cell wall-associated protein kinase. *Genes and Development,* 7**,** 904-910.

CITOVSKY, V., WONG, M. L., SHAW, A. L., VENKATARAM PRASAD, B. V. & ZAMBRYSKI, P. (1992) Visualization and characterization of tobacco mosaic virus movement protein binding to single-stranded nucleic acids. *Plant Cell,* 4**,** 397-411.

CRONSHAW, J., HOEFERT, L. L. & ESAU, K. (1966) Ultrastructural features of Beta leaves infected with beet yellows virus. *Journal of Cell Biology,* 31**,** 429-443.

CROWTHER, D. & MELNICK, J. L. (1961) The incorporation of neutral red and acridine orange into developing poliovirus particles making them photosensitive. *Virology,* 14**,** 11-21.

CUDMORE, S., RECKMANN, I. & WAY, M. (1997) Viral manipulations of the actin cytoskeleton. *Trends in Microbiology,* 5**,** 142-148.

DAIGLE, N. & ELLENBERG, J. (2007) λN-GFP: an RNA reporter system for live-cell imaging. *Nature Methods,* 4**,** 633-636.

DALES, S., EGGERS, H. J., TAMM, I. & PALADE, G. E. (1965) Electron microscopic study of the formation of poliovirus. *Virology,* 26**,** 379-389.

DASILVA, L. L. P., SNAPP, E. L., DENECKE, J., LIPPINCOTT-SCHWARTZ, J., HAWES, C. & BRANDIZZI, F. (2004) Endoplasmic reticulum export sites and Golgi bodies behave as single mobile secretory units in plant cells. *Plant Cell,* 16**,** 1753-1771.

DAVIES, C., HILLS, G. & BAULCOMBE, D. C. (1993) Sub-cellular localization of the 25-kDa protein encoded in the triple gene block of potato virus X. *Virology,* 197**,** 166-175.

DE GRAAFF, M., COSCOY, L. & JASPARS, E. M. J. (1993) Localization and biochemical characterization of alfalfa mosaic virus replication complexes. *Virology,* 194**,** 878-881.

DEMLER, S. A., BORKHSENIOUS, O. N., RUCKER, D. G. & DE ZOETEN, G. A. (1994) Assessment of the autonomy of replicative and structural functions encoded by the luteo-phase of pea enation mosaic virus. *J. Gen. Virol.,* 75**,** 997-1007.

DEOM, C. M., OLIVER, M. J. & BEACHEY, R. N. (1987) The 30-kilodalton gene product of tobacco mosaic virus potentiates virus movement. *Science,* 237**,** 389-394.

DIETRICH, R. A. (2000) Emerging technologies an their application in the study of host-pathogen interactions. IN DICKINSON, M. & BEYNON, J. (Eds.) *Molecular Plant Pathology. Annual Plant Reviews, Volume 4.* Sheffield, England, Sheffield Academic Press Ltd.

DING, B. (1998) Intercellular protein trafficking through plasmodesmata. *Plant Molecular Biology,* 38**,** 279-310.

DING, B., HAUDENSHIELD, J. S., HULL, R. J., WOLF, S., BEACHY, R. N. & LUCAS, W. J. (1992a) Secondary plasmodesmata are specific sites of localization of the tobacco mosaic virus movement protein in transgenic tobacco plants. *Plant Cell,* 4**,** 915-928.

DING, B., TURGEON, R. & PARTHASARATHY, M. V. (1992b) Substructure of freeze-substituted plasmodesmata. *Protoplasma,* 169**,** 28-41.

DIXIT, R., CYR, R. & GILROY, S. (2006) Using intrinsically fluorescent proteins for plant cell imaging. *The Plant Journal,* 45**,** 599-615.

DOLJA, V. V., GRAMA, D. P., MOROZOV, S. Y. & ATABEKOV, J. G. (1987) Potato virus X-related single- and double stranded RNA. Characterisation and identification of terminal structures. *FEBS Lett.,* 214**,** 308-312.

DONALD, R. G., ZHOU, H. & JACKSON, A. O. (1993) Serological analysis of barley stripe mosaic virus-encoded proteins in infected barley. *Virology,* 195**,** 659-668.

DORONIN, S. V. & HEMENWAY, C. (1996) Synthesis of potato virus X RNAs by membrane-containing extracts. *Journal of Virology,* 70**,** 4795-4799.

DOS REIS FIGUEIRA, A., GOLEM, S., GOREGAOKER, S. P. & CULVERT, J. N. (2002) A nuclear localization signal and a membrane association domain contribute to the cellular localization of the tobacco mosaic virus 126-kDa replicase protein. *Virology,* 301**,** 81-89.

DREHER, T. W. & MILLER, W. A. (2006) Translational control in positive strand RNA plant viruses. *Virology,* 344**,** 185-197.

DUNOYER, P., RITZENTHALER, C., HEMMER, O., MICHLER, P. & FRITSCH, C. (2002) Intracellular localization of the peanut clump virus replication complex in tobacco BY-2 protoplasts containing green fluorescent protein-labeled endoplasmic reticulum or Golgi apparatus. *Journal of Virology,* 76**,** 865-874.

ECHEVERRI, A., BANERJEE, R. & DASGUPTA, A. (1998) Amino-terminal region of poliovirus 2C protein is sufficient for membrane binding. *Virus Res.,* 54**,** 217-223.

EGGEN, R. & VAN KAMMEN, A. (1988) RNA replication in Comoviruses. IN AHLQUIST, P., HOLLAND, J. & DOMINGO, E. (Eds.) *RNA Genetics.* Boca Raton, FL, CRC Press.

EHLERS, K. & KOLLMANN, R. (2001) Primary and secondary plasmodesmata: structure, origin, and functioning. *Protoplasma,* 216**,** 1-30.

EPEL, B. L. (1994) Plasmodesmata: composition, structure and trafficking. *Plant Molecular Biology,* 26**,** 1343-1356.

EPEL, B. L. (2009) Plant viruses spread by diffusion on ER-associated movement-protein-rafts through plasmodesmata gated by viral induced host beta-1,3-glucanases. *Sem Cell Dev Biol.,* 20**,** 1074-1081.

ERHARDT, M., MORANT, M., RITZENTHALER, C., STUSSI-GARAUD, C., GUILLEY, H., RICHARDS, K., JONARD, G., BOUZOUBAA, S. & GILMER, D. (2000) P42 movement protein of Beet necrotic yellow vein virus is targeted by the movement proteins P13 and P15 to punctuate bodies associated with plasmodesmata. *Molecular Plant-Microbe Interactions,* 13(5)**,** 520-528.

ERHARDT, M., VETTER, G., GILMER, D., BOUZOUBAA, S., RICHARDS, K., JONARD, G. & GUILLEY, H. (2005) Subcellular localization of the Triple Gene Block movement proteins of Beet necrotic yellow vein virus by electron microscopy. *Virology,* 340**,** 155-166.

ESAU, K. (1967) Anatomy of plant virus infections. *Annual Review of Phytopathology,* 5**,** 45-76.

ESAU, K. & CRONSHAW, J. (1967) Relation of tobacco mosaic virus to the host cells. *Journal of Cell Biology,* 33**,** 665-678.

ESAU, K., CRONSHAW, J. & HOEFERT, L. L. (1967) Relation of beet yellows virus to the phloem and to movement in the sieve tube. *Journal of Cell Biology,* 32**,** 71-87.

ESPINOZA, A. M., MEDINA, V., HULL, R. & MARKHAM, P. G. (1991) Cauliflower mosaic virus gene II product forms distinct inclusion bodies in infected plant cells. *Virology,* 185**,** 337-344.

EVERT, R. F., ESCHRICH, W. & HEYSER, W. (1977) Distribution and structure of the plasmodesmata in mesophyll and bundle-sheath cells of Zea mays L. *Planta,* 136**,** 77-89.

FANNIN, F. F. & SHAW, J. G. (1987) Evidence for concurrent spread of tobacco mosaic virus from infected epidermal cells to neighboring epidermal and mesophyll cells. *Plant Sci.,* 51**,** 305-310.

FAULKNER, C., AKMAN, O. E., BELL, K., JEFFREE, C. & OPARKA, K. (2008) Peeking into pit fields: a multiple twinning model of secondary plasmodesmata formation in tobacco. *Plant Cell,* 20**,** 1504-1518.

FOREST, T., BARNARD, S. & BAINES, J. D. (2005) Active intranuclear movement of herpesvirus capsids. *Nature Cell Biology,* 7**,** 429-431.

FRIDBORG, I., GRAINGER, J., PAGE, A., COLEMAN, M., FINDLAY, K. & ANGELL, S. (2003) TIP, a novel host factor linking callose degradation with the cell-to-cell movement of potato virus X. *Molecular Plant-Microbe Interactions,* 16**,** 132-140.

FROSHAUER, S., KARTENBECK, J. & HELENIUS, A. (1988) Alphavirus RNA replicase is located on the cytoplasmic surface of endosomes and lysosomes. *Journal of Cell Biology,* 107**,** 2075-2086.

FUJIKI, M., KAWAKAMI, S., KIM, R. W. & BEACHY, R. N. (2006) Domains of tobacco mosaic virus movement protein essential for its membrane association. *J. Gen. Virol.,* 87**,** 2699-2707.

FUSCO, D., ACCORNERO, N., LAVOIE, B., SHENOY, S. M., BLANCHARD, J., SINGER, R. H. & BERTR, E. (2003) Single mRNA molecules demonstrate

probabilistic movement in living mammalian cells. *Current Biology,* 13**,** 161-167.
GALLIE, D. R. (1996) Translational control of cellular and viral mRNAs. *Plant Molecular Biology,* 32**,** 145-158.
GALLIE, D. R. (1998) A tale of two termini: A functional interaction between the termini of an mRNA is a prerequisite for efficient translation initiation. *Gene,* 216**,** 1-11.
GARNIER, M., CANDRESSE, T. & BOVÉ, J. M. (1986) Immunocytochemical localization of TYMV-coded structural and non-structural proteins by the protein A-gold technique. *Virology,* 151**,** 100-109.
GARNIER, M., MAMOUN, R. & BOVÉ, J. M. (1980) TYMV RNA replication in vivo: replicative intermediate is mainly single stranded. *Virology,* 104**,** 357-374.
GILBERTSON, R. L. & LUCAS, W. J. (1996) How do viruses traffic on the 'vascular highway'? *Trends in Plant Science,* 1(8)**,** 260-268.
GILLESPIE, T., BOEVINK, P., HAUPT, S., ROBERTS, A. G., TOTH, R., VALENTINE, T. A., CHAPMAN, S. & OPARKA, K. J. (2002) Functional analysis of a DNA-shuffled movement protein reveals that microtubules are dispensable for the cell-to-cell movement of Tobacco mosaic virus. *Plant Cell,* 14**,** 1207-1222.
GILMER, D., BOUZOUBAA, S., HEHN, A., GUILLEY, H., RICHARDS, K. & JONARD, G. (1992) Efficient cell-to-cell movement of beet necrotic yellow vein virus requires 3′ proximal genes located on RNA 2. *Virology,* 189**,** 40-47.
GINGRAS, A. C., RAUGHT, B. & SONENBERG, N. (1999) eIF4 initiation factors: effectors of mRNA recruitment to ribosomes and regulators of translation. *Annual Review of Biochemistry,* 68**,** 913-963.
GOLDIN, M. I. (1963) *Virusnye vkliucheniia v rastitelnoi kletke (Virus inclusions in the plant cell),* Moscow, Academiia Nauk SSSR.
GOLGSTEIN, B. (1926) A cytological study of the leaves and growing points of healthy and mosaic diseased tobacco plants. *Bull. Torrey Bot. Club* 53**,** 499-600.
GOODIN, M., CHAKRABARTY, R. & YELTON, S. (2008) Membrane and protein dynamics in virus-infected plant cells. IN FOSTER, G. D., JOHANSEN, I. E., HONG, Y. & NAGY, P. D. (Eds.) *Methods in Molecular Biology. 451. Plant Virology protocols: From viral sequence to protein function. 2nd edition.* Totowa, USA, Humana Press.
GORBALENYA, A. E. & KOONIN, E. V. (1989) Viral proteins containing the purine NTP-binding sequence pattern. *Nucleic Acids Research,* 17**,** 8413-8440.
GORSHKOVA, E. N., EROKHINA, T. N., STROGANOVA, T. A., YELINA, N. E., ZAMYATNIN, J. A. A., KALININA, N. O., SCHIEMANN, J., SOLOVYEV, A. G. & MOROZOV, S. Y. (2003) Immunodetection and fluorescent microscopy of transgenically expressed hordeivirus TGBp3 movement protein reveals its association with endoplasmic reticulum elements in close proximity to plasmodesmata. *J. Gen. Virol.,* 84**,** 985-994.
GRAMA, C. & MASHKOVSKY, N. (1986) The discovery and study of subgenomic RNA of potato virus X. *Biopolim. Kletka,* 2**,** 328-334.

GREBER, U. F. & WAY, M. (2006) A superhighway to virus infection. *Cell,* 124**,** 741-754.

GRIESBECK, O., BAIRD, G. S., CAMPBELL, R. E., ZACHARIAS, D. A. & TSIEN, R. Y. (2001) Reducing the environmental sensitivity of yellow fluorescent protein. *J. Biol. Chem.,* 276**,** 29188-29194.

GUILFORD, P. J. & FORSTER, R. L. S. (1986) Detection of polyadenylated subgenomic RNAs in leaves infected with daphne virus X. *J. Gen. Virol.,* 67**,** 83-90.

GUPTA, Y. K., NAIR, D. T., WHARTON, R. P. & AGGARWAL, A. K. (2008) Structures of human pumilio with noncognate RNAs reveal molecular mechanisms for binding promiscuity. *Structure,* 16**,** 549-557.

HAMADA, S., ISHIYAMA, K., CHOI, S. B., WANG, C., SINGH, S., KAWAI, N., FRANCESCHI, V. R. & OKITA, T. W. (2003) The transport of prolamine RNAs to prolamine protein bodies in living rice endosperm cells. *Plant Cell,* 15**,** 2253-2264.

HARA-NISHIMURA, I., SHIADA, T., HATANO, K., TAKEUCHI, Y. & NISHIMURA, M. (1998) Transport of storage proteins to protein storage vacuoles is mediated by large precursor-accumulating vesicles. *Plant Cell,* 10**,** 825-836.

HARRIES, P. A., KARUPPAIAH, P., YU, W., SCHOELZ, J. E. & NELSON, R. S. (2009a) The Cauliflower mosaic virus protein P6 forms motile inclusions that traffic along actin microfilaments and stabilize microtubules. *Plant Physiology,* 149**,** 1005-1016.

HARRIES, P. A., PARK, J.-W., SASAKI, N., BALLARD, K. D., MAULE, A. J. & NELSON, R. S. (2009b) Differing requirements for actin and myosin by plant viruses for sustained intercellular movement. *PNAS,* 106**,** 17594-17599.

HARRISON, B. D. & ROBERTS, I. M. (1968) Association of tobacco rattle virus with mitochondria. *J. Gen. Virol.,* 3**,** 121-124.

HARRISON, H., WILEY, D. C. & SKEHEL, J. J. (1996) Virus structure. IN FIELDS, B. N., KNIPE, D. M., HOWLEY, P. M. & EDITION, N. (Eds.) *Fields virology* New York, Lippincott-Raven.

HASELOFF, J., SIEMERING, K. R., PRASHER, D. C. & HODGE, S. (1997) Removal of a cryptic intron and subcellular localization of green fluorescent protein are required to mark transgenic Arabidopsis plants brightly. *PNAS,* 94**,** 2122-2127.

HATTA, T., BULLIVANT, S. & MATTHEWS, R. E. (1973) Fine structure of vesicles induced in chloroplasts of chinese cabbage leaves by infection with turnip yellow mosaic virus *J. Gen. Virol.,* 20**,** 37-50.

HATTA, T. & FRANCKI, R. I. B. (1981) Cytopathic structures associated with tonoplasts of plant cells infected with cucumber mosaic and tomato aspermy viruses. *J. Gen. Virol.,* 53**,** 343-346.

HAUPT, S., COWAN, G. H., ZIEGLER, A., ROBERTS, A. G., OPARKA, K. J. & TORRANCE, L. (2005) Two plant-viral movement proteins traffic in the endocytic recycling pathway. *Plant Cell,* 17**,** 164-181.

HAUPT, S., ZIEGLER, A. & TORRANCE, L. (2008) Localization of viral proteins in plant cells: protein tagging. IN FOSTER, G. D., JOHANSEN, I. E., HONG, Y.

& NAGY, P. D. (Eds.) *Methods in Molecular Biology. 451. Plant Virology protocols: From viral sequence to protein function. 2nd edition.* Totowa, USA, Humana Press.

HAWES, C. (1994) Electron microscopy. IN HARRIS, N. & OPARKA, K. J. (Eds.) *Plant Cell Biology: a practical approach.* Oxford, University Press.

HAWES, C. (2005) Cell biology of plant Golgi apparatus. *New Phytologist,* 165**,** 29-44.

HEFFERON, K. L., DOYLE, S. & ABOUHAIDAR, M. G. (1997) Immunological detection of the 8K protein of potato virus X (PVX) in cell walls of PVX-infected tobacco and transgenic potato. *Arch. Virol.,* 142**,** 425-433.

HEINLEIN, M. (2002) The spread of Tobacco mosiac virus infection: insights into the cellular mechanism of RNA transport. *Cellular and Molecular Life Sciences,* 59**,** 58-82.

HEINLEIN, M., EPEL, B. L., PADGETT, H. S. & BEACHY, R. N. (1995) Interaction of tobamovirus movement proteins with the plant cytoskeleton. *Science,* 270**,** 1983-1985.

HEINLEIN, M., PADGETT, H. S., GENS, J. S., PICKARD, B. J., CASPER, S. J., EPEL, B. L. & BEACHY, R. N. (1998) Changing patterns of localization of the tobacco mosaic virus movement protein and replicase to the endoplasmic reticulum and microtubules during infection. *Plant Cell,* 10**,** 1107-1120.

HEPLER, P. K., PALEVITZ, B. A., LANCELLE, S. A., MCCAULEY, M. M. & LICHTSCHEIDL, I. (1990) Cortical endoplasmic reticulum in plants. *J. Cell Science,* 96**,** 355-373.

HERZOG, E., HEMMER, O., HAUSER, S., MEYER, G., BOUZOUBAA, S. & FRITSCH, C. (1998) Identification of genes involved in replication and movement of peanut clump virus. *Virology,* 248**,** 312-322.

HIATT, C. W. (1960) Differential inactivation of B-virus suspensions of live poliovirus. *Federation Proc.,* 19**,** 405.

HILLMAN, B. I. (1998) Introduction to plant virology. IN FOSTER, G. D. & TAYLOR, S. C. (Eds.) *Methods in Molecular Biology. Volume 81. Plant virology protocols: from virus isolation to transgenic resistance.* Totowa, NJ, Humana Press.

HILLS, G. J., PLASKITT, K. A., YOUNG, N. D., DUNIGAN, D. D., WATTS, J. W., WILSON, T. M. A. & ZAITLIN, M. (1987) Immunogold localization of the intracellular sites of structural and nonstructural tobacco mosaic virus proteins. *Virology,* 161**,** 488-496.

HIRAI, T. & WILDMAN, S. G. (1953) Cytological and cytochemical observations on the early stage of infection of tomato hair cells by tobacco mosaic virus. *Plant Cell Physiology,* 4**,** 265-275.

HOFMANN, C., NIEHL, A., SAMBADE, A., STEINMETZ, A. & HEINLEIN, M. (2009) Inhibition of tobacco mosaic virus movement by expression of an actin-binding protein. *Plant Physiology,* 149**,** 1810-1823.

HOWARD, A. R., HEPPLER, M. L., JU, H. J., KRISHNAMURTHY, K., PAYTON, M. E. & VERCHOT-LUBICZ, J. (2004) Potato virus X TGBp1 induces plasmodesmata gating and moves between cells in several host species whereas CP moves only in N. benthamiana leaves. *Virology,* 328**,** 185-197.

HU, C. D., CHINENOV, Y. & KERPPOLA, T. K. (2002) Visualization of interactions among bZIP and Rel family proteins in living cells using bimolecular fluorescence complementation. *Mol. Cell,* 9**,** 789-798.

HUANG, M. & ZHANG, L. (1999) Association of the movement protein of alfalfa mosaic virus with the endoplasmic reticulum and its trafficking in epidermal cells of onion bulb scales. *Molecular Plant-Microbe Interactions,* 12**,** 680-690.

HUGHES, J. E. & GUNNING, B. E. S. (1980) Glutaraldehyde-induced deposition of callose. *Can. J. Bot.,* 58**,** 250-258.

HUISMAN, M. J., LINTHORST, H. J. M., BOL, J. F. & CORNELISSEN, B. J. C. (1988) The complete nucleotide sequence of potato virus X and its homologies at the amino acid level with various plus-stranded RNA viruses. *J. Gen. Virol.,* 69**,** 1789-1798.

HULL, R. (1992) Down the tube. Tubules extending from protoplasts infected with cowpea mosaic virus may reveal how some viruses move from cell to cell in infected plants. *Current Biology,* 2(5)**,** 224-226.

HULL, R. (2002) *Matthews' Plant Virology. 4th edition*, Academic Press.

ITAYA, A., WOO, Y. M., MASUTA, C., BAO, Y., NELSON, R. S. & DING, B. (1998) Developmental regulation of intercellular protein trafficking through plasmodesmata in tobacco leaf epidermis. *Plant Physiology,* 118**,** 373-385.

IWANOWSKI, D. (1903) Über die Mosaikkrankheit der Tabakpflanze. *Z. Pflanzenkrankh,* 13**,** 1-41.

JEFFREY, A., CHAO, K., CZAPLINSKI, R. & SINGER, H. (2008) Using the bacteriophage MS2 coat protein-RNA binding interaction to visualize RNA in living cells. IN MILLER, L. W. (Ed.) *Probes and tags to study biomolecular function.* Wiley-VCH Verlag GmbH & Co. KGaA.

JONES, L., HAMILTON, A. J., VOINNET, O., THOMAS, C. L., MAULE, A. J. & BAULCOMBE, D. C. (1999) RNA-DNA interactions and DNA methylation in post-transcriptional gene silencing. *Plant Cell,* 11**,** 2291-2301.

JU, H.-J., YE, C.-M. & VERCHOT-LUBICZ, J. (2008) Mutational analysis of PVX TGB3 links subcellular accumulation and protein turnover. *Virology,* 375**,** 103-117.

JU, H. J., BROWN, J. E., YE, C. M. & VERCHOT-LUBICZ, J. (2007) Mutations in the central domain of potato virus X TGBp2 eliminate granular vesicles and virus cell-to-cell trafficking. *Journal of Virology,* 81**,** 1899-1911.

JU, H. J., SAMUELS, T. D., WANG, Y. S., BLANCAFLOR, E., PAYTON, M., MITRA, R., KRISHNAMURTHY, K., NELSON, R. S. & VERCHOT-LUBICZ, J. (2005) The potato virus X TGBp2 movement protein associates with endoplasmic reticulum-derived vesicles during virus infection. *Plant Physiology,* 138**,** 1877-1895.

KALININA, N. O., FEDORKIN, O. N., SAMUILOVA, O. V., MAISS, E., KORPELA, T., MOROZOV, S. Y. & ATABEKOV, J. G. (1996) Expression and biochemical analysis of the recombinant potato virus X 25K movement protein. *FEBS Lett.,* 397**,** 75-78.

KALININA, N. O., RAKITINA, D. V., SOLOVYEV, A. G., SCHIEMANN, J. & MOROZOV, S. Y. (2002) RNA helicase activity of the plant virus movement

proteins encoded by the first gene of the triple gene block. *Virology,* 296**,** 321-329.

KALININA, N. O., SAMUILOVA, O. V., FEDORKIN, O. N., ZELENINA, D. A. & MOROZOV, S. Y. (1998) Biochemical characterization and subcellular localization of a 25K transport protein of potato virus X. *Molekulyarnaya Biologiya,* 32**,** 569-573.

KAPUSCINSKI, J. (1995) DAPI: A DNA-specific fluorescent probe. *Biotechnic and Histochemistry,* 70**,** 220-233.

KARPOVA, O. V., ZAYAKINA, O. V., ARKHIPENKO, M. V., SHEVAL, E. V., KISELYOVA, O. I., POLJAKOV, V. Y., YAMINSKY, I. V., RODIONOVA, N. P. & ATABEKOV, J. G. (2006) Potato virus X RNA-mediated assembly of single-tailed ternary 'coat protein–RNA–movement protein' complexes. *J. Gen. Virol.,* 87**,** 2731-2740.

KAWAKAMI, S., WATANABE, Y. & BEACHY, R. N. (2004) Tobacco mosaic virus infection spreads cell to cell as intact replication complexes. *PNAS,* 101(16)**,** 6291-6296.

KIKUMOTO, T. & MATSUI, C. (1961) Electron microscopy of intracellular potato virus X. I. *Virology,* 13**,** 294-299.

KISELYOVA, O. I., YAMINSKY, I. V., KARPOVA, O. V., RODIONOVA, N. P., KOZLOVSKY, S. V., ARKHIPENKO, M. V. & ATABEKOV, J. G. (2003) AFM study of potato virus X disassembly induced by movement protein. *J. Mol. Biol.,* 332**,** 321-325.

KITAJIMA, E. W. & LAURITIS, J. A. (1969) Plant virions in plasmodesmata. *Virology,* 37**,** 681-685.

KOBAYASHI, K., SARROBERT, C., ARES, X., RIVERO, M. M., MALDONADO, S., ROBAGLI, C. & MENTABERRY, A. (2004) Over-expression of potato virus X TGBp1 movement protein in transgenic tobacco plants causes developmental and metabolic alterations. *Plant Physiology and Biochemistry,* 42**,** 731-738.

KOENIG, R., BEIER, C., COMMANDEUR, U., LÜTH, U., KAUFMANN, A. & LÜDDECKE, P. (1996) Beet soil-borne virus RNA 3 - a further example of the heterogeneity of the gene content of furovirus genomes and triple gene block-carrying RNAs. *Virology,* 216**,** 202-207.

KOONIN, E. V. & DOLJA, V. V. (1993) Evolution and taxonomy of positive-strand RNA viruses: implications of comparative analysis of amino acid sequences. *Critical Reviews in Biochemistry and Molecular Biology,* 28(5)**,** 375-430.

KOZAR, F. E. & SHELUDKO, Y. M. (1969) Ultrastructure of potato and Datura stramonium plant cells infected with potato virus X. *Virology,* 38**,** 220-229.

KRAGLER, F., CURIN, M., TRUTNYEVA, K., GANSCH, A. & WAIGMANN, E. (2003) MPB2C, a microtubule-associated plant protein binds to and interferes with cell-to-cell transport of tobacco mosaic virus movement protein. *Plant Physiology,* 132**,** 1870-1883.

KRAGLER, F., LUCAS, W. J. & MONZER, J. (1998) Plasmodesmata: dynamics, domains and patterning. *Annals of Botany,* 81**,** 1-10.

KRISHNAMURTHY, K., HEPPLER, M., MITRA, R., BLANCAFLOR, E., PAYTON, M., NELSON, R. S. & VERCHOT-LUBICZ, J. (2003) The Potato virus X

TGBp3 protein associates with the ER network for virus cell-to-cell movement. *Virology,* 309**,** 135-151.

KRISHNAMURTHY, K., MITRA, R., PAYTON, M. E. & VERCHOT-LUBICZ, J. (2002) Cell-to-cell movement of the PVX 12K, 18K or coat proteins may depend on the host, leaf developmental stage and the PVX 25K protein. *Virology,* 300**,** 296-281.

KUSOV, Y. Y., PROBST, C., JECHT, M., JOST, P. D. & GAUSS-MULLER, V. (1998) Membrane association and RNA binding of recombinant hepatitis A virus protein 2C. *Arch. Virol.,* 143**,** 931-944.

LACOMME, C., POGUE, G. P., WILSON, T. M. A. & SANTA CRUZ, S. (2001) Plant viruses. IN RING, C. J. A. & BLAIR, E. D. (Eds.) *Genetically engineered viruses: Development and Applications.* Stevenage, UK, Glaxo Wellcome Research and Development, BIOS Scientific Publishers Limited.

LACOMME, C., SMOLENSKA, L. & WILSON, T. M. A. (1998) Genetic engineering and the expression of foreign peptides or proteins with plant virus-based vectors. IN SETLOW, J. K. (Ed.) *Genetic engineering: principles and methods. Volume 20.* New York and London, Plenum Press.

LAI, C. K., JENG, K. S., MACHIDA, K. & LAI, M. M. (2008) Association of hepatitis C virus replication complexes with microtubules and actin filaments is dependent on the interaction of NS3 and NS5A. *Journal of Virology,* 82**,** 8838-8848.

LALONDE, S., EHRHARDT, D. W., LOQUÉ, D., CHEN, J., RHEE, S. Y. & FROMMER, W. B. (2008) Molecular and cellular approaches for the detection of protein-protein interactions: latest techniques and current limitations. *The Plant Journal,* 53**,** 610-635.

LANGE, S., KATAYAMA, Y., SCHMID, M., BURKACKY, O., BRÄUCHLE, C., LAMB, D. C. & JANSEN, R. P. (2008) Simultaneous transport of different localized mRNA species revealed by live-cell imaging. *Traffic,* 9**,** 1256-1267.

LAPORTE, C., VETTER, G., LOUDES, A. M., ROBINSON, D. G., HILLMER, S., STUSSI-GARAUD, C. & RITZENTHALER, C. (2003) Involvement of the secretory pathway and the cytoskeleton in intracellular targeting and tubule assembly of Grapevine fanleaf virus movement protein in Tobacco BY-2 cells. *Plant Cell,* 15**,** 2058-2075.

LAZAROWITZ, S. G. & BEACHY, R. N. (1999) Viral movement proteins as probes for intracellular and intercellular trafficking in plants. *Plant Cell,* 11**,** 535-548.

LE, H., TANGUAY, R. L., BALASTA, M. L., WEI, C. C., BROWNING, K. S., METZ, A. M., GOSS, D. J. & GALLIE, D. R. (1997) Translation initiation factors eIF-iso4G and eIF-4B interact with the poly(A)-binding protein and increase its RNA binding activity. *J. Biol. Chem.,* 272**,** 16247-16255.

LEE, J. Y. & LUCAS, W. J. (2001) Phosphorylation of viral movement proteins - regulation of cell-to-cell trafficking. *Trends in Microbiology,* 9(1)**,** 5-8.

LEISNER, S. M. (1999) Molecular basis of virus transport in plants. IN MANDAHAR, C. L. (Ed.) *Molecular biology of plant viruses.* Boston/Dordrecht/London, Kluwer.

LEISNER, S. M. & TURGEON, R. (1993) Movement of virus and photoassimilate in the phloem: a comparative analysis. *BioEssays,* 15(11)**,** 741-748.

LESEMANN, D. E. (1988) Cytopathology. IN MILNE, R. G. (Ed.) *The Plant Viruses. The filamentous plant viruses.* New York, Plenum Press.

LESHCHINER, A. D., MININA, E. A., RAKITINA, D. V., VISHNICHENKO, V. K., SOLOVYEV, A. G., MOROZOV, S. Y. & KALININA, N. O. (2008) Oligomerization of the potato virus X 25-kD movement protein. *Biochemistry (Moscow),* 73**,** 50-55.

LEYON, H. (1953) Virus formation in chloroplasts *Exptl. Cell Res.,* 4**,** 362-370.

LIEBE, S. & QUADER, H. (1994) Myosin in onion (Allium cepa) bulb scale epidermal cells: involvement in the dynamics of organelles and endoplasmic reticulum. *Plant Physiology,* 90**,** 114-124.

LIM, H. S., BRAGG, J. N., GANESAN, U., LAWRENCE, D. M., YU, J., ISOGAI, M., HAMMOND, J. & JACKSON, A. O. (2008) Triple gene block protein interactions involved in movement of Barley stripe mosaic virus. *Journal of Virology,* 82**,** 4991-5006.

LIU, J. Z., BLANCAFLOR, E. B. & NELSON, R. S. (2005) The tobacco mosaic virus 126-kilodalton protein, a constituent of the virus replication complex, alone or within the complex aligns with and traffics along microfilaments. *Plant Physiology,* 138**,** 1853-1865.

LOUGH, T. J., NETZLER, N. E., EMERSON, S. J., SUTHERLAND, P., CARR, F., BECK, D. L., LUCUS, W. J. & FORSTER, R. L. S. (2000) Cell-to-cell movement of potexviruses: evidence for a ribonucleoprotein complex involving the coat protein and first triple gene block protein. *Molecular Plant-Microbe Interactions,* 13**,** 962-974.

LOUGH, T. J., SHASH, K., XOCONOSTLE-CAZARES, B., HOFSTRA, K. R., BECK, D. L., BALMORI, E., FORSTER, R. L. S. & LUCAS, W. J. (1998) Molecular dissection of the mechanism by which Potexvirus triple gene block proteins mediated cell-to-cell transport of infectious RNA. *Molecular Plant-Microbe Interactions,* 8**,** 801-814.

LUCAS, W. J. (1995) Plasmodesmata: intercellular channels for macromolecular transport in plants. *Current Opinion in Cell Biology,* 7**,** 673-680.

LUCAS, W. J. (2006) Plant viral movement proteins: agents for cell-to-cell trafficking of viral genomes. *Virology,* 344**,** 169-184.

LUCAS, W. J. & WOLF, S. (1993) Plasmodesmata: the intercellular organelles of green plants. *Trends in Cell Biology,* 3**,** 308-315.

LUCAS, W. J., YOO, B. C. & KRAGLER, F. (2001) RNA as a long-distance information macromolecule in plants. *Nature Reviews Molecular Cell Biology,* 2**,** 849-857.

LUPO, R., RUBINO, L. & RUSSO, M. (1994) Immunodetection of the 33K/92K polymerase proteins in cymbidium ringspot virus-infected and in transgenic plant tissue extracts. *Arch. Virol.,* 138**,** 135-142.

MACKENZIE, J. (2005) Wrapping things up about virus RNA replication. *Traffic,* 6**,** 967-977.

MACKENZIE, J. M., JONES, M. K. & WESTAWAY, E. G. (1999) Markers for trans-Golgi membranes and the intermediate compartment localize to induced

membranes with distinct replication functions in flavivirus-infected cells. *Journal of Virology,* 73**,** 9555-9567.
MAGLIANO, D., MARSHALL, J. A., BOWDEN, D. S., VARDAXIS, N., MEANGER, J. & LEE, J. Y. (1998) Rubella virus replication complexes are virus-modified lysosomes. *Virology,* 40**,** 57-63.
MAS, P. & BEACHY, R. N. (1999) Replication of tobacco mosaic virus on endoplasmic reticulum and role of the cytoskeleton and virus movement protein in intracellular distribution of viral RNA. *Journal of Cell Biology,* 147**,** 945-958.
MAS, P. & BEACHY, R. N. (2000) Role of microtubules in the intracellular distribution of tobacco mosaic virus movement protein. *PNAS,* 97**,** 12345-12349.
MATSUSHITA, K. (1965) Tobacco mosaic virus in chloroplast and cytoplasm of infected tobacco leaf. *Plant Cell Physiology,* 6**,** 1-6.
MATTHEWS, R. E. F. (1992) *Fundamentals of plant virology. 3rd edition,* San Diego, London Academic Press.
MAULE, A. J. (2008) Plasmodesmata: structure, function and biogenesis. *Current Opinion in Plant Biology,* 11**,** 680-686.
MAYOR, H. D. (1961) Cytochemical and fluorescent antibody studies on the growth of poliovirus in tissue culture. *Texas Repts. Biol. and Med.,* 19**,** 106-122.
MAYOR, H. D. & DIWAN, A. R. (1961) Studies on the acridine orange staining of two purified RNA viruses: poliovirus and tobacco mosaic virus. *Virology,* 14**,** 74-82.
MAYOR, H. D. & HILL, N. O. (1961) Acridine orange staining of a single-stranded DNA bacteriophage. *Virology,* 14**,** 264-266.
MCLEAN, B. G., ZUPAN, J. & ZAMBRYSKI, P. C. (1995) Tobacco mosaic virus movement protein associates with the cytoskeleton in tobacco cells. *Plant Cell,* 7**,** 2101-2114.
MILLAR, H. A., CARRIE, C., POGSON, B. & WHELAN, J. (2009) Exploring the function-location nexus: using multiple lines of evidence in defining the subcellular location of plant proteins. *Plant Cell,* 21**,** 1625-1631.
MILLER, S. & KRIJNSE-LOCKER, J. (2008) Modification of intracellular membrane structures for virus replication. *Nature Reviews Microbiology,* 6**,** 363-374.
MILLER, W. A. & WHITE, K. A. (2006) Control of plant virus gene expression and replication by long-distance RNA-RNA interactions. *Annual Review of Phytopathology,* 44**,** 447-467.
MIRTA, R., KRISHNAMURTHY, K., BLANCAFLOR, E., PAYTON, M., NELSON, R. S. & VERCHOT-LUBICZ, J. (2003) The potato virus X TGBp2 protein association with the endoplasmic reticulum plays a role in but is not sufficient for viral cell-to-cell movement. *Virology,* 312**,** 35-48.
MOLECULAR_PROBES The Handbook from Invitrogen, viewed 12 July 2009, <http://www.invitrogen.com/site/us/en/home/References/Molecular-Probes-The-Handbook.html>.
MOLODTSOV, M. I., GRISHCHUK, E. L., EFREMOV, A. K., MCINTOSH, J. R. & ATAULLAKHANOV, F. I. (2005) Force production by depolymerizing microtubules: A theoretical study. *PNAS,* 102**,** 4353-4358.

MOORE, A. E. & STONE, B. A. (1972) Effect of infection with TMV and other viruses on the level of β-1,3-glucan hydrolase in leaves of Nicotiana glutinosa. *Virology,* 50**,** 791-798.

MOROZOV, S. Y., DOLJA, V. V. & ATABEKOV, J. G. (1989) Probable reassortment of genomic elements among elongated RNA-containing plant viruses. *Journal of Molecular Evolution,* 29**,** 52-62.

MOROZOV, S. Y., GORBULEV, V. G., NOVIKOV, V. K., AGRANOVSKII, A. A., KOZLOV, Y. V., ATABEKOV, J. G. & BAEV, A. A. (1981) Primary structure of 5- and 3-terminal regions of potato virus X genomic RNA. *Dokl. Akad. Nauk SSSR,* 259**,** 723-725.

MOROZOV, S. Y., LUKASHEVA, L. I., CHERNOV, B. K., SKRYABIN, K. G. & ATABEKOV, J. G. (1987) Nucleotide sequence of the open reading frames adjacent to the coat protein cistron in potato virus X genome. *FEBS Lett.,* 213(2)**,** 438-442.

MOROZOV, S. Y., MIROSHNICHENKO, N. A., SOLOVYEV, A. G., FEDORKIN, O. N., ZELININA, D. A., LUKASHEVA, L. I., KARASEV, A. V., DOLJA, V. V. & ATABEKOV, J. G. (1991) Expression strategy of the potato virus X triple gene block. *J. Gen. Virol.,* 72**,** 2039-2042.

MOROZOV, S. Y. & SOLOVYEV, A. G. (1999) Genome organization in RNA viruses. IN MANDAHAR, C. L. (Ed.) *Molecular biology of plant viruses.* Boston/Dordrecht/London, Kluwer.

MOROZOV, S. Y. & SOLOVYEV, A. G. (2003) Triple gene block: modular design of a multifunctional machine for plant virus movement. *J. Gen. Virol.,* 84**,** 1351-1366.

MOROZOV, S. Y., SOLOVYEV, A. G., KALININA, N. O., FEDORKIN, O. N., SAMUILOVA, O. V., SCHIEMANN, J. & ATABEKOV, J. G. (1999) Evidence for two nonoverlapping functional domains in the potato virus X 25K movement protein. *Virology,* 260**,** 55-63.

MOROZOV, S. Y., ZAKHARYEV, V. M., CHERNOV, B. K., PRASOLOV, V. S., KOZLOV, Y. V., ATABEKOV, J. G. & SKRYABIN, K. G. (1983) The analysis of the primary structure and localization of the coat protein gene in genomic RNA of potato virus X. *Dokl. Akad. Nauk SSSR,* 271**,** 211-215.

MUNRO, S. (1995) An investigation into the role of trans-membrane domains in Golgi protein retention. *EMBO J.,* 14**,** 4695-4704.

NAGARAJ, A. N. (1965) Immunofluorescence studies on synthesis and distribution of tobaccomosaic virus antigen in tobacco. *Virology,* 25**,** 133-142.

NAKAGAWA, T., KUROSE, T., HINO, T., TANAKA, K., KAWAMUKAI, M., NIWA, Y., TOYOOKA, K., MATSUOKA, K., JINBO, T. & KIMURA, T. (2007) Development of series of Gateway binary vectors, pGWBs, for realizing efficient construction of fusion genes for plant transformation. *Journal of Bioscience and Bioengineering,* 104**,** 34-41.

NEBENFÜHR, A., GALLAGHER, L. A., DUNAHAY, T. G., FROHLICK, J. A., MAZURKIEWICZ, A. M., MEEHL, J. B. & STAEHELIN, L. A. (1999) Stop-and-go movements of plant Golgi stacks are mediated by the actino-myosin system. *Plant Physiology,* 121**,** 1127-1141.

NEBENFÜHR, A., RITZENTHALER, C. & ROBINSON, D. G. (2002) Brefeldin A: deciphering an enigmatic inhibitor of secretion. *Plant Physiology,* 130**,** 1102-1108.

NEILSON, J. R. & SHARP, P. A. (2008) Small RNA regulators of gene expression. *Cell,* 134**,** 899-902.

NELSON, R. S. (2005) Movement of viruses to and through plasmodesmata. IN OPARKA, K. J. (Ed.) *Plasmodesmata. Annual Plant Reviews, Volume 18.* Blackwell Publishing Ltd.

NETTLESHIP, S. & FOSTER, G. D. (2000) Viral pathogenicity. IN DICKINSON, M. & BEYNON, J. (Eds.) *Molecular Plant Pathology. Annual Plant Reviews, Volume 4.* Sheffield, England, Sheffield Academic Press Ltd.

NEUMANN, U., BRANDIZZI, F. & HAWES, C. (2003) Protein transport in plant cells: in and out of the Golgi. *Annals of Botany,* 92**,** 167-180.

NEUTHAUS, J.-M. & BOEVINK, P. (2001) The green fluorescent protein (GFP) as a reporter in plant cells. Transformation methods. IN HAWES, C. & SATIAT-JEUNEMAITRE, B. (Eds.) *Plant Cell Biology. 2nd edition.* Oxford, Oxford University Press.

NIESBACH-KLÖSGEN, U., GUILLEY, H., JONARD, G. & RICHARDS, K. (1990) Immunodetection in vivo of beet necrotic yellow vein virus-encoded proteins. *Virology,* 178**,** 52-61.

NOUEIRY, A. O. & AHLQUIST, P. (2003) Brome mosaic virus RNA replication: revealing the role of the host in RNA virus replication. *Annual Review of Phytopathology,* 41**,** 77-98.

NOVAK, J. E. & KIRKEGAARD, K. (1994) Coupling between genome translation and replication in an RNA virus. *Genes and Development,* 8**,** 1726-1737.

NOVOA, R. R., CALDERITA, G., ARRANZ, R., FONTANA, J., GRANZOW, H. & RISCO, C. (2005) Virus factories: associations of cell organelles for viral replication and morphogenesis. *Biology of the Cell,* 97**,** 147-172.

OPARKA, K. J. (2004) Getting the message across: how do plant cells exchange macromolecular complexes? *Trends in Plant Science,* 9**,** 33-41.

OPARKA, K. J., PRIOR, D. A. M., SANTA CRUZ, S., PADGETT, H. S. & BEACHY, R. N. (1997a) Gating of epidermal plasmodesmata is restricted to the leading edge of expanding infection sites of tobacco mosaic virus (TMV). *The Plant Journal,* 12(4)**,** 781-789.

OPARKA, K. J., ROBERTS, A. G., BOEVINK, P., SANTA CRUZ, S., ROBERTS, I. M., PRADEL, K. S., IMLAU, A., KOTLIZKY, G., SAUER, N. & EPEL, B. (1999) Simple, but not branched, plasmodesmata allow the nonspecific trafficking of proteins in developing tobacco leaves. *Cell,* 97**,** 743-754.

OPARKA, K. J., ROBERTS, A. G., ROBERTS, I. M., PRIOR, D. A. M. & SANTA CRUZ, S. (1996) Viral coat protein is targeted to, but does not gate, plasmodesmata during cell-to-cell movement of potato virus X. *The Plant Journal,* 10(5)**,** 805-813.

OPARKA, K. J., ROBERTS, A. G., SANTA CRUZ, S., BOEVINK, P., PRIOR, D. A. M. & SMALLCOMBE, A. (1997b) Using GFP to study virus invasion and spread in plant tissues. *Nature,* 388**,** 401-402.

OPARKA, K. J. & SANTA CRUZ, S. (2000) The great escape: phloem transport and unloading of macromolecules. *Annual Review of Plant Physiology and Plant Molecular Biology,* 51**,** 323-347.

OVERALL, R. L. & BLACKMAN, L. M. (1996) A model of the macromolecular structure of plasmodesmata. *Trends in Plant Science,* 1(9)**,** 307-311.

OZAWA, T., NATORI, Y., SATO, M. & UMEZAWA, Y. (2007) Imaging dynamics of endogenous mitochondrial RNA in single living cells. *Nature Methods,* 4**,** 413-419.

PADGETT, H. S., EPEL, B. L., KAHN, T. W., HEINLEIN, M., WATANABE, Y. & BEACHY, R. N. (1996) Distribution of tobamovirus movement protein in infected cells and implications for cell-to-cell spread of infection. *The Plant Journal,* 10(6)**,** 1079-1088.

PALUKAITIS, P., CARR, J. P. & SCHOELZ, J. E. (2008) Plant-virus interactions. IN FOSTER, G. D., JOHANSEN, I. E., HONG, Y. & NAGY, P. D. (Eds.) *Methods in Molecular Biology. 451. Plant Virology protocols: From viral sequence to protein function. 2nd edition.* Totowa, USA, Humana Press.

PEDERSEN, K. W., VAN DER MEER, Y., ROOS, N. & SNIJDER, E. J. (1999) Open reading frame 1a-encoded subunits of the arterivirus replicase induce endoplasmic reticulum-derived double-membrane vesicles which carry the viral replication complex. *Journal of Virology,* 73**,** 2016-2026.

PENNAZIO, S., D'AGOSTINO, G., APPIANO, A. & REDOLFI, P. (1978) Ultrastructure and histochemistry of the resistant tissue surrounding lesions of tomato bushy stunt virus in Gomphrena globosa leaves. *Physiological Plant Pathology,* 13**,** 165-171.

PERÄNEN, J., LAAKKONEN, P., HYVÖNEN, M. & KÄÄRIÄINEN, L. (1995) The alphavirus replicase protein nsP1 is membrane-associated and has affinity to endocytic organelles. *Virology,* 208**,** 610-620.

PEREMYSLOV, V. V., ANDREEV, I. A., PROKHNEVSKY, A. I., DUNCAN, G. H., TALIANSKY, M. E. & DOLJA, V. V. (2004) Complex molecular architecture of beet yellows virus particles. *PNAS,* 101**,** 5030-5035.

PEREMYSLOV, V. V., HAGIWARA, Y. & DOLJA, V. V. (1999) HSP70 homolog functions in cell-to-cell movement of a plant virus. *PNAS,* 96**,** 14771-14776.

PLANTE, C. A., KIM, K. H., PILLAI-NAIR, N., OSMAN, T. A., BUCK, K. W. & HEMENWAY, C. L. (2000) Soluble, template-dependent extracts from Nicotiana benthamiana plants infected with potato virus X transcribe both plus- and minus-strand RNA templates. *Virology,* 275**,** 444-451.

PLOUBIDOU, A. & WAY, M. (2001) Viral transport and the cytoskeleton. *Current Opinion in Cell Biology,* 13(1)**,** 97-105.

PRASHER, D. C., ECKENRODE, V. K., WARD, W. W., PRENDERGAST, F. G. & CORMIE, M. J. (1992) Primary structure of the Aequorea victoria green-fluorescent protein. *Gene,* 111**,** 229-233.

PRESLEY, J. F., COLE, N. B., SCHROER, T. A., HIRSCHBERG, K., ZAAL, K. J. M. & LIPPINCOTT-SCHWARTZ, J. (1997) ER-to-Golgi transport visualized in living cells. *Nature,* 389**,** 81-85.

PRICE, W. C. (1966) Flexuous rods in phloem cells of lime plants infected with citrus tristeza virus. *Virology,* 29**,** 285-294.

PROD'HOMME, D., LE PANSE, S., DRUGEON, G. & JUPIN, I. (2001) Detection and subcellular localisation of the turnip yellow mosaic virus 66K replication protein in infected cells. *Virology,* 281**,** 88-101.

PROKHNEVSKY, A. I., PEREMYSLOV, V. V. & DOLJA, V. V. (2005) Actin cytoskeleton is involved in targeting of a viral Hsp70 homolog to the cell periphery. *Journal of Virology,* 79**,** 14421-14428.

PURCIFULL, D. E., EDWARDSON, J. R. & CHRISTIE, R. G. (1966) Electron microscopy of intracellular aggregates in pea (Pisum sativum) infected with clover yellow mosaic virus. *Virology,* 29**,** 276-284.

QUADER, H., HOFMANN, A. & SCHNEPF, E. (1987) Shape and movement of the endoplasmic reticulum in onion bulb epidermis cells: possible involvement of actin. *European Journal of Cell Biology,* 44**,** 17-26.

RADTKE, K., DOHNER, K. & SODEIK, B. (2006) Viral interactions with the cytoskeleton: a hitchhiker's guide to the cell. *Cell Microbiol.,* 8**,** 387-400.

RALPH, R. K. & CLARK, M. F. (1966) Intracellular location of double-stranded plant viral ribonucleic acid. *Biochlm. Biophys. Acta.,* 119**,** 29-36.

REDDI, K. K. (1964) Studies on the formation of tobacco mosaic virus ribonucleic acid, V. Presence of tobacco mosaic virus in the nucleus of the host cell. *PNAS,* 52**,** 397-401.

REICHEL, C. & BEACHY, R. N. (1998) Tobacco mosaic virus infection induces severe morphological changes of the endoplasmic reticulum. *PNAS,* 95**,** 11169-11174.

RESTREPO-HARTWIG, M. A. & AHLQUIST, P. (1996) Brome mosaic virus helicase- and polymerase-like proteins colocalize on the endoplasmic reticulum at sites of viral RNA synthesis. *Journal of Virology,* 70**,** 8908-8916.

RESTREPO-HARTWIG, M. A. & AHLQUIST, P. (1999) Brome mosaic virus RNA replication proteins 1a and 2a colocalize and 1a independently localizes on the yeast endoplasmic reticulum. *Journal of Virology,* 73**,** 10303-10309.

RESTREPO, M. A., FREED, D. D. & CARRINGTON, J. C. (1990) Nuclear transport of plant potyviral proteins. *Plant Cell,* 2**,** 987-998.

RING, C. J. A. & BLAIR, E. D. (2001) Introduction: viruses as vehicles and expressers of genetic material. IN RING, C. J. A. & BLAIR, E. D. (Eds.) *Genetically engineered viruses: Development and Applications.* Stevenage, UK, Glaxo Wellcome Research and Development, BIOS Scientific Publishers Limited.

RITZENTHALER, C., LAPORTE, C., GAIRE, F., DUNOYER, P., SCHMITT, C., DUVAL, S., PIEQUET, A., LOUDES, A. M., ROHFRITSCH, O., STUSSI-GARAUD, C. & PFEIFFER, P. (2002) Grapevine fanleaf virus replication occurs on endoplasmic reticulum-derived membranes. *Journal of Virology,* 76**,** 8808-8819.

RITZENTHALER, C., SCHMIT, A. C., MICHLER, P., STUSSI-GARAUD, C. & PINCK, L. (1995) Grapevine fanleaf nepovirus P38 putative movement protein is located on tubules in vivo *Molecular Plant-Microbe Interactions,* 8(3)**,** 379-387.

ROBARDS, A. W. & LUCAS, W. J. (1990) Plasmodesmata. *Annual Review of Plant Physiology,* 41**,** 369-419.
ROBERTS, A. G. & OPARKA, K. J. (2003) Plasmodesmata and the control of symplastic transport. *Plant, Cell and Environment,* 26**,** 103-124.
ROBERTS, D. A. (1952) Independent translocation of sap-transmissible viruses. *Phytopathology,* 42**,** 381-387.
ROBERTS, I. M., BOEVINK, P., ROBERTS, A. G., SAUER, N., REICHEL, C. & OPARKA, K. J. (2001) Dynamic changes in the frequency and architecture of plasmodesmata during the sink-source transition in tobacco leaves. *Protoplasma,* 218**,** 31-44.
RODIONOVA, N. P., KARPOVA, O. V., KOZLOVSKY, S. V., ZAYAKINA, O. V., ARKHIPENKO, M. V. & ATABEKOV, J. G. (2003) Linear remodeling of helical virus by movement protein binding. *J. Mol. Biol.,* 333**,** 565-572.
RODRIGUEZ, A. J., CONDEELIS, J., SINGER, R. H. & DICTENBERG, J. B. (2007) Imaging mRNA movement from transcription sites to translation sites. *Sem Cell Dev Biol.,* 18**,** 202-208.
ROGHI, C. & ALLAN, V. J. (1999) Dynamic association of cytoplasmic dynein heavy chain 1a with the Golgi apparatus and intermediate compartment. *J. Cell Science,* 112**,** 4673-4685.
ROPER, R. L., WOLFFE, E. J., WEISBERG, A. & MOSS, B. (1998) The envelope protein encoded by the A33R gene is required for formation of actin-containing microvilli and efficient cell-to-cell spread of vaccinia virus. *Journal of Virology,* 72**,** 4192-4204.
ROULEAU, M., SMITH, R. J., BANCROFT, J. B. & MACKIE, G. A. (1994) Purification, properties, and subcellular localization of foxtail mosaic potexvirus 26-kDa protein. *Virology,* 204**,** 254-265.
RUBINO, L. & RUSSO, M. (1998) Membrane targeting sequences in tombusvirus infections. *Virology,* 252**,** 431-437.
RUBINO, L., WEBER-LOTFI, F., DIETRICH, A., STUSSI-GARAUD, C. & RUSSO, M. (2001) The open reading frame 1-encoded ('36K') protein of carnation italian ringspot virus localizes to mitochondria. *J. Gen. Virol.,* 82**,** 29-34.
RUPASOV, V. V., MOROZOV, S. Y., KANYUKA, K. V. & ZAVRIEV, S. K. (1989) Partial nucleotide sequence of potato virus M RNA shows similarities to potexviruses in gene arrangement and the encoded amino acid sequence. *J. Gen. Virol.,* 70**,** 1861-1869.
RUSSO, M., TRANCO, D. I. & MARTELLI, G. P. (1983) The fine structure of cymbidium ringspot virus infections in host tissues: Role of peroxisomes in the genesis of multivesicular bodies. *J. Ultrastuct. Res.,* 82**,** 52-63.
SAINT-JORE, C. M., EVINS, J., BATOKO, H., BRANDIZZI, F., MOORE, I. & HAWES, C. (2002) Redistribution of membrane proteins between the Golgi apparatus and endoplasmic reticulum in plants is reversible and not dependent on cytoskeletal networks. *The Plant Journal,* 29**,** 661-678.
SAITO, T., HOSOKAWA, D., MESHI, T. & OKADA, Y. (1987) Immunocytochemical localization of the 130K and 180K proteins (putative replicase components) of tobacco mosaic virus. *Virology,* 160**,** 477-481.

SALONEN, A., AHOLA, T. & KÄÄRIÄINEN, L. (2005) Viral RNA replication in association with cellular membranes. *Curr. Top. Microbiol. Immunol.,* 285**,** 139-173.

SAMUELS, T. D., JU, H.-J., YE, C. M., MOTES, C. M., HOWARD, A. R., BLANCAFLOR, E. B. & VERCHOT-LUBICZ, J. (2007) Potato virus X TGBp1 protein accumulates independently of TGBp2 and TGBp3 to promote virus cell-to-cell movement. *Virology,* 367**,** 375-389.

SANFAÇON, H. (2005) Replication of positive-strand RNA viruses in plants: contact points between plant and virus components. *Can. J. Bot.,* 83**,** 1529-1549.

SANTA CRUZ, S., CHAPMAN, S., ROBERTS, A. G., ROBERTS, I. M., PRIOR, D. A. M. & OPARKA, K. J. (1996) Assembly and movement of a plant virus carrying a green fluorescent protein overcoat. *PNAS,* 93**,** 6286-6290.

SANTA CRUZ, S., ROBERTS, A. G., PRIOR, D. A. M., CHAPMAN, S. & OPARKA, K. J. (1998) Cell-to-cell and phloem-mediated transport of potato virus X: the role of virions. *Plant Cell,* 10**,** 495-510.

SANTOS, A. A., FLORENTINO, L. H., PIRES, A. B. L. & FONTES, E. P. B. (2008) Geminivirus: biolistic inoculation and molecular diagnosis. IN FOSTER, G. D., JOHANSEN, I. E., HONG, Y. & NAGY, P. D. (Eds.) *Methods in Molecular Biology. 451. Plant Virology protocols: From viral sequence to protein function. 2nd edition.* Totowa, USA, Humana Press.

SASAKI, H., NAKAMURA, M., OHNO, T., MATSUDA, Y., YUDA, Y. & NONOMURA, Y. (1995) Myosin-actin interaction plays an important role in human immunodeficiency virus type 1 release from host cells. *PNAS,* 92**,** 2026-2030.

SCHAAD, M. C., JENSEN, P. E. & CARRINGTON, J. C. (1997) Formation of plant RNA virus replication complexes on membranes: role of an endoplasmic reticulum-targeted viral protein. *EMBO,* 16**,** 4049-4059.

SCHAFFER, F. L. (1960) The nature of the noninfectious particles produced by poliovirus infected tissue cultures treated with proflavine. *Federation Proc.,* 19**,** 405.

SCHEPETILNIKOV, M. V., MANSKE, U., SOLOVYEV, A. G., ZAMYATNIN, J. A. A., SCHIEMANN, J. & MOROZOV, S. Y. (2005) The hydrophobic segment of potato virus X TGBp3 is a major determinant of the protein intracellular trafficking. *J. Gen. Virol.,* 86**,** 2379-2391.

SCHIFFERER, M. & GRIESBECK, O. (2009) Application of aptamers and autofluorescent proteins for RNA visualization. *Integr. Biol.,* 1**,** 499-505.

SCHLEGEL, A., GIDDINGS, T. H., LADINSKY, M. S. & KIRKEGAARD, K. (1996) Cellular origin and ultrastructure of membranes induced during poliovirus infection. *Journal of Virology,* 70**,** 6576-6588.

SCHOLTHOF, H. B. (2005) Plant virus transport: motions of functional equivalence. *Trends in Plant Science,* 10**,** 376-382.

SCHWARTZ, M., CHEN, J., JANDA, M., SULLIVAN, M., DEN BOON, J. & AHLQUIST, P. (2002) A positive-strand RNA virus replication complex parallels form and function of retrovirus capsids. *Mol. Cell,* 9**,** 505-514.

SCHWARTZ, M., CHEN, J., LEE, W.-M., JANDA, M. & AHLQUIST, P. (2004) Alternate, virus-induced membrane rearrangements support positive-strand RNA virus genome replication. *PNAS,* 101**,** 11263-11268.

SCHUMMELFEDER, N. (1958) Histochemical significance of the polychromatic fluorescence induced in tissues stained with acridine orange. *J. Histothem. Cytochem.,* 6**,** 392-393.

SEMLER, B. L., KUHN, R. J. & WIMMER, E. (1988) Replication of the poliovirus genome. IN AHLQUIST, P., HOLLAND, J. & DOMINGO, E. (Eds.) *RNA Genetics.* Boca Raton, FL, CRC Press.

SERAZEV, T. V., NADEZHDINA, E. S., SHANINA, N. A., LESHCHINER, A. D., KALININA, N. O. & MOROZOV, S. Y. (2003) Virions and the coat protein of the potato virus X interact with microtubules and induce tubulin polymerization in vitro. *Molecular Biology,* 37**,** 919-925.

SHALLA, T. A. (1968) Virus particles in chloroplasts of plants infected with the U5 strains of tobacco mosaic virus. *Virology,* 35**,** 194-203.

SHALLA, T. A. & SHEPARD, J. F. (1972) The structure and antigenic analysis of amorphous inclusion bodies induced by potato virus X. *Virology,* 49**,** 654-667.

SHANER, N. C., STEINBACH, P. A. & TSIEN, R. Y. (2005) A guide to choosing fluorescent proteins. *Nature Methods,* 2**,** 905-909.

SHAW, P. J. (2001) Introduction to optical microscopy for plant cell biology. Confocal and 3D microscopy. IN HAWES, C. & SATIAT-JEUNEMAITRE, B. (Eds.) *Plant Cell Biology. 2nd edition.* Oxford, Oxford University Press.

SHEAHAN, M. B., STAIGER, C. J., ROSE, R. J. & MCCURDY, D. W. (2004) A green fluorescent protein fusion to actin-binding domain 2 of Arabidopsis fimbrin highlights new features of a dynamic actin cytoskeleton in live plant cells. *Plant Physiology,* 136**,** 3968-3978.

SHEFFIELD, F. M. L. (1939) Micrurgical studies on virus-infected plants. *Proc.. Roy. Soc. (London), Set B.,* 126**,** 529-538.

SHEFFIELD, F. M. L. (1949) The virus in the plant cell. *Exptl. Cell Res. Suppl.,* 1**,** 178-182.

SHIKATA, E. & MARAMOROSCH, K. (1966) Electron microscopy of pea enation mosaic virus in plant cell nuclei. *Virology,* 30**,** 439-454.

SKRYABIN, K. G., MOROZOV, S., KRAEV, A. S., ROZANOV, M. N., CHERNOV, B. K., LUKASHEVA, L. I. & ATABEKOV, J. G. (1988) Conserved and variable elements in RNA genomes of potexviruses. *FEBS Lett.,* 240**,** 33-40.

SMITH, K. M. (1957) *A textbook of plant virus diseases. 2nd edition,* London, J. and A. Churchill Ltd.

SODEIK, B., EBERSOLD, M. W. & HELENIUS, A. (1997) Microtubule-mediated transport of incoming herpes simplex virus 1 capsids to the nucleus. *Journal of Cell Biology,* 136**,** 1007-1021.

SOLOVYEV, A. G., STROGANOVA, T. A., ZAMYATNIN, A. A., FEDORKIN, O. N., SCHIEMANN, J. & MOROZOV, S. Y. (2000) Subcellular sorting of small membrane-associated triple gene block proteins: TGBp3-assisted targeting of TGBp2. *Virology,* 269**,** 113-127.

SONENBERG, N., SHATKIN, A. J., RICCARDI, R. P., RUBIN, M. & GOODMAN, R. M. (1978) Analysis of terminal structures of RNA from potato virus X. *Nucleic Acids Research,* 5**,** 2501-2512.

SPASSOV, D. S. & JURECIC, R. (2002) Cloning and comparative sequence analysis of PUM1 and PUM2 genes, human members of the Pumilio family of RNA-binding proteins. *Gene,* 299**,** 195-204.

SPENCE, J. (2001) Plant histology. IN HAWES, C. & SATIAT-JEUNEMAITRE, B. (Eds.) *Plant Cell Biology. 2nd edition.* Oxford, Oxford University Press.

STAEHELIN, L. A. (1997) The plant ER: a dynamic organelle composed of a large number of discrete functional domains. *The Plant Journal,* 11**,** 1151-1165.

STAEHELIN, L. A. & MOORE, I. (1995) The plant Golgi apparatus: structure, functional organization and trafficking mechanisms. *Annual Review of Plant Physiology and Plant Molecular Biology,* 46**,** 261-288.

STAIGER, C. J. (2000) Signalling to the actin cytoskeleton in plants. *Annual Review of Plant Physiology and Plant Molecular Biology,* 51**,** 257-288.

STANGE, C. (2006) Plant-virus interactions during the infective process. *Cien. Inv. Agr.,* 33 (1)**,** 1-18.

STIDWILL, R. P. & GREBER, U. F. (2000) Intracellular virus trafficking reveals physiological characteristics of the cytoskeleton. *News Physiol. Sci.,* 15**,** 67-71.

STOLS, A. L. H., MEULEN, G. W. H. & TOEN, M. K. I. (1970) Electron microscopy of Nicotiana glutinosa leaf cells infected with potato virus X. *Virology,* 40**,** 168-170.

STORMS, M. M. H., KORMELINK, R., PETERS, D., VAN LENT, J. W. M. & GOLDBACH, R. W. (1995) The nonstructural NSm protein of tomato spotted wilt virus induces tubular structures in plant and insect cells. *Virology,* 214**,** 485-493.

STOUGAARD, J. (1995) Agrobacterium rhizogenes as a vector for transforming higher plants. Application in Lotus corniculatus transformation. IN JONES, H. (Ed.) *Methods in Molecular Biology. Volume 49. Plant gene transfer and expression protocols.* Totowa, NJ, Humana Press.

SUHY, D. A., GIDDINGS JR., T. H. & KIRKEGAARD, K. (2000) Remodeling the endoplasmic reticulum by poliovirus infection and by individual viral proteins: an autophagy-like origin for virus-induced vesicles. *Journal of Virology,* 74**,** 8953-8965.

SUNDELL, C. L. & SINGER, R. H. (1991) Requirement of microfilaments in sorting of actin messenger RNA. *Science,* 253**,** 1275-1277.

SUOMALAINEN, M., NAKANO, M. Y., BOUCKE, K., KELLER, S., STIDWILL, R. P. & GREBER, U. F. (1999) Microtubule-dependent minus and plus end-directed motilities are competing processes for nuclear targeting of adenovirus. *Journal of Cell Biology,* 144**,** 657-672.

SUZUKI, T., MATSUZAKI, T., HAGIWARA, H., AOKI, T. & TAKATA, K. (2007) Recent advances in fluorescent labeling techniques for fluorescence microscopy. *Acta Histochem. Cytochem.,* 40**,** 131-137.

SZECSI, J., DING, X. S., LIM, C. O., BENDAHMANE, M., CHO, M. J., NELSON, R. S. & BEACHY, R. N. (1999) Development of tobacco mosaic virus infection

sites in Nicotiana benthamiana. *Molecular Plant-Microbe Interactions,* 12**,** 143-152.

TAKAHASHI, T. & YOSHIKAWA, N. (2008) Analysis of cell-to-cell and long-distance movement of Apple latent spherical virus in infected plants using green, cyan, and yellow fluorescent proteins. IN FOSTER, G. D., JOHANSEN, I. E., HONG, Y. & NAGY, P. D. (Eds.) *Methods in Molecular Biology. 451. Plant Virology protocols: From viral sequence to protein function. 2nd edition.* Totowa, USA, Humana Press.

TAKEMOTO, D. & HARDHAM, A. R. (2004) The cytoskeleton as a regulator and target of biotic interactions in plants. *Plant Physiology,* 136**,** 3864-3876.

TALIANSKY, M., ROBERTS, I. M., KALININA, N., RYABOV, E. V., RAJ, S. K., ROBINSON, D. J. & OPARKA, K. J. (2003) An umbraviral protein, involved in long-distance RNA movement, binds viral RNA and forms unique, protective ribonucleoprotein complexes. *Journal of Virology,* 77(5)**,** 3031-3040.

TALIANSKY, M., TORRANCE, L. & KALININA, N. O. (2008) Role of plant virus movement proteins. IN FOSTER, G. D., JOHANSEN, I. E., HONG, Y. & NAGY, P. D. (Eds.) *Methods in Molecular Biology. 451. Plant Virology protocols: From viral sequence to protein function. 2nd edition.* Totowa, USA, Humana Press.

TAMAI, A. & MESHI, T. (2001) Cell-to-cell movement of potato virus X: the role of p12 and p8 encoded by the second and third open reading frames of the triple gene block. *Molecular Plant-Microbe Interactions,* 14**,** 1158-1167.

THIVIERGE, K., NICAISE, V., DUFRESNE, P. J., COTTON, S., LALIBERTÉ, J.-F., LE GALL, O. & FORTIN, M. G. (2005) Plant virus RNAs. Coordinated recruitment of host functions by (+) ssRNA viruses during early infection events. *Plant Physiology,* 138**,** 1822-1827.

TILSNER, J., LINNIK, O., CHRISTENSEN, N. M., BELL, K., ROBERTS, I. M., LACOMME, C. & OPARKA, K. J. (2009) Live-cell imaging of viral RNA genomes using a Pumilio-based reporter. *The Plant Journal,* 57**,** 758-770.

TOMENIUS, K., CLAPHAM, D. & MESHI, T. (1987) Localization by immunogold cytochemistry of the virus-coded 30K protein in plasmodesmata of leaves infected with tobacco mosaic virus. *Virology,* 160**,** 363-371.

TOYOOKA, K., OKAMOTO, T. & MINAMIKAWA, T. (2000) Mass transport of a preform of a KDEL-tailed cystein proteinase (SH-EP) to protein storage vacuoles by endoplasmic reticulum-derived vesicle is involved in protein mobilization in germinating seeds. *Journal of Cell Biology,* 148**,** 453-463.

TRUTNYEVA, K., RUGGENTHALER, P. & WAIGMANN, E. (2008) Movement profiles: a tool for quantitative analysis of cell-to-cell movement of plant viral movement proteins. IN FOSTER, G. D., JOHANSEN, I. E., HONG, Y. & NAGY, P. D. (Eds.) *Methods in Molecular Biology. 451. Plant Virology protocols: From viral sequence to protein function. 2nd edition.* Totowa, USA, Humana Press.

TURNER, K. A., SIT, T. L., CALLAWAY, A. S., ALLEN, N. S. & LOMMEL, S. A. (2004) Red clover necrotic mosaic virus replication proteins accumulate at the endoplasmic reticulum. *Virology,* 320**,** 276-290.

TURNER, R. & FOSTER, G. D. (1998) In vitro transcription and translation. IN FOSTER, G. D. & TAYLOR, S. C. (Eds.) *Methods in Molecular Biology. Volume 81. Plant virology protocols: from virus isolation to transgenic resistance.* Totowa, NJ, Humana Press.

TZFIRA, T., RHEE, Y., CHEN, M. H., KUNIK, T. & CITOVSKY, V. (2000) Nucleic acid transport in plant-microbe interactions: The molecules that walk through the walls. *Annual Review of Microbiology,* 54**,** 187-219.

UEDA, K., MATSUYAMA, T. & HASHIMOTO, T. (1999) Visualization of microtubules in living cells of transgenic Arabidopsis thaliana. *Protoplasma,* 206**,** 201-206.

VAGHCHHIPAWALA, Z. E. & MYSORE, K. S. (2008) Agroinfiltration: a simple procedure for systemic infection of plants with viruses. IN FOSTER, G. D., JOHANSEN, I. E., HONG, Y. & NAGY, P. D. (Eds.) *Methods in Molecular Biology. 451. Plant Virology protocols: From viral sequence to protein function. 2nd edition.* Totowa, USA, Humana Press.

VAN DER MEER, Y., SNIJDER, E. J., DOBBE, J. C., SCHLEICH, S., DENISON, M. R., SPAAN, W. J. & LOCKER, J. K. (1999) Localization of mouse hepatitis virus nonstructural proteins and RNA synthesis indicates a role for late endosomes in viral replication. *Journal of Virology,* 73**,** 7641-7657.

VERCHOT-LUBICZ, J. (2005) A new cell-to-cell transport model for potexviruses. *Molecular Plant-Microbe Interactions,* 18**,** 283-290.

VERCHOT-LUBICZ, J., JU, H.-J. & SAMUELS, T. D. (2006) Cell-to-cell movement of Potato virus X. IN SANCHEZ, F., QUINTO, C., LOPEZ-LARA, I. M. & GEIGER, O. (Eds.) *Biology of plant-microbe interactions. Volume 5.* St. Paul, Minnesota, USA, International Society for Molecular Plant-Microbe Interactions.

VERCHOT-LUBICZ, J., YE, C.-M. & BAMUNUSINGHE, D. (2007) Molecular biology of potexviruses: recent advances. *J. Gen. Virol.,* 88**,** 1643-1655.

VERCHOT, J., ANGELL, S. M. & BAULCOMBE, D. C. (1998) In vivo translation of the triple gene block of potato virus X requires two subgenomic mRNAs. *Journal of Virology,* 72**,** 8316-8320.

VITALE, A. & DENECKE, J. (1999) The endoplasmic reticulum - gateway of the secretory pathway. *Plant Cell,* 11**,** 615-628.

VOINNET, O., LEDERER, C. & BAULCOMBE, D. C. (2000) A viral movement protein prevents spread of the gene silencing signal in Nicotiana benthamiana. *Cell,* 103**,** 157-167.

WAIGMANN, E., LUCAS, W. J., CITOVSKY, V. & ZAMBRYSKI, P. (1994) Direct functional assay for tobacco mosaic virus cell-to-cell movement protein and identification of a domain involved in increasing plasmodesmatal permeability. *PNAS,* 91**,** 1433-1437.

WALTER, B. L., PARSLEY, T. B., EHRENFELD, E. & SEMLER, B. L. (2002) Distinct poly(rC) binding protein KH domain determinants for poliovirus translation initiation and viral RNA replication. *Journal of Virology,* 76**,** 12008-12022.

WANG, X., MCLACHLAN, J., ZAMORE, P. D. & TANAKA HALL, T. M. (2002) Modular recognition of RNA by a human Pumilio-homology domain. *Cell,* 110**,** 501-512.

WASTENEYS, G. O. & GALWAY, M. E. (2003) Remodelling the cytoskeleton for growth and form: an overview with some new views. *Annual Review of Plant Biology,* 54**,** 691-722.

WEBER-LOTFI, F., DIETRICH, A., RUSSO, M. & RUBINO, L. (2002) Mitochondrial targeting and membrane anchoring of a viral replicase in plant and yeast cells. *Journal of Virology,* 76**,** 10485-10496.

WEE, E. G.-T., SHERRIER, D. J., PRIME, T. A. & DUPREE, P. (1998) Targeting of active sialyltransferase to the plant Golgi apparatus. *Plant Cell,* 10**,** 1759-1768.

WEI, T. & WANG, A. (2008) Biogenesis of cytoplasmic membranous vesicles for plant potyvirus replication occurs at endoplasmic reticulum exit sites in a COPI- and COPII-dependent manner. *Journal of Virology,* 82**,** 12252-12264.

WEIJERS, D., FRANKE-VAN DIJK, M., VENCKEN, R. J., QUINT, A., HOOYKAAS, P. & OFFRINGA, R. (2001) An Arabidopsis minute-like phenotype caused by a semi-dominant mutation in a Ribosomal protein S5 gene. *Development,* 128**,** 4289-4299.

WEINTRAUB, M., RAGETLI, H. W. J. & LEUNG, E. (1976) Elongated virus particles in plasmodesmata. *Journal of Ultrastructural Research,* 56**,** 351-364.

WHITE, K. A., BANCROFT, J. B. & MACKIE, G. A. (1992) Coding capacity determines in vivo accumulation of a defective RNA of Clover yellow mosaic virus. *Journal of Virology,* 66**,** 3069-3076.

WHITE, R. G., BADELT, K., OVERALL, R. L. & VESK, M. (1994) Actin associated with plasmodesmata. *Protoplasma,* 180**,** 169-184.

WHITHAM, S. A. & WANG, Y. (2004) Roles for host factors in plant viral pathogenicity. *Current Opinion in Plant Biology,* 7**,** 365-371.

WICKENS, M., BERNSTEIN, D. S., KIMBLE, J. & PARKER, R. (2002) A PUF family portrait: 3' UTR regulation as a way of life. *Trends in Genetics,* 18**,** 150-157.

WOLF, S., DEOM, C. M., BEACHY, R. N. & LUCAS, W. J. (1989) Movement protein of tobacco mosaic virus modifies plasmodesmatal size exclusion limit. *Science,* 246**,** 377-379.

WONG, S.-M., LEE, K.-C., YU, H.-H. & LEONG, W.-F. (1998) Phylogenetic analysis of triple gene block viruses based on the TGB 1 homolog gene indicates a convergent evolution. *Virus Genes,* 16**,** 295-302.

WU, J. H. & DIMITMAN, J. E. (1970) Leaf structure and callose formation as determinants of TMV movement in bean leaves as revealed by UV irradiation studies. *Virology,* 40**,** 820-827.

YANG, Y., DING, B., BAULCOMBE, D. C. & VERCHOT, J. (2000) Cell-to-cell movement of the 25K protein of potato virus X is regulated by three other viral proteins. *Molecular Plant-Microbe Interactions,* 13**,** 599-605.

ZAITLIN, M. & BOARDMAN, N. K. (1958) The association of tobacco mosaic virus with plastids. I. Isolation of virus from chloroplast fraction of diseased-leaf homogenates. *Virology,* 6**,** 743-757.

ZAMYATNIN, A. A., SOLOVYEV, A. G., SABLINA, A. A., AGRANOVSKY, A. A., KATUL, L., VETTEN, H. J., SCHIEMANN, J., HINKKANEN, A. E., LEHTO, K. & MOROZOV, S. Y. (2002) Dual-colour imaging of membrane protein targeting directed by poa semilatent virus movement protein TGBp3 in plant and mammalian cells. *J. Gen. Virol.,* 83**,** 651-662.

ZHANG, F. & SIMON, A. E. (2003) A novel procedure for the localization of viral RNAs in protoplasts and whole plants. *The Plant Journal,* 35**,** 665-673.

ZHOU, H. & JACKSON, A. O. (1996) Expression of the barley stripe mosaic virus RNA beta 'triple gene block'. *Virology,* 216**,** 367-379.

ZIMYANIN, V. L., BELAYA, K., PECREAUX, J., GILCHRIST, M. J., CLARK, A., DAVIS, I. & JOHNSTON, D. S. (2008) In vivo imaging of oskar mRNA transport reveals the mechanism of posterior localization. *Cell,* 134**,** 843-853.